UNIVERSIDADE DE LISBOA

FACULDADE DE FARMÁCIA

Development and characterization of novel vehicles for topical drug delivery

Joana Marques Marto

Orientadora: Professora Doutora Helena Margarida Oliveira Marques Ribeiro
Co-orientadores: Professor Doutor António José Leitão das Neves Almeida
Dr. Augusto Eduardo Vieira Borges Oliveira

Tese especialmente elaborada para a obtenção do grau de Doutor em Farmácia na especialidade de Tecnologia Farmacêutica.

2016

UNIVERSIDADE DE LISBOA

FACULDADE DE FARMÁCIA

Development and characterization of novel vehicles for topical drug delivery

Joana Marques Marto

Orientadora: Professora Doutora Helena Margarida Marques Ribeiro
Co-orientadores: Professor Doutor António José Leitão das Neves Almeida
Dr. Augusto Eduardo Vieira Borges Oliveira

Tese especialmente elaborada para a obtenção do grau de Doutor em Farmácia na especialidade de Tecnologia Farmacêutica.

Júri

Presidente: Doutora Matilde da Luz dos Santos Duque da Fonseca e Castro, Professora Catedrática e Diretora da Faculdade de Farmácia da Universidade de Lisboa.

Vogais: Doutor João José Martins Simões de Sousa, Professor Associado com Agregação, Faculdade de Farmácia da Universidade de Coimbra;
Doutor Alberto António Caria Canelas Pais, Professor Associado com Agregação, Faculdade de Ciências e Tecnologia da Universidade de Coimbra;
Doutora Isabel Filipa Martins de Almeida, Professora Auxiliar, Faculdade de Farmácia do Porto;
Dr. Augusto Eduardo Vieira Borges Oliveira, Director de Assuntos Regulamentares, Laboratórios Atral. S.A., na qualidade de especialista de reconhecido mérito e competência, Coorientador;
Doutora Helena Margarida Oliveira Marques Ribeiro, Professora Associada, Faculdade de Farmácia, Universidade de Lisboa; Orientadora;
Doutor Luis Filipe Baptista Pleno Gouveia, Professor Auxiliar, Faculdade de Farmácia da Universidade de Lisboa.

2016

“Se não sais de ti,
não chegas a saber quem és.”

José Saramago

Table of Contents

Agradecimentos

A finalização dos estudos conducentes ao grau de doutor compreenderam desafios intelectuais e pessoais que só foram possíveis de ultrapassar com a entreajuda de todos aqueles que contribuíram para este árduo e longo caminho. É, assim, chegada a hora de expressar os meus mais sinceros agradecimentos a todos os que me orientaram, acolheram e ajudaram na concretização desta aspiração pessoal e que tornaram possível a realização desta dissertação.

À Professora Doutora Helena Margarida Ribeiro, minha orientadora principal, agradeço especialmente pela exemplar orientação que me permitiu crescer cientificamente e, não menos importante, crescer pessoalmente. Agradeço a disponibilidade com que me recebeu e me integrou no seu grupo de trabalho desde o primeiro momento. Ao longo destes anos, agradeço a recetividade constante e a sábia capacidade pedagógica e científica que me permitiram superar dúvidas e reformular decisões. Não posso por isso deixar de destacar a visão crítica e sempre positiva que de uma forma muito clara, objetiva e motivadora conduziram ao aperfeiçoamento do presente trabalho. A sua simpatia, boa disposição, plena dedicação e interesse, permitiram o melhor ambiente que alguém pode desejar enquanto desenvolve um trabalho desta complexidade. Saliento ainda o privilégio que sinto pela amizade que construímos e que se projetará muito para além deste tempo.

Ao Professor Doutor António José Leitão das Neves Almeida, co-orientador desta tese, quero expressar o meu sincero agradecimento pela excelência científica e rigor de desempenho. Agradeço a motivação, a dedicação e a disponibilidade constantes. Agradeço os ensinamentos, as sugestões pertinentes, a visão crítica, clara, oportuna e sempre construtiva no decurso deste trabalho. Saliento a sua conduta humana, apoio e amizade sempre demonstradas em momentos decisivos que resultaram sempre num forte estímulo para prosseguir o caminho que culmina nesta tese.

Ao Dr. Eduardo Oliveira, meu co-orientador científico, quero manifestar o meu agradecimento, realçando a excelência do seu desempenho, enquanto orientador industrial desta tese. Agradeço o apoio e as circunstâncias que me proporcionaram realizar este trabalho, bem como as discussões científicas que me ajudaram a orientar esta tese para necessidades reais da indústria farmacêutica Portuguesa.

Ao Professor Doutor Luis Filipe Gouveia, porque me quis honrar com o seu apoio, pelos conselhos e diálogos científicos, pelas adequadas sugestões formuladas, quero agradecer a sua visão critica e construtiva em momentos decisivos que me ajudaram a atingir os objetivos propostos. O meu reconhecimento para toda a vida.

À Doutora Lídia Maria Diogo Gonçalves, agradeço o rigor pelas boas práticas, chancela do seu trabalho de excelência, e a inteira disponibilidade sempre demonstrada. As suas palavras de encorajamento e de grande amizade revelaram-se determinantes nesta etapa que agora termina.

À Professora Doutora Aida Duarte, expresso os meus agradecimentos pela disponibilidade e partilha de conhecimentos. As discussões científicas críticas contribuíram inquestionavelmente para o aperfeiçoamento da minha forma de trabalhar e pensar. Com um sentido maternal, preocupado e acima de tudo dinâmico, inteligente, objectivo e empreendedor, é inigualável o modo como sempre se e nos destacou.

À Dra. Ana Salgado reconheço o papel determinante em todo o caminho percorrido, a nível profissional e pessoal. Um muito obrigado pela amizade e camaradagem.

À Doutora Sandra Simões e Doutor Pedro Pinto agradeço a colaboração pronta e rigorosa que me dispensaram na execução de alguns trabalhos laboratoriais, bem como o apoio e amizade demostrados.

Ao espírito de grupo, amizade e sentido de entreajuda de todos os colegas da Tecnologia Farmacêutica, e de um modo especial, e sem ordem em particular, à Sara Raposo, Rui Lopes, Diana Gaspar, Maria Paisana, Joana Pinto, Inês Ferreira, Paulo Roque Lino, Ana Matos, Filipa Silva, Joana Bicho, Gonçalo Oliveira, Giuliana Mancini, Andreia Ascenso, Diana Rafael, Ana Cadete, Lara Figueiredo, Ana Varela, Joana Silva, Filipa Guilherme, Ana Neves, Carla Vitorino, Alice Gelpi, Cecilia Sangali, Liliana Aranha, Diogo Baltazar,

Barbara Gregori, Margherita Alegro, João Quintas, André Sá Couto, Nélio Drummond e Ana Costa pelo contínuo apoio que me ajudaram a ultrapassar as fases mais difíceis.

À ADEIM, em especial a Dra. Alexandra Silva e Paula Machado por todo o apoio, espírito de grupo e amizade com que sempre me brindaram e enriqueceram.

À Engenheira Carla Eleuterio, D. Fernanda Carvalho, D. Henriqueta Pinto e D. Fernanda Oliveira, agradeço o bom acolhimento e disponibilidade continuada, que concederam às minhas múltiplas solicitações.

À Doutora Susana Dias Lucas e ao Professor Doutor Rui Moreira um agradecimento pela possibilidade de colaboração com o MedChem Group do iMed.ULisboa, e em especial ao Eduardo Ruivo pelo desenvolvimento da molécula utilizada no Capitulo 4, Secção 2 e no esclarecimento de questões relacionada com a mesma. Agradeço ainda todo o apoio, partilha, paciência, sorrisos e alegrias com que diariamente me enriqueceram este percurso e com que me ajudaram a superar as etapas mais difíceis.

Ao Professor Doutor Alberto Pais Canelas do Departamento de Química da Universidade de Coimbra, agradeço a disponibilidade e o interesse manifestado por este trabalho. Ao Professor Doutor Filipe Antunes, Professor Doutor João Pina e Doutor Sérgio Silva agradeço todos os ensinamentos, esclarecimentos, sugestões e diálogos científicos que em muito contribuíram para a qualidade desta tese. À Doutora Sandra Nunes e Dra. Tânia Firmino não posso deixar de agradecer a contagiante boa disposição que proporcionaram a vivência de momentos de descontração únicos.

À Professora Doutora Vera Isaac do Laboratório de Cosmetologia da Faculdade de Ciências Farmacêuticas da UNESP, agradeço a simpatia e amizade com que me recebeu em Araraquara e o interesse demonstrado na colaboração do meu trabalho. Também à Doutora Bruna Chiari-Andreo apresento o meu muito obrigada por toda a disponibilidade no laboratório e no esclarecimento de questões relacionadas com as mesmas, por todas as considerações científicas e sugestões que culminaram no trabalho publicado e que será apresentado nesta tese.

A Doutora Tania Carvalho, Ana Margarida Santos, Andreia Pinto e Bruna Almeida do Laboratório de Histologia e Patologia Comparada no Instituto de Medicina Molecular pelo trabalho de histologia. Agradeço-lhes as valiosas observações e sugestões para a melhor

análise das amostras e os esclarecimentos prestados sobre as mesmas sempre que uma dúvida surgia.

O meu agradecimento também aos estudantes Inês Jorge, Patrícia Manteigas e Joice Lana pela sua contribuição na realização do intenso trabalho de laboratório.

À Professora Doutora Ana Francisca Bettencourt e à Professora Maria João Silva por todo o carinho, bem como apoio e amizade demostrados.

À Dra. Inês Casais pelo *design* gráfico da presente dissertação.

À empresa DS Produtos Químicos Lda., em especial ao Sr. Óscar Brás, pela disponibilização de várias matérias-primas e ajuda em algumas questões científicas.

À direcção e restantes membros do Departamento de Farmácia Galénica e Tecnologia Farmacêutica e ao Departamento de Microbiologia bem como do grupo Nano2B, antigo NanoDDS e da FFULisboa por sempre ter encontrado as melhores condições para um correcto desenrolar de trabalhos bem como pelo ambiente cientificamente rico e potenciador de conhecimento.

Aos meus amigos e em especial ao André, pela sua inestimável paciência, tempo interminável... e contenção das minhas angústias finais.

À minha Mãe, Pai e família. Ao apoio incondicional que me deram ao encarar este projecto e com o qual me continuam ajudar a avançar sempre em frente, fomentando a conclusão dos objectivos a que me proponho, sempre rumo a um crescimento saudável e feliz. São as pessoas que me enchem o peito a razão do meu viver e estou-lhes e estarei sempre eternamente agradecida!

Aos Laboratórios Atral S.A., agradeço as condições económicas que me proporcionaram realizar esta tese bem como todo o apoio dispensado.

À Fundação para a Ciência e Tecnologia agradeço a bolsa de doutoramento SFRH/BDE/51599/2011 que nos permitiu efectuar o presente conjunto de trabalhos.

Abstract

Topical drug delivery is challenging since the skin acts as a natural and protective barrier. The skin has been an important route for drug delivery when topical, local or systemic effects are desired. The outcome of topical dermatological drug treatment is significantly influenced by the choice of vehicle. In recent years there has been an increased interest in developing improved delivery systems and, exploring new ways of using approved excipients, such as, starch. Due to its unique properties, starch has been extensively used in various topical pharmaceutical application, i.e. as a sensorial enhancer, a stabilizer and drug delivery polymer, providing protection and control release of the drug molecule.

The base-concept of this study was to develop and characterize novel starch-based vehicles for dermatological application, easily scaled-up to industry and produced by methods that can allow the decrease of production costs, and further investigate the resulting systems behavior in *in vitro* and *in vivo* conditions.

Starch-based vehicles were prepared successfully using QbD approach with the understanding of the high risk process and formulation parameters involved and optimized design space with a multifactorial combination of critical parameters to obtain predetermined specifications.

Three different model drugs were incorporated into the optimized starch-based vehicles. Minocycline hydrochloride (MH) was incorporated in Pickering emulsions, a human neutrophil elastase inhibitor (ER143), a new molecule developed by the MedChem Group at iMed.ULisboa, was encapsulated into starch nanocapsules and melatonin was added on Pickering emulsions sunscreen, in order to fully characterize these new formulations, and further study its topical delivery and *in vitro* and *in vivo* efficacy.

The *in vitro* antibacterial activity studies for Pickering emulsions containing MH revealed that the released drug exceeded the minimum inhibitory concentration of MH against *S.aureus. In*

vitro release studies showed a prolonged release of the MH, with an initial burst effect. Regarding *in vitro* permeation studies, MH does not pass through the entire skin layer, suggesting a minimal potential for the systemic absorption of the MH upon topical administration. *In vivo* results showed that topical administration of MH was effective in *S. aureus* superficial infections treatment.

Starch nanocapsules presented a mean particle size ranging from 200 to 250 nm and a positive zeta potential. *In vitro* permeation studies showed that the starch nanocapsules were suitable for the delivery of ER143, allowing a high control of the drug release, contributing to a high skin retention and/or permeation profiles of ER143. *In vivo* results showed that erythema and edema were attenuated in 98%, following the local application of ER143-loaded starch nanocapsules.

Regarding Pickering emulsions sunscreen, formulation studies demonstrated that starch particles presented no intrinsic photoprotection properties, they proved to be a sun protection factor promoter by a synergistic effect. Besides the excellent sunscreen activity confirmed by *in vitro* and *in vivo* results, the final formulations proved to be also suitable for topical use according to the rheological assessment and stability throughout the study period (3 months).

Additionally, the safety and biological effects of the placebos (vehicles without drug) was assessed by using both *in vitro* and *in vivo* studies, as an adequate equilibrium between the safety and efficacy effects.

Overall, these findings highlight the starch-based vehicles as promising for the development of topical delivery systems, covering innovative therapeutic approaches.

Keywords: New delivery systems; Pickering emulsions; quality by design; starch; polymeric nanocapsules; topical delivery.

Resumo

A pele revela-se particularmente adequada para a aplicação tópica de fármacos ao favorecer o estabelecimento de um contacto íntimo do fármaco com o tecido-alvo a tratar e por dessa aplicação decorrer habitualmente um mínimo de efeitos sistémicos. No entanto, a administração tópica de fármacos continua a ser um desafio, uma vez que a terapêutica das doenças da pele está condicionada por duas características fundamentais deste órgão: a sua função de barreira, determinada pela estrutura da camada córnea que, por si, constitui o factor limitante da absorção percutânea e a sua sensibilidade ao contacto repetido com substâncias químicas. Normalmente as reacções adversas resultantes da aplicação tópica de fármacos não são imputáveis exclusivamente às substâncias activas utilizadas, sendo-o também aos excipientes, agentes conservantes ou substâncias aromáticas incluídos na preparação. Por esta razão impõe-se a investigação de novos excipientes ou o melhoramento dos existentes através da aplicação de novas abordagens.

São actualmente bem conhecidos os factores que condicionam a absorção e a difusão dos fármacos aplicados topicamente. Em primeiro lugar, a estrutura e características físico-químicas da substância activa e, seguidamente o tipo de excipiente que vai influenciar o grau de penetração do fármaco ativo, podendo ainda melhorar o grau de hidratação da pele e ter efeito emoliente e protector. Contudo, para terem actividade terapêutica, os fármacos têm que ultrapassar a camada córnea, o que consiste no transporte de uma substância para uma determinada camada da pele. A maior parte dos fármacos não consegue permear a pele, pelo que é necessário um veículo para os transportar ou para aumentar a libertação no local de ação.

Assim, o desenvolvimento e melhoramento de novas formulações para aplicação cutânea é uma estratégia interessante para a administração de fármacos cuja acção é local ou

transdérmica, representando uma alternativa que permite superar aspectos indesejados relacionados com as características farmacocinéticas e farmacodinâmicas dos fármacos.

O desenvolvimento de novas formas farmacêuticas implica um esforço considerável que é muitas vezes consumido na elaboração de especificações rigorosas de forma a garantir a sua estabilidade física, química e microbiológica. Estes novos produtos, concebidos para aplicação tópica de acordo com critérios específicos têm, até ao presente, sido produzidos em escala laboratorial ou em equipamentos de escala piloto. Para além dos requisitos de eficácia e segurança do medicamento, a facilidade de produção, de uma forma reprodutível, em equipamento industrial de produção rápida e económica é, frequentemente um factor que diferencia um produto com sucesso de outro que é encarado como uma curiosidade científica. Para ter sucesso o produto tem que ser capaz de ser processado e embalado em grande escala. Na instalação piloto uma fórmula é traduzida num produto viável e robusto pelo desenvolvimento de um método de produção fiável e prático que permita uma transição fácil entre o laboratório e uma instalação industrial.

Assim, a optimização de formulações e a utilização de sistemas transportadores constitui uma estratégia válida, nomeadamente com recurso a novos veículos, produzidos com excipientes devidamente regulamentados como os lípidos sólidos, o alginato e o amido.

Devido às suas propriedades únicas, o amido tem sido amplamente utilizado em diversas aplicações farmacêuticas. No entanto, uma potencial aplicação tem sido pouco explorada: a sua utilização em formas farmacêuticas para aplicação tópica. Devido à multifuncionalidade do amido, muitos desenvolvimentos são esperados nesta área, o que pode representar uma visão renovada para a indústria farmacêutica. Assim, um desenvolvimento farmacêutico racional, que integre formulações simples, de baixo custo e facilmente traspostas para a escala industrial, irá ajudar no desenvolvimento de veículos adequados.

Este projeto teve como principais pressupostos o desenvolvimento e caracterização de formulações com veículos inovadores, seguros, de menor custo e com vantagens terapêuticas para uso dermatológico e, de valor acrescentado para a empresa financiadora.

Foram desenvolvidos e optimizados vários veículos à base de amido, utilizando abordagem *quality by design* (QbD) e de acordo com a ICH Q8(R2). Após desenvolvidos e detalhadamente caracterizados, recorrendo a técnicas de DSC, FTIR, microscopia, fluorescência, ângulos de contacto, reologia, biocompatibilidade, o objetivo foi estudar os

perfis de libertação e permeação através de membranas sintéticas e pele de leitão, e realizar estudos *in vivo* de eficácia, comparando os resultados obtidos com a formulação de referência no mercado.

Finalmente, os efeitos biológicos e a avaliação de segurança foram realizados para os veículos de acordo com a legislação europeia de cosméticos em vigor.

Foram seleccionados 3 fármacos modelo para os diferentes veículos desenvolvidos e optimizados. Um antibiótico, cloridrato de minociclina (MH) foi incorporado em emulsões de Pickering, um inibidor da elastase de neutrófilos humanos (ER143), uma nova molécula desenvolvida pelo grupo de investigação MedChem do iMed.ULisboa, foi encapsulado em nanocápsulas de amido e por fim, a melatonina, um potente antioxidante, foi incorporada num protetor solar, utilizando como forma farmacêutica as emulsões de Pickering. Os fármacos modelo incorporados nos diferentes veículos foram utilizados com o intuito de caracterizar intensivamente os novos medicamentos/produtos de saúde desenvolvidos, e compreender os mecanismos de libertação e permeação, assim como estudar a sua eficácia terapêutica *in vitro* e *in vivo*.

Relativamente as emulsões de Pickering contendo MH, os estudos *in vitro* para determinar a actividade antibacteriana revelaram que o fármaco libertado das formulações é superior a concentração mínima inibitória contra *Staphylococcus aureus*. Estudos de libertação *in vitro* revelaram que o perfil de libertação do fármaco depende da concentração do agente estabilizador, grânulos de amido e da natureza da fase externa da emulsão. Todas as formulações estudadas exibem uma libertação controlada do fármaco. Estudos de permeação *in vitro* demostraram que as formulações em estudo tem pouca influencia na permeação do MH, dado que o MH não permeou a pele, revelando possuir um perfil de segurança adequado para os antibióticos de aplicação tópica. Resultados *in vivo* com murganhos demostraram que a administração tópica de MH foi eficaz no tratamento de infecções superficiais por *S. aureus*.

As nanocápsulas de amido desenvolvidas e optimizadas apresentam um tamanho médio de partícula entre 200 a 250 nm e um potencial zeta positivo (> 25 mV). A abordagem QbD permitiu compreender a formação deste veículo e concluir que a concentração de tensioactivo (não iónico) e a quantidade de lípido (núcleo oleoso) influenciam o tamanho da nanocápsula. Estudos de permeação *in vitro* demonstraram que o veículo desenvolvido era adequado para a administração tópica de ER143, permitindo um elevado controlo da libertação da molécula, o

que contribui para uma elevada retenção da pele. Os resultados obtidos no ensaio de *tape stripping* em pele de leitão, confirmaram os resultados, demostrando que a quantidade de ER143 que atingiu as camadas viáveis da pele é baixa (10.64 %), ficando parte do fármaco retido na camada córnea (22.70 %). No entanto, os estudos *in vivo* demostraram que as formulações desenvolvidas diminuíram o edema e o eritema na orelha do murganho em mais de 92 %. Adicionalmente, foi demostrado que a eficácia das formulações é semelhante à da formulação comercial relativamente aos estudos da actividade anti-inflamatória.

Relativamente ao protector solar desenvolvido e, utilizando o conceito de emulsões de Pickering, foi possível obter uma emulsão estabilizada por filtros solares físicos (dióxido de titânio e oxido de zinco) e grânulos de amido. A melatonina, um poderoso antioxidante que retarda o envelhecimento cutâneo, é uma molécula extremamente instável quando exposta à radiação solar, sendo um desafio a sua estabilização química num protector solar. No entanto, estudos *in vitro* de fotoestabilidade provaram que a tecnologia de emulsões de Pickering permitiu estabilizar quimicamente a melatonina, mantendo-a com as suas características durante a exposição solar. Estudos *in vitro* de determinação do fator de protecção solar (FPS) demonstraram que o amido não possui propriedades intrínsecas de fotoproteção, no entanto, provou ser um promotor do FPS, por efeito sinérgico. Além da excelente protecção solar (FPS 50^{+}) confirmada pela determinação *in vitro,* os resultados *in vivo*, evidenciaram que as formulações finais foram adequadas para aplicação tópica. Todos os resultados revelaram um excelente compromisso entre a estabilidade, proteção contra radiação ultravioleta, eficácia, segurança e cosmeticidade.

Os estudos dos efeitos biológicos (perda de água trans epidérmica, corneometria, sebometria e microcirculação) dos veículos estudados permitiram concluir que estes contribuíram para o aumento da hidratação e da microcirculação. Adicionalmente a avaliação de segurança concluiu que estes veículos são seguros para aplicação tópica nas condições previstas.

No geral, estes resultados evidenciam os veículos à base de amido como promissores para o desenvolvimento de sistemas de libertação tópica, podendo ser utilizados em abordagens terapêuticas inovadoras.

Palavras-chave: Administração tópica; amido; emulsões de Pickering; nanocapsulas de amido; novos veículos; *quality by design.*

List of Figures

Chapter 3

Section 1

Section 2

Chapter 4

Section 1

Chapter 7

List of Tables

Section 2

Chapter 4

Section 1

Section 2

Chapter 5

Chapter 6

Abbreviations & Symbols

AFM	Atomic force microscopy
AIC	Akaike Information Criterion
AM	Amylose
ANOVA	Analysis of variance
AP	Amylopectin
ASt	Aluminum starch octenylsuccinate
ATCC	American type culture collection
ca.	Approximately
Bw	Body weight
CCD	Central Composite Design
CLSM	Confocal laser scanning microscopy
CT	Caprylic/capric triglyceride
CQAs	Critical quality attributes
DDM	Disc diffusion method
DE	Dissolution efficiency
DL	Drug loading
DMSO	Dimethyl sulfoxide
DoE	Design of Experiments
DPH	1,6-diphenyl-1,3,5-hexatriene
DSC	Differential scanning calorimetry
e.g.	For example
ER143	Novel synthetic HNE inhibitor
EE	Encapsulation efficiency
EMA	European Medicines Agency
EP	European Pharmacopoeia
FDA	Food and Drug Administration
FTIR	Fourier transform infrared spectroscopy
GRAS	Generally regarded as safe
G'	Storage modulus
G''	Loss modulus
H&E	Hematoxylin and eosin
HLB	Hydrophilic lipophilic balance
HNE	Human neutrophil elastase
HPLC	High-performance liquid chromatography
HRIPT	Human repeated insult patch test
ICH	International Conference on Harmonization
IC_{50}	Half maximal inhibitory concentration
InstSt	Pregelatinized modified starch
ISO	International Standard Organisation
LD_{50}	Median lethal dose
LP	Liquid paraffin
J	Permeation flux

J_{SS}	Steady-state flux
K	Partition coefficient
K_p	Permeability coefficient
MH	Minocycline hydrochloride
MHASt	Pickering emulsions containing minocycline hydrochloride
MIC	Minimum inhibitory concentration
MoS	Margin of safety
MPF	Monochromatic protection factor
MSC	Model selection criterion
MTT	3-[4,5-dimethylthiazol-2-yl]-2, 5-diphenyltetrazolium bromide
NOAEL	No observed (adverse) effect level
PAR	Proven Acceptable Range
PBS	Phosphate buffer saline
PI	Propidium Iodide
PreG	Pregelatinized starch
QbD	Quality by design
QTPP	Quality target product profile
RH	Relative humidity
ROS	Reactive oxygen species
SC	S*tratum corneum*
SCCS	Scientific Committee on Consumer Safety
SD	Standard deviation
SDS	Sodium dodecyl sulfate
SED	Systemic exposure dose
SEM	Scanning electron microscope
SLS	Sodium lauryl sulfate
SPF	Sun protection factor
StNC	Starch-based nanocapsules
St-BV	Starch-based vehicles
TEM	Transmission electron microscopy
TEWL	Trans-epidermal water loss
TPA	Texture profile analysis
UV	Ultraviolet
VE	Viable epidermis
WRR	Water resistance retention
ZP	Zeta potential
θ	Contact angle

Aims and Organization of the Thesis

The research project leading to this thesis, which began 1st February 2012, integrated the development of innovative starch-based topical systems for the delivery of model drugs and was especially oriented to meet the industrial needs of a pharmaceutical Portuguese company. All the research and scientific work, results from a joint partnership between a Portuguese pharmaceutical company – Laboratórios Atral S.A and the Faculty of Pharmacy of the University of Lisbon, Portugal. The financial support of the entire research project, including the PhD grant, was equally shared by Laboratorios Atral S.A and by Portuguese Foundation for Science and Technology (SFRH/BDE/51599/2011), between February 2012 and January 2016.

The experimental work that supports this thesis was performed at the Departamento de Farmácia Galénica e Tecnologia Farmacêutica of the Faculty of Pharmacy of the University of Lisbon, with the exception of the sun protection factor determination of the Pickering emulsion sunscreen that was performed at Laboratório de Cosmetologia of the Faculty of Pharmacy of the UNESP (São Paulo, Brazil) and, rheological and fluorescence studies that was performed at Faculdade de Ciências e Tecnologia da Universidade de Coimbra, Departamento de Química.

Considering the increase of the complexity and competitiveness of the pharmaceutical market, it is of high importance for all pharmaceutical companies to pursuit the development of innovative pharmaceutical forms and products, in order to guarantee the quality of the products and, consequently, to strengthen the position of the companies in the market. In this sense, Laboratorios Atral S.A needs to be constantly alert to the feedback from consumers, as well as to the market developments in order to detect gaps, new opportunities and/or possible ways of improving their products. Thus, it is very important for Laboratorios Atral S.A to improve their products, as well as to develop new products.

Topical drug delivery is a challenging area, presenting many known advantages, such as avoiding the first passage effect and also a local therapeutic effect. Despite all these

advantages, topical drug delivery remains limited to a narrow range of drugs, since skin act as a barrier in the delivery of many molecules at a therapeutic level. To overcome this obstacle, the most favored strategy is to select suitable vehicles for dermatologic therapy, such as, emulsions, gels and, more recently, nanoparticulate systems. In recent years there has been an increased interest in developing improved delivery systems and, exploring new ways of using approved excipients, such as, starch. Exploring innovative applications for approved excipients with a history of safe use in medicine is a smart strategy to obtain improved medicinal products. Due to its unique properties, starch has been extensively used in various topical pharmaceutical applications.

The current and emerging approaches of optimizing the topical delivery of dermatological agents include the use of chemical enhancers, liposomes, nanoparticulate carriers, iontophoresis, ultrasound, among others. These delivery approaches are a significant improvement over conventional systems (creams, lotions, ointments and pastes) and have the potential to enhance efficacy and tolerability, improve patient compliance, and also fulfill other unmet needs of the topical dermatological market.

Thus, the emphasis of this project relayed on the development and characterization of starch-based vehicles for dermatological application. During the formulation development, the aim was also to develop vehicles that are physically stable, including the minimum number of excipients, and requiring as little energy as possible during their preparation, i.e. by using a cold process.

Additionally, the safety and biological effects of the placebos (product without drug) was assessed by using both *in vitro* and *in vivo* studies, as an adequate equilibrium between the safety and efficacy effects.

The thesis is organized as a collection of chapters, each one in the format of a research article that has been published or submitted for publication. The first chapter is introductory to the work, comprising a book chapter that contains the state-of-the-art. The following chapters have the structure of research articles.

Therefore, this thesis is organized as follows:

Chapter 1 consists on a literature review about the main functions of the skin, a detailed description about the physiology and anatomy of the main barrier for the percutaneous absorption – the *stratum corneum* (SC), as well as the main diffusion routes through the skin. This chapter provides a brief overview of starch historical, structural and chemical background, and its used in the pharmaceutical and cosmetic field. A summary of starch-

based topical vehicles for dermal delivery of model drugs is also given, as well as the role and their effect on the medicine and cosmetic product performance.

Chapter 2 describes the effect of the temperature on the physicochemical properties of five different native types of starch (rice, wheat, potato, corn and pregelatinized starch) and two different modified types of starch. Thus, seven starches were studied by means of differential scanning calorimetry (DSC), hot-stage microscopy and rheology. Starches were also evaluated concerning biocompatibility under *in vitro* conditions. Micropolarity and aggregation of the starch chains were monitored by fluorescence spectroscopic technique.

Chapter 3 describes the pharmaceutical development of Pickering emulsions stabilized by starch granules according to the guideline ICH Q8 (R2). It is divided in two sections:

- In **Section 1** a QbD approach was applied to the development of Pickering emulsions stabilized by starch granules, using a cold emulsification process. Stability studies, mechanical and rheological evaluation, *in vitro* cytotoxicity tests and microbiological studies are presented.

- **Section 2** describes the loading of minocycline hydrochloride into the previously optimized emulsions. Studies include preparation, *in vitro* antibacterial studies, *in vitro* cytotoxicity tests and *in vitro* release and permeation studies, as well as, *in vivo* antibacterial studies.

Chapter 4 describes the pharmaceutical development of starch nanocapsules according to the guideline ICH Q8 (R2). It is divided in two sections:

- In **Section 1** the role of the different factors that affect starch nanocapsule size distribution and zeta potential prepared by the emulsification–solvent evaporation method was assessed using a QbD approach. An optimal formulation was selected and fully characterized in terms of molecular interactions (DSC and FTIR), morphology (TEM and AFM), as well as *in vitro* cell uptake studies.

- ⋆ **Section 2** describes the formula optimization of ER143-loaded starch nanocapsules. This section also presents the releasing profile and skin permeation and penetration of ER143–loaded starch nanocapsules, as well as the *in vivo* anti-inflammatory studies. The formulation optimized was selected to the complete physical characterization.

Chapter 5 describes the safety assessment of starch-based vehicles (Pickering emulsions and starch nanocapsules) as well as its biological effects on human volunteers, as starch-based vehicles have also potential for being marketed as a cosmetic product.

Chapter 6 describes the development of an innovative sunscreen formulation based on Pickering emulsions concept, stabilized by physical UV filters and starch associated to melatonin as a key strategy for prevention against UV-induced skin damage. The formulations were characterized in terms of mechanical, physical and chemical stability by a thorough pharmaceutical control. In addition, the sun protection factor (SPF) and topical delivery were also evaluated, as well as the *in vitro* and *in vivo* biological properties of the final formulations.

Chapter 7 summarizes the highlights of the thesis regarding the experimental results, the impact of the work in the industrial field and near-future perspectives.

1 General Introduction

This page was intentionally left blank

Novel starch-derived topical delivery systems

This chapter was adapted from the *in press* chapter book in:

J Marto, I Jorge, AJ Almeida, HM Ribeiro. Novel starch-based topical delivery systems, in Carrier-Mediated Dermal Delivery: Applications. in: the Prevention and Treatment of Skin Disorders. Ascenso A, *et al*., Editors. 2016. Pan Stanford Publishing. II.1.

This page was intentionally left blank

Graphical Abstract

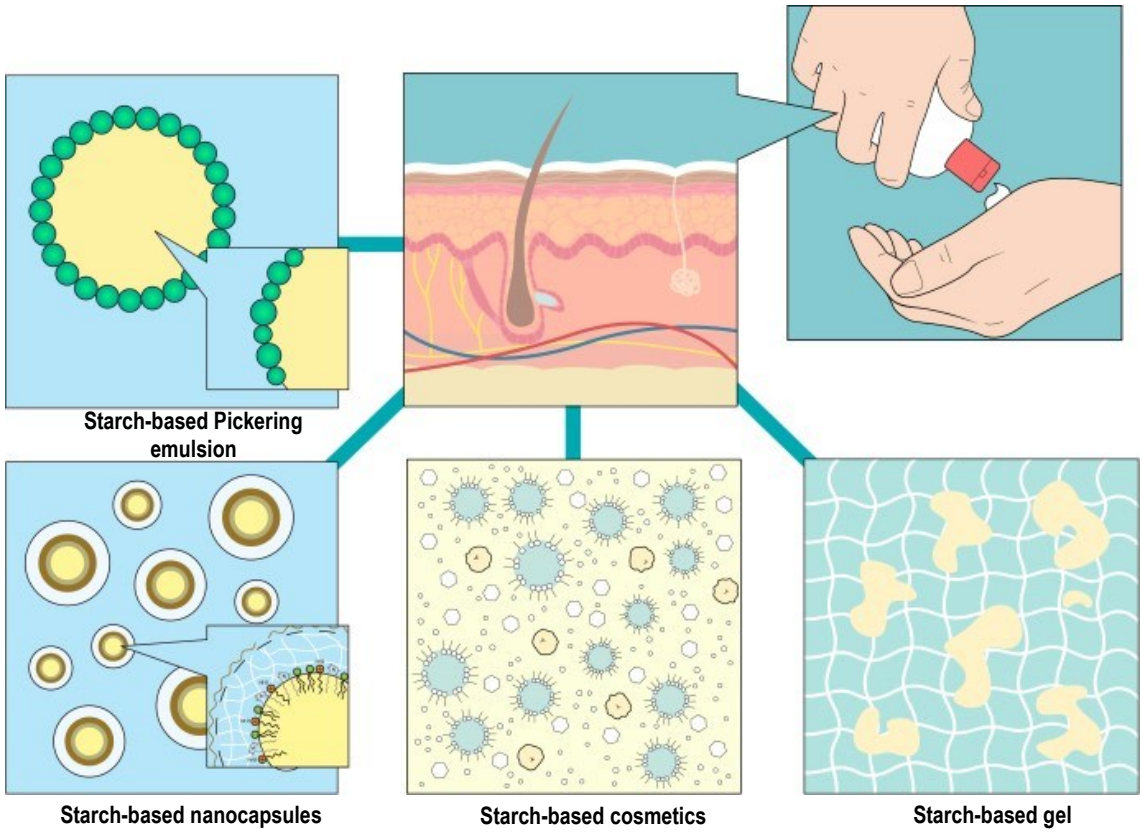

Highlights:

- Starch is a GRAS excipient with endless advantages, that could potentially grant a renewed vision for the pharmaceutical and cosmetic industry.
- Starch has been extensively used in various topical pharmaceutical applications as a sensorial enhancer, stabilizer and drug delivery polymer.
- The improvement of the native starch originates modified starches with better physicochemical properties, allowing its use as a more efficient pharmaceutical and cosmetic excipient.
- Starch-based vehicles as a smart strategy to obtain improved medicinal products.

This page was intentionally left blank

1 Introduction

1.1 Starch: functional characteristics and relevance

In the past decade, the demand for natural and eco-friendly products has been growing. Natural polymers, with emphasis on starch, are a valuable option to comply with this green request, whilst creating products with the desired sensorial attributes.

Starch occurs as an odorless, tasteless, fine, white powder and the chemical formula of its molecule is $(C_6H_{10}O_5)_n$, where n=300-1000 [1]. It is composed by two polymers of *D*-glucose (Fig. 1.1): amylose (AM), an essentially unbranched α[1→4] linked glucan, and amylopectin (AP), which has chains of α[1→4] linked glucoses arranged in a highly branched structure with α[1→6] branching links [2].

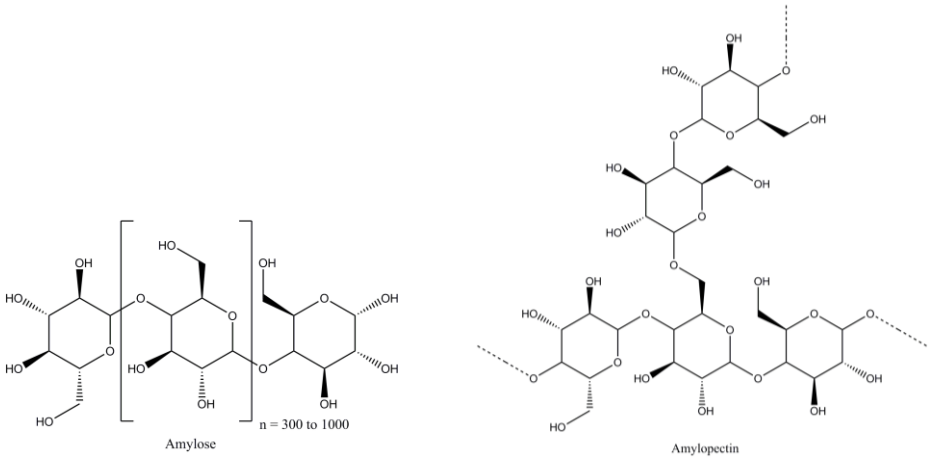

Fig. 1.1 - Structural formula of starch.

AM has a molecular weight of approximately 10^5-10^6 Da and a degree of polymerization (DP) of 324-10000 glucose units [2-4]. Unlike AP, AM has a low degree of branching, which gives AM the tendency to form insoluble semi-crystalline aggregates [2]. It forms helical complexes with iodine, fatty acids and monoglycerides [4, 5]. AP, the major component of all starches, is a much larger molecule with a molecular weight of approximately 10^7-10^9 Da and with a heavily branched structure [4]. The basic organization of the chains is described in terms of the A, B and C chains: the outer A chains are unsubstituted and glycosidically linked at their potential reducing group through C_6 of a glucose residue to an inner B chain; these B chains are in turn defined as chains bearing other chains as branches; the single C chain per molecule likewise carries other chains as branches, but contains the sole reducing terminal residue of glucose [2, 5]. In general, the ratio of AM to AP and their structural variability strongly depend on the

botanical origin. Normal starches contain approximately 70 to 80 % of AP and 20 to 30 % of AM (Fig. 1.2) [5, 6].

Minor components of starch include lipids, proteins and minerals. Starches, in particular cereal starches, contain inner lipids in the form of free fatty acids and lysophospholipids. The minerals found in starch are calcium, magnesium, phosphorus, potassium and sodium [3, 5].

Phosphorus in starch is mainly present in two forms: phosphate monoesters and phospholipids. Phosphate monoesters are covalently bound to the AM fraction of the starch, increasing its paste clarity and viscosity, and phospholipids gives opaque and lower-viscosity pastes [7].

Starch granules range in size (from 1 to 100 μm diameter), shape (polygonal, spherical, ovoid and lenticular) and in content, structure and organization of the AM and AP molecule, accordingly to each botanical variety and growth conditions (Table 1.1) [1-3]. In addition, starch granules usually contain a central line known as the "Maltese cross" or hilum, and this characteristic reduces the birefringence of the starch granules [8].

This variety in form and function gives starch not only advantages but also disavantages as the variableness of the raw material can affect the proper pharmaceutical manufacturing. Modified starches were developed to allow a wider range of processing conditions, and nowadays are extensively used to overcome the variability of the native starches.

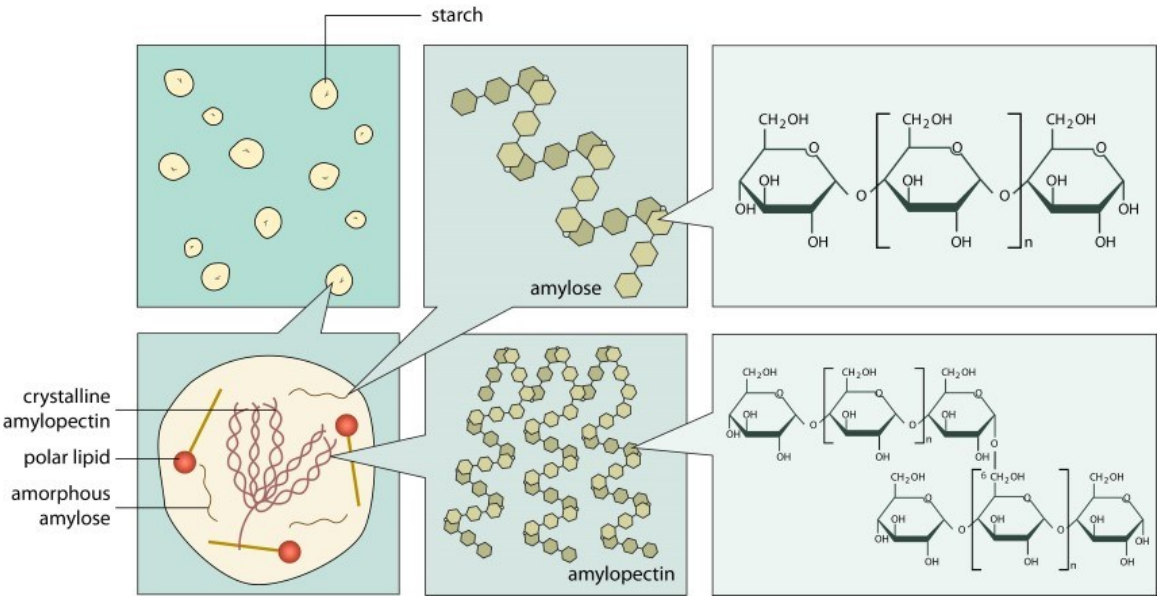

Fig. 1.2 – Starch granules composition [5, 9].

Table 1.1 - Characteristics of starch granules from different botanical sources [3-6, 8, 10-13].

Botanical Origin	Maize	Wheat	Potato	Cassava	Barley	Pea	Oat	Rice	Corn
Type	Cereal	Cereal	Tuber	Root	Cereal	Legume	Cereal	Cereal	Cereal
Granule shape	Round, polygonal	Round, lenticular	Oval, spherical	Oval, truncated	Lenticular, spherical	Oval, rentiform	Polyhedral	Angular, polygonal	Angular
Granule size (µm)	2-30	1-45	5-100	4-35	15-25	5-30	3-10	2-8	11.5±0.3
Phosphate (%, w/w)	0.02	0.06	0.08	0.01	-	-	-	-	-
Protein (%, w/w)	0.35	0.40	0.06	0.1	0.32	-	0.46	0.1	0.4
Lipid (%, w/w)	0.70	0.80	0.05	0.10	0.18	0.30-0.40	0.66	0.6-1.4	0.6-0.8
Amylose content (% total starch)	25-28	25-29	18-21	18-24	21-24	24	22.12	21-25	28.5
Amylopectin content (% total starch)	-	80-90	80-90	-	-	-	-	-	-
Ash (%, w/w)	0.07-0.10	0.16-0.27	0.10-0.33	0.30	0.18	-	0.40	-	-

1.1.1 Modified starch: a strategy to prepare high performance starch

Modified starch has been developed to fulfill pharmaceutical industry needs. Modified starch is an excipient that offers functional advantages such as gelling and thickening.

In general, AM synthesis requires just a single gene, while AP modification involves the combined action of several enzymes. Modification of starch can be achieved by using a derivatization technique, such as etherification, esterification, cross-linking and dual modification of starch; by decomposition or conversion using acid or enzymatic hydrolysis and oxidation of starch; or by physical treatment, using heat or moisture. Chemical modification requires the introduction of functional groups into the starch molecule, resulting in a markedly altered physicochemical characteristics, such as gelatinization, pasting and retrogradation behavior [14].

Three different enzymatic strategies are available to modify starch biosynthesis in plants, in order to obtain starch polymers with innovative functional properties: knocking out biosynthetic enzymes through selection of mutations; pulling down biosynthetic enzyme expression by mutations or by directing antisense RNA against them; or expressing heterologous genes related or unrelated to the biosynthetic pathway [5]. Mutation of the locus that encodes the granule-bound starch synthase (GBSS[1]) creates a starch with no AM. These waxy starches, high in AP gelatinizes easily, yielding clear pastes. On the other hand, high-AM starches are also of great interest as they have a high gelling strength. This phenotype is caused by a mutation in the gene that encodes the starch-branching enzyme (SBE) IIb, which is also known as “amylose extender” [15].

The antisense inhibition of the gene that encodes the α-glucan water dikinase (GWD) (the enzyme which causes the incorporation of phosphate groups into starch) results in a starch that has low phosphate content and viscosity [5, 10].

1.1.2 Starches: from granules to novel applications

Starch is the most abundant storage reserve of carbohydrates in plants. It is found in many different plant organs, including seed, fruits, tubers and roots. This natural material is an edible food substance and is considered as non-toxic and non-irritant. Moreover, starch is also biocompatible, biodegradable and inexpensive [10, 16-18].

[1] The granule-bound starch synthase (GBSS) is the glucosyltransferase specifically responsible for elongating amylose polymers and was the only protein known to be required for its biosynthesis.

Due to these advantages, starch is widely used: in the food industry as an ingredient, emulsifier, gelling, thickener and encapsulating agent; as a source of energy (after its conversion to ethanol); in the paper industry, as adhesive and coating agent; in the textile industry, as printing thickener and a warp sizing agent; and in pharmaceutical industry, where is used as a binder, diluent and disintegrant [1, 2, 17-19]. However, one potential highly attractive application remains to be explored: its use in topical drug delivery systems. In the dermatological area, generic raw materials requirements include skin compatibility and skin protection, efficacy, sensory properties and environmental compatibility [20].

1.2 Skin: the epidermal barrier

The skin is an important part of the integumentary system, as it protects the body from external damage. Skin performs several functions, such as acting as a sensorial organ, promoting the body thermoregulation, allowing the excretion of substances, producing vitamin D (endocrine functions), promoting physical, chemical and immunological defense and protecting against dehydration, UV radiation and external pathogens [21-24].

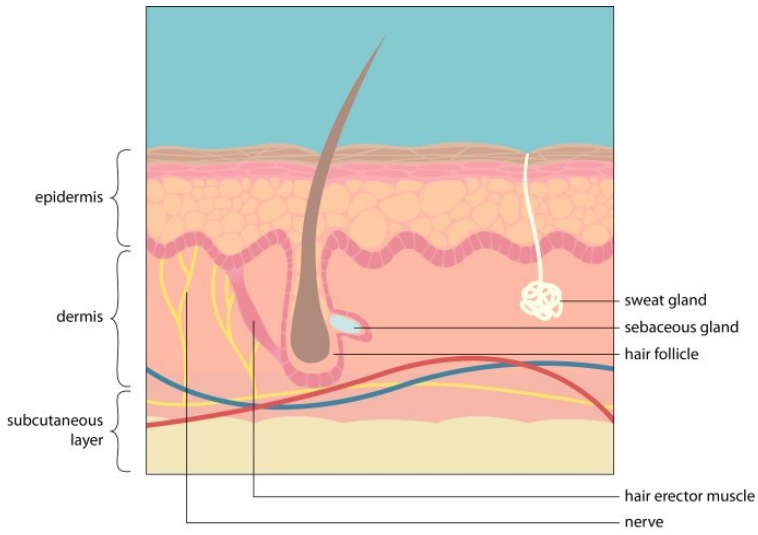

Fig. 1.3 – Skin structure (adapted from [22]).

The skin can be divided in three main layers (Fig. 1.3): *(i)* the more external being the epidermis constituted by keratinocytes, melanocytes, Langerhans cells and Merkel cells, among others; *(ii)* the middle layer, the dermis, which is mainly composed by the fibrillary structural protein collagen and contains capillaries, sebaceous and sweat glands, hair follicles and nerves; and *(iii)* finally, the hypodermis, the most internal layer and

constituted by adipose tissue [22, 24-28]. The epidermis has a multilayer structure consisting of basal, spinous and granular cell layers. Each layer is defined by position, shape, morphology, composition and state of differentiation of keratinocytes. The last stage of the keratinocyte differentiation is associated with deep changes in their structure, resulting in their transformation into physically and chemically resistant squamous cells, called corneocytes – these cells make the uppermost layer of the epidermis, called *stratum corneum* (SC). The SC is the layer that controls absorption, constituting a barrier to the delivery of many molecules at therapeutic level [23, 25, 29, 30].

Stratum corneum properties are based on the special content and composition of its lipids, the structural arrangement of the intercellular lipid matrix and the lipid envelope surrounding the cells in the SC. The lipids form bi-layers surrounding the corneocytes, producing a "brick-and-mortar" model, the bricks, being the corneocytes packed with keratin, and the intercellular lipids acting as the mortar. These intercellular lipids are mainly ceramides and free fatty acids, but also cholesterol, cholesteryl ester and a small fraction of cholesterol sulphate [25, 29, 31, 32].

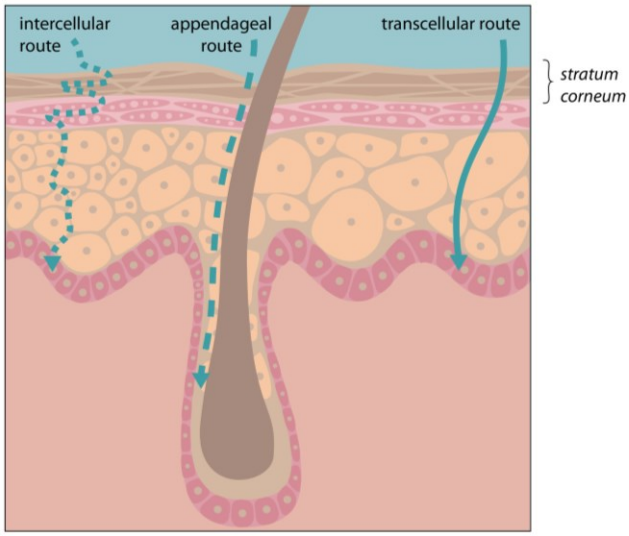

Fig. 1.4 - Possible transport pathways through the *stratum corneum* (adapted from [33]).

Molecules can penetrate into the skin using one of the following ways: intercellular route, transcellular route or appendageal route (Fig. 1.4). The latter is the least significant mechanism since it takes place through the eccrine glands or hair follicles, and since both represent a low surface area (only 0.1% of the total surface area of human skin). Nonetheless, drug delivery by this route may be important for permeation of slowly

diffusing compounds and very high molecular weight substances (nanoparticles, for instance). In the transcellular route, the molecule crosses through the cells. Finally, the intercellular route is the longest pathway, but also the most predominant, in which the molecules passes by the intercellular spaces [21, 25, 27, 30, 32, 34].

As such, drug delivery through skin may pose some difficulties due to its tortuous route, problematic sequential diffusion and partitioning between the polar head groups and the alkyl chains of the intercellular bilayers of lipids [27, 30]. Fig. 1.5 summarizes some strategies to overcome the SC barrier [32, 35-37]. In most cases, an association of multiple strategies is used in order to assure the dermal and/or transdermal drug delivery.

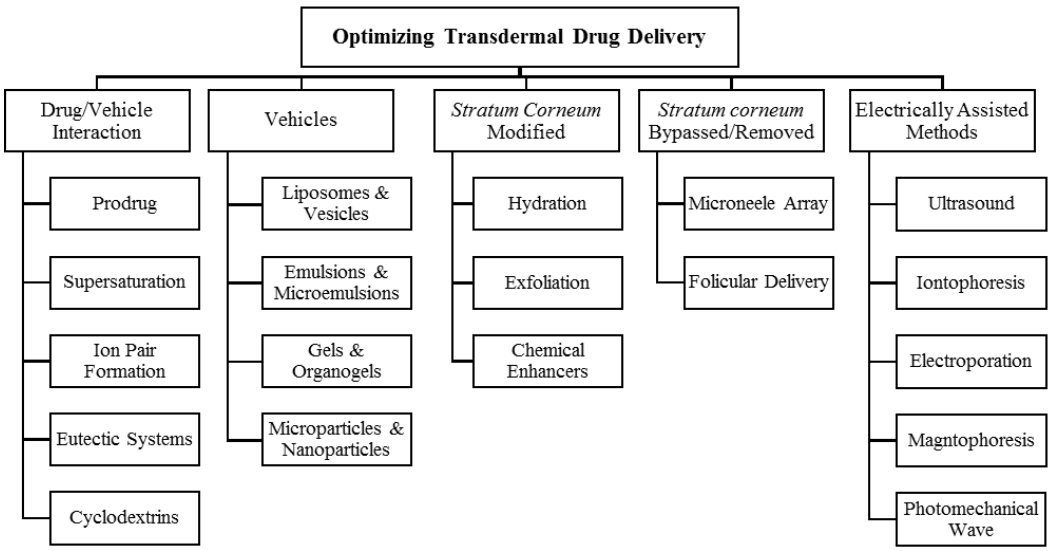

Fig. 1.5 - Some methods for optimizing transdermal drug delivery (adapted from [32, 35-37]).

Other factors, besides penetration mechanisms, can influence the molecular permeation, such as: skin temperature and peripheral circulation (higher temperature increases penetration due to vasodilation), condition of the skin (normal, abraded or diseased), area of application, contact time and frequency of re-application, moisturizing level of the skin, pre-treatment of the skin, physical properties of the penetrating substance (solubility, molecular size, particle size, crystalline form, volatility, polarity, ionization, partition), vehicle and the penetrating substance-vehicle relationship [21, 27, 38].

The permeation flux (J) of a substance through the SC can be described by Fick's first law of diffusion:

Equation 1: $J = \frac{D_m c_{s,m}}{L} \times \frac{c_v}{c_{s,v}}$

In Equation 1, D_m represents the diffusion coefficient of the substance in the skin membrane, $c_{s,m}$ its solubility in the membrane, L the diffusion path length across the skin, c_v the concentration of the substance dissolved in the vehicle and $c_{s,v}$ the solubility of the substance in the vehicle. Therefore, at least three permeation strategies can be postulated based on Fick's first law of diffusion: *(i)* to increase the diffusion coefficient of the drug; *(ii)* to increase the substance partitioning into the skin; and *(iii)* to increase the saturation level of the substance in the vehicle. The first two strategies require an effect of the vehicle on the barrier function of the SC, whereas the last one is based on vehicle-drug interaction [21, 25].

These permeation strategies can be achieved with chemical penetration enhancers acting within the skin. The ideal enhancer should be: non-toxic, non-irritating and non-allergic; appropriate for formulation into diverse topical forms and compatible with other excipients and drugs; and cosmetically acceptable [36, 39, 40].

The diffusion coefficient can be increased by disordering the lipids of the SC. Among the chemical compounds commonly used to achieve this goal are fatty acids, namely oleic acid, azone, a cyclic amide, sulphoxides (e.g. DMSO), terpenes, surfactants and alcohols. These compounds have shown to induce phase separation in the SC lipid domains, creating a lipid disorder and, reducing barrier function, resulting in a reduced diffusional resistance of the skin [25, 30, 35, 40, 41].

Other chemical enhancers act by increasing the substance solubility in the skin, being of special interest in the delivery of hydrophobic drugs. Examples of this type of agents are propylene glycol, ethanol, diethylene glycol monoethyl ether, and *N*-methyl pyrrolidone. These solvents penetrate the SC and change its properties by altering the chemical environment, thus increasing the partitioning of a second substance into the skin [25, 30, 32, 35, 36].

Finally, the saturation level can be enhanced by increasing the substance concentration in the vehicle or by decreasing the solubility of the substance in the vehicle, both resulting in an enhanced thermodynamic activity and in an increased skin permeation [40]. One way to achieve this, can be through supersaturation, where a high chemical potential, however thermodynamically unstable solution is produced [21, 27].

The perfect chemical enhancer has yet to be discovered and the existing ones are often associated with skin irritation, representing a disadvantage [32]. Additionally, synergy and combinations of chemical enhancers may offer some opportunities in transdermal formulations [39].

Another approach to drug dermal delivery of drugs is the use of prodrugs. In this case, chemical modification of the drug facilitates drug permeation, i.e. by addition of a cleavable chemical group for example [39, 42]. From the Fick's first law of diffusion, one can deduce the ideal properties of a penetrating skin molecule: low molecular weight, adequate solubility in oil and water (optimal partition coefficient) and high concentration of the substance in the vehicle [35].

General ointments, creams, lotions, gels and nanoparticulate carriers are the preferred vehicles for dermatological therapy, since they remain *in situ* and deliver the drug over extended periods of time [43].

In addition, to the chemical enhancers and vehicles mentioned above, there are also physical methods for enhancing skin permeation, such as iontophoresis, noncavitational ultrasound, electroporation, cavitation ultrasound, microneedles, thermal ablation and microdermabrasion [43].

The main advantages of topical drug delivery systems are the extended duration of action and, consequently the reduction of dosing frequency. Furthermore, topical drug delivery is useful protection tool for potent drugs as it provides a reduction of systemic adverse effects [44]. Finally, it also allows a reduced drug dose due to the shortened metabolization pathway of the transdermal route *versus* the gastrointestinal pathway, which increases the overall bioavailability of the drug [45].

1.3 Topical delivery systems

Delivery systems for topical drug therapy aim to produce the desired therapeutic effect at specific sites in the epidermal tissue. Many studies have been performed to investigate the effect of topical dosage forms on dermal and transdermal drug delivery. Semisolid formulations, such as creams, gels and lotions, are the preferred pharmaceutical vehicles for topical therapy due to the fact that they remain *in situ* and, in general, provide a extended release of the drug. More recently, nanoparticulate carriers have been recognized as alternative topical delivery systems, due to their small size and larger superficial area which increases skin drug uptake [43].

Starch can be a valuable ingredient when formulating semisolid vehicles. Waxy starches, which are poor in AM, gelatinize easily, producing clear pastes that will not be a gel. Hydrophobic modified starches can be used as a stabilizer and thickener. On the contrary,

starches with high level of phosphate, for instance potato starch, have higher swelling power and stable-paste properties [10].

1.3.1 Conventional topical delivery systems

1.3.1.1 Emulsions

Emulsions are heterogeneous systems composed by two immiscible liquids, one of which is uniformly dispersed as fine droplets throughout the other. These systems are thermodynamically unstable and their study and development is one of the most difficult and complex subjects in the pharmaceutical field [46]. Nevertheless, emulsions, in the form of creams, lotions or foams, are extensively used due to their therapeutic properties and as vehicles to deliver drugs and cosmetic agents through the skin. Furthermore, these dosage forms facilitate drug permeation into and through the skin by their occlusive effects and/or by the incorporation of penetration-enhancing molecules.

Current pharmaceutical emulsions are most commonly stabilized by synthetic surfactants, that can be toxic or may alter the pharmacokinetics of co-administered drugs [47]. Consequently, solid-stabilized emulsions, also called Pickering emulsions[2], may be regarded as an interesting strategy to encapsulate drugs in pharmaceutical formulations [48, 49]. Pickering emulsions are emulsions stabilized by solid particles instead of classic emulsifiers (Fig. 1.6) [50]. Many solid particles can be used in Pickering emulsions and they can be organic, such as polymer latex or starch, or inorganic, such as silica and clay particles [18, 51]. The stabilization of emulsion droplets by solid particles is possible due to their dual wettability. This phenomenon enables the spontaneous accumulation of particles at the oil-water interface and stabilizes it against coalescence by volume exclusion and steric hindrances [17, 52].

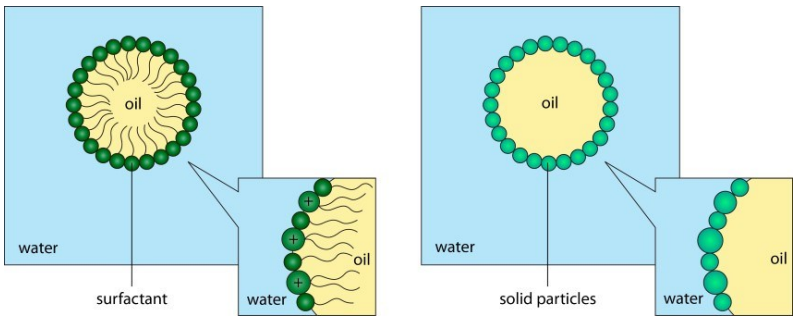

Fig. 1.6 - Surfactant-based emulsion (left) and a Pickering emulsion (right).

[2] This type of emulsion was named after S.U. Pickering, who described the phenomenon in 1907 [50].

In this type of emulsions, one of the liquids will wet the solid particle more than the other, as the poorest wetting liquid becoming the disperse phase. The importance of the wettability of the particles at the oil-water interface is quantified by the contact angle (θ) that the particle makes with it, which in turn will determine the type of emulsion. If θ, measured through the aqueous phase, is smaller than 90º, the emulsion will be o/w and, by contrast, if θ is greater than 90º, the emulsion will be w/o [49, 53, 54].

The effectiveness of the solid in stabilizing emulsions will depend on the particle size, particle shape, particle concentration, particle wettability and on the interactions between particles [17, 53].

Since this type of emulsions is free of emulsifiers, it can avoid some adverse effects often linked to surfactants, like skin irritation, making Pickering emulsions very attractive for many application fields, in particular cosmetic and pharmaceutical [50, 53].

This promising approach has already been studied by some authors (Table 1.2). Wille *et al.* [55] developed an o/w Pickering microemulsion using a vegetable oil mix (hydrogenated cotton seed oil, soybean oil and coconut oil*)*, corn starch, glycerol and cationic surfactants, one of which is benzalkonium chloride (BKC), an antimicrobial agent. The lotion proved itself to form an occlusive barrier to water loss and have a skin moisturizing effect, thus enhancing skin hydration. When submitted to a human repeat insult patch test (HRIPT), the lotion, being hypoallergenic, had no potential for inducing dermal irritation or sensitization. This lotion achieved 6 months stability with good antimicrobial action, where the BKC was slowly release upon skin application. This longer stability when compared to others author's studies is explained by the addition of disteryldimonium chloride (DMDC), a cationic surfactant used as a rheological modifier. This study reinforces the skin compatibility of starch in topical emulsions.

Avoiding chemical surfactants, Marku *et al.* [53] developed an o/w Pickering emulsion, using a octenyl succinic anhydride modified quinoa starch (OSA) and obtained an emulsion with suitable properties for topical application: homogenous white-creamy appearance, high permeability and stability (8 weeks). During the phase studies, it was observed that no stable emulsion was possible to form at oil concentrations superior to 70 % and that, creaming systems were obtained when the oil concentration was inferior to 41 %. The increase in starch to oil ratio gave a lower average droplet size and a narrower droplet size distribution. Regarding the three types of oils studied, caprylic/capric triglycerides (Miglyol® 812) and liquid paraffin (LP) provided creams with similar properties (rheological properties and droplet size), while the sheanut oil (a solid fat)

showed a higher mean droplet size and higher viscosity and yield stress. Texture and cosmetic properties of the creams were evaluated by a small panel of volunteers and, as result, the difference between the liquid oils and the solid fat was seen: Miglyol® 812 and LP creams were assessed as watery and slippery, while sheanut oil cream showed better permeability, but it was thicker, stickier, glossier and left residues on the skin. The *in vitro* skin permeation tests showed a steady state flux of approximately 8.0 μg/(cm^2/h) for all emulsions. When compared to the buffer experiments, where the flux was 4.2 μg/(cm^2/h), it was possible to conclude that the emulsion system increased the permeation into the skin.

The versatility of starch for stabilizing emulsion can be seen in the study performed by Matos *et al.* [17], where OSA was also used in the development of a double w/o/w Pickering emulsion. To the inner water phase was added sodium chloride (NaCl) and the continuous oil phase consisted of Miglyol® 812 and of a lipophilic surfactant: polyglycerol polyricinoleate 90 (PGPR 90). In the outer aqueous phase was added a sodium phosphate buffer, since it has showed to enhance the oil droplets separation. With the addition of PGPR 90, a decreased mean droplet size was possible to obtain and a higher viscosity of the oil phase, which resulted in a less pronounced sedimentation of the inner aqueous phase. This double emulsion showed high encapsulation efficiency (around 98.6 %) and high encapsulation stability (91.1-95.2 % after 3 weeks of study), confirming the high chemical stability of this double Pickering emulsion.

Concerning emulsions, it is possible to conclude that starch is a very versatile excipient. Its use in pharmaceutics can produce nature-friendly products with suitable and interesting cosmetic properties.

Table 1.2 - Pickering emulsions for topical drug delivery.

Type of emulsion	Qualitative and quantitative composition (%, w/w)						Physical characteristics			
	Type of starch	Type of lipid	Drug	Other Excipients	Starch quantity	Lipid quantity	Droplet size distribution (μm)	Viscosity (at 25 °C)	Stability	Ref.
o/w	OSA	Miglyol® 812	-	-	214 mg/ml of oil	56 %	43 ± 3	7.2x10^6 mPa.s	8 weeks	[53]
		LP					48 ± 2	3.0x10^6 mPa.s	8 weeks	
		Sheanut oil					73 ± 17	1.7x10^7 mPa.s	8 weeks	
o/w	Corn	Hydrogenated vegetables oils	BKC	Glycerol, cyclopentasiloxane, DMDC, dimethicone and Citricidal®	3.3 %	8.8 %	0.25 – 5.0	8–10x10^4 mPa.s	6 months	[55]
w/o/w	OSA	Miglyol® 812	-	Phosphate buffer, NaCl, PGPR 90	214 mg/ml of oil	33 %	40 ± 5	-	3 weeks	[17]

o/w – oil in water emulsions; w/o – water in oil emulsions; w/o/w - water-in-oil-in-water (w/o/w) multiple emulsions; OSA - octenyl succinic anhydride modified quinoa starch; Miglyol® 812 - caprylic/capric triglycerides; LP – liquid paraffin; BKC - benzalkonium chloride; DMDC - disteryldimonium chloride; Citricidal® - grape fruit seed extract; PGPR 90 - polyglycerol polyricinoleate 90; NaCl - sodium chloride.

1.3.1.2 Gels

Gels can be defined as a semisolid system consisting of a dispersion made up of either small inorganic particle or large organic molecule enclosing and interpenetrated by liquid, forming a three dimensional interlaced network structure that provides solid-like properties [43, 56]. The European Pharmacopeia (Ph. Eur.) discriminates two types of gels: lipophilic gels (oleogels) and hydrophilic gels (hydrogels) [57].

Gels, as a topical dosage form, have the main advantage of allowing the drug to be absorbed directly at a specific site and avoiding the first-pass metabolism at the liver, offering a great advantage when compared to other delivery systems. Therefore, the therapeutic effects of the drugs are achieved effectively and the systemic side effects are minimized or avoided. Examples of drugs commonly delivered in gels include nonsteroidal antiinflammatory drugs (NSAIDs), antibacterial, antifungal and antihistaminic agents. The drug release from a gel preparation occurs by diffusion of the drug molecules through the gel network or by erosion or dissolution of the gel texture at the interface [58].

The formulation of an effective gel requires the use of an appropriate gelling agent, usually a polymer which can be synthetic (e.g. carbomers or carboxyvinil polymer), semisynthetic (e.g. methylcellulose, carboxymethylcellulose (CMC) or hydroxyethylcellulose) or natural (e.g. gums or starches) [43]. The main characteristics of such polymer include the inertness, safety, biocompatibility with other ingredients, appropriate adhesion to the skin, allowance of drug permeation, irritation-free and biodegradability. When in formulation, the polymer presents swelling and rheological properties suitable for solidifying or stiffening the system [58]. Lately, natural polymers for topical gels have been reported, such as carrageenan, xantham gum, chitosan and several starches.

Starch gelatinization is a process that by dissociation the double-helices and loss of the "Maltese cross" transforms starch from an ordered semicrystalline state to an amorphous one. Starch gelatinization is normally achieved by heating starch above a certain temperature, the "gelatinization temperature" (Table 1.3), in the presence of water or other plasticizers (e.g., glycerol, ethylene glycol, and 1,4-butanediol) (Fig. 1.7), or using alkaline solutions (e.g., sodium hydroxide and potassium hydroxide), neutral salt solutions (e.g., calcium chloride and lithium chloride), and solvents as dimethyl sulfoxide (DMSO) [8, 19, 59]. Wheat starch has the lowest gelatinization temperature, followed by potato, cassava and maize starches. Regular rice starches show a high variation in gelatinization temperature, which can in part be attributed to their high variation of AM content [59]. After gelatinization, the amorphous starch readily absorbs water and develops viscosity to

form a paste. Upon cooling, some starch pastes can create gels. The difference between starch paste and gel lies in that starch paste possesses a certain fluidity, whereas starch gel not, due to its defined shape [60].

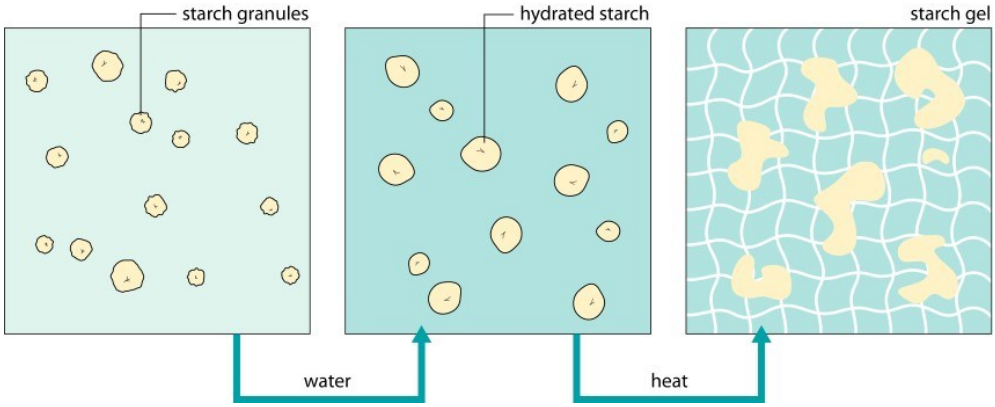

Fig. 1.7 – Mechanism of starch-based gel formation.

Table 1.3 - Gelatinization properties of native starches (adapted from [60]).

Type	To (°C)	Tp (°C)	Tc (°C)	Range (°C)	ΔH (J/g)
Normal Maize	64.1 ± 0.2	69.4 ± 0.1	74.9 ± 0.6	10.8	12.3 ± 0.0
Waxy Maize	64.2 ± 0.2	69.2 ± 0.0	74.2 ± 0.4	10.4	15.4 ± 0.2
Normal Rice	70.3 ± 0.2	76.2 ± 0.0	80.2 ± 0.0	9.9	13.2 ± 0.6
Waxy Rice	56.9 ± 0.3	63.2 ± 0.3	70.3 ± 0.7	13.4	15.4 ± 0.2
Sweet Rice	58.6 ± 0.2	64.7 ± 0.0	71.4 ± 0.5	12.8	13.4 ± 0.6
Wheat	57.1 ± 0.3	61.6 ± 0.2	66.2 ± 0.3	9.1	10.7 ± 0.2
Barley	56.3 ± 0.0	59.5 ± 0.0	62.9 ± 0.1	6.6	10.0 ± 0.3
Mung bean	60.0 ± 0.4	65.3 ± 0.4	71.5 ± 0.4	11.5	11.4 ± 0.5
Chinese taro	67.3 ± 0.1	72.9 ± 0.1	79.8 ± 0.2	12.5	15.0 ± 0.5
Tapioca	64.3 ± 0.1	68.3 ± 0.2	74.4 ± 0.1	10.1	14.7 ± 0.7
Potato	58.2 ± 0.1	62.6 ± 0.1	67.7 ± 0.1	9.5	15.8 ± 0.4
Green leaf canna	59.3 ± 0.3	65.4 ± 0.4	80.3 ± 0.3	21.0	15.5 ± 0.4
Lotus root	60.6 ± 0.0	66.2 ± 0.0	71.1 ± 0.2	10.5	13.5 ± 0.1
Green banana	68.6 ± 0.2	72.0 ± 0.2	76.1 ± 0.4	7.5	17.2 ± 0.1
Water chestnut	58.7 ± 05	70.1 ± 0.1	82.2 ± 0.2	24.1	13.6 ± 0.5

T_o - onset temperature; T_p - peak temperature; T_c - conclusion temperature; range of gelatinization - Tc - To; ΔH - enthalpy change.

Amylose content, relative crystallinity, AP chain length distribution and phosphorus content affect the gelatinization behavior of starches [59, 61, 62]. Short AP chains (DP<14) prevent crystalline order, whereas longer chains (DP>18) produce more stable crystals.

Consequently, increased levels of longer chains shift gelatinization to higher temperatures, whereas short chains decrease the gelatinization temperatures [59, 61]. In potato and cassava starches, it was showed that increased crystallinity and increased AM content resulted in higher ΔH values [61]. Other studies on potato starch showed that at high level of AM content, higher phosphorus content, enhanced re-crystallization of AP during retrogradation of starch gel, associated with a well-formed gel structure and more ordered molecules in the gel, producing a more structured gel [62].

The use of starch gels for topical delivery of pharmaceutical drugs reports back to the 1900s when El-Khordagui *et al.* [63] studied the physicochemical properties of a maize starch gel, using riboflavin as a model drug. A clear gel was obtained with a suitable swelling ability. Riboflavin showed diffusion-controlled release kinetics, influenced mainly by initial loading levels and starch concentration. This was one of the first reported evidence that starch has the ability to produce gels with adequate properties for topical vehiculation of drugs.

More recently, Pal *et al.* [64] formulated a corn starch hydrogel with salicylic acid to protect injured skin and keep the wound surface appropriately moist to increase the healing process. The resulted hydrogel membrane had a tensile strength of 35.92 ± 1.87 mPa, a value similar to the failure strength of skin, meaning that this hydrogel membrane can have a potential application as artificial skin, giving a cushioning effect to the wound. Regarding the drug release, salicylic acid presented a diffusion coefficient through the gel of 4.1×10^{-6} $cm^2 s^{-1}$, delivering the drug directly to the site of action.

Kittipongtana *et al.* [65] on their studies formulated a clear sodium carboxymethyl mung bean starch gel for the topical delivery of ibuprofen, confirmed its clearness by the very low absorption at UV 700 nm ($A < 0.10$). The starch gel presented high viscosity and acceptable spreadability, sticking well onto the skin. The gel was subject to satisfaction evaluation in human volunteers. Statistical analysis showed that the factors significantly affecting satisfaction were the spreading of gel base and the ease of rubbing, as such these properties are the ones to improve, in order to maximize end user satisfaction. The gel also received high score on grittiness and disappearance after applying. Texture and skin irritation were also evaluated through volunteer's opinion. Despite the lack of safety and effectiveness tests, the subjective test performed on volunteers testified for the starch gel satisfactory macroscopic and organoleptic properties.

In another study, Kittipongtana *et al.* [58] prepared a carboxymethyl mung bean starch gel that showed a shear thinning flow with thixotropy behavior, suggesting adequate

spreadability. Concerning the organoleptic characteristics, the gel had a good macroscopic appearance, tackles, greaseless and easily washable. Piroxicam was used as a model drug and a controlled release was observed, however, the amount of piroxicam released was low (< 5 %). In addition, they also tested the stability of the gel production and concluded that it remained stable after 2 months of storage at room temperature.

Nazim *et al.* [66] investigated the use of a potato starch gel as a topical vehicle for rofecoxib, a NSAID, with the purpose to avoid the gastrointestinal disorders often associated with oral administration of these drugs. The physical appearance of the gels was found to be white opaque to white translucent with good homogeneity. By testing different concentrations of potato starch (5-15 %), they concluded that higher concentrations of starch give slightly higher pHs and reduce gel spreadability by increasing viscosity. The rofecoxib release was 16.65 % and 16.39 % for 5 % (w/w) and 10% (w/w) potato starch, respectively. This difference can be attributed to the higher viscosity of gels containing more starch. These formulations were stable up to 24 weeks.

Gabriel *et al.* [67] studied the use of modified *Enset*[3] and cassava starches as gelling agents. Translucent gels with good and smooth homogeneous appearance were obtained, with pH values ranging from 6.8–7.2, within physiologically accepted pH. The formulations with lower starch concentration presented better extrudability and higher spreadability. The release studies conducted using ibuprofen demonstrated that the cumulative percentage of drug released over 12 h ranged from 43.8 % to 84.5 %. The release profiles exhibited a burst effect in the first hour followed by a sustained and controlled release profile. The authors concluded that the nature of the modified starches influenced the rheological properties (spreadability and extrudability) and the release properties (cumulative release and diffusion coefficient). The modified release of the drug can be of valuable advantage, when delivering drugs such as, analgesics or antiinflammatories, providing extended drug action.

Nazim *et al.* [56] conducted another work where a clotrimazole starch gel was developed. This antifungal gel presented good mechanical and macroscopic properties. It was easily washable and had no greasiness. The rheological parameters, with a viscosity of 6.9 x 10^3 mPa.s and a spreadability of 2.6 cm, were suitable for topical application and the pH of

[3] *Ensete ventricosum*, Musaceae is starch-rich staple food widely used in the southern and south-western regions of Ethiopia and closely related to the banana tree, but does not produce banana. *Enset* is often referred as "False Banana" [67].

6.96 assured skin compatibility. *In vitro* drug release was 85 % during 6 h. Stability studies were carried for a period of 3 months according to ICH guidelines and all parameters maintained within the specifications during the period of storage.

As summarized in Table 1.4, it is possible to conclude that a lot of investigation on starch gels has been done and continuous advances on the subject have been achieved. The starch on these gels helps forming a strong and stable matrix due to the AP and AM presence, providing a controlled and sustaining drug release. This slower release, in addition to the starch biocompatibility, is what makes starch gels an attractive delivery system for pharmaceutical industry.

1.3.1.3 Starch in personal care: a multifunctional ingredient

Not only starch is edible, but it has also a huge potential on the creation of innovative and skin-friendly cosmetics. Starch, due to its high derma-compatibility and unique properties, is used in cosmetic products for all skin types and, specially, for sensitive skin.

Personal care starches range from basic unmodified starches for body powders to very specific and innovative starches for gels, films and other unique applications.

Peigen *et al*. [68] proposed to explore new starch resource for cosmetic industry. The plants *Paeonia suffruticosa Andr*., *Paeonia lactiflora Pall*. and *Curcuma phaeocaulis Val*. were explored and the studies indicated different moisture, fat and protein contents, as well as high water binding capacity and clarity, bringing forward high potential application in the cosmetics industry.

Other researchers extracted an innovative and cost-effective native starch from sago. The sago starch, a fine and white powder, was added in perfumed and cool body powders and demonstrated to provide the required physicochemical properties and acceptable levels of specific properties according to Thai Industrial Standards (TIS 443-2525 - Skin Powders properties - *i.e.*, slip, covering power, adhesiveness, absorbency, bloom and spreading power), without causing skin irritation. Sago starch-containing body powders showed good results of users' satisfaction, evidencing to be an excellent ingredient for skin care and one of the best applications to exploit endemic plants [69].

Table 1.4 - Pharmaceutical starch gels for topical delivery.

Starch	Drug	Other excipients	Concentration of starch	pH	Viscosity	Spreadability	Drug Release	Type of Membrane	Kinetic model	Stability	Macroscopic Appearance	*In vivo* studies	Ref.
Maize starch	Riboflavin 0.044 % (w/v)	Sodium Salicylate	10 % (w/v)	-	-	-	28.5±1.7 %	-	Higuchi kinetic D:2.6±0.1 $1x10^{-6}$ cm^2s^{-1}	-	Optically clear gel	-	[63]
Corn starch	Salicylic acid 0.025 % (w/w)	Ethanol, Glutaraldehyde	2.26 % (w/w)	6.37-7.57	Tensile strength of 35.92±1.87 mPa	-	-	Corn starch hydrogel membrane	D: $4.1x10^{-6}$ cm^2s^{-1}	-	-	-	[64]
Sodium carboxymethyl mungbean starch	Ibuprofen 0.5 % (w/w)	Propylene glycol, Denatured alcohol, Triethanolamine	2 % (w/w)	9.0-9.22	High viscosity; 5.1-15.3 mPa.s	Good spreadability on the skin	-	-	-	-	Clear gel	The satisfaction was influenced by the spreadability and the ease of rubbing.	[65]
Carboxymethyl mungbean starch	Piroxicam 0.5 % (w/w)	Propylene glycol, Denatured alcohol, Triethanolamine	3 % (w/w)	9.0-9.2	Shear-thinning fluid with thixotropy behavior; $4.8x10^4$ mPa.s	Good spreadability	5 %	Spectra/Por®7 regenerated cellulose membrane	-	2 months	Clear gel; Tackles, greaseless and easily washable	-	[58]
Potato starch	Rofecoxib 1 % (w/w)	Sodium salicylate 15 % (w/w)	5 – 10 % (w/w)	6.37-6.38	$2.0\ x10^3$-$11.9\ x10^4$ mPa.s	47.14-110 $g.cm.s^{-1}$	16.4–6.6 %	Cellophane membrane	-	6 months	White opaque and good homogeneity	-	[66]
		Sodium benzoate 15 % (w/w)		7.54-7.57	$3.2\ x10^3$ -$22.4\ x10^4$ mPa.s	5.36-82.5 $g.cm.s^{-1}$							
Carboxymethyl cassava starch	Ibuprofen 5 % (w/w)	-	8 – 12 % (w/w)	6.80–6.86	Shear-thinning fluid; 2.9-3.0 $x10^5$ mPa.s	5.4±1.2 – 8.8±1.7 cm	50.6–77.6 %	Cellulose acetate membrane	Higuchi kinetic D: 4.6±0.04 $x10^{-6}$ cm^2s^{-1} to 14.8±0.12 $x10^{-6}$ cm^2s^{-1}	3 months	Translucent gels with good homogeneity	-	[67]
Carboxymethyl *Enset* starch		-	6 – 10 % (w/w)	7.17-7.22			43.8–84.5 %						
Corn starch	Clotrimazole 1% (w/w)	Sodium salicylate 15 % (w/w)	10 % (w/w)	6.0-7.5	6960 mPa.s	2.6 cm	85 %	Cellophane membrane	-	3 months	Opaque in appearance. Good homogeneity, extrudability and gel strength	-	[56]

D - drug diffusion coefficient.

Also, an interesting work of extraction of starch from *Okenia hypogaea*, which belongs to the family of the Nyctaginacea, was performed by Solorza-Feriaa *et al*., and the results obtained suggested that *Okenia* starch could be used as a cosmetic raw material, due to the fact that starches with small size granules have a high adsorbent capacity, making it suitable to regulate the oily and shiny appearance of skin, or could also be used as carriers, because it can adsorb substances such as colorants and perfumes [70].

Modified starches, namely, thermally-inhibited starches are also used in cosmetic compositions, such as skin and hair care products as emulsifier, thickener and aesthetic control agent [71].

In cosmetic industry, starch is used in skin and hair care products where it can substitute the silicone oils. Concerning hair care products, the advantage of starch in this type of product consists in simpler formulation technology and improved care performance with regard to volume of the hair, due to the absence of depot-forming effects, as typical of silicone oils. Albrecht *et al.* [72] formulated a hair shampoo with pregelatinized cross-linked starch derivatives in a concentration of 0.2 % to 10 % (w/w), and concluded that shampoos with starch derivatives can improve the volume, the shine and the after feel of hair.

McCuag [73] also used the unique properties of starch to develop a long life deodorant, using starch treated with *N*-alkanoyl amino acid, as a substitute for talc in a composition, comprising also citric acid. The starch improved the spreadability and the organoleptic characteristics of the product, once it gives a smooth and silky afterfeel.

Starch can also function as an oil control agent, as described by McCook *et al.* [74] when developing formulations for topical treatment for oily skin. Biedermann *et al.* [75] have also referred to this property of starch in their work on skin care products for regulating the oily and shiny appearance of skin.

Formulations containing natural polymer hydrophobically modified starch-based have been studied for their sensory modifier quality. Polonka *et al.* [76] studied a method for making a sensory modifier comprising a polysaccharide carbohydrate rich in AM, such as waxy corn starch or tapioca starch. After treatment with an anhydrous solvent (for example: dipropylene glycol, polyethylene glycol and/or diglycerine), the combined starch and solvent mixture was heated to a temperature from 70 to 80 ºC for 1.5 to 4.5 hours. The sensory modifiers prepared by this method yielded no gelation in a 70 % water formulation and present very desirable sensory benefits. Chorilli *et al*. [77] evaluated the volunteers' acceptance of a sunscreen formulation containing aluminium starch octenylsuccinate,

compared with a control formulation (without polymer), and determined that the sensory modifier starch added to the formulation was able to promote softness and velvet feel to the sunscreen and it was able to mitigate and noticeably reduce the oiliness of the skin. In addition, the starch showed a soft and dry afterfeel, while also improving the spreadability of the product.

Further to these applications of modified starch in cosmetic, Guth *et al.* [78] reported that the addition of 5% aluminium starch octenylsuccinate can enhance sun protection factor (SPF) of a titanium dioxide formulation by 40 % (w/w) [79]. Martino *et al.* [80] described the use of 0.5-30 % (w/w) starch as a sunscreen agent, providing protection against ultraviolet radiation (UV) A and B. The starch can be used alone in these formulations, in mixtures or in combination with other known UVA or UVB filters to provide several SPF values (Fig. 1.8).

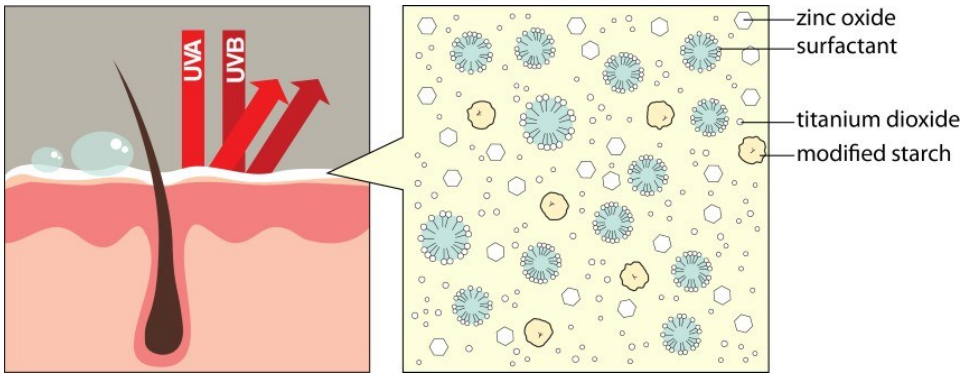

Fig. 1.8 – Mechanism of action of sunscreens/solid particles with UV radiation.

Personal care products have traditionally been sold as semi-solid or liquid dosage forms. These cosmetics normally include a considerable amount of water in the formula. However, due to the water content in cosmetics, the inclusion of lipophilic active ingredients is limited to either the solubilization or emulsification within aqueous phase. As a result, Gott *et al*. [81] described a successful application of a modified starch in another category of cosmetic products. The concept was to develop a multifaceted starch-based solid cosmetic product, especially foamed solids. When immersed in water, the foamed starch rapidly dissolves, releasing the active cosmetic agent or the perfume, which can then deposit or treat human skin or hair.

The same authors proved that a perfume is perceived with greater intensity when added to a modified starch rather than one incorporated into an unmodified type of starch. The selected starch was a destructurized starch, which is generated under certain conditions of

temperature, pressure, shear, limited water and sufficient time. Other authors [82] developed a starch-based porous dissolvable solid substrate in the form of a unit dose personal care product. This cosmetic can be conveniently and quickly dissolved in the palm of the consumer's hand to reconstitute a semi-solid or a liquid cosmetic, for a suitable application on the skin or the hair, respectively, while efficiently deliver lipophilic active ingredients, during consumer usage.

Thus, depending on the application, the level of starch added can range from 1–100%. These results demonstrated that starch is a multifaceted, alternative and eco-friendly ingredient, compatible with a wide variety of other personal care ingredients.

1.3.2 Non-conventional topical delivery systems

1.3.2.1 Polymeric nanoparticles

Polymeric nanoparticles (particle size between 1 and 1000 nm) can be classified as nanospheres or nanocapsules. Nanospheres are solid-core structures and nanocapsules are hollow-core structures, as schematized in Fig. 1.9 [44, 83, 84]. Thus, nanocapsules differ from nanospheres for being a reservoir type of system, while nanospheres are a polymeric matrix system. The core acts as a reservoir for drugs or active substances, or several, which can be dissolved or dispersed. In addition, the core itself can have biological activity or effects (octylmethocinnamate is a UV chemical sunscreen, turmeric oil has antibacterial, antifungal, antioxidant properpies, among others). It is usually composed of triglycerides, an active ingredient, and other chemical substances, such as capric/caprylic triglycerides and sorbitan monostearate or vegetable oils and sorbitan monostearate [85]. On the other hand, surface is directly related to the nature of the polymer, natural or synthetic (ideally non-toxic and biodegradable) and the surfactants used. Usually, synthetic polymers make more reproducible and purer formulations [85-87].

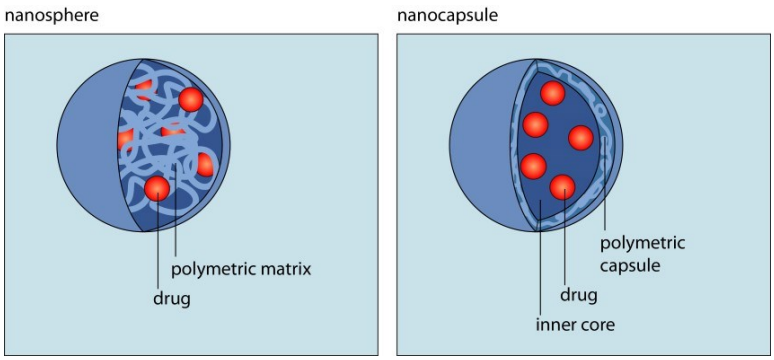

Fig. 1.9 - Schematic representation of nanospheres and nanocapsules (adapted from [88]).

Polymeric nanoparticles can be classified as ionic (anionic or cationic) or non-ionic (presence or absence of charge on their surfaces). The presence of charge can increase the hydration forces at the surface of the nanocapsules, supporting repulsion among the particles in suspension and reducing aggregation. On the other hand, non-ionic nanocapsules have a great physicochemical compatibility with other ingredients of dosage forms [85].

These nanocarriers can be useful as reservoirs or matrixes for lipophilic or hydrophilic drugs, delivering them in the SC. The use of polymeric materials for encapsulating drugs or other active substances is an important approach to cover the physical and chemical intrinsic properties of substances. The skin penetration and transport seem to be largely dependent on the chemical composition of ingredients, encapsulation mechanism (that will influence the drug release mechanism), the nanoparticles' size and formulations' viscosity [85, 89].

The active ingredient in nanocapsules and nanospheres can be incorporated in different patterns: dissolved in the nanosphere matrix, adsorbed at the nanosphere surface, dissolved in the liquid-phase nanocapsules and adsorbed at the nanocapsules surface (Fig. 1.10) [90, 91].

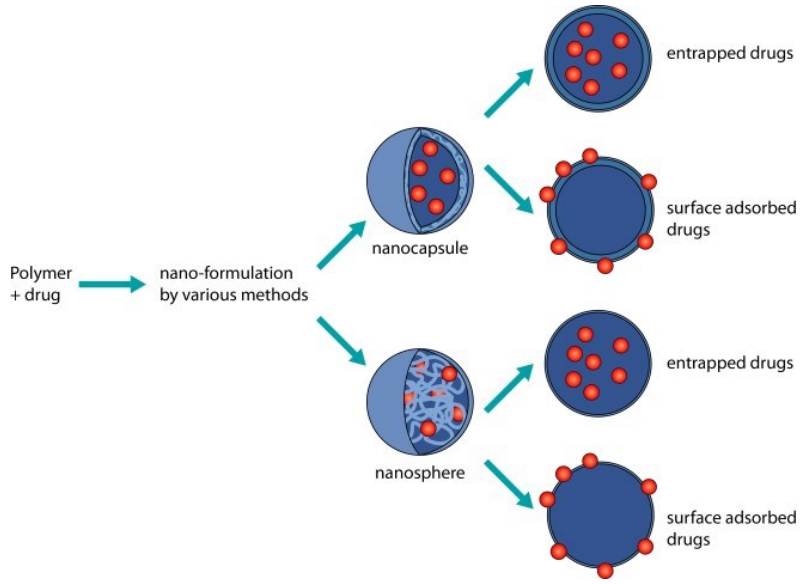

Fig. 1.10 - Different mechanisms of drug incorporation into polymeric nanoparticles (adapted from [84, 88]).

Nanoparticles preparation techniques are based on their physicochemical properties. They are made by emulsification-diffusion by solvent displacement, emulsification-

polymerization, *in situ*-polymerization (interfacial polymerization), gelation (cross-linking), nanoprecipitation (solvent displacement), solvent evaporation/extraction, inverse salting out, dispersion polymerization and other techniques derived from these ones [44, 83]. Drug loading into the nanoparticles can be achieved essentially by two methods: either by incorporating the drug at the time of the nanoparticle production, or by adsorbing the drug after nanoparticle formation, upon incubation in a drug solution. The capacity of adsorption is related to the hydrophobicity of the polymer and the superficial area of the nanoparticles, when comparing the two methods, which it can be possible to conclude that a larger amount of drug can be entrapped using the incorporation method rather than the adsorption one [92].

The advantages and limitations of using nanocarriers arise from their peculiar features: small size, high surface energy, composition, architecture, among others. However, comprehensive characterization, analytical evaluation, toxicological and pharmacological assessment are necessary to determine the efficacy of using these nanostructures as drug delivery systems [83]. Nonetheless, the use of well-known polysaccharides (for example, chitosan, alginate, starch and, so on) as drug vehicles has the additional benefit of the safety, toxicity and availability issues being substantially simplified [93]. Polymeric nanoparticles, for instance, starch nanoparticles, are an excellent option for topical delivery, because they can be tailor-made in different sizes and it is possible to modify surface polarity in order to improve skin penetration [44, 83]. Moreover, nanoparticle carriers made of bioadhesive materials, such as starch, can form an occlusive film and prolong the residence time, increasing the absorbance of the loaded drugs (Fig. 1.11) [93].

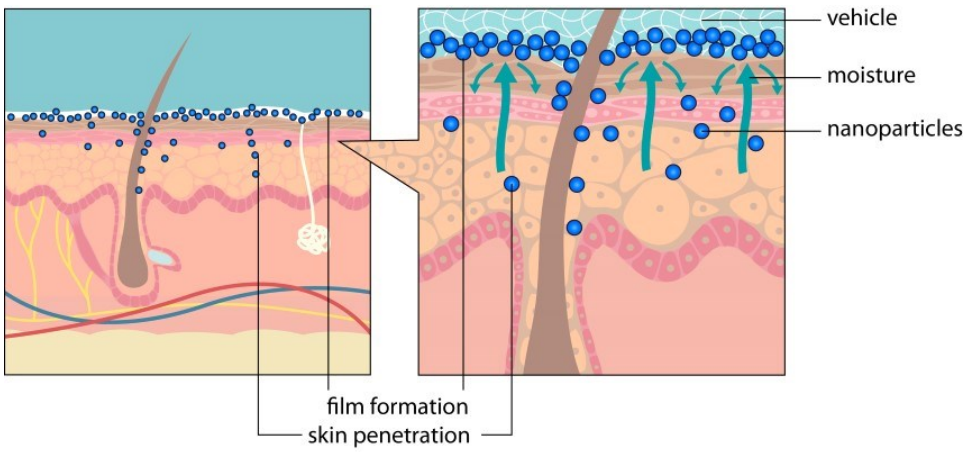

Fig. 1.11 - Film formation associated with the occlusion effect of nanoparticles (adapted from [85]).

Santander-Ortega *et al.* [16] formulated nanocapsules using propyl-maize starch with high degree of substitution. A simple o/w emulsion diffusion technique was used to formulate the nanocapsules, therefore avoiding the use of hazardous solvents. The incorporation of polyvinyl alcohol (PVA) improved the nanocapsule hydrodynamic size distribution and a mono-modal size distribution was obtained. The drug encapsulation did not produce any intelligible change in the spherical shape or soft surface of the nanoparticles and did not alter their original mean size. The encapsulation efficiency was higher than 95 % for flufenamic acid (FFA) and for testosterone and, higher than 80 % for caffeine. Nanocapsules loaded with FFA and with testosterone showed a sustained release without any burst effect and a nearly linear profile in the *in vitro* release tests, while the nanocapsules loaded with caffeine showed a much faster release within the first 10 hours before reaching a *plateau* phase (close to zero release kinetic). This difference in the release patterns might be explained by the more hydrophilic character of the caffeine. The analysis of the drug permeation profiles, using Franz diffusion cells, suggested that for FFA the release from the starch nanoparticles was the rate limiting factor, whereas for caffeine the skin barrier was the rate limiting factor. Regarding testosterone, there was no effect of the nanoencapsulation on skin permeation since very similar permeation profiles were obtained with both, free and encapsulated drug. The high encapsulation efficiency of the nanocapsules in this study is of great importance, when demonstrating the advantages of polymeric starch nanoparticles for topical delivery of drugs.

In different studies, Saboktakin *et al.* [45] used modified carboxymethyl corn starch and hyperbranched 1,4-*cis* polybutadine (1,4-PBD) as novel polymer matrix for transdermal drug delivery systems. The nanospheres showed a solid and consistent structure, with good spherical geometry. They presented a relatively broad size distribution, ranging from 40 to 100 nm. The incorporation of the drug clonidine into the nanospheres produced a smooth surface and compact structure, being the average drug entrapment 92.2 ± 0.1 %. The primary mechanism for release of clonidine from the matrix system *in vitro* is swelling, diffusion and disintegration. In this research, clonidine showed a delayed release, only starting after 2 hours. This delayed release profile reinforces the importance of starch nanoparticles for the drug retention onto the skin, providing a long lasting drug action.

More recently, El-Feky *et al.* [94] investigated the use of native maize starch in the production of nanospheres for the transdermal delivery of indomethacin (IND) and acyclovir (ACV), two poorly soluble drugs. The nanospheres were produced using the nanoprecipitation method and the loaded nanospheres were analyzed and characterized in

what concerns mean particle size, potential zeta, entrapment efficiency and *in vitro* release. For the nanospheres loaded with 20 mg of IND, the mean particle diameter was 32.67 nm and showed a polydispersity index (PDI), an indicator of particle size distribution, 0.519, suggesting some heterogeneity. The zeta potential was -29.1 mV, which is sufficiently high to ensure physical stability, due to the electrostatic repulsion forces, avoiding aggregation. The nanospheres loaded with 50 mg of ACV showed a mean particle diameter of 15.69 nm with a PDI of 0.423. In what concerns to the surface charge, the ACV nanoparticles showed a zeta potential of -35.9 mV, indicating that the prepared nanospheres are stable for a long time. The entrapment efficiency was determined by a spectrophotometric method and was 63.72 % for IND and 74.24 % for ACV, where the smallest spheres are capable of entrapping more drug inside and in the outer sphere, due to the larger surface area. The *in vitro* release of IND showed an initial burst in the first 60 min, releasing 4.65 % of the drug, followed by a more sustained release. On the other hand, in the ACV nanospheres, no initial burst was observed, suggesting that the ACV drug was not weakly adsorbed onto the nanosphere surface.

Finally, an interesting work of encapsulation of a NSAID resulted in suitable and cost-effective cross-linked starch nanospheres, for the transdermal delivery, using diclofenac sodium (DS) as a model drug. The nanocarrier is based on cross-linked starch nanospheres, which were synthesized using native starch. Cross-linking was achieved by reacting sodium tripolyphosphate (STPP) at different concentrations and DS-loaded cross-linked starch nanospheres were synthesized according to the nanoprecipitation method in the presence of Tween® 80, as a surfactant. A two-level factorial design was selected for the prediction of optimized formulation for DS-loaded cross-linked starch nanospheres. The resultant nanospheres were characterized using world-class facilities such as TEM, DLS, FTIR, XRD and DSC. The efficiency of DS loading was also evaluated by entrapment efficiency, as well as *in vitro* release and histopathological study on rat skin. The optimum nanoparticles formulation selected by the JMP® software was the formula that composed of 5 % (w/w) maize starch, 0.058 % (w/w) DS, 0.5 % (w/w) STPP and 0.4 % (w/w) Tween® 80, with particle diameter of about 21.04 nm, PDI of 0.2 and zeta potential of −35.3 mV. It is also worth noting that this selected formula shows an average entrapment efficiency of 95.01 % and sustained DS release up to 6 h. Histophathological studies using the best formula on rat skin advocate the use of designed transdermal DS-loaded cross-linked starch nanospheres as it is safe and non-irritant to rat skin. The authors concluded that the starch nanospheres could be considered a good carrier for DS drug, regarding the

enhancement in its controlled release and successful permeation, thus offering a promising nanoparticulate system for the transdermal delivery of NSAID [95].

The previously referred works are summarized in Table 1.5. Despite nanoparticles for topical drug delivery have many given proofs, starch nanoparticles remained little explored.

Table 1.5 - Nanoparticles for topical drug delivery.

Type of Nanoparticles	Starch	Drug(s)	Other excipient(s)	Encapsulation efficiency (%)	Size (nm)	PDI	Zeta Potential (mV)	Drug Release (%)	Permeation (cm s^{-1})	*In vivo* studies	Ref.
Nanocapsules	Maize starch	FFA	Ethyl acetate 0.1 % (w/w) and PVA 1 % (w/w)	> 95	185.5	0.06	-12.3 ± 1.5	26	3.11 x 10^{-6}	-	[16]
		Testosterone		> 95	176.6	0.43	-12.7 ± 0.6	56	0.43 x 10^{-6}	-	
		Caffeine		> 80	183.3	0.11	-10.3 ± 1.2	75	0.11 x 10^{-6}	-	
Nanospheres	Carboxymethyl corn starch 3 % (w/w)	Clonidine 0.04 % (w/w)	1,4 - PBD	92.2 ± 0.1	40 – 100	-	-	100	-	-	[45]
Nanospheres	Native maize starch 5 % (w/w)	IND 0.02 % (w/w)	Tween® 80 and STPP	63.7	32.67	0.519	-29.1	12	-	-	[94]
		ACV 0.05 % (w/w)		74.2	15.69	0.423	-35.9	11	-	-	
Nanospheres	Native maize starch 5 % (w/w)	DS 0.058 % (w/w)	Tween® 80 0.4% (w/w) and STPP 0.5% (w/w)	95.01	21.04	0.2	-35.3	20 (4 h)	-	The histophathological studies advocate the use of starch nanoparticles as it is safe and non-irritant to rat skin.	[95]

FFA - Flufenamic acid; IND - Indomethacin; ACV - Acyclovir; DS - Diclofenac sodium; PVA - Polyvinyl alcohol; PBD - 1,4-*cis* Polybutadine; Tween® 80 – polysorbate 80; STPP - Sodium tripolyphosphate; PDI - Polydispersity index.

2 Conclusions

Starch properties and advantages as a pharmaceutical excipient are well studied and it is widely used in the technology of oral formulations. Its use in topical formulations is only now emerging, mostly due to the consumers' demand for natural products and to the industry quest for low cost excipients.

In what concerns starch emulsions, formulators went back in time and now are reinventing the Pickering emulsions. At present, none of the commercialized product uses this technology, but some patents have been submitted and some work is yet to be done: increasing the stability and reduced the aging problems of flocculation and coalescence. On the other hand, the use of starch in cosmetics is rising faster with its use in skin care and hair care products, due to starch ability to decrease oiliness, and in sunscreen products, due to the SPF-enhancing power of starch.

So far, starch gels have been the most investigated. Several studies using a model drug have proved their success in topical drug delivery, allied with good organoleptic appearance and skin feeling. The elevated gelatinization temperature of starch remains the limitative factor of these topical systems, requiring more energy in its preparation. In that line, modified starches have been intensively studied since they gelatinize at room temperature and they have great potential to solve this drawback.

Although the nanoparticles are the most recent trend in pharmaceutical technology, starch nanoparticles remain roughly unexplored. This represents a valuable opportunity for research and investment, since they present themselves as the future. The advances in modified starches result in tailor-made excipients, where properties can be shaped and enhanced in order to assure the desired ones. Starch nanoparticles have many advantages, starting with the use of natural and environment-friendly materials, passing through low immunogenicity and ending with modified drug release and better drug permeation.

In addition, there is a lack of comparative studies between different formulations and different pharmaceutical dosage forms, which makes it challenging to understand what are the critical physicochemical factors to study when developing topical delivery systems. Furthermore, it is difficult to correlate each topical delivery system with its efficacy, since there is also a lack of quantitative percutaneous data.

In this review, in the field of topical starch-based delivery systems, no study presented *in vivo* skin permeation studies, neither *in vivo* skin safety studies. Moreover, the scale-up to industry has not yet been carried out, which brings along some difficulties to anticipate

their cost-benefit, thus still remaining a challenge to be overcome by industry and their researchers.

Considering the consumers' demand for more eco-friendly cosmetics, pharmaceutical industry should take that trend into consideration and develop novel starch-based vehicles. Starch's high skin compatibility and recognized property as sensory modifier, both important features when addressing topical vehicles, make it the perfect candidate for novel topical delivery systems.

3 References

1. Rowe RC, Sheskey PJ, Quinn ME. Handbook of Pharmaceutical Excipients. 6 ed. London: Pharmaceutical Press; 2009.

2. Copeland L, Blazek J, Salman H, Tang MC. Form and functionality of starch. Food Hydrocolloids. 2009;23(6):1527-1534.

3. Tester RF, Karkalas J, Qi X. Starch—composition, fine structure and architecture. Journal of Cereal Science. 2004;39(2):151-165.

4. Hoover R, Hughes T, Chung HJ, Liu Q. Composition, molecular structure, properties, and modification of pulse starches: A review. Food Research International. 2010;43(2):399-413.

5. Buléon A, Colonna P, Planchot V, Ball S. Starch granules: structure and biosynthesis. International Journal of Biological Macromolecules. 1998;23(2):85-112.

6. Schirmer M, Höchstötter A, Jekle M, Arendt E, Becker T. Physicochemical and morphological characterization of different starches with variable amylose/amylopectin ratio. Food Hydrocolloids. 2013;32(1):52-63.

7. Singh N, Singh J, Kaur L, Singh Sodhi N, Singh Gill B. Morphological, thermal and rheological properties of starches from different botanical sources. Food Chemistry. 2003;81(2):219-231.

8. Alcázar-Alay SC, Meireles MAA. Physicochemical properties, modifications and applications of starches from different botanical sources. Food Science and Technology (Campinas). 2015;35(2):215-236.

9. Pérez S, Bertoft E. The molecular structures of starch components and their contribution to the architecture of starch granules: A comprehensive review. Starch-Stärke. 2010;62(8):389-420.

10. Jobling S. Improving starch for food and industrial applications. Current Opinion in Plant Biology. 2004;7(2):210-218.

11. Jenkins PJ, Donald AM. The influence of amylose on starch granule structure. International Journal of Biological Macromolecules. 1995;17(6):315-321.

12. Majzoobi M, Saberi B, Farahnaky A, Mesbahi G. Comparison of Physicochemical and Gel Characteristics of Hydroxypropylated Oat and Wheat Starches. International Journal of Food Engineering2014. p. 657.

13. Hoover R, Ratnayake WS. Starch characteristics of black bean, chick pea, lentil, navy bean and pinto bean cultivars grown in Canada. Food Chemistry. 2002;78(4):489-498.

14. Singh J, Kaur L, McCarthy OJ. Factors influencing the physico-chemical, morphological, thermal and rheological properties of some chemically modified starches for food applications—A review. Food Hydrocolloids. 2007;21(1):1-22.

15. Seung D, Soyk S, Coiro M, Maier BA, Eicke S, Zeeman SC. Protein targeting to starch is required for localising granule-bound starch synthase to starch granules and for normal amylose synthesis in arabidopsis. PLoS Biology. 2015;13(2):e1002080-e1002080.

16. Santander-Ortega MJ, Stauner T, Loretz B, Ortega-Vinuesa JL, Bastos-González D, Wenz G, Schaefer UF, Lehr CM. Nanoparticles made from novel starch derivatives for transdermal drug delivery. Journal of Controlled Release. 2010;141(1):85-92.

17. Matos M, Timgren A, Sjöö M, Dejmek P, Rayner M. Preparation and Encapsulation Properties of Double Pickering Emulsions Stabilized by Quinoa Starch Granules. Colloids and Surfaces A: Physicochemical and Engineering Aspects. 2013;423(0):147-153.

18. Timgren A, Rayner M, Sjöö M, Dejmek P. Starch particles for food based Pickering emulsions. Procedia Food Science. 2011;1(0):95-103.

19. Ai Y, Jane J-l. Gelatinization and rheological properties of starch. Starch - Stärke. 2015; 67(3-4):213-224 .

20. Röper H. Renewable Raw Materials in Europe — Industrial Utilisation of Starch and Sugar. Starch - Stärke. 2002;54(3-4):89-99.

21. Hadgraft J. Skin deep. European Journal of Pharmaceutics and Biopharmaceutics. 2004;58(2):291-299.

22. Menon GK. New insights into skin structure: scratching the surface. Advanced Drug Delivery Reviews. 2002;54, Supplement:S3-S17.

23. Prow TW, Grice JE, Lin LL, Faye R, Butler M, Becker W, Wurm EM, Yoong C, Robertson TA, Soyer HP, Roberts MS. Nanoparticles and microparticles for skin drug delivery. Advanced Drug Delivery Reviews. 2011;63(6):470-491.

24. Junqueira LC, Carneiro J. Histologia Básica. 11 ed. Rio de Janeiro: Guanabara Koogan; 2008.

25. Moser K, Kriwet K, Naik A, Kalia YN, Guy RH. Passive skin penetration enhancement and its quantification in vitro. European Journal of Pharmaceutics and Biopharmaceutics. 2001;52(2):103-112.

26. Jungersted JM, Hellgren LI, Jemec GBE, Agner T. Lipids and skin barrier function – a clinical perspective. Contact Dermatitis. 2008;58(5):255-262.

27. Hadgraft J. Skin, the final frontier. International Journal of Pharmaceutics. 2001;224(1–2):1-18.

28. James WD, Berger T, Elston D. Andrews' diseases of the skin: clinical dermatology: Elsevier Health Sciences; 2015.

29. Bouwstra JA, Honeywell-Nguyen PL, Gooris GS, Ponec M. Structure of the skin barrier and its modulation by vesicular formulations. Progress in Lipid Research. 2003;42(1):1-36.

30. Lane ME. Skin penetration enhancers. International Journal of Pharmaceutics. 2013;447(1–2):12-21.

31. Fartasch M. The nature of the epidermal barrier: structural aspects. Advanced Drug Delivery Reviews. 1996;18(3):273-282.

32. Prausnitz MR, Mitragotri S, Langer R. Current Status and Future Potencial of Transdermal Drug Delivery. Nature Reviews Drug Discovery. 2004;3(2):115-124.

33. Williams AC, Barry BW. Penetration enhancers. Advanced Drug Delivery Reviews. 2012;64:128-137.

34. Barrett C. Skin penetration. Journal of the Society of Cosmetic Chemists 1969;20(48):499.

35. Barry BW. Novel mechanisms and devices to enable successful transdermal drug delivery. European Journal of Pharmaceutical Sciences. 2001;14(2):101-114.

36. Williams AC, Barry BW. Penetration Enhancers. Advanced Drug Delivery Reviews. 2012;64, Supplement(0):128-137.

37. Neubert RHH. Potentials of new nanocarriers for dermal and transdermal drug delivery. European Journal of Pharmaceutics and Biopharmaceutics. 2011;77(1):1-2.

38. Barrett CW. Skin penetration. Journal of Society of Cosmetic Chemists. 1968;20:487-499.

39. Prausnitz MR, Langer R. Transdermal drug delivery. Nature Biotechnology. 2008;26(11):1261-1268.

40. Hadgraft J. Passive enhancement strategies in topical and transdermal drug delivery. International Journal of Pharmaceutics. 1999;184(1):1-6.

41. Walker RB, Smith EW. The role of percutaneous penetration enhancers. Advanced Drug Delivery Reviews. 1996;18(3):295-301.

42. Naik A, Kalia YN, Guy RH. Transdermal drug delivery: overcoming the skin's barrier function. Pharmaceutical Science & Technology Today. 2000;3(9):318-326.

43. Raposo SC, Simões SD, Almeida AJ, Ribeiro HM. Advanced systems for glucocorticoids' dermal delivery. Expert Opinion on Drug Delivery. 2013;10(6):857-877.

44. Escobar-Chávez JJ. Nanocarriers for transdermal drug delivery. Skin. 2012;19:22.

45. Saboktakin MR, Akhyari S, Nasirov FA. Synthesis and characterization of modified starch/polybutadiene as novel transdermal drug delivery system. International Journal of Biological Macromolecules. 2014;69(0):442-446.

46. Ribeiro HM, Morais JA, Eccleston GM. Structure and rheology of semisolid o/w creams containing cetyl alcohol/non-ionic surfactant mixed emulsifier and different polymers. International Journal of Cosmetic Science. 2004;26(2):47-59.

47. Bouyer E, Mekhloufi G, Rosilio V, Grossiord J-L, Agnely F. Proteins, polysaccharides, and their complexes used as stabilizers for emulsions: Alternatives to synthetic surfactants in the pharmaceutical field? International Journal of Pharmaceutics. 2012;436(1–2):359-378.

48. Chen J, Vogel R, Werner S, Heinrich G, Clausse D, Dutschk V. Influence of the particle type on the rheological behavior of Pickering emulsions. Colloids and Surfaces A: Physicochemical and Engineering Aspects. 2011;382(1–3):238-245.

49. Binks BP. Particles as surfactants—similarities and differences. Current Opinion in Colloid & Interface Science. 2002;7(1–2):21-41.

50. Chevalier Y, Bolzinger M-A. Emulsions stabilized with solid nanoparticles: Pickering emulsions. Colloids and Surfaces A: Physicochemical and Engineering Aspects. 2013;439(0):23-34.

51. Kaewsaneha C, Tangboriboonrat P, Polpanich D, Eissa M, Elaissari A. Preparation of Janus colloidal particles via Pickering emulsion: An overview. Colloids and Surfaces A: Physicochemical and Engineering Aspects. 2013;439(0):35-42.

52. Fan H, Striolo A. Mechanistic study of droplets coalescence in Pickering emulsions. Soft Matter. 2012;8(37):9533-9538.

53. Marku D, Wahlgren M, Rayner M, Sjöö M, Timgren A. Characterization of starch Pickering emulsions for potential applications in topical formulations. International Journal of Pharmaceutics. 2012;428(1–2):1-7.

54. Schmitt V, Ravaine V. Surface compaction versus stretching in Pickering emulsions stabilised by microgels. Current Opinion in Colloid & Interface Science. 2013;18(6):532-541.

55. Wille JJ. Encapsulation of a biocide in a starch-oil microemulsion lotion: antimicrobial activity and clinical safety of benzalkonium chloride. In: Méndez-Vilas A, editor. Science against microbial pathogens: communicating current research and technological advances: Formatex; 2011.

56. Nazim S, Shaikh S. Formulation and evaluation of clotrimazole hydrotropic starch gel. Indo American Journal of Pharmaceutical Research. 2014;4(2):1181-1186.

57. EP. European Pharmacopoeia 8. Strasbourg: Council Of Europe : European Directorate for the Quality of Medicines and Healthcare; 2014.

58. Kittipongpatana OS, Burapadaja S, Kittipongpatana N. Carboxymethyl Mungbean Starch as a New Pharmaceutical Gelling Agent for Topical Preparation. Drug Development and Industrial Pharmacy. 2009;35(1):34-42.

59. Waterschoot J, Gomand SV, Fierens E, Delcour JA. Production, structure, physicochemical and functional properties of maize, cassava, wheat, potato and rice starches. Starch - Stärke. 2015;67(1-2):14-29.

60. Ai Y, Jane J-l. Gelatinization and rheological properties of starch. Starch - Stärke. 2015;67(3-4):213-224.

61. Gomand SV, Lamberts L, Derde LJ, Goesaert H, Vandeputte GE, Goderis B, Visser RGF, Delcour JA. Structural properties and gelatinisation characteristics of potato and cassava starches and mutants thereof. Food Hydrocolloids. 2010;24(4):307-317.

62. Lu Z-H, Donner E, Yada RY, Liu Q. The synergistic effects of amylose and phosphorus on rheological, thermal and nutritional properties of potato starch and gel. Food Chemistry. 2012;133(4):1214-1221.

63. El-Khordagui LK. Hydrotrope-gelled starch: Study of some physicochemical properties. International Journal of Pharmaceutics. 1991;74(1):25-32.

64. Pal K, Banthia A, Majumdar D. Starch based hydrogel with potential biomedical application as artificial skin. African Journal of Biomedical Research. 2006;9(1).

65. Kittipongpatana OS, Burapadaja S, Kittipongpatana N. Development of Pharmaceutical Gel Base Containing Sodium Carboxymethyl Mungbean Starch. CMU Journal of Natural Sciences 2008;7(1):23-32.

66. Nazim S, Dehghan M, Shaikh S, Shaikh A. Studies on hydrotrope potato starch gel as topical carrier for rofecoxib. Pelagia Research Library. 2011:227-235.

67. Gabriel T, Belete A, Gebre-Mariam T. Preparation and Evaluation of Carboxymethyl Enset and Cassava Starches as Pharmaceutical Gelling Agents. 2013.

68. Xia Y, Gao W, Wang H, Jiang Q, Li X, Huang L, Xiao P. Characterization of tradition Chinese medicine (TCM) starch for potential cosmetics industry application. Starch-Stärke. 2013;65(5-6):367-373.

69. Boonme P, Pichayakorn W, Prapruit P, Boromthanarat S, editors. Application of sago starch in cosmetic formulations. Advances in Sago Research and Development; 2012; Kota Samarahan.

70. Solorza-Feriaa J, Paredes-Lópezb O, Bello-Péreza LA. Isolation and partial characterization of Okenia (Okenia hypogaea) starch. Starch-Stärke. 2002;54:193-197.

71. Jeffcoat RP, J.; Ronco, D. L.; Solarek, D. B.; Hanchett, D. J., inventor National Starch and Chemical Investment Holding Corporation, assignee. Cosmetics Containing Thermally-Inhibited Starches. United States.1999.

72. Albrecht H, Heitmann B, Ruppert S, inventors; Beiersdorf Ag, assignee. Hair shampoo containing pregelatinized, cross-linked starch derivatives. United States. 2007.

73. McCuaig D, inventor Dorothy McCuaig, assignee. Of zinc oxide, citric acid and a starch spreading agent. United States.1997.

74. McCook J, Stephens T, inventors; Mccook John P, Stephens Thomas J, assignee. Topical treatment of acne, seborrheic dermatitis, and oily skin with formulations containing histamine antagonists. United States. 2004.

75. Biedermann KA, Schubert HL, Parran Jr JJ, inventors; The Procter & Gamble Company, assignee. Topical compositions for regulating the oily/shiny appearance of skin. United States.2000.

76. Polonka J, inventor Conopco, Inc., assignee. Sensory modifier. United States.2013.

77. Rigon RB, Piffer AR, Lima AAS, Bighetti AE, Chorilli M. Influence of Natural Polymer Derived from Starch as a Sensory Modifier in Sunscreen Formulations. International Journal of Pharmacy and Pharmaceutical Sciences. 2013;5(1).

78. Guth J, Martino G, Pasapane J, RONC D. Polymeric Approaches to Skin Protection. Cosmetics and Toiletries. 1991;106(12):71-74.

79. Nair B, Yamarik TA. Final report on the safety assessment of aluminum starch octenylsuccinate. International Journal of Toxicology. 2002;21 Suppl 1:1-7.

80. Martino GT, Pasapane J, Nowak FA, inventors; National Starch And Chemical Investment Holding Corporation, assignee. Granular starch as sunscreen agent in aqueous compositions. United States.1993.

81. Gott R, Schmitt W, Sabin R, Londin J, Dobkowski B, Cheney M, Vinski P, Slavtcheff C, Paredes R, inventors; Unilever Home & Personal Care Usa, Division Of Conocpo, Inc., assignee. Fragranced solid cosmetic compositions based on a starch delivery system. United States.2004.

82. Glenn RW, Kaufman KM, Hutchins VTH, Dubois ZG, inventors; The Procter & Gamble Company, assignee. Porous, dissolvable solid substrates and surface resident starch perfume complexes. United States.2013.

83. Escobar-Chávez JJ. Current Technologies to Increase the Transdermal Delivery of Drugs: Bentham Science Publishers; 2010.

84. Kumari A, Yadav SK, Yadav SC. Biodegradable polymeric nanoparticles based drug delivery systems. Colloids and Surfaces B: Biointerfaces. 2010;75(1):1-18.

85. Beck R, Guterres S, Pohlmann A. Nanocosmetics and nanomedicines: new approaches for skin care: Springer; 2011.

86. Patravale V, Mandawgade S. Novel cosmetic delivery systems: an application update. International Journal of Cosmetic Science. 2008;30(1):19-33.

87. Arora N, Agarwal S, Murthy R. Latest Technology Advances in Cosmaceuticals. International Journal of Pharmaceutical Sciences & Drug Research. 2012;4(3).

88. Guterres SS, Alves MP, Pohlmann AR. Polymeric Nanoparticles, Nanospheres and Nanocapsules, for Cutaneous Applications. Drug Target Insights. 2007;2:147-157.

89. Guterres SS, Alves MP, Pohlmann AR. Polymeric nanoparticles, nanospheres and nanocapsules, for cutaneous applications. Drug Target Insights. 2007;2:147.

90. Patravale VB, Mandawgade SD. Novel cosmetic delivery systems: an application update. International Journal of Cosmetic Science. 2008;30(1):19-33.

91. Arora N, Agarwal S, Murthy R. Latest Technology Advances in Cosmaceuticals. International Journal of Pharmaceutical Sciences and Drug Research. 2012;4(3):168-182.

92. Soppimath KS, Aminabhavi TM, Kulkarni AR, Rudzinski WE. Biodegradable polymeric nanoparticles as drug delivery devices. Journal of Controlled Release. 2001;70(1–2):1-20.

93. Liu Z, Jiao Y, Wang Y, Zhou C, Zhang Z. Polysaccharides-based Nanoparticles as Drug Delivery Systems. Advanced Drug Delivery Reviews. 2008;60(15):1650-1662.

94. El-Feky GS, El-Rafie MH, El-Sheikh MA, El-Naggar ME, Hebeish A. Utilization of Crosslinked Starch Nanoparticles as a Carrier for Indomethacin and Acyclovir Drugs. Nanomedicine & Nanotechnology. 2015;6(1).

95. El-Naggar ME, El-Rafie M, El-Sheikh M, El-Feky GS, Hebeish A. Synthesis, characterization, release kinetics and toxicity profile of drug-loaded starch nanoparticles. International Journal of Biological Macromolecules. 2015;81:718-729.

2 Preformulation studies on native and modified starches

This page was intentionally left blank

Graphical Abstract

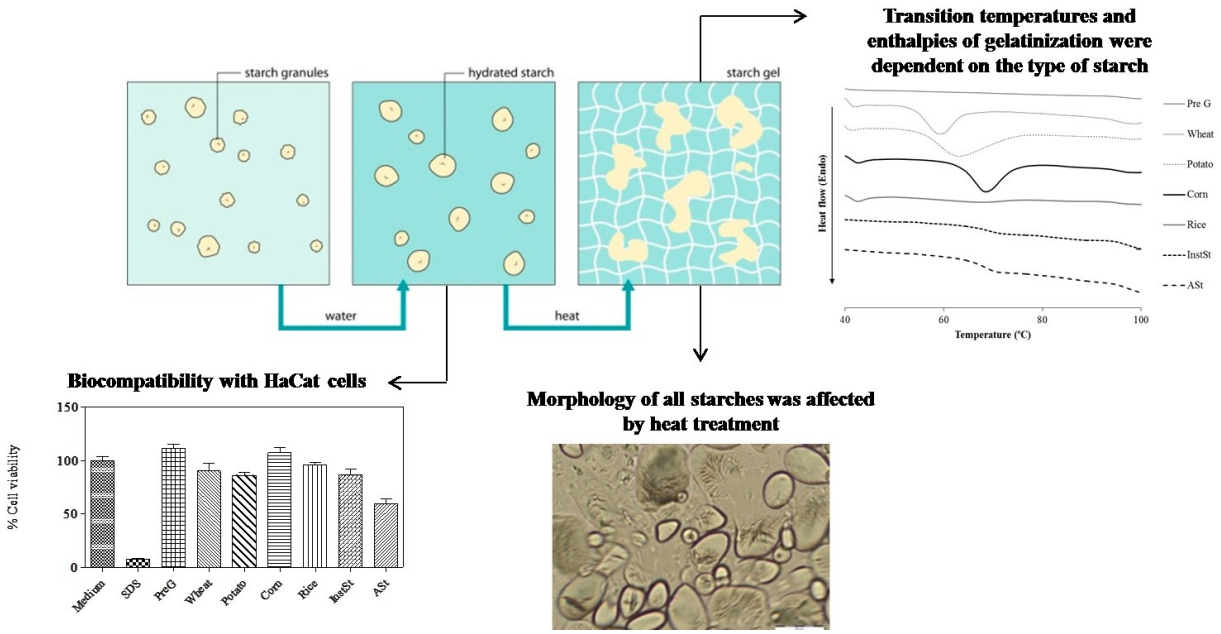

Highlights:

- Native and modified starches are one of the most promising multifunctional material for drug delivery.
- Comprehensive preformulation studies are crucial to understand which starch type is the best for each.
- The results confirmed a high variability dependent to the origin of starch.
- Native and modified starches offer a solution that ideally addresses the needs on pharmaceutical and cosmetic industry.

This page was intentionally left blank

1 Introduction

The pharmaceutical industry is undergoing a period of great transformation as the patents of many medicines expire and are being successfully challenged by generic medicines. This loss is not being automatically compensated by new products. The increased costs to stay ahead of the competition are causing a loss in productivity and a focus on cost reduction [1]. Therefore, scientists and technologists need to develop not only new delivery systems that are substantially better than the existing ones, but also to explore new ways of using old excipients [2]. For that reason, exploring approved excipients can be an easy and safe strategy to obtain improved benefit/risk solutions.

Excipients are the largest components of pharmaceutical formulation. In general, excipients are defined as additives used to convert active pharmaceutical ingredients into pharmaceutical dosage forms suitable for administration to patients. However, excipients no longer maintain the initial concept of inactive support as they are known to influence biopharmaceutical aspects and technological factors [2-4]. In fact, they play a critical role in the preparation of pharmaceutical products, helping to preserve the efficacy, safety and stability of active pharmaceutical ingredients and ensuring that they address the promised benefits to the patients. The ideal excipient is a quest that will never be fully achieved, because what is excellent today may be outmoded tomorrow. Nevertheless, it is indisputable that an optimal use of excipients can provide pharmaceutical manufacturers with cost-savings in drug development, enhanced functionality and advantages in drug formulation innovation [2, 5, 6].

Excipients can be derived from natural sources, be chemically synthesized as well as prepared semi-synthetically, starting from natural sourced materials. Regardless of that, synthetic excipients have become usual in today's pharmaceutical dosage forms [5]. On the other hand, natural excipients still have an important role and application in the pharmaceutical industry, which may be explained not only by the fact that they are biodegradable and non-toxic raw materials of low cost and relative abundance compared to synthetic materials, but also because natural resources are renewable and if cultivated or harvested in a sustainable manner, they can provide a constant supply of raw material. Furthermore, their extensive applications in drug delivery systems are explained by their unique properties, which so far have not been achieved by any other materials [2].

Starch is the second most abundant biomass material in nature and is one of the natural polymers produced by many plants. Starch granules are mainly found in seeds, roots and tubers, as well as in stems, leaves, fruits and even pollen [7-9]. Worldwide, the main

sources of starch are maize, wheat, potatoes, rice and cassava. In 2018, the world starch market is projected to reach a value of $77.4 billion, including native and modified starches. The high value of the output explain the current need for manufacturers and researchers to look for new properties or high value applications [2, 10]. Starch occurs is an odorless and tasteless, soft, fine, white-colored powder comprising very small spherical or ovoid granules whose size may vary from less than 100 nm to a few micrometers, and shape are characteristic for each botanical variety The basic chemical formula of the starch molecule is $(C_6H_{10}O_5)_{300\text{-}1000}$ [7, 10-12]. Starch powder comprise microscopic granules with multi-level structures from macro to molecular scales, i.e. starch granules (< 1 - 100 μm), alternating with amorphous and semi-crystalline shells (growth rings) (100 - 400 nm), crystalline and amorphous lamellae (periodicity) (9 - 10 nm) and macromolecular chains (nm) [7, 13-15].

When starch is used as an extract from a plant, it is called “native starch”. If starch suffers one or more modifications to gain specific properties, it is known as “modified starch”. The structure of starch has been under research for decades, but because of its complexity, a universally accepted model is still lacking [7]. Starch is a polysaccharide comprising glucose monomers bind by α-1,4 linkages. The simplest form of starch is the linear polymer amylose (AM) and amylopectin (AP) is the branched form.

The major aim of this study is to find novel uses for starch to obtain improved medicinal products. However, previous to the development of any novel starch-based drug delivery system, preformulation investigations are needed to identify those physicochemical properties of starches that may influence the formulation design, method of manufacture, and biopharmaceutical properties of the resulting product. For this purpose, preformulation studies were performed to evaluate the effects of temperature on the physicochemical properties of five different native types of starch (rice, wheat, potato, corn and pre-gelatinized starch) and two modified starches using differential scanning calorimetry (DSC), hot-stage microscopy and rheological experiments, with both large strain (rotational) tests at different shear rates and small strain (oscillatory) tests. The results obtained confirm the suitability of starch as a drug delivery agent and its potential for use in innovative applications in the pharmaceutical and cosmetic industries.

2 Material and methods

2.1 Materials

The different starches used in this work were aluminum starch octenylsuccinate (ASt) (DryFlo® Plus) purchased from AkzoNobel (Amsterdam, Netherlands), Pregelatinized modified starch (Instant Pure-Cote® B793) (InstSt) was a gift from Grain Processing Corporation's (Muscatine, USA), rice starch, wheat starch, corn starch, potato starch and pregelatinized starch (Pre G) were a kind gift from Laboratórios Atral, S.A. (Castanheira do Ribatejo, Portugal). The oils used were liquid paraffin (LP) purchased from Mosselman (Ghlin, Belgium) and caprylic/capric acid triglyceride (Tegosoft® CT) (CT) a kind gift from Evonik Industries AG (Essen, Germany). Purified water was obtained by reverse osmosis and electrodeionization (Millipore, Elix 3) being afterwards filtered (pore 0.22 μm).

2.2 Methods

2.2.1 Starch granules characterization

2.2.1.1 Morphology of starch granules

The morphology of starch granules was studied using a light microscope (Olympus BX51, Japan) with 10-100x objectives with normal and polarized light (UANT, Olympus). The system was equipped with a 1280×960 resolution camera (Olympus XC30, Japan) and with the software Olympus Stream Essentials®, version 1.8.

2.2.1.2 Wettability measurements

The measurement of the contact angle of water, liquid paraffin (LP) and caprylic/capric acid triglyceride (CT) on starches in air was performed at room temperature using ConAnXL - a Microsoft Excel based workbook and Add-in software. Starches solid surfaces were prepared by compressing suitable amounts of starch under a pressure of 10 metric tons using a KBr Press Model MP-15. A drop of the liquid was then carefully deposited onto the solid surface with a micropipette. The contact angle was defined as the angle between the starch surface and the tangent to the surface of the drop. All the measurements were performed in triplicate (n=3).

2.2.2 Sample preparation

Aqueous suspensions of different starches (ASt, InstSt, rice, wheat, potato, corn and Pre G) were prepared by adding 5% of dry polymer to water. Due to the long hydration times, suspensions were kept stirring for 24 hours before use.

2.2.3 Structure analysis of starch aqueous solutions

2.2.3.1 Rheological studies

The rheological properties of the solutions were examined at high shear rates using rotational shear tests and in the viscoelastic region using oscillation tests. The rheological measurements were conducted on a Reologica® Stresstech (ATS RheoSystems, USA) stress controlled rheometer equipped with automatic gap setting. A bob cup measurement system (CC 15) with a solvent trap was used to test all samples. The temperature control was achieved using a water bath system. All experiments based on a temperature ramp were performed from 30 to 90 °C at a fixed heating rate of 1 °C/min. A number of viscosity measurements were conducted in steady-state conditions. Prior to this, a viscometry test was carried out in order to determine both Newtonian and non-Newtonian regimes. Dynamic or shear viscosity was analyzed by rotational shear experiments. Oscillation tests were performed to determine the storage modulus, G′, and loss modulus, G″. A test of linearity, the oscillation stress sweep, was used to obtain the values of shear stress for which the viscoelastic functions are independent from the magnitude of the applied stress. The applied frequency was chosen ensuring that, at the initial conditions, G″ is dominant.

2.2.3.2 Thermoanalytical measurements and hot stage microscopy

Thermoanalytical measurements were performed with a TA Instrument DSC Q200 system (TA Instruments, New Castle, USA). The sample and the reference (air) were placed in hermetically sealed pans. A scan speed of 10 °C/min and 10-20 mg of sample (aqueous solution of each starch) gave the best compromise between resolution, temperature, accuracy and attenuation.

A light microscope (Olympus BX51, Japan) equipped with a THMS350V (Linkam, Surrey, England) hot stage was used to visualize the behavior of the emulsions under stress conditions. Contact thermal microscopy was conducted by heating the samples from 30 to 90 °C using heating rate of 1 °C/min. All samples were tested one day after preparation and stored at room temperature.

2.2.3.3 Steady state fluorescence measurements

The samples were prepared *in situ* by adding 30 µl of the pyrene and 1,6-diphenyl-1,3,5-hexatriene (DPH) solution to 3 ml of 5 % starch suspensions.

The fluorescence spectra were recorded with a Horiba–Jobin–Ivon Fluorolog 3-22 spectrometer and were corrected for the instrumental response of the system. The steady state fluorescence anisotropies as a function of temperature were measured using Glan-Thompson polarizers for recording the fluorescence spectra with vertical-vertical (I_{vv}) and vertical-horizontal (I_{vh}) orientation of the excitation and emission polarizers. The anisotropy values were calculated with Equation 1 [16].

Equation 1: $$\langle r \rangle = \frac{I_{vv} - GI_{vh}}{I_{vv} + 2GI_{vh}}$$

where the grating factor G is G=I_{hv}/I_{hh}.

The samples were equilibrated for at least 5-10 min at each temperature before the measurements.

2.2.4 Biocompatibility assay

2.2.4.1 Cell culture conditions

Spontaneously immortalized human keratinocyte cell line, HaCaT, (CLS, Germany) were grown in RPMI-1640® (Gibco, UK) medium supplemented with 10 % (w/v) fetal bovine serum (FCS, Life Technologies. Inc., UK), penicillin (100 IU/ml) and streptomycin (100 µg/ml) in a humidified 95 % O_2, 5 % CO_2 environment at 37 °C. For the subculture, cells growing as monolayer were detached from the tissue flasks by treatment with 0.05 % (w/v) trypsin/EDTA (Invitrogen, UK). The viability and cell count were monitored routinely using Trypan blue dye exclusion method [17].

2.2.4.2 Biocompatibility assay

The biocompatibility of starch polymers was quantitatively evaluated *in vitro* using general cell viability endpoint MTT reduction (3-(4,5-dimethyl-2-thiazolyl)-2,5-diphenyl- 2H-tetrazolium bromide) [1,2] and propidium iodide (PI) dye exclusion assays [3]. MTT is a yellow and water-soluble tetrazolium dye that is converted by viable cells to a water-insoluble, purple formazan. PI is a red fluorescent probe, which is a cell membrane impermeant and, therefore, does not allow the entrance the dye into viable cells and only enters compromised cells. When PI gains access to nucleic acids, and intercalates them, the

fluorescence increases dramatically and is used to identify the presence of compromised cells.

Cell viability was assessed after 48h of incubation of HaCat with 2 mg/ml concentration of starch particles. The day before experiment, HaCaT were seeded in sterile flat bottom 96 well tissue culture plates (Griner, Germany) in RPMI-1640® culture medium, supplemented with 10 % fetal serum bovine, 100 units of penicillin G (sodium salt), 100 µg of streptomycin sulfate and 2mM L-glutamine, at a cell density of 2 x 10^5 cells/ml. Cells were incubating at 37 ºC and 5 % CO_2. On the next day, medium was replaced by fresh medium containing the different samples to be analyzed and each concentration was tested in five wells per plate. The negative control was the culture medium and positive control sodium dodecyl sulfate (SDS) at 0.1 mg/ml. After the time of exposition, medium was replace by 0.3 mM PI in culture medium (Stock solution 1.5 mM in DMSO, diluted with culture medium 1:5000). Fluorescence was measured (excitation, 485 nm; emission, 590 nm) in Microplate Reader (FLUOstar Omega, BMGLabtech, Germany), and then, the MTT assay was performed. The culture medium was replaced by medium containing 0.5 mg/ml MTT. The cells were further incubated for 3h. In the plates containing reduced MTT, the media was removed and the intracellular formazan crystals were solubilized and extracted with dimethylsulfoxide (DMSO). After 15 min at room temperature the absorbance was measured at 570 nm in the same microplate reader.

The relative cell viability (%) compared to control cells was calculated by the following equations:

$$\text{Equation 2: Cell viability (\%) for the MTT assay} = \frac{[Absorvance_{\,570\,nm}]sample}{[Absorvance_{\,570\,nm}]\,control} \times 100$$

$$\text{Equation 3: PI ratio} = \frac{[Fluorescence]sample}{[Fluorescence]control}$$

One-way analysis of variance (ANOVA) and Tukey–Kramer post-hoc multiple comparison test were used to identify the significant differences between the groups and were performed using GraphPad PRISM® 5 software. An alfa error of 5% was chosen to set the significance level.

3 Results and discussion

Seven aqueous suspensions of different starches (ASt, InstSt, rice, wheat, potato, corn and PreG) were fully characterized in terms of morphology, molecular interactions, mechanical properties and, as well as *in vitro* biocompatibility properties. Two distinctive modified

starches (ASt and InstSt) were compared to five pharmacopeia starches with well-established physicochemical properties.

3.1 Starch granules

3.1.1 Particle size measurements and morphology of starch granules

Starch consists of two glucose polymers: AM and AP, which are components of the starch granule. The relative proportion and structural differences between amylose and amylopectin, as well as the botanical source of the starch, contribute to the significant differences in starch characteristics and properties. However, physical, chemical and enzymatic starch modification may alter several aspects, such as, its texture, viscosity, stability, transparency and film-forming properties.

In this section, the size and morphology of starch granules were evaluated by optical microscopy. Table 2.1 gathers data pertaining the morphology of native and modified starch granules. They were different from each other in size and shape. Among the native starches, the particle size of rice starch was smallest among the tested samples. The size of potato starch granules was larger than PreG, wheat and corn starch. PreG, rice and corn starch were spherical and polygonal in shape and wheat and potato starch had both oval and spherical shapes. InstSt and ASt granules are irregular polygonal shaped, but the last one exhibits smooth edges. Additionally, polarized light micrographs of starches showed for PreG, wheat, potato, corn, rice and ASt a positive birefringence, suggesting a crystalline structure of starch granules.

Particularly, rice starch due to its fine particle size (7-9 μm) exhibits extraordinary soft-touch. The large surface area permits a fine distribution of both functional and active ingredients and also ensures effective delivery to the skin. This inherent fineness provides an extraordinary increase in the surface area, resulting in extraordinary adsorption and absorption characteristics. Starch granules in their native or modified form can exhibit birefringence that is proportional to their crystalline structure. Birefringence patterns in starch granules represent the radial arrangement of AP molecules. Loss of birefringence in starch granules is associated with deformation, due to its modification [18]. Due to the strong crystalline structure of potato starch and semi–crystalline structure of Pre G, wheat, corn, rice and ASt starches, the granules do not solubilize in water at room temperature, which is an advantage for the emulsions stabilized by solid particles, as well as, for improved spreading, pleasant and silky-soft touch properties of topical systems. In natural antiperspirant agents, insoluble starches adsorb perspiration released by the skin. The pores

are not blocked because the particles do not swell on the skin, with an advantage that there is no whitening effect of the product applied on the skin.

Specifically, ASt is a hydrophobically modified natural polymer. Due to its birefringence and, consequently insolubility in both aqueous and anhydrous excipients, ASt mitigate the apparent oiliness of formulations, leaving a soft, dry and matte finish on the skin, functioning as an absorbent, an anticaking agent and a viscosity increasing agent [19]. Furthermore, due to the small size of ASt and its hydrophobicity, the granules can be effective stabilizers of emulsions [20].

On the other hand, InstSt is an amorphous pregelatinized modified starch (Table 2.1). So, the most distinctive property of InstSt is the ability to form a cold gel. This starch provides products with suitable viscosity without the need of high temperatures, which means that the pharmaceutical and cosmetic industries do not need to pre-treat the starch. Due to its excellent and promising characteristics, InstSt can be used in a wide variety of applications where film-forming properties are desired for coatings, barriers, texture modification, binding or adhesives. It can be used also to replace other polymers such as hydroxypropyl methylcellulose, hydroxypropyl cellulose, gums, gelatin, among others.

Table 2.1 - Optical micrographs of native and modified starch granules and characteristics of starch granules from different botanical sources [7, 9, 18, 21-26].

		Starch						
		Pre G	Wheat	Potato	Corn	Rice	InstSt	ASt
Microscopic aspect	Bright-field	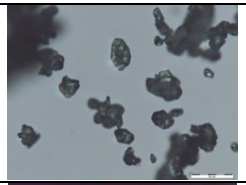	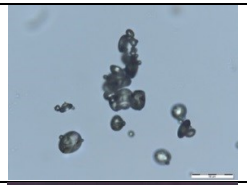		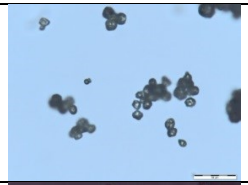	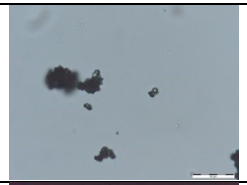		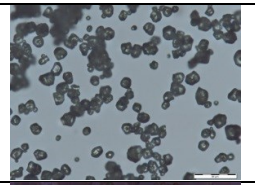
	Polarized light	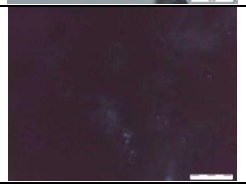	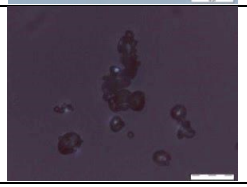	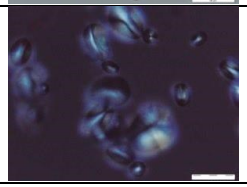	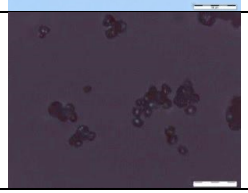	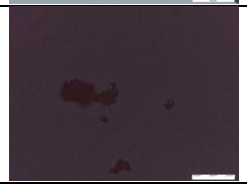	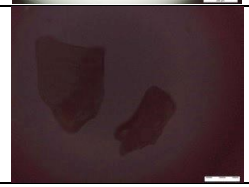	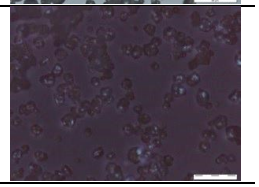
Type		-	Cereal	Tuber	Cereal	Cereal	-	Cereal
Granule shape		-	Round, lenticular	Oval, spherical	Angular	Angular, polygonal	-	Angular
Granule size (μm)		~ 65	1-45	5-100	3-100	2-8	-	
Phosphate (%, w/w)		-	0.06	0.08	-	-	-	-
Protein (%, w/w)		-	0.4	0.06	0.4	0.1	0.35	-
Lipid (%, w/w)		-	0.80	0.05	0.6-0.8	0.6-1.4	-	-
Amylose content (% total starch)		~ 27	25-29	18-21	26-28.5	21-25	-	>40
Amylopectin content (% total starch)		~ 73	80-90	80-90	-	-	-	-
Ash (%, w/w)		-	0.16-0.27	0.10-0.33	0.11	-	<0.5	<0.7

3.1.2 Wettability measurements

Wettability is a useful parameter to provide information on surface properties of starch granules. The wettability of a solid surface can be determined by measuring the contact angle. In addition, affinity of starch towards water and other excipients seems to be an important parameter determining its physical, chemical and several functional properties.

Table 2.2 shows the contact angle of water, liquid paraffin and caprylic/capric acid triglyceride on different starches. All kinds of standard starches present the contact angle of water and of both types of oil lower than 90°, empathizing their hydrophilicity. The contact angle of water on ASt was higher than 90°, while contact angle of both types of oil was lower than 90°, showing ASt is hydrophobic. In this case, the presence of aluminum octenylsuccinate ensures the hydrophobic properties of ASt. This modification affects drastically the starch performance, being suitable for w/o Pickering emulsions stabilization and it may be also used to adsorb excess oil from the skin. The wettability properties of solid particles determine the type of emulsion (o/w or w/o). Water-wet particles tend to stabilize o/w emulsions whereas oil-wet particles tend to stabilize w/o emulsions. To adsorb at interface, particles need to be partly wetted by both phases [20]. Concerning this evidence, ASt is the only type of starch that presents capability to stabilize Pickering emulsions due to its dual wettability properties.

On the other hand, it should be noticed that native and modified hydrophilic starches are widely used in pharmaceutical technology to formulate hydrogel-based controlled release delivery systems. The porous structure of the starch gel allows drugs to be loaded within the gel network, thus providing a controlled drug release from the hydrogel network [27].

Table 2.2 - Contact angle of water, liquid paraffin and caprylic/capric acid triglycerides with starches (mean ± SD, n=6).

Starch	Contact Angle (θ °)		
	Water	Liquid paraffin	Caprylic/capric acid triglyceride
Pre G	29.1 ± 4.7	14.2 ± 1.7	16.1 ± 0.7
Wheat	28.2 ± 3.4	17.1 ± 2.0	18.3 ± 0.8
Potato	31.4 ± 0.1	15.2 ± 2.3	17.8 ± 4.6
Corn	31.9 ± 3.5	16.1 ± 1.1	16.7 ± 1.8
Rice	27.6 ± 1.2	15.5 ± 0.7	16.8 ± 0.9
InstSt	52.3 ± 3.0	13.7 ± 0.6	15.1 ± 2.0
ASt	109.0 ± 0.4	15.8 ± 1.1	16.5 ± 0.1

3.2 Structure analysis of starch aqueous solutions

3.2.1 Dynamic and oscillation measurements

Rotational shear experiments measure the ability of each system to resist to structural deformation during the standardized shearing procedure. For all starches suspensions, the viscosity started to increase at temperatures between 60 and 75 °C (Fig. 2.1 (a)). The increasing viscosity of starches dispersions during heating was attributed to the swelling of the starch granules, mainly regarding the volume fraction and morphology, which is supported by DSC and hot stage microscopy data.

Oscillatory measurements can be used to study the structure of a material, in which the deformation during the oscillation has to be kept small. An important point is to check whether measurements are made in the linear viscoelastic regime, otherwise the results of the frequency experiments will depend not only on the frequency but also on the applied stress or deformation. The viscoelasticity of heated starch dispersions was found to be strongly dependent on the type of starch. For wheat, corn, potato and rice starch, G'' is much higher than G', meaning a dominant viscous behavior (Fig. 2.1 (b and c)). The G’ and G’’ increased upon heating, probably due to the onset gelatinization of the polymer. As expected, for Pre G, during the heating, the G’ decreased and the G’’ increased due to the previous treatment (Table 2.3).

These results confirm that the native starches are essentially insoluble in cold water. To improve its functional properties and increase their versatility in different processing conditions, starches can be physically gelatinized to make them cold water-soluble, or chemically modified to enhance their viscosity and gelling profiles, which is the case of InstSt. Nevertheless, InstSt exhibits low viscosity in solution, which is appropriate to prepare starch nanoparticles, since the size of nanoparticles depends on polymer concentration and viscosity in solution [28]. According to some authors, AP contributes to swelling and pasting of starch granules, while AM and lipids, on the contrary, inhibit the swelling of starch granules [28]. In addition, phosphorus is one of the non-carbohydrate components present in the starch granules that affects its functional properties. Monoester phosphates are associated with the amylopectin fraction by covalent bonds, increasing the clarity and viscosity of the paste, whereas the presence of phospholipids results in opaque and low viscosity pastes. It has been reported that concentration, volume fraction of the swollen granules and the deformability of the granules influence the viscosity of starch gelatinization during heating [29].

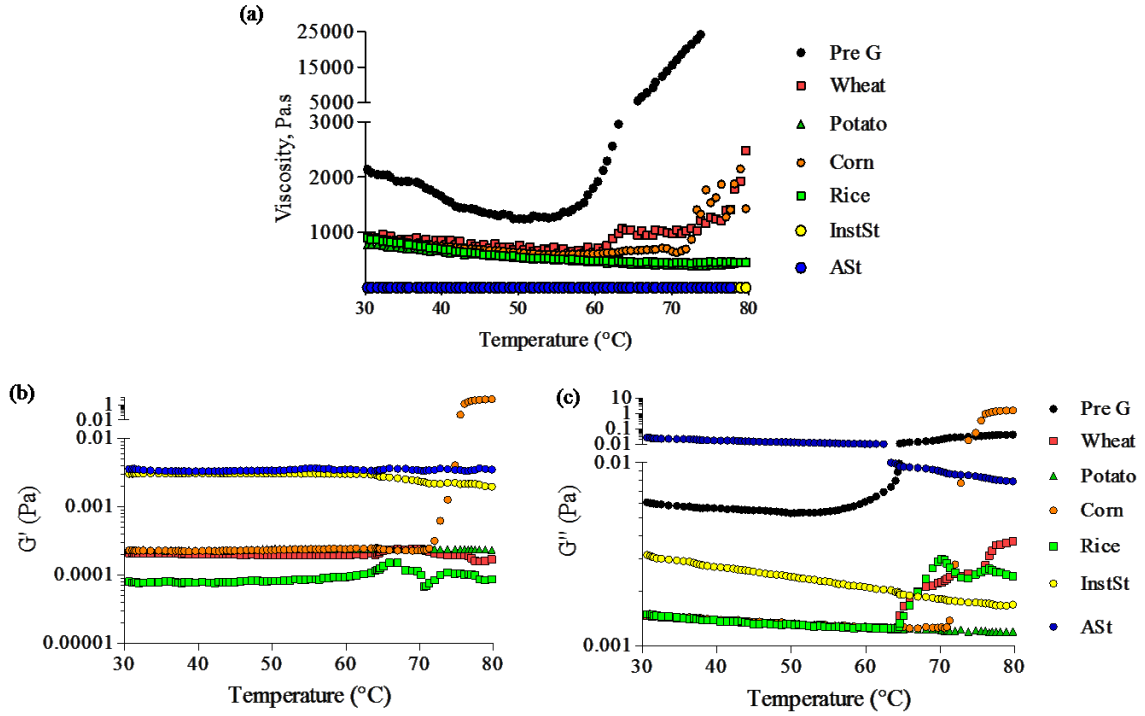

Fig. 2.1 - (a) Viscosity of different starches at different temperatures. (b) Dependence of storage (G') and (c) loss (G'') moduli for different starches at different temperatures.

Table 2.3 - Storage modulus (G') and loss modulus (G'') as a function of the temperature, for different starches.

Starch	Temperature (˚C)					
	40 ˚C		60 ˚C		80 ˚C	
	G'	G''	G'	G''	G'	G''
Pre G	3.04×10^{-3}	6.29×10^{-3}	2.33×10^{-3}	2.12×10^{-3}	1.96×10^{-3}	4.00×10^{-2}
Wheat	1.98×10^{-4}	1.25×10^{-3}	2.42×10^{-4}	2.23×10^{-3}	1.70×10^{-4}	4.09×10^{-3}
Potato	2.40×10^{-4}	1.26×10^{-3}	2.38×10^{-4}	1.22×10^{-3}	2.35×10^{-4}	1.19×10^{-3}
Corn	2.39×10^{-4}	1.28×10^{-3}	2.29×10^{-4}	1.27×10^{-3}	5.58	1.72
Rice	9.30×10^{-5}	1.32×10^{-3}	1.00×10^{-4}	2.98×10^{-3}	8.60×10^{-5}	2.37×10^{-3}
InstSt	3.04×10^{-3}	2.08×10^{-3}	2.33×10^{-3}	1.81×10^{-3}	1.96×10^{-3}	1.66×10^{-3}
ASt	3.51×10^{-3}	1.00×10^{-2}	3.38×10^{-3}	1.00×10^{-2}	3.50×10^{-3}	1.00×10^{-2}

3.2.2 Thermoanalytical measurements and hot stage microscopy

DSC technique can detect changes in heat flow associated with first-order transitions (melting) and second-order transitions (glass transition) of polymers. When heated in the presence of water excess, starch granules suffer an irreversible transition known as gelatinization, which represent the melting of starch crystallites. Briefly, starch granules swell, absorb water and lose the crystalline structure [30].

The gelatinization of starch is an endothermic process, meaning that it can be measured using DSC. Wheat, potato, corn, rice and ASt starch showed single endothermic peaks

between 60 °C and 80 °C and the transition temperatures and enthalpies of gelatinization were found dependent on the type of starch (Fig. 2.2). This phenomenon can be explained by the fact that during heating, the semi-crystalline structure of starch is broken and water molecules associate by hydrogen bonding to hydroxyl groups exposed on the AM and AP molecules. This association causes swelling and increases granule size and solubility [31].
On the other hand, PreG and InstSt showed no DSC peaks because they are non-crystalline materials, whereas some native starches present crystalline material (Table 2.1).
As can be seen in Table 2.4, an increase in the temperature from 25 to 70ºC caused the swelling and morphology alteration of the seven types of starch granules. It was observed that the granules gelatinized at different temperatures. Additionally, the light microscopy images revealed that the morphology of all starches was affected by heat treatment.
Finally, the results obtained confirmed the previous findings obtained from the rheological studies.

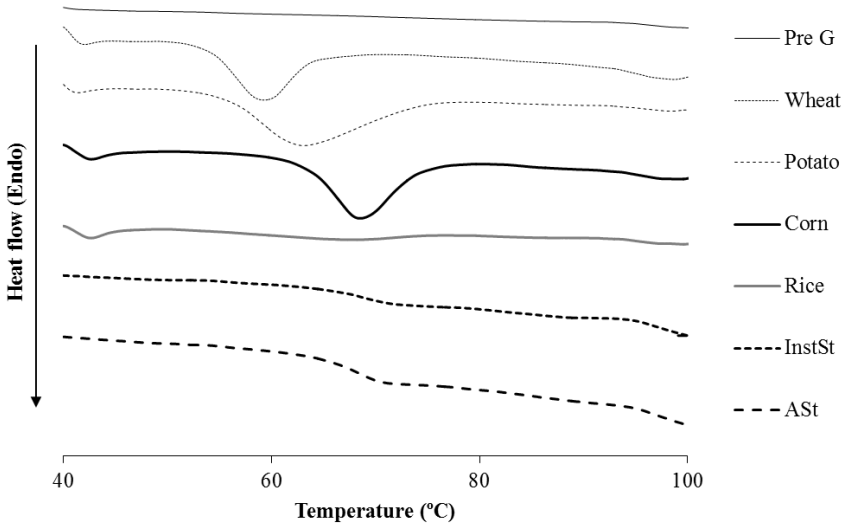

Fig. 2.2 – DSC scanning thermograms of different starches.

Table 2.4 - Micrographs of different starches at different temperatures (25 and 70 °C) during the heating process (Scale bar = 50 μm).

Starch	Temperature (°C)	
	25 °C	70 °C
PreG		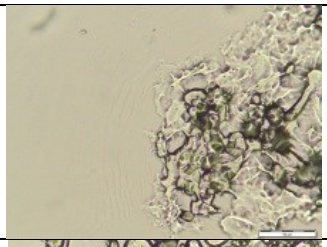
Wheat	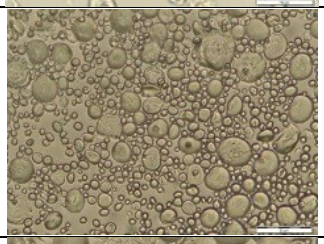	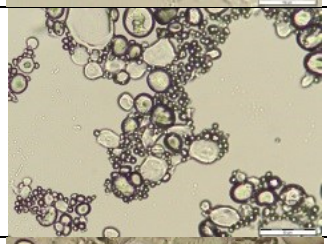
Potato	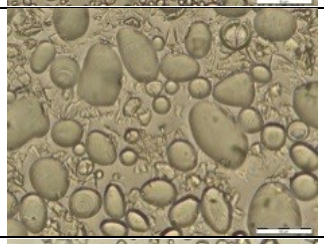	
Corn	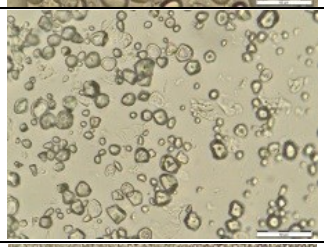	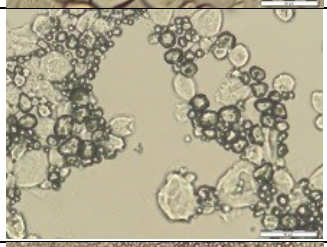
Rice	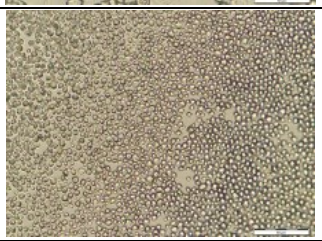	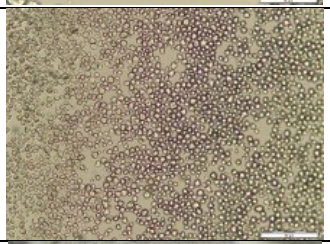
InstSt		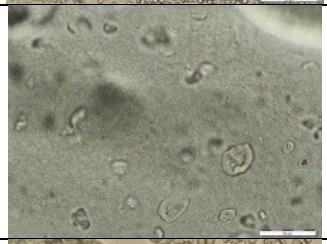
ASt		

3.2.3 Steady state fluorescence measurements

Fluorescence techniques have shown to be very valuable for monitoring changes in fluidity (microviscosity) upon an external stimulus such as temperature [16]. Thus to further investigate the phase transition temperature range for the different starch derivatives, steady-state fluorescence emission measurements were performed using (i) 1,6-diphenyl-1,3,5-hexatriene (DPH) and (ii) pyrene as environment sensitive probes. One of the best known fluorescence microviscosity probes is DPH [16, 32]. In this case phase transitions can be identified from the behavior of the fluorescence depolarization of DPH as a function of temperature. The extent of the fluorescence depolarization reflects the degree to which a population of photoselected excited chromophores loses its initial selective orientation and becomes randomized. From this, we can obtain information on the molecular motions, which depend on the size and the shape of the probe molecules and on the fluidity of their microenvironment. The steady-state fluorescence emission anisotropies for DPH in the different starch solutions were collected as a function of temperature. The anisotropy values at the maximum emission wavelength (in the 420-430 nm range) were plotted as a function of temperature, see Fig. 2.3. With exception of rice, potato and ASt, where no significant changes were seen in the DPH anisotropy values in the 30-90 ºC range, for corn, wheat, PreG and InstSt a significant change in the anisotropy values was found with the increase of viscosity (gelatinization) of these moieties (Fig. 2.3), which corroborates the dynamic and oscillation results. From Fig. 2.3 it can be seen that for the latter starch derivatives the gelatinization process started in the 55-80 ºC temperature range. It is also worth noting that while for wheat and PreG the DPH anisotropy values increase concomitantly with the increase of viscosity, for corn and InstSt opposite behavior was found, thus showing that the DPH fluorescence emission in these moieties is less polarized. Another approach to detect the phase transition associated with the gelatinization process of the starch derivatives involved the pyrene ability to form intermolecular excimers by association of an excited pyrene molecule with an unexcited molecule of the same species. Within this framework the excimer is characterized by the appearance of a broad structureless emission, red-shifted from the monomer emission. Birks *et al.* [33] have shown that the formation of intramolecular excimers is a diffusion controlled process in a variety of solvents and therefore, viscosity and concentration dependent. Changes in the fluidity of a medium can thus be monitored through the variation of the ratio of the excimer-to-monomer bands (I_E/I_M) of pyrene with the temperature. The fluorescence emission spectra for pyrene containing solutions of the starch derivatives were investigated

as a function of temperature. However, only for the derivatives InstSt and ASt the plots of $\ln(I_E/I_M)$ vs the reciprocal of the temperature yielded the characteristic Steven-Ban plots (Fig. 2.4) [34]. In these plots the maxima of the parabola, where the excimer-to-monomer ratio reaches its maximum, indicates the transition between the low- (LTL) and high-temperature (HTL) regimes [35]. For InstSt and ASt the excimer-to-monomer maximum values point out to a transition phase occurring in the 60-75 ºC range (Fig. 2.4), thus in agreement with the results previously found for the starch derivatives.

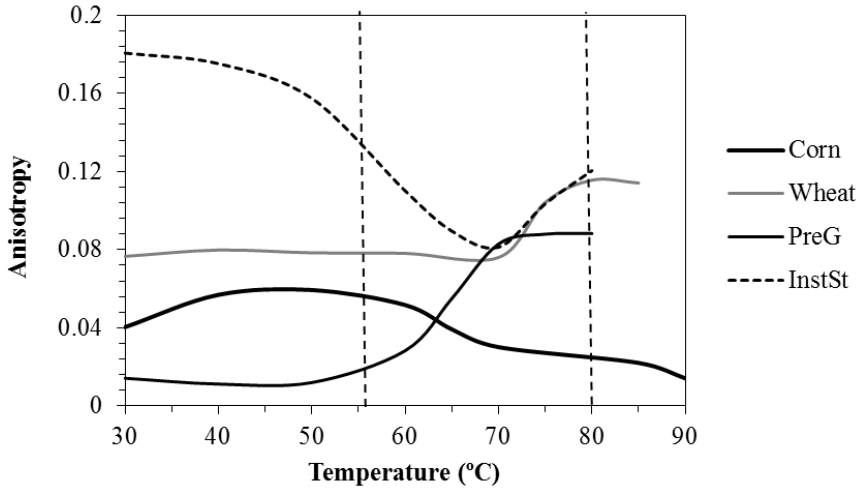

Fig. 2.3- Steady-state fluorescence emission anisotropy values for 1,6-diphenyl-1,3,5-hexatriene (DPH) in the starch aqueous solutions collected as a function of temperature.

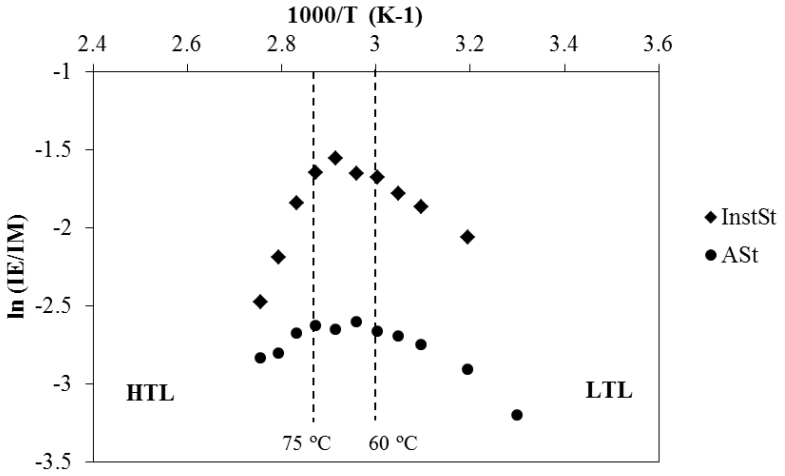

Fig. 2.4 - Arrhenius plots for the excimer-to-monomer intensity ratio (I_E/I_M) of pyrene in aqueous solutions of the starch derivatives InstSt and ASt.

3.3 Biocompatibility assay

The measurements were planned to obtain insight into the biocompatibility of starches, when they were exploited in the pharmaceutical and cosmetic application field. Consequently, the *in vitro* cytotoxicity of starches was investigated using HaCaT cell line to determine the biocompatibility. Human keratinocytes, which are affected first by drugs or actives components, are recognized to be involved in a multiplicity of inflammatory and immune responses of the skin. Hence, HaCat should be a more suitable cell model for evaluating sensitivity of the skin to potential irritants [36].

The cell viability of HaCaT cells incubated with different starches was assessed using the MTT assay. After 48 h, no significant cytotoxicity effect was observed after incubation with different starches, which demonstrated that the starches were extremely biocompatible and reliable for additional bioacceptability *in vivo* assessments. Nonetheless, ASt caused a decrease in cell viability of 62.4 ± 8.7 % (Fig. 2.5). The possible toxic effects of a substance are intensely related to its concentration and biochemical surroundings, which must be carefully studied before pharmaceutical or cosmetic use. However, ASt is safe if used in cosmetic formulations at concentrations lower than/up to 30 % [19].

Propidium iodide (PI) assays detect the breakdown of plasma membrane integrity, resulting in the uptake of cell-impermeable dyes such as PI. ASt also caused some membrane integrity compromise compared with the control (0.1 mg/ml SDS exposed cells) (Fig. 2.6). However, we need to take into account that in *in vitro* assays, monolayer cells are more sensitive than *in vivo* or 3D *in vitro* models.

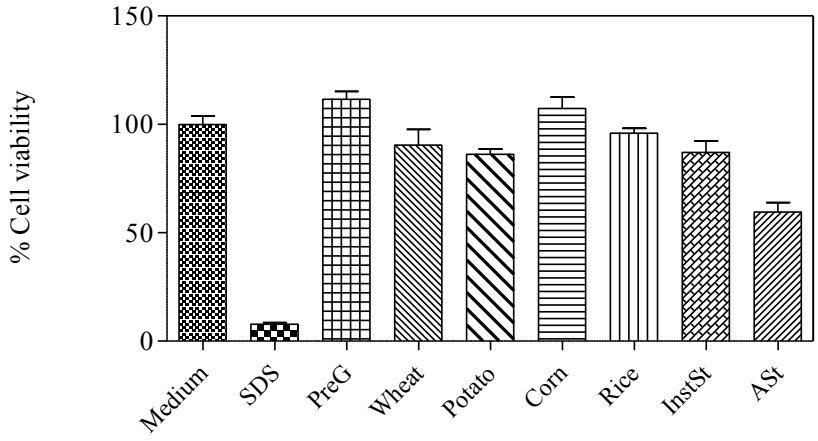

Fig. 2.5 - Viability of HaCaT cells after 48 h of incubation with different starches at concentration of 2 mg/ml (mean ± SD, n=5). SDS - sodium dodecyl sulfate.

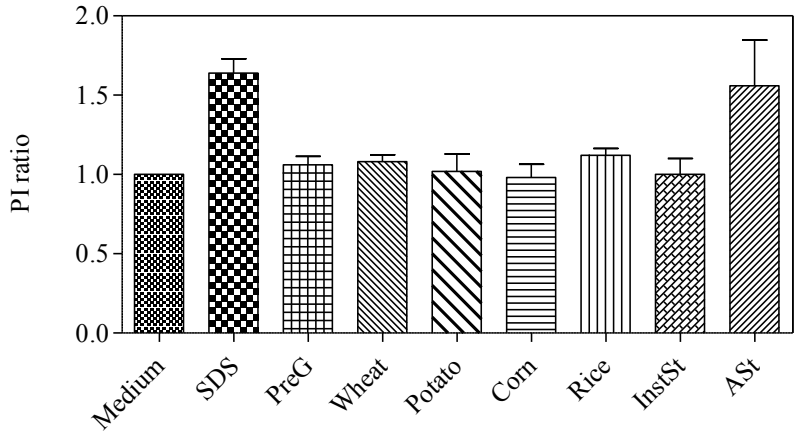

Fig. 2.6 - Membrane integrity of HaCaT cells after 48 h of incubation with different starches at concentration of 2 mg/ml (mean ± SD, n=5). PI - propidium iodide; SDS - sodium dodecyl sulfate.

4 Conclusions

The increasing scientific and industrial interest for starch as biomaterial has led to the development of numerous methods for preparing modified starches for pharmaceutical and cosmetic applications. These studies demonstrated that native and modified starches have an enormous potential for use in innovative applications in pharmaceutical and cosmetic formulations. The results also confirmed a high variability related to their origin. Native starches showed endothermic peaks between 60 and 80 °C. The type of starch influences the transition temperatures and enthalpies of gelatinization. The light microscopy data revealed that the morphology of all starches change upon heating. The viscoelasticity of heated starch dispersions was found to be strongly dependent on the type of starch. For wheat, corn, potato and rice starch, G'' is much higher than G', pointing out a dominant viscous behaviour. Both G' and G'' increased with temperature, probably due to the onset gelatinization of the polymer. In addition, the *in vitro* cytotoxicity and biocompatibility of starches on HaCaT cell line was investigated and the results obtained illustrated the practicability and efficiency performance characterized by the biocompatibility of starches. Therefore, preformulation studies were crucial to develop a portfolio of information about starches allowing detailed formulation design to be carried out, as well as selecting the best starch type for the intended purpose.

5 References

1. Ermens H. Pharmaceutical excipients—the past and future. Business Briefing: Pharmagenerics. 2004:1-3.

2. Ochubiojo EM, Rodrigues A. Starch: from food to medicine: INTECH Open Access Publisher; 2012.

3. Rodrigues A, Emeje M. Recent applications of starch derivatives in nanodrug delivery. Carbohydrate Polymers. 2012;87(2):987-994.

4. Monsuur F, Poncher J. Raising expectations of excipients. Chimica oggi. 2010;28(5).

5. Dharmendra S. Natural Excipients A Review. International Journal of Pharmaceutical & Biological Archive. 2012;3(5).

6. Ogaji IJ. Advances in natural polymers as pharmaceutical excipients. Pharmaceutica Analytica Acta. 2012.

7. Buléon A, Colonna P, Planchot V, Ball S. Starch granules: structure and biosynthesis. International Journal of Biological Macromolecules. 1998;23(2):85-112.

8. Sajilata M, Singhal RS, Kulkarni PR. Resistant starch–a review. Comprehensive Reviews in Food Science and Food Safety. 2006;5(1):1-17.

9. Tester RF, Karkalas J, Qi X. Starch—composition, fine structure and architecture. Journal of Cereal Science. 2004;39(2):151-165.

10. Le Corre D, Bras J, Dufresne A. Starch nanoparticles: a review. Biomacromolecules. 2010;11(5):1139-1153.

11. Rowe RC, Sheskey PJ, Quinn ME, Association AP, Press P. Handbook of pharmaceutical excipients: Pharmaceutical press London; 2009.

12. USP. United States Pharmacopeia-National Formulary, USP 35-NF 30. Rand McNally, Rockville, USA; 2013.

13. Song D, Thio YS, Deng Y. Starch nanoparticle formation via reactive extrusion and related mechanism study. Carbohydrate Polymers. 2011;85(1):208-214.

14. Pérez S, Bertoft E. The molecular structures of starch components and their contribution to the architecture of starch granules: A comprehensive review. Starch-Stärke. 2010;62(8):389-420.

15. Xie F, Pollet E, Halley PJ, Avérous L. Starch-based nano-biocomposites. Progress in Polymer Science. 2013;38(10):1590-1628.

16. Valeur B, Berberan-Santos MN. Molecular fluorescence: principles and applications: John Wiley & Sons; 2012.

17. Strober W. Trypan Blue Exclusion Test of Cell Viability. Current Protocols in Immunology: John Wiley & Sons, Inc.; 2001.

18. Alcázar-Alay SC, Meireles MAA. Physicochemical properties, modifications and applications of starches from different botanical sources. Food Science and Technology (Campinas). 2015;35(2):215-236.

19. Nair B, Yamarik TA. Final report on the safety assessment of aluminum starch octenylsuccinate. International journal of toxicology. 2002;21 Suppl 1:1-7.

20. Marto J, Gouveia L, Jorge IM, Duarte A, Gonçalves LM, Silva SMC, Antunes F, Pais AACC, Oliveira E, Almeida AJ, Ribeiro HM. Starch-based Pickering emulsions for topical drug delivery: A QbD approach. Colloids and Surfaces B: Biointerfaces. 2015;135:183-192.

21. Jobling S. Improving starch for food and industrial applications. Current Opinion in Plant Biology. 2004;7(2):210-218.

22. Schirmer M, Höchstötter A, Jekle M, Arendt E, Becker T. Physicochemical and morphological characterization of different starches with variable amylose/amylopectin ratio. Food Hydrocolloids. 2013;32(1):52-63.

23. Jenkins PJ, Donald AM. The influence of amylose on starch granule structure. International Journal of Biological Macromolecules. 1995;17(6):315-321.

24. Majzoobi M, Saberi B, Farahnaky A, Mesbahi G. Comparison of Physicochemical and Gel Characteristics of Hydroxypropylated Oat and Wheat Starches. International Journal of Food Engineering2014. p. 657.

25. Hoover R, Hughes T, Chung HJ, Liu Q. Composition, molecular structure, properties, and modification of pulse starches: A review. Food Research International. 2010;43(2):399-413.

26. Moore GRP, Canto LRd, Amante ER, Soldi V. Cassava and corn starch in maltodextrin production. Química Nova. 2005;28(4):596-600.

27. Ismail H, Irani M, Ahmad Z. Starch-based hydrogels: present status and applications. International Journal of Polymeric Materials and Polymeric Biomaterials. 2013;62(7):411-420.

28. Tester RF, Morrison WR. Swelling and gelatinization of cereal starches. I. Effects of amylopectin, amylose, and lipids. Cereal Chemistry Journal. 1990;67(6):551-557.

29. Lu Z-H, Donner E, Yada RY, Liu Q. The synergistic effects of amylose and phosphorus on rheological, thermal and nutritional properties of potato starch and gel. Food Chemistry. 2012;133(4):1214-1221.

30. Jenkins PJ, Donald AM. Gelatinisation of starch: a combined SAXS/WAXS/DSC and SANS study. Carbohydrate research. 1998;308(1):133-147.

31. Singh N, Singh J, Kaur L, Sodhi NS, Gill BS. Morphological, thermal and rheological properties of starches from different botanical sources. Food Chemistry. 2003;81(2):219-231.

32. Dale RE, Chen LA, Brand L. Rotational relaxation of the" microviscosity" probe diphenylhexatriene in paraffin oil and egg lecithin vesicles. Journal of Biological Chemistry. 1977;252(21):7500-7510.

33. Birks J, Lumb M, Munro I, editors. 'Excimer'Fluorescence. V. Influence of Solvent Viscosity and Temperature. Proceedings of the Royal Society of London A: Mathematical, Physical and Engineering Sciences; 1964: The Royal Society.

34. Stevens B, Ban M. Spectrophotometric determination of enthalpies and entropies of photoassociation for dissolved aromatic hydrocarbons. Transactions of the Faraday Society. 1964;60:1515-1523.

35. Seixas de Melo J, Pina J, Pina F, Lodeiro C, Parola A, Lima J, Albelda MT, Clares MP, Garcia-Espana E, Soriano C. Energetics and dynamics of naphthalene polyaminic derivatives. Influence of structural design in the balance static vs dynamic excimer formation. The Journal of Physical Chemistry A. 2003;107(51):11307-11318.

36. Olschlager V, Schrader A, Hockertz S. Comparison of primary human fibroblasts and keratinocytes with immortalized cell lines regarding their sensitivity to sodium dodecyl sulfate in a neutral red uptake cytotoxicity assay. Arzneimittel-Forschung. 2009;59(3):146-152.

3

Starch-based Pickering emulsions

This page was intentionally left blank

Section 1

Starch-based Pickering emulsions for topical drug delivery: a QbD approach

This Section was adapted from the published paper in:

J Marto, LF Gouveia, IM Jorge, A Duarte, LM Gonçalves, SMC Silva, F Antunes, AACC Pais, E Oliveira, AJ Almeida, HM Ribeiro (2015) Starch-based Pickering emulsions for topical drug delivery: A QbD approach, Colloids and Surfaces B: Biointerfaces, 135:183-192.

This page was intentionally left blank

Graphical Abstract

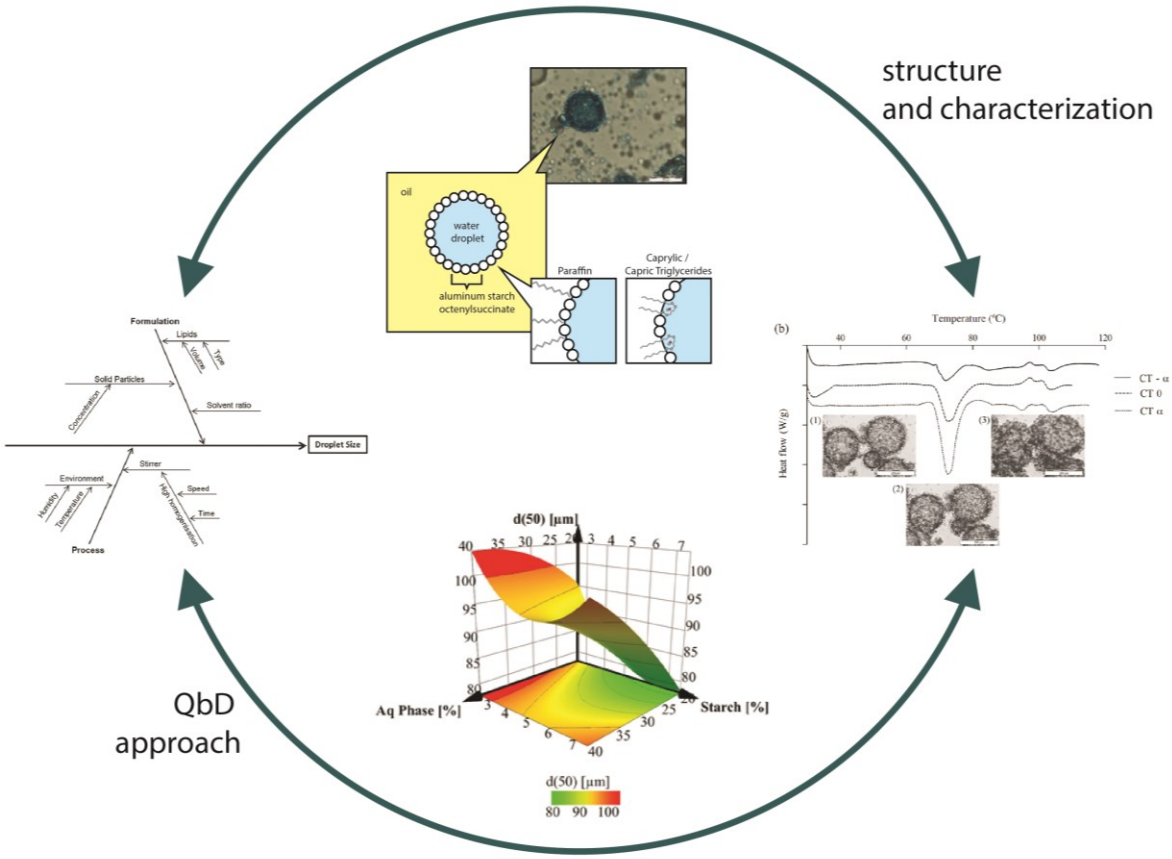

Highlights:

- A QbD approach was successfully applied to obtain starch Pickering emulsions.
- Formulation and process parameters allowed modulating droplet size.
- Starch amount highly influenced Pickering emulsions stability.
- Starch Pickering emulsions with suitable rheological and mechanical properties.
- Pickering emulsions were self-preserving and non-irritant for skin application.

This page was intentionally left blank

1 Introduction

Dosage forms for dermatological use are intended to produce the desired therapeutic action at specific sites in the skin tissue. Pharmaceutical emulsions emerge as a good solution for skin drug deposition in spite of their thermodynamic instability that makes their development a complex challenge in pharmaceutical technology. Current pharmaceutical emulsions are mostly stabilized by synthetic surfactants, which can be intrinsically toxic or may alter the distribution and elimination of co-administered drugs [1]. Consequently, solid-stabilized emulsions, i.e. Pickering emulsions, constitute an interesting alternative, whereby the stabilization of emulsion droplets by solid particles is due to particle dual wettability [2]. This interesting property allows the spontaneous accumulation of particles at the oil-water interface, which is stabilized against coalescence by volume exclusion and steric hindrances [3]. In this type of emulsions, the liquid with the poorest wetting properties is considered the disperse phase. The wettability of the particles at the oil-water interface is quantified by the contact angle, θ, between the particle and the interface. If the water contact angle is lower than 90º, the emulsion is o/w and, conversely, if the water contact angle is higher than 90º, the emulsion is w/o. However, if the particles have very low contact angles (too hydrophilic) or very high contact angles (too lipophilic), they tend to be dispersed in either the aqueous phase or oil phase, respectively, leading to unstable emulsions [4, 5]. These solid-stabilized emulsions avoid the application of hazardous surfactants, and show improved stability, especially at high internal phase ratio, allowing easy fabrication of stable large droplets up to millimeter size, when compared to classical surfactant-based emulsions [6]. Many types of solid particles, either organic (e.g. polymer latex or starch) or inorganic (e.g. silica and clay particles), have been used for stabilizing Pickering emulsions [2, 7, 8]. The use of starch to stabilize emulsions has been attracting substantial research interest due to their distinctive characteristics and promising technological applications.

In this study, a quality by design (QbD) approach was applied to the development of starch-based Pickering emulsions, so the quality is built by detailed understanding of the product and process [9]. It includes the definition of a Design Space thus creating a multidimensional combination and interaction of formulation variables and process parameters that have been demonstrated to provide assurance of quality. In this context the design of experiments (DoE) allows the measurement of interaction effects and includes the complete multidimensional experimental region. For these reasons, DoE is the perfect strategy to develop and optimize a pharmaceutical product, aiming at the product quality at

a cost-effective manner [10]. Therefore, it the present work the QbD approach was performed not only to extract the maximum amount of information from the collected data, but also to establish the influence of multiple factors on the formulation properties of starch-based Pickering emulsions. The direct effect of each factor was studied and the respective interaction with other factors was also evaluated in detail, demonstrating the emulsifying ability of starch granules and its successful application on pharmaceutical and cosmetic fields.

2 Material and methods

2.1 Materials

The materials used are described in Chapter 2, section 2.1. Span® 80 and Tween® 80 were obtained from Merck (Kenilworth, USA).

2.2 Methods

2.2.1 Characterization of starch granules

2.2.1.1 Particle size and morphology of ASt granules

Particle size distribution was determined using a Malvern Mastersizer 2000 (Malvern Instruments, UK) coupled with a Hydro S accessory. The real refractive index was set to 1.54. The data were expressed in terms of relative distribution of volume of particles, and given as diameter values corresponding to percentiles of 10 %, 50 % and 90 % (mean ± SD, n=6). The span value is a statistical parameter useful to characterize the wideness of the particle size distribution. In order to achieve an acceptable turbidity, about 5 ml of each sample, corresponding to an obscuration between 10 % - 20 %, was added to the sample chamber containing 120 ml of filtered purified water using a stirrer at 1750 rpm during 5 min and ultra-sonication at 50 %.

The morphology of aluminum starch octenylsuccinate (ASt) granules was confirmed as previously described in Chapter 2 section 2.2.1.1.

2.2.1.2 Wettability measurements

The measurement of the contact angle of water, liquid paraffin (LP) and caprylic/capric acid triglyceride (CT) on ASt in air was performed according to the procedure described previously in Chapter 2, section 2.2.1.2.

2.2.2 Preparation of the starch-stabilized emulsions (ASt-emulsion)

The w/o emulsion stabilized by ASt granules was developed using purified water as disperse phase and CT or LP as continuous phase. The ASt particles were first dispersed in the oil phase using a vortex mixer until total dispersion. The oil and aqueous phases were then mixed together with an UltraTurrax® T25 homogenizer (IKA®-Werke GmbH & Co. KG, Germany). In order to avoid bias, the order of preparation of the batches was random (Table 3.1.2.).

2.2.2.1 Type of emulsion

The emulsion type was confirmed by the dilution method and staining technique. In the first, a drop of emulsion was added to a certain volume of water and another oil. If it disperses in one of them, then that liquid is the continuous or external phase of the emulsion. The liquid, in which it remains as a drop, is the discontinuous or internal phase. In the second method, a drop of methylene blue (hydrophilic dye) was added to the emulsion and then the emulsion was inspected in an optical microscope to detect whether or not the water phase was the continuous one.

2.2.2.2 Droplet size distribution

The emulsions were analyzed for droplet size as previously described in Chapter 2, section 2.2.1.1. One drop of each emulsion was added to a glass slide without covering glass, and diluted with two drops of oil. The droplet size was determined using the image analysis software Olympus Stream Essentials®. The size data was expressed in terms of relative size distribution of particles, and given as diameter values corresponding to percentiles of 50%, 90% and span value [11].

2.2.3 Identification of Quality Target Product Profile (QTPP) and Critical Quality Attributes (CQAs)

The QTPP describes the product quality and forms the basis for defining the CQAs and critical process parameters (CPPs) [9]. The first step is to define the desired QTPP, which depend upon scientific, regulatory and practical considerations and previous work. One of the important features of an emulsion is its droplet size distribution, namely, d(50), d(90) and span, because it influences other important characteristics such as rheology and stability. Thus, the list of the key QTPP are given in Table 3.1.1

Table 3.1.1 - QTPP of ASt-emulsions.

QTPP element	Target
Route of administration	Topical [12]
Dosage form	Emulsion (Pickering emulsion)
	Droplet size distribution: • d(50) – 75-150 µm • d(90) – 150-300 µm • Span – 1-3
Stability	At least 12 weeks shelf-life at room temperature [13]

2.2.4 Risk analysis of CQAs

An Ishikawa diagram was used to categorize the potential causes of noncompliance, which enables the identification of the CQAs that have the greatest chance of generating product failure. This approach also allows prioritizing the possible risk factors associated to emulsion stability as well as the process parameters. The first step in the risk assessment was to gather up systematically all the possible factors that could influence product quality. For this purpose, the identification of critical variables and the levels used in DoE was based on the literature and previous work. With the information collected, Ishikawa diagrams were constructed to identify the potential risks. The droplet size, i.e. d(50), d(90) and Span, was defined and further delineated to identify potential risks and after the analysis, three variables were identified for optimization in the following studies.

2.2.5 Design space assessment

The process and the formula of the emulsions were optimized using a two-factor Central Composite Design (CCD). For the process optimization, the independent variables were the rotation speed (S) of the homogenizer (UltraTurrax® T25) and the stirring time (T) of the emulsification. The independent variables for formula optimization were the percentage of aqueous phase (Aq) and the percentage of ASt in the aqueous phase (St).

To investigate the variables affecting the responses studied, three CCD were performed, one for the process only with LP and two for the formula with CT and LP, as the oil phase. The α value chosen to ensure design rotability was 1.147 for formula and 1.414 for process optimization.

This design required 11 experimental runs, including three replicated center points for a more uniform estimation of the prediction variance over the entire design space. Data were

analyzed using the MODDE® Pro 11 software (Umetrics, Sweden) and effects were considered significant when the estimated *p* values were lower than 0.1 (the chosen alfa error), to increase statistical power. The following mathematical quadratic model was fitted to the data:

Equation 1: $Y = \beta_0 + \beta_1 X_1 + \beta_2 X_2 + \beta_{12} X_1 X_2 + \beta_{11} X_1^2 + \beta_{22} X_2^2$

This model describes the zero and second order effects as well as the interactions between the independent variables. In this equation, β_0 is the arithmetic mean response, β_1, β_2, β_{11} and β_{22} are the linear and quadratic coefficients of the independent variables and β_{12} the interaction term, respectively. The higher the magnitude of each coefficient, the higher is the respective main effect on the system. A positive coefficient sign indicates that an increase in the parameter level leads to an increase in droplet size. Taking into account the interaction coefficient, the response must be studied in terms of how the variation of one factor modulates the effect of another factor (Table 3.1.2).

Table 3.1.2 - Formula and process CCD matrix and experimental matrix.

Design matrix		ID	Experimental matrix for formula optimization		Design matrix		ID	Experimental matrix for process optimization	
Aq (%, w/V)	St (%, w/V, wrt Aq)		Aq (%, w/V)	St (%, w/V, wrt Aq)	S (k rpm)	T (s)		S (k rpm)	T (s)
-1	-1	F1	20.00	8.33	-1	-1	P1	11.5	61
1	-1	F2	40.00	8.33	1	-1	P2	20.5	61
-1	1	F3	20.00	25.00	-1	1	P3	11.5	259
1	1	F4	40.00	25.00	1	1	P4	20.5	259
-1. 147 (-α)	0	F5	18.53	16.67	-1. 414 (-α)	0	P5	9.6	160
1. 147 (α)	0	F6	41.47	16.67	1. 414 (α)	0	P6	22.3	160
0	-1.147 (-α)	F7	30.00	7.10	0	-1.414 (-α)	P7	14.5	20
0	1. 147 (α)	F8	30.00	26.23	0	1. 414 (α)	P8	14.5	300
0	0	F9	30.00	16.67	0	0	P9	14.5	160
0	0	F10	30.00	16.67	0	0	P10	14.5	160
0	0	F11	30.00	16.67	0	0	P11	14.5	160

Aq - Aqueous Phase; St – ASt; S - Speed; T – Time.

2.2.6 Stability of w/o ASt-emulsions

All formulations were stored during 12 weeks at 25 ± 2 °C, protected from the light by aluminium foil. Samples were analyzed for macroscopic appearance before the storage period and on 1, 2, 3, 4 and 12 weeks of storage. Macroscopic appearance was assessed by visual inspection.

2.2.7 ASt-emulsions' mechanical and structure properties

2.2.7.1 Rheological studies

2.2.7.1.1 Dynamic viscosity

Shear rate *vs* shear stress measurements were performed at 25°C using a HAAKE MARS III Rotational Rheometer, equipped with automatic gap setting (Thermo Scientific™, Waltham, USA). Rotational viscosity was determined using a C35 mm cone geometry, with an angle of 1 º. All measurements were carried out at a temperature of 25 °C using a peltier system. Dynamic measurements were carried out by rotational shear experiments, between 1 and 1000 Pa on a logarithmic increment, in order to investigate the effect of each formulation component on the viscosity. Each test was performed at least in duplicate (n = 2).

2.2.7.1.2 Oscillation measurements

Oscillatory measurements were performed to investigate the behavior of the formulations at small deformations. Oscillation frequency sweep tests were performed at frequencies ranging between 0.01 and 1 Hz. Viscoelastic experiments for emulsions were obtained by exposing the samples to a forced oscillation deformation. Prior to the oscillation tests, stress sweep tests were performed to determine the values of shear stress for which the viscoelastic functions are independent from the magnitude of the applied stress. Each test was performed at least in duplicate (n = 2) using new samples for each measurement.

2.2.7.2 Texture profile analysis (TPA)

A Texture Analyzer TA.XT Plus (Stable Micro Systems Ltd., Godalming, UK) was used to examine textural characteristics (hardness, elasticity, compressibility, adhesiveness and cohesiveness) of the emulsion. TPA mode was carried out using an analytical probe (P/10, 10 mm Delrin), which was twice depressed into the sample at a defined rate (5 mm/s) to a desired depth (15 mm), allowing 15 s of delay between consecutive compressions. The samples were placed into cylindrical tubes with the same dimensions (at a fixed height). Six replicates were performed at 25 ºC for each formulation. Data collection and calculation were performed using the Texture Exponent 3.0.5.0 software package of the instrument.

2.2.7.3 Differential Scanning Calorimetry (DSC) and hot stage microscopy

The DSC analyses and hot stage microscopy were performed according to the procedure described previously in Chapter 2, section 2.2.3.2. Both analyses were conducted by heating the samples from 30 ºC to 120 ºC using a 10 °C/min heating rate.

2.2.8 *In vitro* cytotoxicity studies

2.2.8.1 Cell culture conditions

The cell culture conditions are described in Chapter 2, section 2.2.5.1.

2.2.8.2 Cytotoxicity assay

To determine *in vitro* emulsions effects on cell viability, cells (cultured in 96-well microplates) were incubated with emulsions stabilized by ASt particles and emulsions stabilized by surfactants for 24 h and cell viability was determined using the MTT assay as described in detail in Chapter 2, section 2.2.5.2. Each condition was assayed in triplicate and every experiment was performed at least three times, with a total of nine replicates (n=9). The percentage of viable cells was compared to the viability of cells treated with medium.

2.2.9 Antimicrobial activity

The antimicrobial activity was assessed according to a modification of membrane filtration method described in the European Pharmacopoeia 8 (Ph. Eur.) (5.1.3.) [14]. Briefly, 24 samples of 20 ml were prepared separately, and afterwards contaminated with an inoculum of 10^8 microorganisms per milliliter of *Pseudomonas aeruginosa* ATCC 9027, *Staphylococcus aureus* ATCC 6538, *Candida albicans* ATCC 10231 and *Aspergilus brasiliensis* ATCC 16404. The antimicrobial activity of the emulsions was evaluated during 28 days. Results were expressed as the log reduction of the colony-forming units (cfu) at 0, 48 h, 7, 14 and 28 days. The bacteria should be diminished at least by about 2 log-steps after two days, by about 3 log-steps after 7 days and on day 28 their number must not be increased. In the case of fungi, the cfu should be reduced at least about 2 log-steps after 14 days and on day 28 the cfu should be not increased for A criteria and 1 log-step after 14 days and on day 28 the cfu should be not increased for B criteria.

3 Results and discussion

3.1 Characterization of starch granules

3.1.1 Particle size measurements of ASt granules

As native starch granules are not hydrophobic, they are inappropriate to adsorb in oil–water interface. Nevertheless, the hydrophobicity can be added to starch granules by chemical or physical modifications [15]. A common way to chemically modify starch is by using octenyl succinic anhydride, resulting in the aluminum starch octenylsuccinate (ASt) used in the present study for its amphiphilic character. It is used in pharmaceutical and personal care products at concentrations as high as 30 % as an anticaking agent and a thickening agent [16]. Emulsions stabilized by starch granules constitute an interesting vehicle for topical drug delivery [17].

Microscopy analysis showed ASt granules are irregular polygonal shaped with smooth edges. Using polarized light revealed a positive birefringence (Fig. 3.1.1), predicting a semi-crystalline structure whereby the granules do not disperse in water at room temperature, which is an advantage for the emulsions stabilized by solid particles. The ASt granules showed a particle size ranging from 10 to 20 μm, with a main peak at 13 μm and d(10), d(50) and d(90) values of 7.28 ± 0.01 μm, 13.52 ± 0.01 μm and 20.85 ± 0.02 μm, respectively, supporting the use of ASt granules as effective stabilizers of emulsions [2, 4].

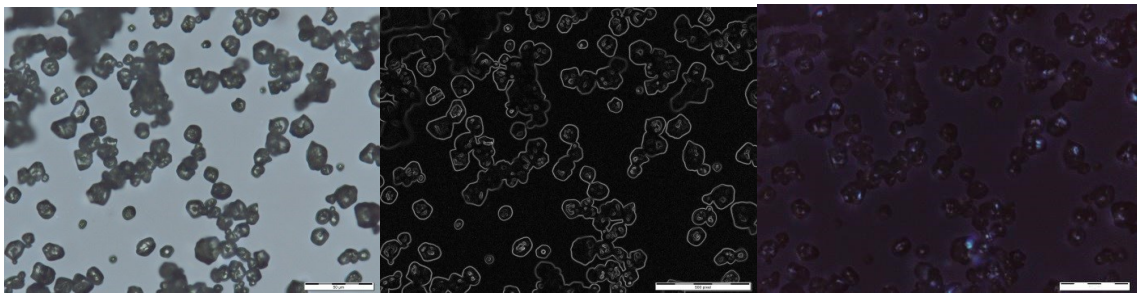

Fig. 3.1.1 - Morphology of ASt under (a) bright-field. (b) sobel filter and (c) polarized light (Scale bar = 50μm).

3.1.2 ASt wettability

For emulsions stabilized by surfactants, the hydrophilic–lipophilic balance (HLB) defines which emulsion type (o/w or w/o) is preferentially stabilized, thus quantifying the effect of the different interactions at interfaces. In the case of solid particle adsorption at oil-water interfaces, the HLB in surfactant systems is paralleled with particle wettability, characterized by the contact angle (θ) between the oil-water interface with the particle

surface [18]. Hence, the wettability properties of solid particles determine the type of emulsion (o/w or w/o). Water-wet particles tend to stabilize o/w emulsions whereas oil-wet particles tend to stabilize w/o emulsions. Ideally, for a w/o emulsion would be beneficial an oil-wet particle, i.e. larger angles in contact with water and smaller with oil.

Fig. 3.1.2 shows the contact angle of water ($\theta > 90º$), LP ($\theta < 90º$) and CT ($\theta < 90º$) on ASt, showing that ASt is hydrophobic. The production of hydrophobic coatings on the surface of the solid particles leads to their dispersion within the oil and results in w/o emulsions [19]. In this case, the presence of aluminum octenylsuccinate ensures the hydrophobic properties of ASt. In emulsions stabilized by solid particles the hydrocarbon chains at the particle surface are orientated outwards. The length of the hydrocarbon chains determines the phase continuity of the emulsion. Consequently, the octenylsuccinate modification leads to contact angles > 90° due to the increase in the density of coverage and alkyl chains with more than 12 carbon atoms. Thus, the octenylsuccinate modification provides ASt with the suitable wettability to strongly adsorb at the oil–water interface and consequently form very stable emulsions.

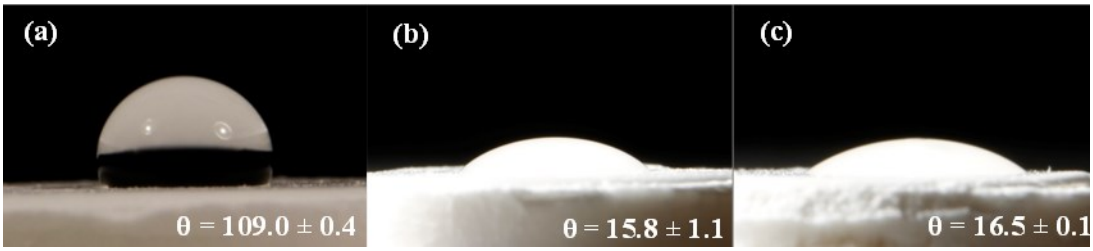

Fig. 3.1.2 - Contact angles of aluminium starch octenylsuccinate in (a) water, (b) LP and (c) CT.

3.1.3 Type of emulsion

Fig. 3.1.3 shows the emulsion stabilized by ASt. Modified starch granules have been used successfully to create emulsions stabilized by solids in a close-packed around spherical drops. All of the starch was adsorbed at the oil-water interface and few free ASt were observed in light microscopy (Fig. 3.1.3). This further indicates that the starch granules present a very high degree of affinity for the oil-water interface.

Theoretically, the type of emulsion was already defined, w/o, however to assure it further studies concerning the determination of the type of the emulsion were performed. The emulsions were inspected visually and a drop of emulsion was added to water and to oil. The drop in the oil dispersed easily while on the water it remained as an isolated drop.

Accordingly, the developed emulsions were w/o. Also a drop of methylene blue was added to the emulsion to detect whether or not the water phase was the dispersed one. As observed in Fig. 3.1.3, the methylene blue, a hydrophilic dye only tainted the droplets which means that we are in the presence of a w/o emulsion.

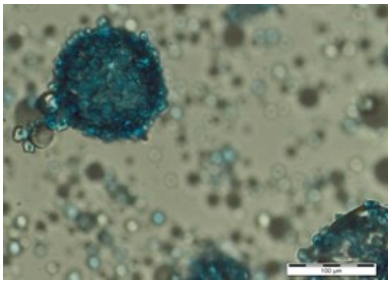

Fig.3.1.4 - Emulsion stabilised by starch granules dyed with methylene blue (Scale bar = 100 μm).

3.1.4 Risk analysis of CQAs

The first and the most important element when using the QbD concept to assist formulation and process design, is to pre-define the desired final QTPP. This study focused on one critical formulation and process quality attribute, i.e. droplet size distribution.

Factors potentially affecting the quality attributes of the emulsions stabilized by ASt granules were divided into two categories: formula and process related. Within these two categories, critical variables were identified (Fig. 3.1.4) and the effects of these variables on the droplet size were studied.

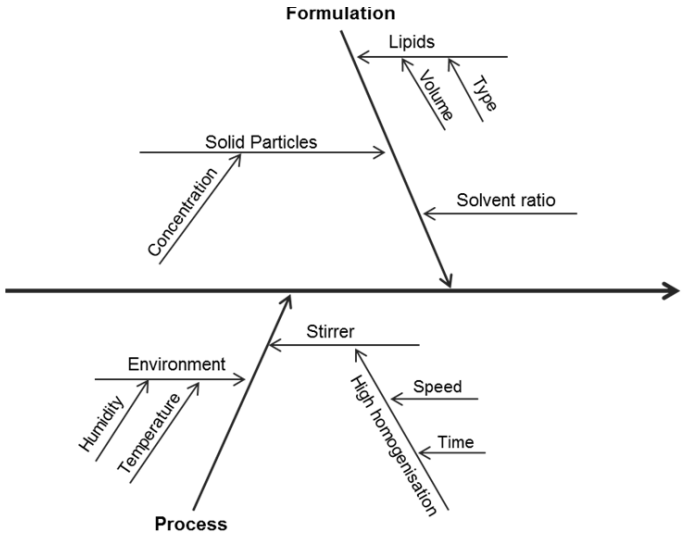

Fig. 3.1.4 - Ishikawa diagram illustrating factors that may have impact on the droplet size of an ASt-emulsion.

The major critical variables identified as possible cause of product variability were the stirring speed, stirring time, concentration of solid particles and solvent ratio. This screening has the advantage of minimize the number of experiments required to identify the most critical factors affecting the response.

The amount of ASt used in the designed experiments was estimated assuming a monolayer of close-packed spherical particles of ASt laid at the interface of monodisperse aqueous droplets with the oily continuous phase. The covering density (k) of this packing can be calculated using Equation 2.

Equation 2: $k = \frac{\pi}{3*\sqrt{3}} \approx 0.6046$

The calculation of the total amount (expressed in g) of ASt needed to fully cover the aqueous droplets was made using Equation 3, where D_S and D_d are the diameters of the ASt particles and disperse droplets, respectively, V_{aq} is the volume (in ml) of the aqueous phase and ρ the true density of the ASt (experimentally determined using gas picnometry as 0.7 g/cm^3) (Fig. 3.1.5).

Equation 3: $M_s \leq 2\ \rho\ V_{aq} \cdot k \frac{D_d^3 - (D_d - 2D_s)^3}{D_d^3(1-k) + (D_d - 2D_s)^3(2+k)}$

Using Equation 3, approximately 6 g of ASt are needed to fully cover the aqueous disperse droplets when considering a diameter of 13.52 µm for the ASt particles, a 150 µm diameter for the dispersed droplets and a total volume of 30 mL for the disperse phase. Hence, a 5 g amount of ASt was selected as the CCD "0" level and 2.5 and 7.5 g as the "-α" and "α" levels, respectively.

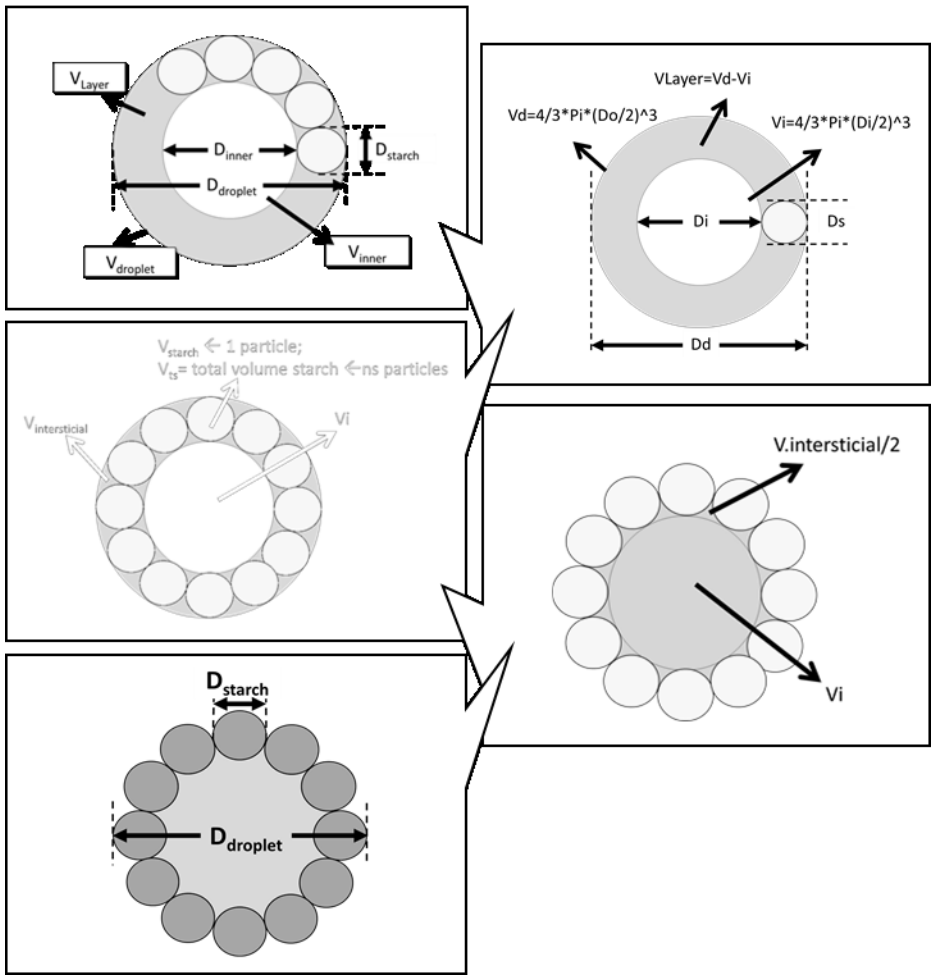

Fig. 3.1.5 - Schematic representation of the rationale to calculate the total amount of ASt needed to fully cover the aqueous droplets.

3.1.5 Response surface analysis

The collected experimental data were analyzed and polynomial models were fitted. An analysis of variance (ANOVA) was also performed and *p* values were calculated for the variables. The information derived from the models was expanded graphically using isoresponse curves. A good correlation was obtained between the observed and predicted values as indicated by the R^2 value between 0.80 and 0.89 for all variables in both optimization studies.

In Table 3.1.3 the effect column reflects each factor's relative strength, the higher the absolute, greater the effect of that factor on the response.

Table 3.1.3 - Summary of regression analysis results for measured responses, for process and formula optimization.

CCD	Oil phase		d(50)		d(90)		Span	
			Coeff	± SE	Coeff	± SE	Coeff	± SE
Process	LP	k	1.903	0.009	2.471	0.005	3.077	0.176
		S	0.042	0.007	NS	NS	NS	NS
		T	-0.051	0.007	-0.028	0.002	NS	NS
		S*S	0.048	0.007	-0.023	0.003	-0.402	0.128
		T*T	0.040	0.007	NS	NS	NS	NS
		S*T	-0.052	0.011	-0.021	0.033	NS	NS
Formula	CT	k	2.084	0.019	2.952	0.018	3.663	0.095
		Aq	0.014	0.005	NS	NS	0.039	-0.008
		St	-0.059	0.010	-0.177	0.011	-0.520	0.029
		Aq*Aq	-<0.001	<0.001	-<0.001	<0.001	-0.001	0.001
		St*St	0.011	0.002	0.012	0.002	0.008	0.004
		Aq*St	-0.002	0.001	NS	NS	0.006	0.001
	LP	k	2.021	0.012	2.367	0.014	1.410	0.079
		Aq	0.007	0.002	0.019	0.004	NS	NS
		St	-0.082	0.026	-0.091	0.018	-0.034	0.017
		Aq*Aq	NS	NS	NS	NS	NS	NS
		St*St	0.005	0,002	0.007	0.002	NS	NS
		Aq*St	NS	NS	NS	NS	NS	NS

CCD – Central composite design; CT – Tegosoft® CT; LP – Liquid paraffin; Aq - Aqueous Phase; St – ASt; S - Speed; T – Time.
Coeff– Coefficient Scaled and centered; SE – Standard Error; k – Constant; NS (no significant) – $p > 0.10$.

A positive value indicates an effect that increases the response, and a negative value represents an inverse relationship between the response and the factor. A general interpretation indicates that in the process optimization, an increase in stirring time and/or stirring speed originates lower droplet size (d50, d90). Due to the second order and interactions terms of the underlying model, some combinations of the variables do not follow this general trend. In what concerns the process optimization, the response surfaces of the fitted models are shown in Fig. 3.1.6.

For d(50), all variables were statistically significant. However the stirring speed appears to have no impact on the d(90). On the other hand, regarding the span the only significant variable was the stirring speed. Consequently, it is possible to conclude that both stirring speed and stirring time show a negative correlation. Therefore, an increased stirring time produced smaller droplets and a higher stirring speed originated a narrower distribution of

droplet size. In fact, the increase of the homogenization time can cause droplet disruption due to shear stress and cavitation forces, thus decreasing their size [20]. It was also demonstrated that increasing the stirring speed originates a decrease in droplet size, which also decreases with the time for the higher speed experiment, confirming previous publications [21].

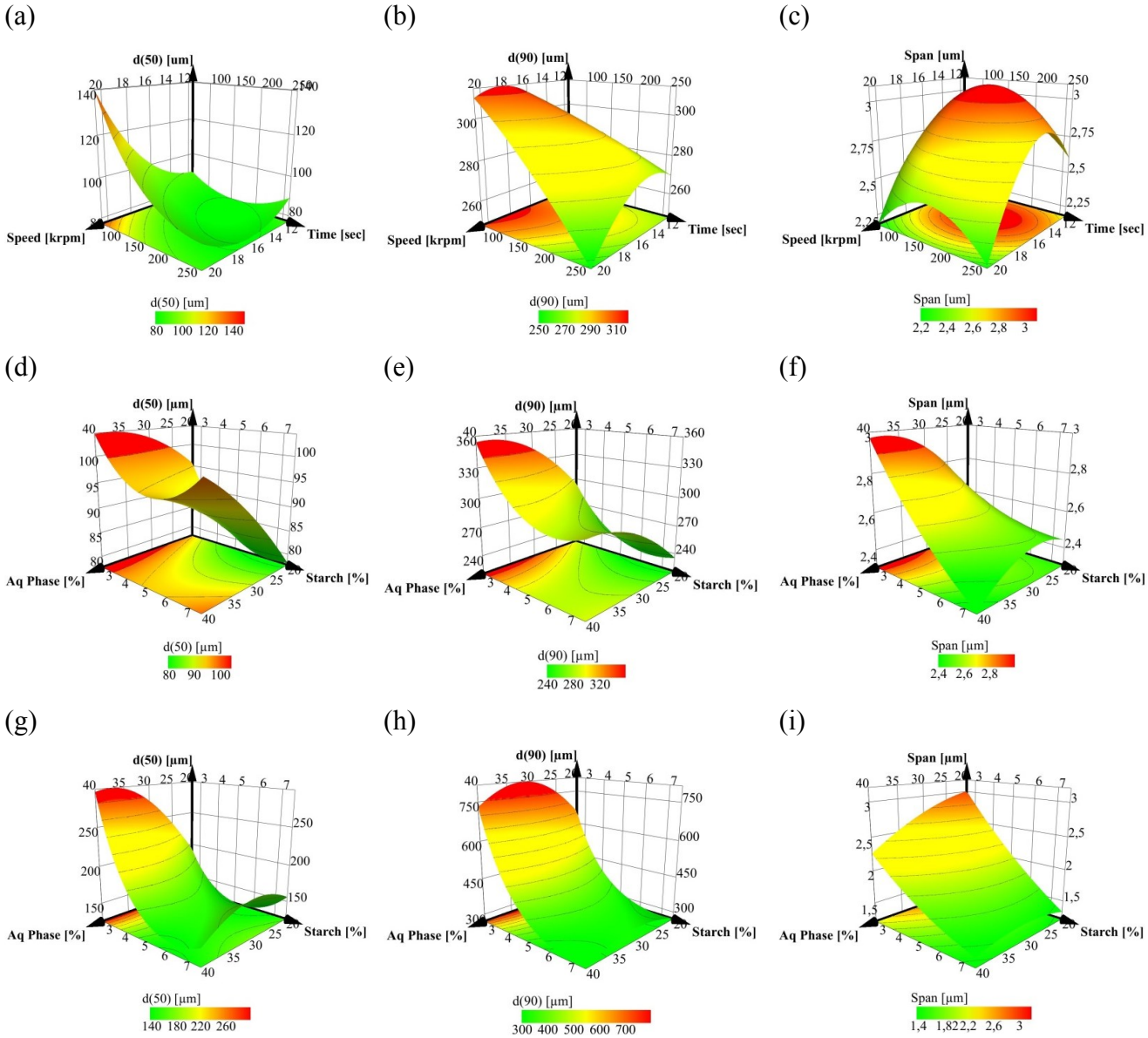

Fig. 3.1.6 - Isoresponse curves (graph floor) and response surface plots of relative size distribution (µm), respectively: (a) d(50) (b) d(90) and (c) span, for process optimization using LP as the oil phase, (d) d(50), (e) d(90) and (f) Span, for formula optimization using LP as the oil phase and (g) d(50), (h) d(90) and (i) Span, for formula optimization using CT as the oil phase.

For CT and LP formula optimization study, the results indicated that although an increase in ASt concentration and a decrease in the aqueous phase contributed to a narrower droplet size distribution, the former had a more dominant effect.

Considering CT formula optimization, for d(50) and d(90), the aqueous phase and ASt amounts were the variables significantly affecting the droplet size distribution. Indeed, a negative correlation was observed for the percentage of ASt in all dependent variables, meaning that an increase in the ASt amount in the emulsion will result in a decrease in droplet size. According to several authors, the size of the droplets decreases with increasing solid particle concentration, leading to the formation of emulsions throughout the entire mixture volume without any coalescence or phase separation. However, if the droplet size approaches the size of the solid particles, flow oscillations induced by the particles dominate the droplet break-up leading to increased polydispersity [22].

As expected, the phase ratio influenced the droplet size distribution [23]. With an increase in percentage of aqueous phase, the smaller droplets tend to aggregate, originating single and larger droplets. Consequently, the span value tends to increase due to a lesser surface coverage around the droplets, leading to coalescence. A negative correlation was also found for Span meaning that an increase in ASt concentration leads to a narrower droplet size distribution.

Considering the LP results, the statistically significant variables ($p < 0.10$) that affect the d(50) and d(90) were the percentage of aqueous phase and the percentage of ASt, while for span the only variable with statistical significance was the percentage of ASt. Thus it can be inferred that a decrease in the percentage of aqueous phase, as well as an increase in the ASt, produces smaller droplets. Similar results concerning the formula have been reported elsewhere, showing the strong affinity of starch for the oil-water interface, resulting in a maximum coverage of the droplet surface and the formation of smaller droplets [6]. The same has been observed for emulsions stabilized with other solid materials [24]. This suggests a similar behavior at oil-water interface as that of surfactants, confirming the fact that HLB in surfactant systems is paralleled by particle wettability in emulsions stabilized by particles [18].

3.1.6 Design space

The design space (DS) concept is defined as “the multidimensional combination and interaction of input variables (material attributes) and process parameters that have been

demonstrated to provide assurance of quality". Working within the DS is not considered as a change; however the movement out of the DS is considered as a relevant change in the process [9]. A comprehensive DS leads to a more robust and flexible process to adjust the variations and getting closer to predicted CQAs.

In this study, response surface methodology was applied to establish the DS. The process key parameters that had been demonstrated to affect emulsions quality were used to construct the DS (Fig. 3.1.7). Every single point corresponds to a combination of stirring time and stirring speed. The green area corresponds to a range of combinations for which the size remains within the pre-defined acceptable limits. This overlay plot provides a range within the value of a critical process parameter that will not affect the final response, in other words, as long as each variable is maintained within its range, the droplet size can be successfully predicted and controlled. The DS was established for formula optimization, which was delineated in the green region in Fig. 3.1.7. The dotted frame in the DS plot defines the optimal conditions that can be inserted into the irregular DS volume (Proven Acceptable Range – PAR).

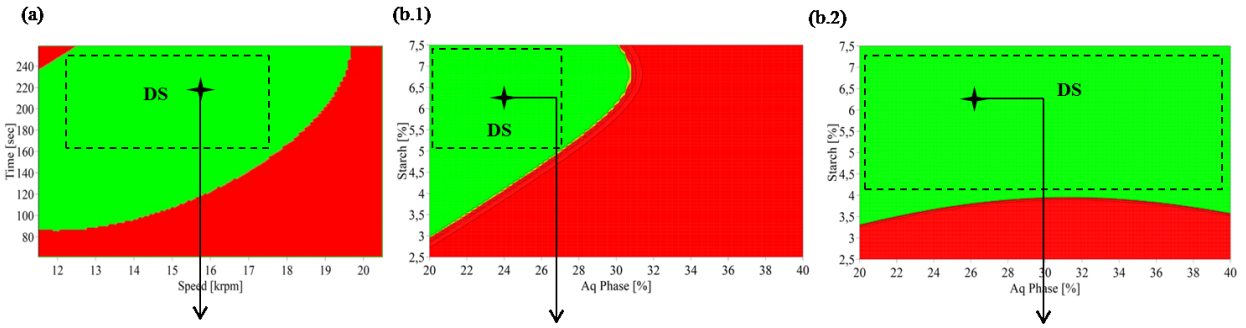

Factor	Setpoint	Factor contribution
S (K rpm)	15.9	42.8
T (Sec)	216	57.2

Factor	Setpoint	Factor contribution
Aq Phase (%)	24.6	65.9
Ast (%)	6.3	34.1
LP (%)	69.1	-

Factor	Setpoint	Factor contribution
Aq Phase (%)	26.2	31.3
Ast (%)	6.0	68.7
CT (%)	67.8	-

Fig. 3.1.7 - Plots evidence the DS for (a) the process and (b) the formula with (b.1) LP and (b.2) CT as the oil phase, respectively.

3.2 Characterization of ASt-emulsions

In order to evaluate and characterize the influence of the external phase type, and the amount of ASt on the stability, rheological behavior and *in vitro* studies, the internal phase volume was fixed (30 %) and the levels – α, 0 and α of the formula's CCD were studied.

3.2.1 Stability of ASt-emulsions

Instability of emulsions may result from a variety of physicochemical destabilizing processes, such as creaming, flocculation, coalescence or phase inversion. The macroscopic characteristics of emulsions were assessed by visual inspection throughout 12 weeks at 25±2°C. From this study, it was concluded that the process had no significant impact on the aging of the emulsions since no coalescence or phase separation were observed in these emulsions. On the other hand, the formula has some impact on emulsion stability.

The ASt-emulsions were in general rather unstable with sedimentation, occurring quickly after homogenization, although easily redispersed until 2 weeks into the study.

The effectiveness of the solid in stabilizing emulsions depends on particle size, shape, concentration, wettability (contact angle) and interactions between particles [3, 5]. The contact angle influences the adhesion energy of the particle, which can be expressed as $E=\pi\alpha^2\gamma(1\pm cos\theta)^2$, where α is the radius of the particle, γ is the surface tension and the sign inside the bracket is negative for removal into the aqueous phase and positive for removal into the oil phase [4, 7]. As the adhesion energy increases in proportion to the square of particle size, the larger particles provide better emulsion stability. In fact, particles above a certain size (~ 10 nm) are almost irreversibly adsorbed at the oil-water interface and the desorption energy per particle is of an enormous magnitude, indicating that this is an insurmountable energy barrier to droplet shrinkage beyond a tightly packed monolayer particles. As a result, Pickering emulsions present a higher stability against coalescence and even Oswald ripening. In the present study coalescence occurred first in the emulsions with the lowest level of ASt, in the second week of storage, followed by phase separation on week 4. Nevertheless, a contribution from the lower viscosity of these emulsions to instability may not be precluded, as discussed below. This also applies to the emulsions prepared with the central level of ASt. ASt-emulsions with the highest level of ASt maintained their stability during the 12 weeks of study. The dispersion of ASt granules reduces the droplet diffusion in concentrated solutions and stabilizes the contact between droplets, improving the emulsion stability. Overall, as ASt concentration increases, the stability of emulsion also increases.

3.2.2 ASt-emulsions' mechanical and structure properties

3.2.2.1 Dynamic viscosity

Rotational shear experiments measure the ability of each system to resist to structural deformation during the standardized shearing procedure. The viscosity values were determined at $1s^{-1}$ and showed a decrease upon shear rate increase (Table 3.1.4).

Table 3.1.4 - Apparent viscosity values were obtained at a shear rate of $1s^{-1}$, and storage modulus (G') and loss modulus (G'') were obtained at a shear stress of 10 Pa (mean ± SD, n=2).

Formulations		Apparent viscosity (Pa.s)	Storage modulus, G' (Pa)	Loss modulus, G'' (Pa)
LP	α	86.61 ± 0.20	35170.1 ± 25.0	9738.5 ± 13.2
	0	78.33 ± 0.11	29810.9 ± 104.1	7885.1 ± 67.4
	- α	54.18 ± 0.38	17430.0 ± 25.7	4039.0 ± 39.1
CT	α	66.16 ± 0.42	543.5 ± 9.5	184.7 ± 5.7
	0	9.60 ± 0.54	0.7 ± 0.3	2.1 ± 0.7
	- α	3.06 ± 0.33	0.2 ± 0.1	0.7 ± 0.2

As expected, an increase in the concentration of ASt promotes the increase in the viscosity of the formulations due to the interaction between ASt particles. This could be related to the destruction and formation of the emulsion network structure [25-27]. This non-Newtonian behavior is primarily due to a marked dependency of the viscosity with the shear rate, known as shear-thinning. The inclusion of ASt seems to increase the viscosity of the ASt-emulsions, while the inclusion of lipid notably influenced this parameter, depending on the lipid used (Table 3.1.4). This effect is more pronounced when the lipid CT is employed. Conversely, there is a minimal variation of the viscosity upon ASt increase, in formulations containing LP. The viscosity profile of a formulation provides important information about the production, processing and performance. Lower shear rates can be related to storage conditions and provide valuable information about the stability of Pickering emulsions, through the occurrence of sedimentation and phase separation phenomena. Structural differences in the formulations can be inferred from the flow curves. As the emulsions behave as a shear-thinning fluid, they are suitable for topical administration.

3.2.2.2 Oscillation measurements

Fig. 3.1.8 shows the variation of the G' and G' with shear stress. For each formulation tested, G' increases with an increase in the amount of ASt (Table 3.1.4). This behavior is typical of a viscoelastic liquid. The CT-based emulsions exhibit a sharper decrease in the storage modulus (G'), as a result of the reduction of the size of the emulsified droplets, when compared to LP-based emulsions. However, the system maintained the solid-like properties (G' > G'') due to the presence of the stabilizer agent, which assured stability during the stress tests and presented long-term storage stability. This indicates that the structures of the ASt-emulsions with high concentration of ASt and LP as external phase are more robust than those containing CT and lower concentration of ASt.

The tan (δ) is defined as the ratio between the loss modulus (G'') and the storage modulus (G') and is dimensionless. A value of tan (δ) > 1 indicates a liquid-like behavior whereas a value < 1 means solid-like behavior. At high shear stresses, the emulsions with LP exhibit a lower tan (δ) value compared to the emulsions containing CT, indicating that the latter has a weaker structure. At lower shear stresses both emulsions present a tan (δ) < 1, indicating that the G' component of the system is dominant.

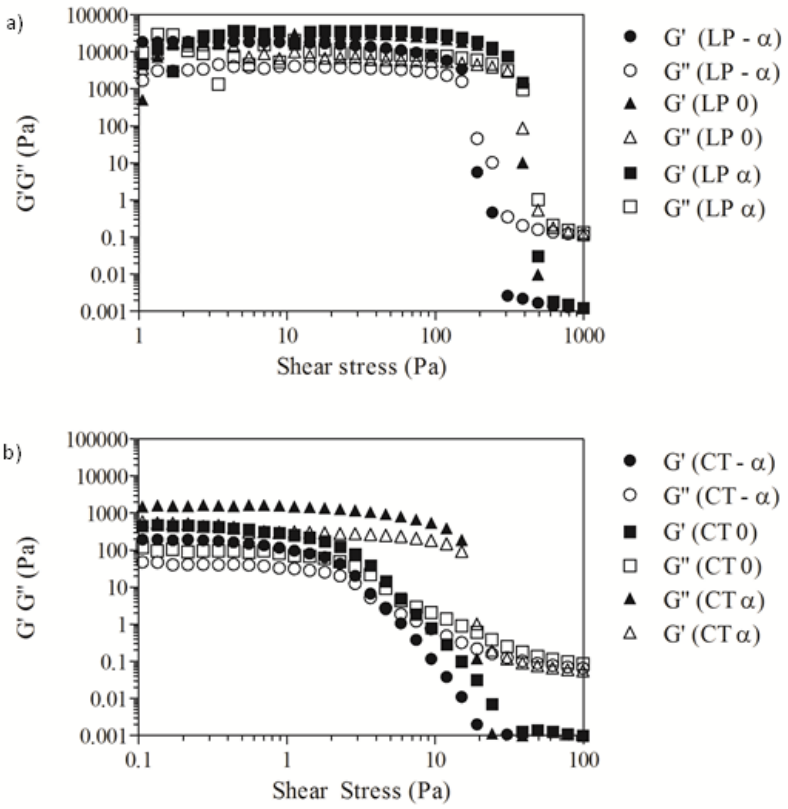

Fig. 3.1.8 - Dependence of storage (G') and loss (G'') moduli with shear stress for ASt-emulsion a) LP and b) CT. All the experiments were carried out at 25ºC.

3.2.2.3 TPA

The ASt-emulsions demonstrated a wide range of mechanical properties dependent on the formulation design. The amount of ASt and the type of external phase strongly affected the rheological behavior of the formulations, which may influence adhesion onto the skin and consequently affect the drug release rates. The TPA technique is relevant and adequate for the mechanical characterization of pharmaceutical semisolid formulations, in order to determine interactions between formulation components, being a good complement for the rheological information. Through this approach, parameters such as hardness, adhesiveness, compressibility, elasticity and cohesiveness can be extracted from the compression graphics (Table 3.1.5).

Concerning the emulsion hardness, which expresses the easiness with which the emulsion is applicable onto the skin, it increases with ASt addition. It should be noted that the viscosity of polymeric-based dosage forms increased as their concentrations were increased. Additionally, CT-based formulations were characterized by smaller hardness parameter. The same trend was observed for compressibility, which is correlated to the spreadability of the emulsions on the skin surface, and adhesiveness, which is essentially a surface characteristic, and depends on a combined effect of adhesive and cohesive forces. The ASt-emulsions showed a wide range of compressibility and adhesiveness values, again dependent on the concentrations of ASt and on the external phase type. The compressibility and adhesiveness increased markedly for LP, and for high amounts of ASt. In turn, CT improved the adhesiveness of the ASt-emulsions only when the ASt concentration exceeded 7.5% (w/w). As such, represented LP is a more suitable external phase for all concentrations of ASt.

The elasticity value is defined as the rate at which the deformed sample returns to the original form after removing the force. The amount of ASt and external phase type did not impact on this parameter, and the obtained values are suitable for skin application, as according to Jones *et al.* [28], lower values of elasticity indicate greater emulsion elasticity. Concerning cohesiveness, it provides information on the structural reformation following emulsion application. According to Table 3.1.5, it can be observed that the amount of ASt does not noticeably contribute to cohesiveness. TPA indicated that CT-based formulations were more cohesive than those LP-based formulations.

Once more, the results reflect an easier application and a higher adhesion, which is suitable to the compliance and to retain the ASt-emulsions in contact with the skin.

Table 3.1.5 - Mechanical properties of ASt-emulsions extracted from the TPA mode (mean ± SD, n=3).

Formulations		Compressibility (g.sec)	Hardness (g)	Adhesiveness (g.sec)	Elasticity	Cohesiveness
LP	- α	112.97 ± 5.84	79.14 ± 5.72	80.56 ± 4.27	0.99 ± 0.01	0.55 ± 0.02
	0	146.83 ± 1.71	102.93 ± 0.80	109.77 ± 8.35	1.00 ± 0.01	0.56 ± 0.03
	α	161.54 ± 5.09	109.75 ± 5.26	103.04 ± 9.13	0.99 ± 0.01	0.52 ± 0.02
CT	- α	44.20 ± 0.32	32.01 ± 1.76	41.67 ± 7.58	0.99 ± 0.01	0.66 ± 0.04
	0	52.56 ± 5.27	37.65 ± 3.78	42.52 ± 3.74	0.98 ± 0.01	0.62 ± 0.03
	α	138.65 ± 5.66	96.31 ± 4.17	112.54 ± 5.04	0.98 ± 0.01	0.60 ± 0.02

3.2.2.4 DSC and hot stage microscopy

The thermograms obtained between 30 ºC and 120 ºC showed an endothermic peak at 68-82 ºC for all samples (Fig. 3.1.9). The thermo-microscopic investigations demonstrate no visible change in the emulsions until 60 ºC. Emulsions maintained their integrity up to 70ºC but above this temperature a dramatic change in structure occurred with the loss of the initial structure (Fig. 3.1.9 a3 and b3). Rearrangements of the water droplets can occur and this phenomenon is certainly associated with starch gelatinization and swelling.

The barrier properties of the oil-water interface of the emulsions stabilized by ASt granules can be improved by heating. Starch granules swell and gelatinize when heated in aqueous medium, improving the physical barrier of the emulsions. The gelatinization process, which is an endothermic reaction, includes the swelling of starch granules, amylose leakage and loss of molecular and crystalline properties. It was shown that by heating under carefully chosen conditions, the surface of the ASt granules can be partially gelatinized, creating an enhanced barrier in the interface and an impermeable layer around the droplets, preserving droplet stabilization [8].

The kinetic parameters of the main peak (onset, peak and endset temperatures and integral value) calculated by DSC software analysis are given in Table 3.1.6. The integral value that corresponds to the area under the curve gives the extent of the total enthalpy change and can be correlated with physical stability of the systems [29]. The results confirm that α-ASt-emulsions correspond to the strongest structures. Correlating these values with the rheological, mechanical and stability results, one can conclude that α-LP and α-CT-ASt-emulsions present the strongest and more stable structures.

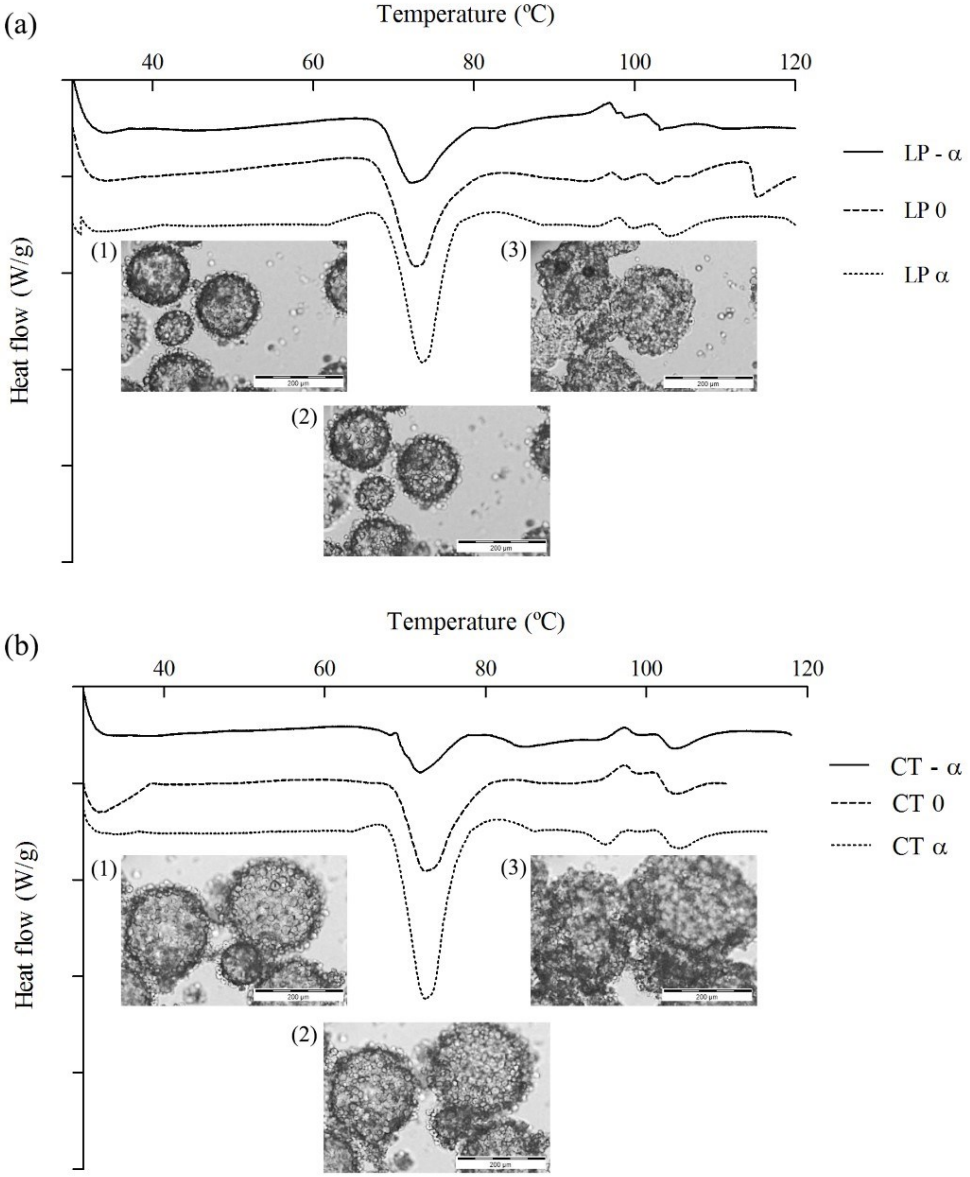

Fig. 3.1.9 - DSC thermograms of ASt-emulsions: (a) LP and (b) CT with photomicrographs of α-ASt-emulsions during a heating program with 10 °C/min between 30 °C and 120 °C. At 60 ºC (1), at 70 ºC (2) and at 80 ºC (3) (Scale bar = 200 µm).

Table 3.1.6 - Calorimetric parameters of ASt-emulsions.

Formulations		T_{onset} (°C)	T_{endset} (°C)	T_{peak} (°C)	Integral value (W ºC g^{-1})
LP	- α	68.58 ± 0.18	81.61 ± 0.46	72.35 ± 0.20	-0.46 ± 0.08
	0	68.69 ± 0.37	82.31 ± 0.25	72.36 ± 0.54	-0.78 ± 0.03
	α	68.95 ± 0.29	80.07 ± 0.45	72.51 ± 0.12	-1.36 ± 0.15
CT	- α	68.53 ± 0.83	78.86 ± 0.93	72.04 ± 0.16	-0.26 ± 0.05
	0	69.34 ± 0.18	79.02 ± 0.16	72.56 ± 0.14	-0.58 ± 0.03
	α	68.59 ± 0.27	79.13 ± 1.44	73.35 ± 0.40	-1.11 ± 0.11

3.2.2.5 Microscopy analysis

Micrographs show the size of the droplets and the microstructure of the systems depend on the amount of ASt used (Fig. 3.1.10). Moreover, in α-ASt-emulsions, several small inner drops of water, with homogeneous size were observed dispersed in the oil phase. In the –α-ASt-emulsions and intermediate (0 level) amounts of ASt, larger inner oil droplets with a non-homogenous size were seen. The droplet size differences between these emulsions are probably due to a coalescence phenomenon occurring in -α and 0-ASt-emulsions.

Concerning the external phase, no significant influence on the microstructure of the emulsions was detected. Finally, microscopy analysis corroborated the DoE results, evidencing a decrease in droplet size with the increase of ASt concentration.

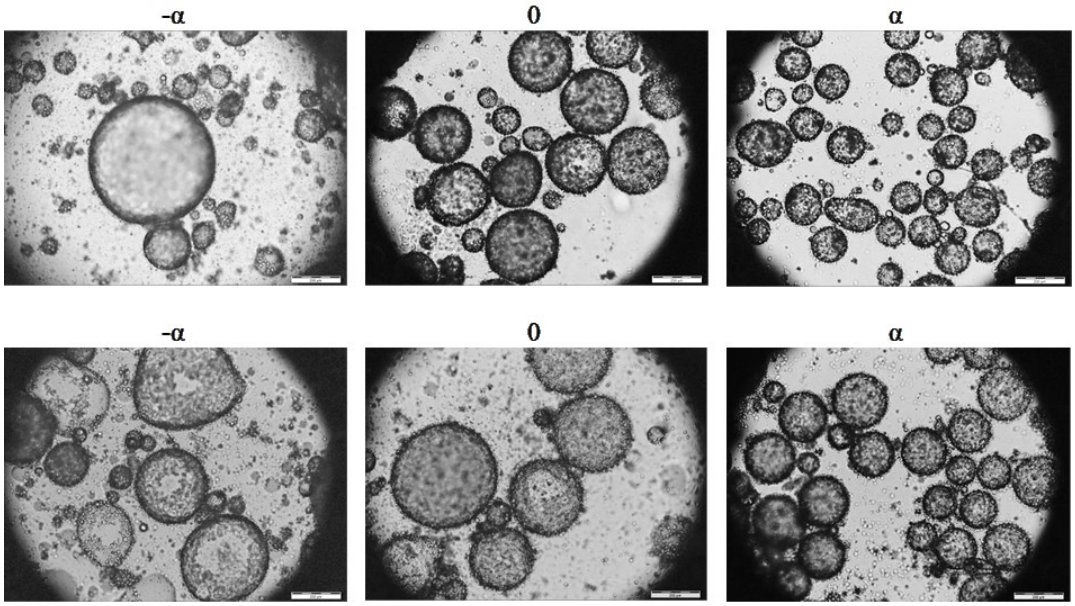

Fig. 3.1.10 - Micrographs of (above) LP and (below) CT emulsions after 1 week of preparation (Scale bar = 200 μm).

3.2.3 *In vitro* cytotoxicity studies

To investigate the potential cytotoxicity of the emulsions, the cell viability was evaluated by performing a MTT assay in HaCaT cells. Emulsions with low (- α level), medium (0) and high (α level) ASt concentrations and also with different external phases (LP and CT) were selected for cytotoxicity testing. Emulsions stabilized by surfactants (CE) (Span® 80 and Tween® 80) were used as controls. The ASt-stabilized emulsions were not cytotoxic to HaCaT cells at the tested concentration (Fig. 3.1.11). The incorporation of surfactants into the emulsions (LP CE and CT CE) maintains HaCat cell viability.

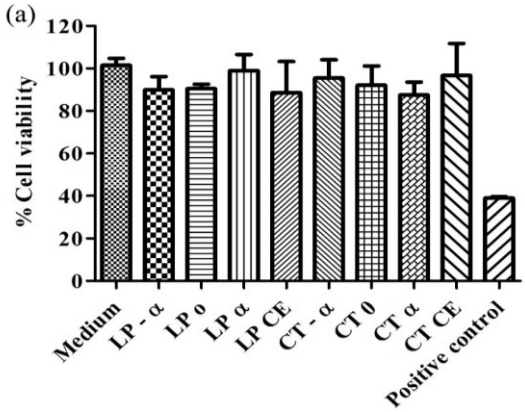

Fig. 3.1.11 - Cell viability of HaCaT cells after 24 h of incubation with ASt-emulsions, emulsions stabilized by surfactants (CE) and positive control (SDS - sodium dodecyl sulfate) (mean ± SD, n=10).

It should be noticed that cytotoxicity assays are generally regarded as a method that is able to provide a cost-effective, and reproducible index of viability for skin cells and an alternative for skin irritation assessment, but it cannot be expected that the behavior of cultured cells is exactly consistent with that of the skin. Unlike the skin tissue, the groups of cells cultured for the cytotoxicity assay is noticeably less complex in number and cell types when compared to the skin tissue. Therefore, the results should be regarded as an indicator of potential and relative toxicity and irritation of the compounds to the skin cells. Human keratinocytes, which are affected first by drugs or actives components, are recognized to be involved in a multiplicity of inflammatory and immune responses of the skin. Hence, keratinocytes should be a more suitable cell model for evaluating sensitivity of the skin to potential irritants [30].

In the present study, cells were exposed to test samples during 24 h with the cell viability above 50 %. Hence, all emulsions stabilized by ASt can be considered as non-irritant, and the different amount of ASt used can be considered as safe. These results are supported by previous conclusions that indicated the absence of any skin irritation or sensitization at tested concentrations as high as 30.5 % [16].

3.2.4 Antimicrobial activity

ASt-emulsions with low (-α level), medium (0) and high (α level) ASt concentrations and also with different external phases (LP and CT) were selected for testing for antimicrobial activity. In general, for bacteria (*P. aeruginosa and S. aureus*), a decrease in the cfu was found after the first 48 h and for *C. albicans* and *A. brasiliensis* a 2 log reduction was

noticed after 7 days, followed by undetectable or no increase cfu for the subsequent observation days. Thus, all emulsions complied with the A criteria for bacteria and fungi and B criterium for yeasts. The emulsions revealed an antimicrobial activity, which complies with the requirements of the preservation efficacy test for topical formulations according to Ph. Eur. (5.1.3.). The lipid and also the amount of ASt seem to influence the antimicrobial activity of the vehicle, probably, due to the relatively high oil content. However, few studies confirmed this theory.

The w/o emulsions, where the oil is the continuous phase, are less prone to microbial contamination, compared to o/w emulsions, because the oil constitutes another obstacle for the proliferation of microorganisms [31]. Microorganisms require water for growing and, therefore, formulations that somehow limit water availability help control microbial growth. Different classes of microorganisms exhibit different tolerance to low water content and the obtained results confirmed this statement. As a rule, bacteria have higher water requirements than yeasts, and yeasts higher requests than molds [32]. Synergistically, medium chain saturated fatty acids, such as caprylic (C8) and capric (C10) triglycerides have been found to possess antimicrobial activity against various bacteria and fungi in *in vitro* studies [33]. Particularly, capric acid, a 10-carbon saturated fatty acid, causes a fast and an effective killing of *C. albicans* [34].

Interestingly, starch is an excellent nutrient source but it was proved that corn starch did not improve yeast proliferation on human skin [35, 36], while some authors demonstrated the synergistic action of starch on the antifungal activity of additional excipients [37]. The present study confirms these particular w/o emulsions present self-preservation properties with the advantages of avoiding the adverse effects often associated with antimicrobial preservatives [38].

3.2.5 Microstructure of ASt-emulsions

In view of the results, a hypothetical model for the microstructure of the ASt-emulsions may be proposed with a certain degree of accuracy. Fig. 3.1.12 depicts model whereby the stabilization of w/o emulsions by solid particles involves three main consecutive phenomena: 1) dispersed ASt granules forming a pendular state in the continuous phase (oil phase - yellow), i.e., the particles are kept suspended in the liquid that preferentially wet the particles. This happens when the contact angle is low and the added liquid wets the particles; 2) a spherical agglomeration, in which the drops of the internal phase form the nuclei of particle agglomerates. In this case, the contact angle with the internal phase is >

90° and the added liquid fails to wet the particles; and 3) a w/o emulsion is produced adding more quantity of the internal phase. The particles in suspension irreversibly adsorb onto fresh liquid-liquid interfaces and the inner droplets are rapidly coated with particles creating an emulsion stabilized by ASt particles [39].

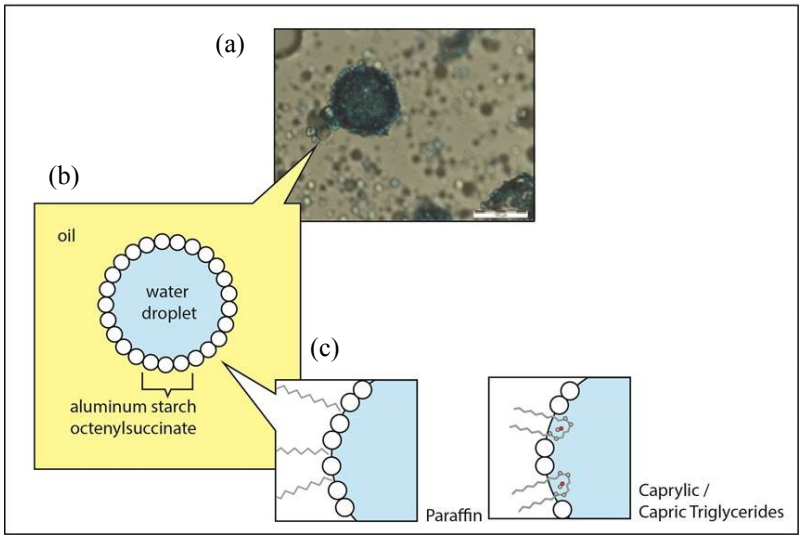

Fig. 3.1.12 - Structure of the proposed model for w/o emulsion stabilized by ASt granules. a) water-soluble dye methylene blue, which only stained the disperse droplets, demonstrating that a w/o emulsion has been formed; b) water droplet; c) molecules involved in the interfacial phenomenon.

4 Conclusions

The design planning methodology has clearly shown its usefulness in the optimization of process and formula and, therefore, the present work provides a framework for the understanding the formation of emulsions stabilized by ASt. The production of these emulsions was optimized in terms of composition (qualitative and quantitative) and process using a QbD approach. It was possible to obtain a DS for ASt-emulsion preparation with minimum variability and assuring product quality, thus benefitting industry in terms both of time and costs. Concerning physical stability, the emulsions with high levels of ASt remained stable for at least 12 weeks. This is quite remarkable if we consider that a high concentration of ASt is within the range of the DS established to obtain a structured with the desirable droplet size ASt-emulsion. In addition, these developed formulations can be considered self-preserving and non-irritant, increasing the shelf-life of the product. ASt-stabilized emulsions are therefore an attractive, promising, simple and novel platform for the production of pharmaceutical and cosmetics vehicles.

5 References

1. Bouyer E, Mekhloufi G, Rosilio V, Grossiord JL, Agnely F. Proteins, polysaccharides, and their complexes used as stabilizers for emulsions: alternatives to synthetic surfactants in the pharmaceutical field? International Journal of Pharmaceutics. 2012;436(1-2):359-378.

2. Chevalier Y, Bolzinger M-A. Emulsions stabilized with solid nanoparticles: Pickering emulsions. Colloids and Surfaces A: Physicochemical and Engineering Aspects. 2013;439(0):23-34.

3. Matos M, Timgren A, Sjöö M, Dejmek P, Rayner M. Preparation and encapsulation properties of double Pickering emulsions stabilized by quinoa starch granules. Colloids and Surfaces A: Physicochemical and Engineering Aspects. 2013;423(0):147-153.

4. Binks BP. Particles as surfactants—similarities and differences. Current Opinion in Colloid & Interface Science. 2002;7(1–2):21-41.

5. Marku D, Wahlgren M, Rayner M, Sjöö M, Timgren A. Characterization of starch Pickering emulsions for potential applications in topical formulations. International Journal of Pharmaceutics. 2012;428(1–2):1-7.

6. Frelichowska J, Bolzinger MA, Pelletier J, Valour JP, Chevalier Y. Topical delivery of lipophilic drugs from o/w Pickering emulsions. International Journal of Pharmaceutics. 2009;371(1-2):56-63.

7. Kaewsaneha C, Tangboriboonrat P, Polpanich D, Eissa M, Elaissari A. Preparation of Janus colloidal particles via Pickering emulsion: An overview. Colloids and Surfaces A: Physicochemical and Engineering Aspects. 2013;439(0):35-42.

8. Timgren A, Rayner M, Sjöö M, Dejmek P. Starch particles for food based Pickering emulsions. Procedia Food Science. 2011;1(0):95-103.

9. ICHQ8(R2). ICH Harmonised tripartite guideline pharmaceutical development Q8(R2). www.ich.org; 2012.

10. Dejaegher B, Heyden YV. Experimental designs and their recent advances in set-up, data interpretation, and analytical applications. Journal of Pharmaceutical and Biomedical Analysis. 2011;56(2):141-158.

11. BS. Methods for determination of particle size distribution. Part 4, Guide to microscope and image analysis methods. British Standards 3406-4:19931993. p. 36.

12. Rayner M, Marku D, Eriksson M, Sjöö M, Dejmek P, Wahlgren M. Biomass-based particles for the formulation of Pickering type emulsions in food and topical applications. Colloids and Surfaces A: Physicochemical and Engineering Aspects. 2014;458(0):48-62.

13. ICHQ1A(R2). ICH of Technical Requirement for Registration of Pharmaceuticals for Human Use, Stability Testing of new Drugs and Products. www.ich.org; 2003.

14. EP. European Pharmacopoeia 8. Strasbourg: Council Of Europe : European Directorate for the Quality of Medicines and Healthcare; 2014.

15. Chang F, He X, Fu X, Huang Q, Qiu Y. Preparation and characterization of modified starch granules with high hydrophobicity and flowability. Food Chemistry. 2014;152(0):177-183.

16. Nair B, Yamarik TA. Final report on the safety assessment of aluminum starch octenylsuccinate. International Journal of Toxicology. 2002;21 Suppl 1:1-7.

17. Sweedman MC, Tizzotti MJ, Schäfer C, Gilbert RG. Structure and physicochemical properties of octenyl succinic anhydride modified starches: A review. Carbohydrate Polymers. 2013;92(1):905-920.

18. Aveyard R, Clint JH, Horozov TS. Aspects of the stabilisation of emulsions by solid particles: Effects of line tension and monolayer curvature energy. Physical Chemistry Chemical Physics. 2003;5(11):2398.

19. Schulman JH, Leja J. Control of contact angles at the oil-water-solid interfaces. Emulsions stabilized by solid particles (BaSO4). Transactions of the Faraday Society. 1954;50(0):598-605.

20. Vitorino C, Carvalho FA, Almeida AJ, Sousa JJ, Pais AA. The size of solid lipid nanoparticles: an interpretation from experimental design. Colloids and Surfaces B: Biointerfaces. 2011;84(1):117-130.

21. Maaß S, Paul N, Kraume M. Influence of the dispersed phase fraction on experimental and predicted drop size distributions in breakage dominated stirred systems. Chemical Engineering Science. 2012;76(0):140-153.

22. Lam S, Velikov KP, Velev OD. Pickering stabilization of foams and emulsions with particles of biological origin. Current Opinion in Colloid & Interface Science. 2014;19(5):490-500.

23. Anisa ANI, H.Nour A. Affect of Viscosity and Droplet Diameter on water-in-oil (w/o) Emulsions: An Experimental Study. World Academy of Science, Engineering and Technology. 2010;4(2):4.

24. Li C, Li Y, Sun P, Yang C. Pickering emulsions stabilized by native starch granules. Colloids and Surfaces A: Physicochemical and Engineering Aspects. 2013;431:142-149.

25. Morishita C, Kawaguchi M. Rheological and interfacial properties of Pickering emulsions prepared by fumed silica suspensions pre-adsorbed poly(N-isopropylacrylamide). Colloids and Surfaces A: Physicochemical and Engineering Aspects. 2009;335(1–3):138-143.

26. Silva SMC, Pinto FV, Antunes FE, Miguel MG, Sousa JJS, Pais AACC. Aggregation and gelation in hydroxypropylmethyl cellulose aqueous solutions. Journal of Colloid and Interface Science. 2008;327(2):333-340.

27. Lippacher A, Muller RH, Mader K. Liquid and semisolid SLN dispersions for topical application: rheological characterization. European journal of pharmaceutics and biopharmaceutics : official journal of Arbeitsgemeinschaft fur Pharmazeutische Verfahrenstechnik e.V. 2004;58(3):561-567.

28. Jones DS, Woolfson AD, Djokic J. Texture profile analysis of bioadhesive polymeric semisolids: Mechanical characterization and investigation of interactions between formulation components. Journal of Applied Polymer Science. 1996;61(12):2229-2234.

29. Labes-Carrier C, Dumas JP, Mendiboure B, Lachaise J. DSC as a tool to predict emulsion stability. Journal of Dispersion Science and Technology. 1995;16(7):607-631.

30. Olschlager V, Schrader A, Hockertz S. Comparison of primary human fibroblasts and keratinocytes with immortalized cell lines regarding their sensitivity to sodium

dodecyl sulfate in a neutral red uptake cytotoxicity assay. Arzneimittel-Forschung. 2009;59(3):146-152.

31. Dweck AC. Natural preservatives. Cosmetics and Toiletries. 2003;118(8):45-50.

32. Varvaresou A, Papageorgiou S, Tsirivas E, Protopapa E, Kintziou H, Kefala V, Demetzos C. Self-preserving cosmetics. International Journal of Cosmetic Science. 2009;31(3):163-175.

33. Kabara JJ, Swieczkowski DM, Conley AJ, Truant JP. Fatty acids and derivatives as antimicrobial agents. Antimicrobial Agents and Chemotherapy. 1972;2(1):23-28.

34. Bergsson G, Arnfinnsson J, Steingrimsson O, Thormar H. In vitro killing of Candida albicans by fatty acids and monoglycerides. Antimicrobial Agents and Chemotherapy. 2001;45(11):3209-3212.

35. Santana IL, Goncalves LM, de Vasconcellos AA, da Silva WJ, Cury JA, Del Bel Cury AA. Dietary carbohydrates modulate Candida albicans biofilm development on the denture surface. PloS one. 2013;8(5):e64645.

36. Leyden JJ. Corn starch, Candida albicans, and diaper rash. Pediatric Dermatology. 1984;1(4):322-325.

37. Boukraa L, Bouchegrane S. Additive action of honey and starch against Candida albicans and Aspergillus niger. Revista Iberoamericana de Micologia. 2007;24(4):309-311.

38. Shaughnessy CN, Malajian D, Belsito DV. Cutaneous delayed-type hypersensitivity in patients with atopic dermatitis: Reactivity to topical preservatives. Journal of the American Academy of Dermatology. 2014;70(1):102-107.

39. Aveyard R, Clint JH, Horozov TS. Aspects of the stabilisation of emulsions by solid particles: Effects of line tension and monolayer curvature energy. Physical Chemistry Chemical Physics. 2003;5(11):2398-2409.

Section 2

Minocycline-loaded starch-based Pickering emulsions: *in vitro* and *in vivo* studies

This page was intentionally left blank

Graphical Abstract

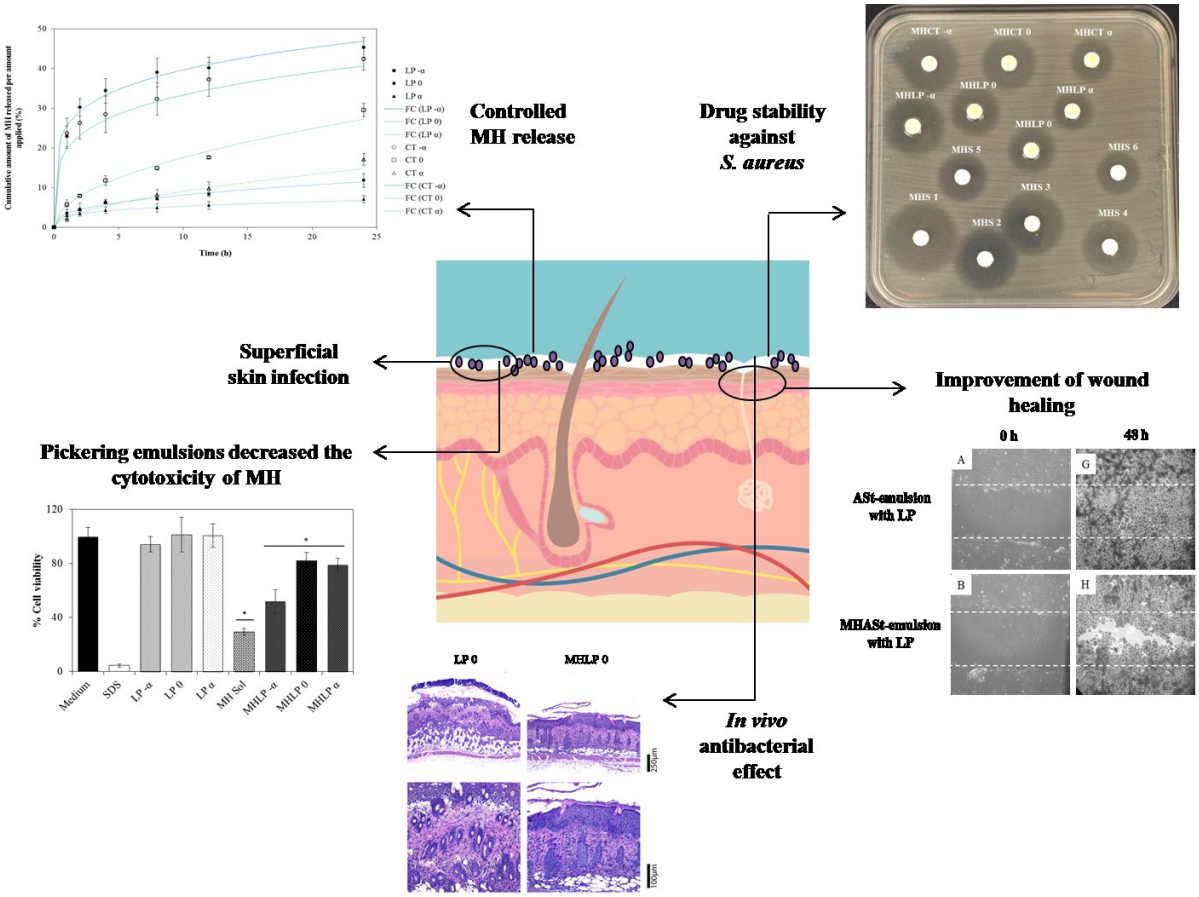

Highlights:

- Pickering emulsions containing minocycline (MH) (MHASt-emulsions) showed sustained drug release through synthetic membranes.
- No retention of the MH was detected in the skin and the drug did not pass through the entire skin layer.
- Antibacterial activity studies for MHASt-emulsions revealed that the drug released exceeded the minimum inhibitory concentration of MH against *S. aureus*.
- MHASt-emulsions decreased the cytotoxicity of MH and greatly improved wound healing.
- MHASt-emulsions are safe vehicles for topical antibiotherapy.

This page was intentionally left blank

1 Introduction

The skin is the major organ that protects the body from microorganisms and other environmental pathogens. In injuries such as burns and trauma, the skin becomes vulnerable to microbial invasion due to the skin's integrity loss and local and systemic immunity suppression. As a result, superficial infection may not only delay the wound healing process, but also can cause systemic infection under severe conditions, such as burns and bedsores, among others [1]. The most common Gram-positive bacterial pathogen that colonizes wounds and causes infection is *Staphylococcus aureus*. Topical antibiotics are used to treat skin infection or as prophylaxis to prevent skin from further infection [2].

Minocycline hydrochloride (MH), a tetracycline analog, has proven to be effective in eradicating topical pathogens implicated in superficial infections, especially those caused by Gram-positive bacteria [3, 4]. Apart from its antibacterial activity, MH shows additional important pharmacological effects for the management of skin diseases, including collagenase inhibition, anti-inflammatory action and antioxidant activity [5]. There is a concern regarding MH systemic side effects, namely opportunistic yeast infection (*Candida spp.*), gastrointestinal disturbance and cutaneous symptoms (pigmentation). In addition, the oral administration of MH requires long-term treatments [6]. For these reasons, the topical route could be advantageous for the administration of MH. Moreover, it has also been reported that drug concentration in skin layers resulting from a single topical application is much higher than those obtained after prolonged oral administration, and persists there at measurable amounts for four or more days [7, 8]. Hence, the topical application of MH requires a much lower amount of drug to achieve similar integumentary levels compared with the amount required via oral administration [1, 9].

There is a recent trend for producing novel carriers loaded with antibiotics to increase drug's solubility and allow topical application. Literature describes topical dosage forms loaded with MH with concentrations ranging from 0.25 - 4% [1, 9, 10]. In fact, numerous drug delivery strategies have been tried to develop MH topical formulations, such as ointments [9], hydrogels [1, 3], foams [11] and microspheres [10, 12]. Despite these studies, topical MH advanced formulations still remain in the experimental therapeutic field. For instance, Pickering emulsions have been studied for biomedical and pharmaceutical applications because of their non-toxic and non-carcinogenic characteristics and good skin biocompatibility [13].

Thus, the purpose of this study was to develop and fully characterize novel starch-based Pickering emulsions for topical delivery of MH in order to increase its efficacy and safety. The *in vitro* release and permeation studies and the *in vivo* efficacy studies were also evaluated in detail, demonstrating the successful application of starch-based Pickering emulsions and highlighting their potential for sustained drug release, acting as a promising vehicle for delivery of topical antibiotics.

2 Material and methods

2.1 Materials

The materials used are described in Chapter 2, section 2.1. Minocycline hydrochloride (MH) was obtained from Laboratórios Atral S.A. (Castanheira do Ribatejo, Portugal).

2.2 Methods

2.2.1 Preparation of MH-loaded starch-stabilized emulsions (MHASt-emulsions)

Six w/o emulsions stabilized by ASt granules were prepared considering the optimization studies previously described (Chapter 3, Section 1). Purified water was used as disperse phase, where MH was previously dissolved, and CT or LP were used as continuous phase. The ASt particles were first dispersed in the oil phase using a vortex mixer until total dispersion (2.5 %, 5.0 % and 7.5 % of starch). The oil and aqueous phases were then mixed together with an UltraTurrax® T25 homogenizer (IKA®-Werke GmbH & Co. KG, Germany). The compositions of the MHASt-emulsions are described in Table 3.2.1.

Table 3.2.1 - Qualitative and quantitative composition of the optimized MHASt-emulsions (please refer to Chapter 3, Section 1 for details).

Formulations	Quantitative composition (%, w/w)											
	ASt-emulsion with LP			ASt-emulsion with CT			MHASt-emulsion with LP			MHASt-emulsion with CT		
	-α	0	α	-α	0	α	-α	0	α	-α	0	α
Phase A (external)												
Liquid paraffin	72.50	70.00	67.50	-	-	-	72.45	69.95	67.45	-	-	-
Caprylic/capric acid triglyceride	-	-	-	72.50	70.00	67.50	-	-	-	72.45	69.95	67.45
Phase B (solid particles)												
Aluminum starch octenylsuccinate	2.50	5.00	7.50	2.50	5.00	7.50	2.50	5.00	7.50	2.50	5.00	7.50
Phase C (internal)												
Purified water	25.00	25.00	25.00	25.00	25.00	25.00	25.00	25.00	25.00	25.00	25.00	25.00
Minocycline hydrochloride	-	-	-	-	-	-	0.05	0.05	0.05	0.05	0.05	0.05

2.2.2 Microscopic aspect of MHASt-emulsions

The microscopic aspect of MHAst-emulsions was confirmed, using the methodology previously described in Chapter 3, Section 1, section 2.2.2.2.

2.2.3 Stability of MHASt-emulsions

All formulations were stored according to the procedure previously described in Chapter 3, Section 1, section 2.2.6.

2.2.4 *In vitro* release studies

Release of MH from Pickering emulsions was measured in infinite dose conditions using hydrophilic polysulfone membranes filters (Tuffryn®, 0.45 µm) from Pall Corporation (New York, USA) with a diffusion area of 1 cm^2. The membranes were washed and equilibrated with receptor phase during 12 h and then, set between the donor and receiver compartments of the Franz diffusion cells (receptor volume: 3 ml, permeation area: 1 cm^2). The receptor phase was purified water. The system was maintained at 37 ± 2 ºC for about 30 min before the experiment starts. The samples were then applied (0.3 g ± 0.1 g) evenly on the surface of the membrane in the donor compartment and immediately sealed with Parafilm® to prevent evaporation. Samples of the receptor phase (200 µl) were collected at predefined times (1, 2, 4, 8, 12 and 24 h). After sampling, the same volume was replaced with fresh receptor phase kept at the same temperature. These release tests were performed using 6 Franz cells per formulation. The amount of released drug was assayed by using the flow injection analysis described below.

The data obtained from *in vitro* release studies were computed using DDsolver [14], which is an Excel-plugin module, and the resultant data were fitted to five different kinetic models [15, 16]:

1) Zero order

Equation 1: $F = K_0 \times t$

Where, K_0 is the zero order release constant.

2) First order

Equation 2: $F = 100 \times (1 - e^{-K_1 \times t})$

Where, K_1 is the first order release constant.

3) Higuchi model

Equation 3: $F = K_H \times \sqrt{t}$

Where, K_H is the Higuchi release constant.

4) Korsmeyer-Peppas

Equation 4: $F = K_{KP} \times t^n$

Where, K_{KP} is the release constant incorporating structural and geometric characteristics of the drug-dosage form and *n* is the diffusional exponent indicating the drug-release mechanism.

5) Weibull

Equation 5: $F = 100 \times \left(1 - e^{-\frac{(t-Ti)^\beta}{\alpha}}\right)$

Where, α is the scale parameter which defines the time scale of the process; β is the shape parameter which characterizes the curve as either exponential (β=1), sigmoid, S-shaped, with upward curvature followed by a turning point (β>1), or parabolic, with a higher initial slope and after that consistent with the exponential (β<1). T_i is the location parameter, which represents the lag time before the onset of the dissolution or release process and, in most cases, will be near to zero.

In all models, F is the fraction (%) of released drug in time, t. The adjusted coefficient of determination ($R^2_{adjusted}$) was estimated for each model, fitted and used as a model ability to describe a given dataset.

The dissolution efficiency (DE) was calculated from the area under the dissolution curve up to a certain time *t*, according to the following equation [17]:

Equation 6: $DE = \frac{\int_0^t y \times dt}{y_{100} \times t} \times 100$

Where *y* is the percentage of dissolved drug at time *t*. In the present study DE was calculated at 24 h ($DE_{24\,h}$).

2.2.5 Topical delivery studies of *MH*

2.2.5.1 In vitro skin permeation

The skin permeation of MH was measured using Franz diffusion cells and newborn pig skin obtained from a local slaughterhouse. The entire skin was cut into sections (1 cm^2 permeation area). Purified water was used as the receptor phase that assured perfect sink conditions during all experiment period. The cells were immersed in a bath system at 37 ± 2 °C under stirring (200 rpm). The formulations samples were applied (0.3 ± 0.1 g, infinite dose experiment) on the skin surface in the donor compartment further sealed by Parafilm® in order to prevent the water evaporation (occlusive conditions). Samples were collected from the receptor fluid at pre-determined time points 2, 4, 8, 12 and 24 h and replaced with an equivalent amount (200 µl) of fresh receptor medium. The MH content in the withdrawn samples was determined as below described.

2.2.5.2 In vitro skin retention

In vitro skin retention or penetration study was performed by tape stripping according to the method recommended by OECD Guideline 428 [18]. The MHASt-emulsions (0.3 ± 0.1 g) were spread over the newborn pig skin (1 cm^2) in contact with 4 ml of receptor phase as described before. After 24 h, skin samples were rinsed to remove the excess of formulation and dried with filter paper. After the skin samples had been attached and fixed on a smooth surface, the *stratum corneum* (SC) was removed using 20 adhesive tapes (Scotch® 3M, UK). In order to ensure the reproducibility of the tape stripping technique, a cylinder (2 kg) on foam and an acrylic disk were used and the pressure was applied for 10 s for each tape. All the tapes (excluding the first one) with the removed SC and the remaining skin (viable epidermis and dermis - ED) were cut into small pieces used for the extraction process previously validated. In this extraction process, 3 ml of ethanol was added to the SC tapes and ED pieces. Both samples were vigorously stirred for 2 min in a vertical mixer (Kinematica AG), and sonicated for 20 min to lyse cells. The final solution was centrifuged (30000 rpm, 10 min) and the supernatant was filtered (0.2 µm) and assayed as above described to quantify the amount (%) of MH retained in these skin layers (SC + ED).

2.2.5.3 Flow injection analysis of MH content

The samples were analyzed using a HP 1100 series System liquid chromatography (VWR, USA) equipped with a pump (G1310A), an autosampler (G1329A) and an UV detector (G1328A). Peaks were detected at 280 nm and the corresponding areas were estimated by

the Value Solution ChemStation software. Purified water pumped at 1.0 ml/min was used as sample (10 µl) carrier. The auto sampler chamber was maintained at room temperature. The running time was 0.5 min.

2.2.6 *In vitro* cytotoxicity studies

2.2.6.1 Cell culture conditions

The cell culture conditions are described in Chapter 2, section 2.2.5.1.

2.2.6.2 Cytotoxicity assays

To determine *in vitro* emulsions effects on cell viability, cells were incubated with ASt-emulsions and MHASt-emulsions for 24 h and cell viability was determined using the MTT assay as described in detail in Chapter 2, section 2.2.5.2. The percentage of viable cells was established relatively to cells treated with vehicle, for drug in solution, and for drug into emulsions. Inhibitory concentrations (IC_{50}) were calculated using GraphPad Prism® software v5.0 (GraphPad Software, Inc., USA) by the sigmoidal curve fitting method.

2.2.6.3 Scratch wound healing migration assay

Cells were seeded onto six-well plates and cultured until high confluence. The monolayer was wounded by scraping it with a sterile tip. The wells were washed twice with medium without serum and then finally with complete culture medium. The healing process was examined during the time with an optical microscope and the wounds microphotographs were obtained at time 0, 24 and 48 h after making the wound. The area of the wounds for the different time-points were compared with the wound area at time 0, in order to evaluate the migration rate of cells.

2.2.7 *In vitro* determination of the antibacterial activity of MH in ASt-emulsions

The standard curve and the minimum inhibitory concentration (MIC) of MH against *Staphylococcus aureus* ATCC 6538 was first determined. Different concentrations of MH solutions were prepared in sterile distilled water and tested against *S. aureus* using the standard disc diffusion method (DDM), in accordance with the Clinical and Laboratory Standards Institute Standards (CLSI) guidelines [19].

To accomplish this, the microorganism inoculum was prepared from 18 h broth culture and the suspension was then adjusted to a turbidity of 0.5 McFarland (~1.5×10^8 colony-forming

units (cfu/ml). Then, the Mueller-Hinton agar (MHA) (Thermo Scientific™ Oxoid™, UK) was poured into petri dishes and inoculated with 100 µl of the suspension containing ~1.5×10^8 cfu/ml of bacteria. Sterile paper discs (6 mm; Thermo Scientific™ Oxoid™, UK) were loaded with 15 µl of MH solution with different concentrations, ranging from 17 to 545 µg/ml. After incubation at 37 °C for 24 h, the mean of the inhibition zone diameters and the standard deviation were calculated and, the lowest concentration of MH capable of inhibiting growth after 24 h of incubation was then recorded as the MIC. The MIC of MH against *S. aureus* was determined by plotting the square of inhibition zone diameter from back of plate using a caliper, against the corresponding log drug concentrations.

2.2.7.1 Disc diffusion method

The antibacterial activity of the MH on the different ASt-emulsions was tested using the DDM described by the CLSI. The DDM allowed the evaluation of the different modifications in ASt-emulsions on the antibacterial activity, namely the effect of starch concentration and lipid type. MH was used as the positive control and a blank disc was used as the negative control. The antibacterial activity was tested according to the procedure described previously in section 2.2.7. After incubation time, the efficacy of each tested formulation was determined by measuring the inhibition zone.

2.2.7.2 Skin adapted agar diffusion test

This method is an adaptation of a well-known *in vitro* assay (DDM) to verify the effectiveness of antibiotic product contained in topical formulations. In this adapted test, instead of antibiotic impregnated discs, newborn pig skin discs were used. Skin discs were made with 13 mm biopsy punches and disinfected using ethanol at 70%. An aliquot of 15 µl of test formulations were applied on skin discs that were then incubated on mannitol salt agar plate (MSA) (Thermo Scientific™ Oxoid™, UK) inoculated with *S. aureus* 24 h at 37°C. After incubation time, the efficacy of each tested formulation was determined by measuring the inhibition zone diameter.

Another skin adapted test was performed. In this test, an aliquot of 15 µl of test formulations were applied twice daily for 1 day on infected skin discs with *S. aureus* (~ 1.5×10^8 cfu/ml) that were then incubated on MSA, during 24 h at 37 °C. After incubation time, the efficacy of tested formulations was determined by cfu determination. Carry-over effect was minimized by performing the cfu determinations >18 h after the last treatment.

2.2.8 In vivo studies

2.2.8.1 In vivo antibacterial activity studies: tape-stripping and infection model

Animal tape-stripping and infection experiments were performed according to Kugelberg *et al*. [20]. Briefly, eight-week-old female BALB/c mice (Instituto Gulbenkian de Ciências, Oeiras, Portugal) were used. All animals were acclimatized before the experiments and housed in plastic cages under standard laboratory conditions, fed commercial chow and acidified drinking water *ad libitum*. All animal experiments were carried out with the permission of the local animal ethical committee in accordance with the EU Directive (2010/63/EU), Portuguese law (DL 113/2013) and all relevant legislations. Mice were anesthetized by intraperitoneal injection of a mixture of ketamine (75 mg/kg body weight) and medetomidine (1 mg/kg body weight), the hair of the dorsum, midline, was clipped and the skin was stripped 4 times with adhesive tapes (Transpore™, 3M) with ca. 4 cm^2 of area.

In order to standardize the degree of barrier disruption elicited by the tape stripping, the transepidermal water loss (TEWL) was measured by using Tewameter TM 210 (C+K Electronics GmbH, Germany). TEWL is calculated automatically and is expressed in $g/h.m^2$. By tape stripping the back of the mice the TEWL reached approximately 50 $g/h.m^2$. The skin became visibly red but no bleeding occurred. After stripping, a bacterial infection was initiated by placing on the skin 20 µl containing ~ 3.7×10^8 cfu/ml of *S.aureus* ATCC 6538 culture from an overnight culture.

Six groups of animals, each containing 5 mice were used. The infected mice were treated with 10 mg/ml clyndamicine phosphate topical solution (Commercial solution (CS) - Dalacin® T, Pfizer) (Group 1), with ASt-emulsion with LP (Group 2), with MHASt-emulsion with LP (Group 3), with ASt-emulsion with CT (Group 4), or with MHASt-emulsion with CT (Group 5), and a group of infected mice remained untreated working as the infection control (Group 6). An additional group of three stripped mice but not infected was used to control the stripping damage on the skin. For each treatment, a volume of 100 µl was applied epicutaneously. The first application was made 4 h post-infection. Thereafter, beginning at 16 h after the first treatment, additional applications were made twice daily with an 8 h interval for a period of 4 days. For all treatment/control groups the experiments endded 18 h after the last topical treatment and the CFU were determined, as follows. An area of ca. 4 cm^2, centered on the lesion, was scrubbed ten times with a swab moistened in brain heart infusion broth (BHI) (Thermo Scientific™ Oxoid™, UK). Swabs were serially diluted in BHI and then plated on duplicate MSA, which were subsequently

incubated overnight at 37 °C. Typical colonies were then determined as the total number of cfu/ml using log10-transformed data. Data were analyzed using the GraphPad PRISM® 5 software (San Diego, CA, USA) and the groups were considered significant when the estimated *p* values were lower than 0.1 (the chosen α error), to increase statistical power.

2.2.8.2 Skin histology

In order to assess the histological features of the lesions, mice from all groups previously describe were sacrificed with CO_2 narcosis, and skin wounds were excised with a wide margin of normal skin (approx. 2 mm) and processed for routine histology. Briefly, excised wounds were immediately placed onto a small piece of cardboard, with the subcutaneous tissue facing down, and immersed in 10% neutral buffered formalin (Sigma-Aldrich®, Germany). After fixation, trimming was performed longitudinally, in the direction of the hair flow and centered on the wound. Samples were embedded in paraffin, sectioned at 4 μm, and stained with hematoxylin and eosin (H&E). Histopathological analysis was performed by a pathologist blinded to experimental groups using Nanozoomer SQ slide scanner and NDP.view2 software (Hamamatsu). The criteria used to stage the lesion and to perform semi-quantitative analysis of the inflammatory cell infiltration are resumed in Table 3.2.2 [21].

Table 3.2.2 - Histopathological criteria used for wound healing staging and for semi-quantitative analysis of inflammation [21].

Numerical score	Tissue-specific parameters		Inflammation
	Epidermis	Dermis	
1	ulceration	inflammation	none
2	early stage regeneration	inflammation and tissue formation	minimal
3	severe hyperplasia with crust formation	tissue formation	mild
4	hyperplasia	tissue remodeling, early	moderate
5	resolved	tissue remodeling, late	severe
6	-	resolved	-

2.2.9 Statistical analysis

Two or one-way analysis of variance when appropriate (ANOVA) and Tukey–Kramer post-hoc multiple comparison test were used to identify the significant differences between

the groups and were performed using GraphPad PRISM® 5 software. An α error of 5% was chosen to set the significance level unless stated otherwise.

3 Results and discussion

3.1 Formulation development

3.1.1 Drug substance: MH as a model drug

The active substance used as a model drug in the emulsions was MH due to its hydrophilic character. It has a molecular weight of 493.9 g/mol and a LogP of -0.65, making it an unsuitable candidate for topical delivery [22]. The MH (7-dimethylamino-6- demethyl-6-deoxytetracycline hydrochloride) is a yellow crystalline powder and is essentially odorless and has a somewhat bitter taste (Fig. 3.2.1). The main physicochemical properties of MH are described in Table 3.2.3.

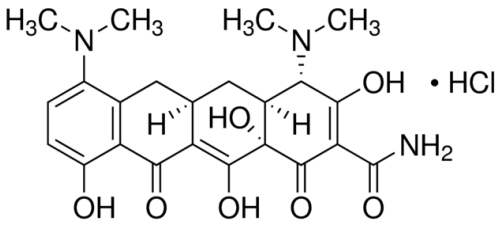

Fig. 3.2.1 - Chemical structure of MH [22].

It is a semi-synthetic tetracycline, which has broad spectrum activity against many aerobic and anaerobic Gram-positive and Gram-negative bacteria, including some strains of staphylococci and streptococci resistant to tetracycline. MH is generally more active than other tetracyclines against Gram-positive organisms. It has a wide range of potential clinical indications such as respiratory tract, and sexually transmitted infections, acne vulgaris and skin structure infection [22]. Apart from its antibacterial activity, MH shows additional significant pharmacological effects, including collagenase inhibition and anti-inflammatory action [3].

Table 3.2.3 - Physicochemical properties of MH according to [22] and [23].

Molecular formula	$C_{23}H_{28}ClN_3O_7$
Molecular weight	493.9 g/mol
Solubility	Sparingly soluble in water, slightly soluble in ethanol (96˚). It dissolves in solutions of alkali hydroxides and carbonates.
Melting point	217 ºC
LogP	-0.65
Maximum absorption (λ max)	263 nm (0.1N HCl) and 243 nm (0.1N NaOH)

3.1.2 Optimization of MHASt-emulsions

In previous work (Chapter 3, Section 1), the optimization of experimental conditions to obtained stable ASt-emulsions was established and, pharmaceutically acceptable formulations were achieved. This previous work clearly indicates that ASt-emulsions characteristics are highly influenced by the amount of starch and lipid type.

3.1.2.1 Microscopy analysis

Optical microscopy images of MHASt-emulsions revealed the emulsions' microstructure and showed that MH does not influence the droplet size distribution, when compared with ASt-emulsions (Chapter 3, Section 1). The size of the droplets and the microstructure of MHASt-emulsions stabilized by ASt only depend on the amount of ASt used (Fig. 3.2.2). Moreover, in α-MHASt-emulsions, several small inner drops of water, with homogeneous size were observed being dispersed in the oil phase. The MHASt-emulsions with low and intermediate amounts of ASt, exhibited a heterogeneous structure with larger inner oil droplets. The droplet size differences between these emulsions are probably due to insufficient coverage at the oil-water interface. Thus, aggregation of droplets may lead to coalescence and the formation of larger droplets until the phases become separated.

3.1.3 Stability of MHASt-emulsions

The macroscopic characteristics of MHASt-emulsions were assessed by visual inspection throughout 12 weeks at 25 ± 2 °C. It was concluded that the MH does not influence the MHASt-emulsions stability, since no more coalescence or phase separation were observed in these emulsions, when compared with ASt-emulsions (Chapter 3, Section 1).

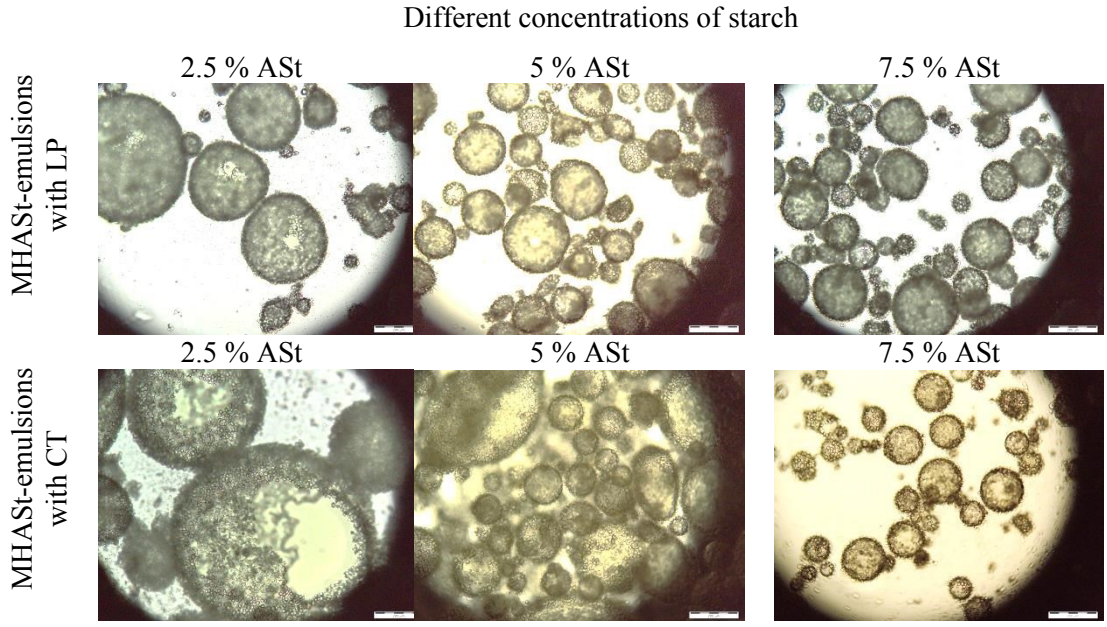

Fig. 3.2.2 - Micrographs of (above) LP and (below) CT MHASt-emulsions after 1 week of preparation (Scale bar = 200 μm). ASt - Aluminum starch octenylsuccinate.

In the present study, coalescence occurred firstly in the emulsions with the lowest level of ASt, in the second week of storage, followed by phase separation on week 4. This is also occurred with the emulsions prepared with the central level of ASt. The α-MHASt-emulsions, with the highest level of ASt, maintained their stability during the 12 weeks after preparation. With sufficient coverage at the interface, which is the case of α-MHASt-emulsions, ASt particles act as barriers against droplet coalescence that enhance the emulsion stability [24, 25]. Unlike surfactants, ASt particles do not reduce the oil-water interfacial tension, but they strongly get adsorbed at the oil-water interface. However, particle adsorption on the oil-water interface is a slow process and needs to be enhanced by mixing [26].

3.2 *In vitro* release studies

The results MH release as a function of time, during 24 h, through the Tuffryn® membrane are shown in Fig. 3.2.3. As graphically illustrated, the studied emulsions successfully release the drug. From the ANOVA statistical analysis, it can be concluded that there were significant differences between the formulations containing different amounts of starch and also between the lipid type used ($p < 0.05$).

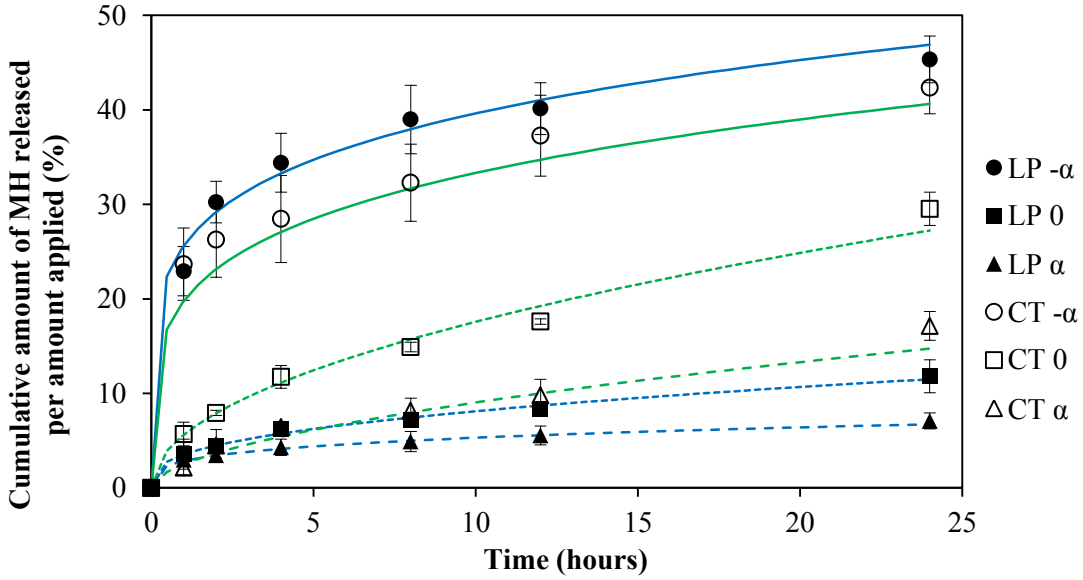

Fig. 3.2.3 - Release profile and fitting curve of Korsmeyer-Peppas model for MH from MHASt-emulsions through Tuffryn® membrane in water at 37 ºC (mean ± SD, n = 6). LP – MHASt-emulsions with LP; CT - MHASt-emulsions with CT; - α – 2.5 % ASt; 0 – 5 % ASt; α – 7.5% ASt.

In order to achieve a controlled released of the MH, it is crucial to have the drug strictly confined in the water droplets of w/o MHASt-emulsions. Therefore, the choice of LP and CT as continuous phase was motivated by the very low solubility of MH in both external phases that makes the partition coefficient of MH between aqueous and oil phases to be very low. MH was used as a model water-soluble compound in skin absorption studies mainly because of its low LogP value (LogP = − 0.65), indicating that MH was restricted to the water phase of the emulsion.

The lipid and also the amount of starch seem to influence the release of MH from the vehicle. In fact, after 1 h, the MH release was higher from emulsions containing less starch when compared with emulsions containing more starch. At the end of the study (24 h), when it is compared the emulsions with the same concentration of starch, the emulsions with CT had a higher accumulated amount of released MH.

Additionally, the release pattern of MH from the emulsions with low concentration of starch had a burst release at the early stage. This phenomenon occurs due to the incomplete coverage by ASt particles at the interface that will allow a faster and easier release of MH from the droplet. The release of MH from the emulsions with high concentration of starch was considerably slowed down compared to the emulsions with lower concentration of starch, suggesting that the shell of starch particles around the droplets acted as a barrier to

interfacial diffusion. This barrier might retard the release by the presence of "starch-packed" granules and the increased viscosity. In contrast, the extent of drug release was often greater from formulations comprising low concentration of starch.

Indeed, it is quite a general characteristic that drug encapsulation provides a sustained delivery. This was often observed for systems such as liposomes and solid lipid nanoparticles [27, 28]. The possible encapsulation inside w/o Pickering emulsions droplets has often been put away, because the starch granules form a rigid shell around the droplets. MH transport mechanism could be a result of MH adsorption at starch surface. Moreover, it is known that many solutes can be adsorbed at the surface of solid particles [29, 30].

In order to describe the kinetics of drug release and the discernment of the release mechanisms, the drug release data were fitted to first order, Higuchi, Korsmeyer-Peppas and Weibull kinetic models and then analyzed. The results showed that the Korsmeyer-Peppas kinetic model best fitted the 24 h release profile as confirmed by the highest values for $R^2_{adjusted}$ and model selection criterion (MSC) and lowest values for Akaike Information Criterion (AIC) [14]. The parameter n in the Korsmeyer-Peppas equation is related to the mechanism of drug release, i.e. if the exponent $n < 0.5$, then the drug release mechanism is Fickian diffusion, if $0.5 < n < 1$, then it is non-Fickian or anomalous diffusion and if the exponent value is 1 or greater is indicative of Case-II Transport or typical zero-order release [31]. The determined values of diffusion exponent (n) ranged between 0.18 and 0.49 (Table 3.2.4 and 3.2.5). These results indicated that the drug release from these MHASt-emulsions followed the Fickian diffusion, which means that the drug is released *via* usual molecular diffusion through the system [31]. This finding indicates that the rate-controlling mechanism in the drug release process is the diffusion of the dissolved drug through the vehicle network to the external medium, which is in agreement with other studies [32, 33].

The DE values were used to compare the potential parameters and evaluate the dissolution profiles of different emulsions. Those values for the total time profile (24 h) indicated higher dissolution efficiency for the emulsions with low concentration of starch ($p < 0.05$) (Table 3.2.4 and 3.2.5). Emulsions containing high percentage of starch showed lower dissolution efficiency and a slow dissolution. These results justify the existence of a relation between starch concentration, lipid type and DE, which however, was confirmed only for the results of the cumulative amounts of released MH.

Table 3.2.4 - Kinetic parameters obtained after fitting the release data from the MHASt-emulsions with LP to different release models (mean ± SD, n=6).

	Model	K	$R^2_{adjusted}$	AIC	$T_{50\%}$ (h)	$T_{90\%}$ (h)	$DE_{24\ h}$ (% ± SD)
-α-MHASt-emulsion with LP	First order	0.05	0.723	55.3	14.3	47.5	38.4 ± 5.4
	Higuchi	14.68	0.731	38.3	12.0	39.0	
	Korsmeyer-Peppas	25.63	0.973	25.6	56.3	2388.9	
		n - 0.18					
	Weibull	α - 3.14	0.972	26.3	83.9	12432.0	
		β - 0.20					
		Ti - 0.53					
0-MHASt-emulsion with LP	First order	0.01	0.838	30.4	111.1	369.1	8.1 ± 0.2
	Higuchi	2.53	0.960	16.6	390.1	1263.9	
	Korsmeyer-Peppas	3.53	0.989	4.2	13683.2	185438.2	
		n - 0.39					
	Weibull	α - 27.17	0.985	5.1	148476.5	10288670.6	
		β - 0.35					
		Ti - 0.40					
α-MHASt-emulsion with LP	First order	0.00	0.273	24.5	182.2	605.1	5.3 ± 0.9
	Higuchi	1.63	0.871	13.1	979.1	3172.1	
	Korsmeyer-Peppas	2.84	0.997	9.3	71257.0	723399.2	
		n - 0.27					
	Weibull	α - 31.79	0.996	11.7	902911.8	39677378.5	
		β - 0.24					
		Ti - 0.40					

K – release constant; $R^2_{ajusted}$ - adjusted coefficient of determination; AIC - Akaike Information Criterion; $T_{50\%}$ - time required for 50% dissolution; $T_{75\%}$ - time required for 75% dissolution; $T_{90\%}$ - time required for 90% dissolution; DE_{24h} – dissolution efficiency at 24h of release study; n - release exponent; α – scale parameter; β – shape parameter; Ti – location parameter.

Table 3.2.5 - Kinetic parameters obtained after fitting the release data from the MHASt-emulsions with CT to different release models (mean ± SD, n=6).

		Model	K	$R^2_{adjusted}$	AIC	$T_{50\%}$ (min)	$T_{90\%}$ (min)	$DE_{24\ h}$ (% ± SD)
-α-MHASt-emulsion with	CT	First order	0.05	0.139	50.1	15.8	52.6	40.1 ± 8.3
		Higuchi	11.99	0.775	40.7	18.2	58.8	
		Korsmeyer-Peppas	25.10	0.988	22.2	38.8	743.7	
			n - 0.20					
		Weibull	α - 3.31	0.974	28.3	283.7	2577.2	
			β - 0.21					
			Ti - 0.40					
0-MHASt-emulsion with	CT	First order	0.02	0.886	31.6	43.8	145.7	17.9 ± 0.3
		Higuchi	5.65	0.981	18.3	78.4	254.0	
		Korsmeyer-Peppas	5.60	0.988	14.4	85.8	291.9	
			n - 0.40					
		Weibull	α - 14.72	0.974	22.1	153.9	1015.0	
			β - 0.47					
			Ti - 0.42					
α-MHASt-emulsion with	CT	First order	0.01	0.8693	25.6	94.5	313.8	9.3 ± 1.7
		Higuchi	2.91	0.9884	8.6	317.0	1027.2	
		Korsmeyer-Peppas	2.50	0.9967	0.5	228.4	660.9	
			n - 0.49					
		Weibull	α - 33.44	0.9846	11.8	507.4	2717.3	
			β - 0.51					
			Ti - 0.40					

K – release constant; $R^2_{ajusted}$ - adjusted coefficient of determination; AIC - Akaike Information Criterion; $T_{50\%}$ - time required for 50% dissolution; $T_{75\%}$ - time required for 75% dissolution; $T_{90\%}$ - time required for 90% dissolution; DE_{24h} – dissolution efficiency at 24h of release study; n - release exponent; α – scale parameter; β – shape parameter; Ti – location parameter.

3.3 Topical delivery studies of MH

No retention was detected in the skin within 24 h of exposure and MH did not pass through the entire skin layer, suggesting a minimal potential for the systemic absorption of MH upon topical administration. Nonetheless, it is important to understand how Pickering emulsions can be used to modulate the drugs penetration through the SC and to control the drug release at different skin sites, as Pickering emulsions are useful and multifunctional topical vehicles [24].

Concerning the particles from Pickering emulsions, several studies demonstrated the possibility of particles acting as carriers through the skin [24, 30, 34]. Particles smaller than 3 μm penetrate both by diffusion through the SC and by the hair follicles path. On the other hand, particles of size ranging from 3 to 10 μm manly penetrate into hair follicles and particles larger than 10 μm remain on the skin surface, which is the case of ASt particles (Chapter 3, Section 1) [35]. Thus, it is not expected that ASt particles may act as a skin carrier in MHASt-emulsions.

Hydration of the SC is one of the primary procedures to increase the penetration of most active molecules. Water has the ability to open up the compact structure of the horny layer. The water content of the horny layer can be increased either by delivering water from the vehicle to the skin or by preventing water loss from the skin when partially occlusive formulations are applied to the skin, becoming an important skin permeation pathway for hydrophilic molecules. Thus, the long term topical application of w/o emulsions decreases the water retention and increases the hydration of the skin, providing a healthier skin barrier with a higher permeation aptitude [36, 37]. This phenomenon was confirmed by *in vivo* studies obtained in the microcirculation results and after a long term application of ASt-emulsions (Chapter 7). Concerning the external phase type, polar solvents, such as CT, greatly increase the penetration into the skin [38]. On the other hand, LP is a non-polar solvent, creating an occlusive barrier onto the membrane. Several authors demonstrated that occlusion effect is widely used to enhance the penetration of applied drugs in clinical practice [39, 40]. However, occlusion does not increase percutaneous absorption of all chemicals. It may increase the penetration of lipid-soluble, non-polar molecules but has less effect on polar molecules, which is the case of MH [41].

Thus, regarding highly lipophilic molecules, Pickering emulsions promote high accumulation in the SC. The practical utility of such behavior is either preventing skin penetration of molecules that should be retained at the skin surface, e.g. sunscreens and topical antibiotics or using the SC as a reservoir for slow release of the drug to the deeper skin layers. One indication of Pickering emulsions, regarding a pharmaceutical application, is for a sustained and targeted release to the viable epidermis, from drug reservoir in the deeper layers of SC. This same mechanism has been claimed for nano- and microparticles skin drug delivery [34].

3.4 *In vitro* studies

3.4.1 *In vitro* cytotoxicity studies

To investigate the potential cytotoxicity of the MHASt-emulsions, cell viability was evaluated using HaCaT cell line in a MTT assay. Firstly, the IC_{50} of the drug in solution was determined by a non-linear regression analysis, and subsequently, the found concentration was used to determine the cell viability after application of the emulsions. The cytotoxicity of MH in water (525 µg/ml) was also analyzed.

The solubilized MH in water or formulated in emulsions presented different behaviors in terms of cell toxicity. It was found that the IC_{50} of the MH aqueous solution was 50.9 ± 1.0 µg/ml. However, using the same concentration, it was observed that the emulsions decreased the cytotoxicity of MH (Fig. 3.2.4). Finally, MH incorporation in emulsions protects the human cells keratinocytes from the cytotoxicity of the drug. Cell viability increased to more than 50%, depending on the starch concentration. As we can see in Fig. 3.2.3 and Fig. 3.2.4, drug diffusion started to happen in the emulsions with the lowest level of starch, decreasing the cell viability and, this could be due to the fact that with less starch, the interface between oil and water might not be fully covered, leading to an earlier drug diffusion.

Additionally, according to the OECD guideline, an irritant substance is predicted if the mean relative tissue viability is found below 50% of the mean viability of the negative controls for a 15 – 60 min of exposition time [42]. Thus, the formulations can be intended as non-irritant and the used amount of starch and MH can be considered as safe. These results are in line with findings described in the literature, whereby starch concentrations as great as 30.5 % are devoided of skin irritation or sensitization [43].

Moreover, emulsions stabilized by solid particles can be distinguished from emulsions stabilized with classic emulsifiers concerning their irritative potential, for the reason that emulsifiers have the potential to act as penetration enhancers by disturbing SC integrity and hence may enable or enhance diffusion of other molecules through the skin [44, 45]. On the other hand, the starch granules, due to their high molecular weight (> 10000 Da), are not able to penetrate the SC. As a general rule, chemicals with a molecular weight greater than 500 Da do not penetrate the skin. This upper limit on molecular size mainly results from the physical arrangement of lipids between adjacent corneocytes of the SC [46, 47].

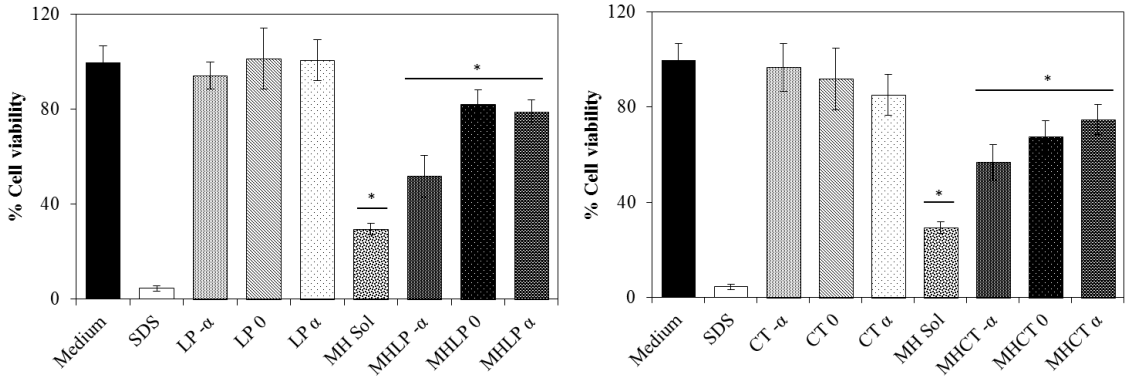

Fig. 3.2.4 - Viability of HaCaT cells after 24 h of incubation with MH at the concentration of 525 μg/ml, either in the free form or incorporated into the emulsions (a) LP (b) CT; - α – 2.5 % ASt; 0 – 5 % ASt; α – 7.5% ASt; SDS - sodium dodecyl sulfate (mean ± SD, n=10) (* $p < 0.05$).

3.4.2 Scratch wound healing migration assay

To assess an additional usefulness to ASt-emulsions and MH, we performed *in vitro* scratch wound healing assays with HaCaT cells in the presence or absence of MH. In order to evaluate the influence of ASt-emulsions and MH on the wound healing, 0-ASt-emulsions were studied.

In untreated HaCaT cells, 0-MHASt-emulsions and MH solution did not repair scratch wounds after 48 h, but treatment with 0-ASt-emulsions led to complete closure of the wound in 48 h (Fig. 3.2.5). Thus, irrespective of the addition of MH, ASt-emulsions greatly improved wound healing. In addition, there was no significant difference between the ASt-emulsions with LP and CT or between MHASt-emulsions with LP and CT. According to several authors, modified starches have been reported to accelerate wound healing and presented highly absorptive capacity [48, 49]. On the other hand, the migration of HaCaT cells could be blocked by MH due to its cytotoxicity (Fig. 3.2.4).

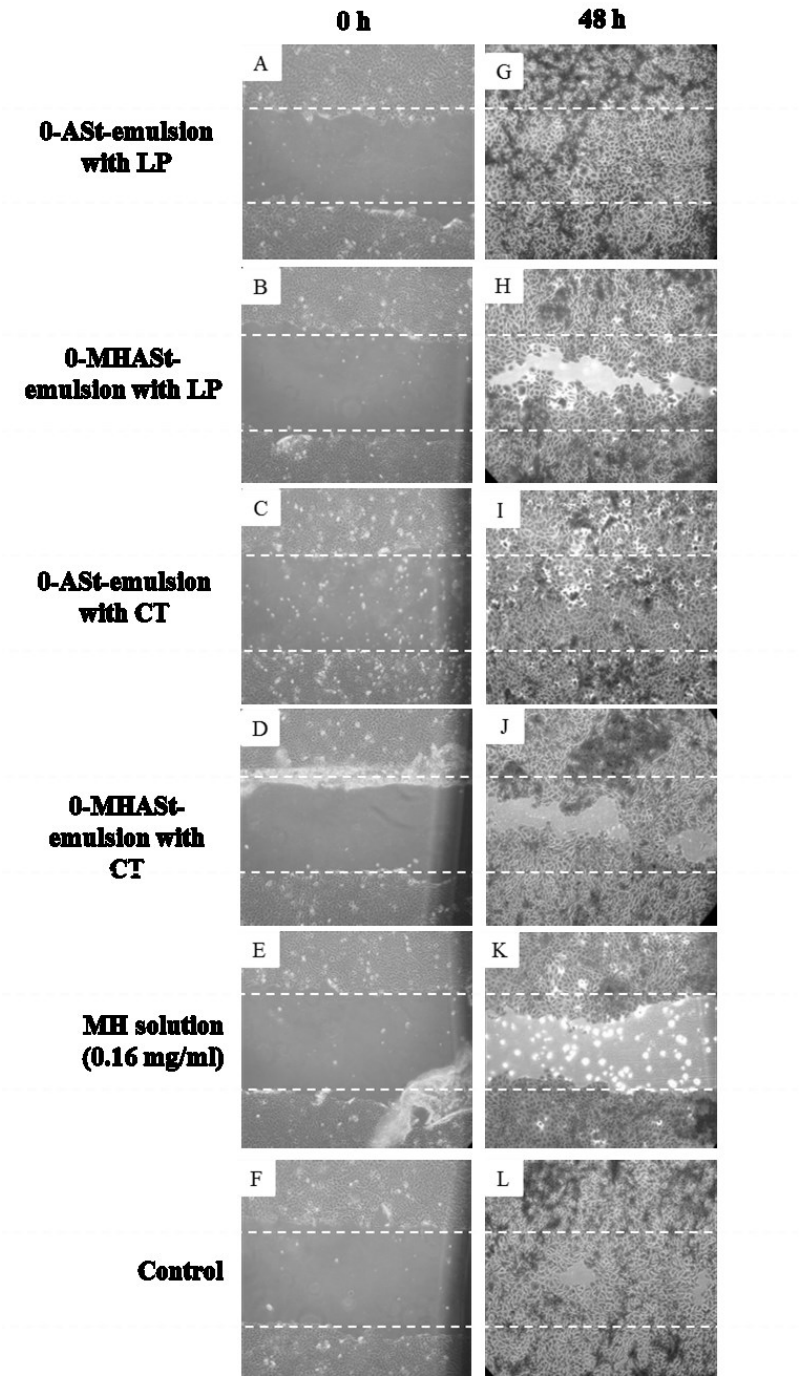

Fig. 3.2.5 - Representative time-lapse images of HaCaT keratinocyte scratch assays immediately after the scratches had been made and then after 48 h in the presence of 0--emulsions with LP (A, G), 0-MHASt-emulsions with LP (B, H), 0-ASt-emulsions with CT (C, I), 0-MHASt-emulsions with CT (D, J), MH solution (E, K) or control medium (F, L). The cells were allowed to migrate for 48 h, fixed and photographed. Outlines of the original wounds are marked with dashed lines. Original magnification 40×.

3.4.3 *In vitro* determination of the antibacterial activity of MH in ASt-emulsions

The *in vitro* antibacterial activity of MH in MHASt-emulsions was tested against *S. aureus* ATCC 6538. All tested MHASt-emulsions gave a mean inhibition zone after 24 h incubation between 14.9-22.8 mm, which significantly exceeded that of the calculated MIC value for MH (13.38 mm) against the same microorganism (Table 3.2.6). All ASt-emulsions showed no growth inhibition of microorganism. These results revealed that the amount of released drug from the formula exceeded the MIC against the tested microorganism (0.190 µg/ml) (Table 3.2.6).

Table 3.2.6 - Comparison of zone of inhibition produced by MHASt-emulsions after 24 h of incubation (mean ± SD, n=3).

Formulations		Zone of inhibition (mm)	Concentration of MH released (µg/ml)
MHASt-emulsions with LP	- α	22.8 ± 0.7	1.90 ± 0.12
	0	19.3 ± 0.2	1.12 ± 0.03
	α	14.9 ± 0.3	0.45 ± 0.05
MHASt-emulsions with CT	- α	22.5 ± 0.4	1.88 ± 0.04
	0	20.1 ± 0.9	1.41 ± 0.15
	α	16.5 ± 1.0	0.75 ± 0.19
Blank disc	-	-	-

LP – Liquid paraffin; CT - caprylic/capric acid triglyceride; - α – 2.5 % ASt; 0 – 5 % ASt; α – 7.5% ASt

3.4.4 Skin adapted agar diffusion test

This test intends to assess local susceptibility rates, with the diameter of the inhibition zone being proportional to the sensitivity of the microorganism and the efficacy of the antibacterial drug. Fig. 3.2.6 illustrates two possible outcomes of this test [50].

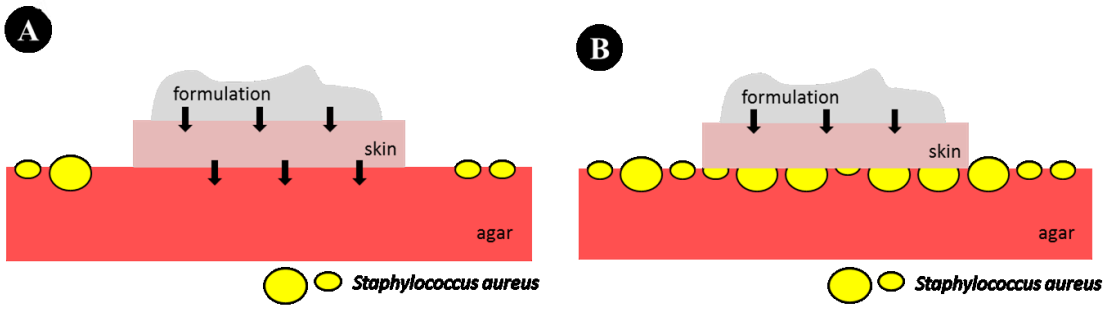

Fig. 3.2.6 - Skin adapted agar diffusion test cross sections. A - Drug skin permeation (black arrows) inhibits *S. aureus* growth and an inhibition zone is observed around the skin disk. B - Drug skin retention (black arrows) does not inhibit *S. aureus* growth. No inhibition zone is observed under the skin neither around the skin disk.

Results obtained on skin adapted agar diffusion test revealed no drug skin permeation (Fig. 3.2.7), i.e. the situation illustrated in Fig. 3.2.6 B. These findings are in accordance with permeation measurements that confirmed the absence of permeated MH from MHASt-emulsions, thus no zone of inhibition was observed around the skin disk, neither under it. Furthermore, no inhibition was observed after incubation in the blank disc containing only skin without formulation. However, aqueous solutions of MH promoted zone of inhibition surrounding the skin discs, which corresponds to the diffusion of MH and lower skin adhesion. Since MH was confined inside the water droplets of ASt-emulsions, direct MH transfer to the skin may take place if water droplets are deposited on the skin surface, confirming earlier findings reported by other authors [30], who demonstrated that w/o Pickering emulsion droplets adhered better to the skin surface than the water droplets.

Fig. 3.2.7 - Skin adapted agar diffusion test. MHS – Solution of MH ranging from 17 to 545 µg/ml. MHLP – MHASt-emulsion with liquid paraffin; MHCT – MHASt-emulsions with caprylic/capric acid triglyceride.

In another study, skin discs were inoculated with *S. aureus* (~ 5.7×10^8 cfu/ml) and were treated twice daily with MH solution (272.5 µg/ml), ASt-emulsions and MHASt-emulsions. Total bacterial loads in the skin discs were determined 18 h after the last treatment. The effect of different external phases (liquid paraffin or caprylic/capric acid triglyceride), or starch at various concentrations, was studied. The topical treatment with MHASt-emulsions resulted in a significant reduction of the bacterial loads in the skin discs

compared with ASt-emulsions (Fig. 3.2.8). For MH solution and MHASt-emulsions treated skin discs, no bacteria were detectable after 1 day of treatment ($p < 0.05$). Not surprisingly, the ASt-emulsions without MH had weak or no antimicrobial activity at all, but it was important to explore any potential antimicrobial effect of excipients in these formulations. No significant difference was observed between the external phases. However, when testing α-MHASt-emulsions, a slight increase on bacterial burden was observed, which is in line with the *in vitro* release studies. As long as the release of MH from α-MHASt-emulsions was considerably decreased, suggesting that the close-packed layer of starch particles around the droplets acted as a barrier to interfacial diffusion [34].

Based on these results, and considering the data obtained from stability and *in vitro* release studies, 0-ASt-emulsions and 0-MHASt-emulsions were selected for *in vivo* studies.

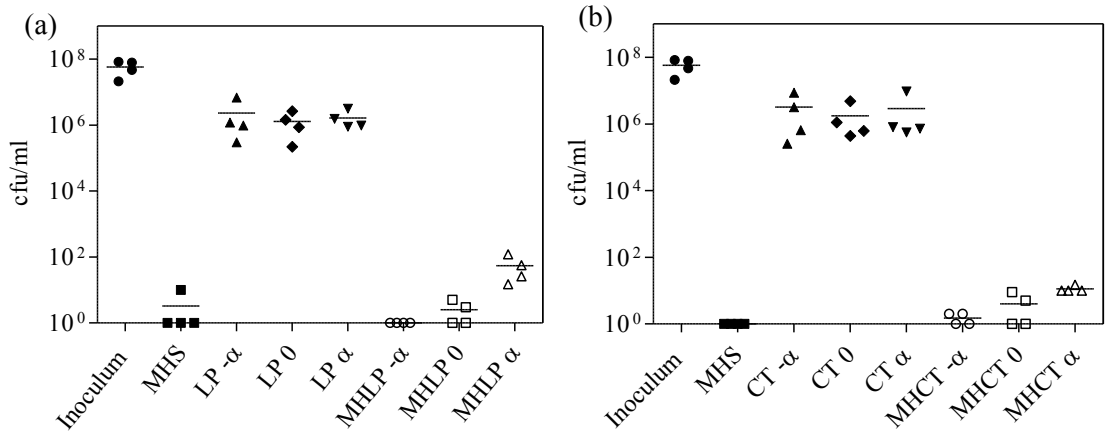

Fig. 3.2.8 – Effect of different formulations on antibacterial activity (a) MHASt-emulsion with liquid paraffin; (b) MHASt-emulsion with caprylic/capric acid triglyceride; - α – 2.5 % ASt; 0 – 5 % ASt; α – 7.5% ASt. Skin discs were infected with S. aureus ATCC 6538. The number of bacteria (cfu/ml) from each skin disc is represented by the symbol for the corresponding experimental group. The median value of the data for each group is shown as a horizontal bar (mean ± SD, n=4).

3.5 *In vivo* studies

3.5.1 *In vivo* antibacterial activity studies: tape-stripping infection model

The number of cfu recoverable from the skin 4 h after application of ~3.7×10^8 cfu/ml of *S. aureus* ATCC 6538 was 7.39 ± 0.36 log10 (Table 3.2.7). The different treatment regimens started after this initial 4 h period. There was no significant difference ($p < 0.1$) in the numbers of cfu/ml when 4 h *versus* 4 days of untreated mice were compared (6.83 ± 0.67 log10). This is an evidence of the successful establishment of a staphylococcal

infection in this model. There was a slightly greater reduction in the numbers of cfu/ml that was statistically significant ($p < 0.1$) when 4 h *versus* 4 days of ASt-emulsions and MHASt-emulsions treatment were compared (Table 3.2.7). The comparison of the treatments with ASt-emulsions and MHASt-emulsions revealed a reduction in the numbers of cfu/ml that was statistically significant ($p < 0.1$).

Table 3.2.7 - Bacterial counts obtained in the various treatment groups.

Group	Mean bacterial count (log10 cfu/ml)
Inoculum	7.67 ± 0.27
4 h post-infection	7.39 ± 0.36
Untreated (day 4)	6.83 ± 0.67
Commercial solution (day 4)	0.70 ± 0.96
0-ASt-emulsion with LP (day 4)	4.33 ± 0.45
0-MHASt-emulsion with LP (day 4)	0.52 ± 0.83
0-ASt-emulsion with CT (day 4)	4.09 ± 0.78
0-MHASt-emulsion with CT (day 4)	1.05 ± 0.98

Concerning the *in vivo* results, 0-MHASt-emulsions have been shown to provide sufficient MH concentration, i.e. exceeding the MICs of susceptible *S. aureus*. In this study, it was observed that 4 days of topical treatment with MHASt-emulsions resulted in significantly reduced bacterial loads (Fig. 3.2.9).

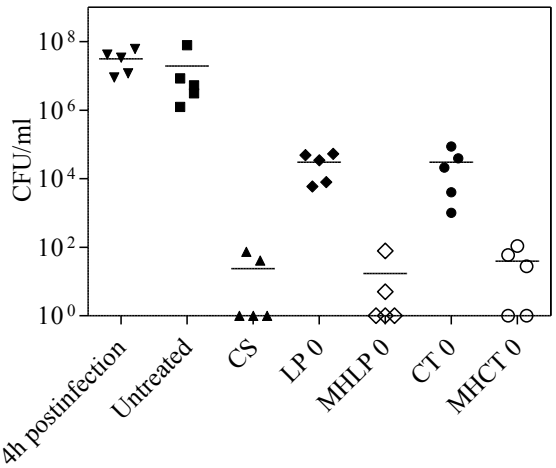

Fig. 3.2.9 – Effect of different formulations on antibacterial activity. Tape-stripped mice were infected with *S. aureus* ATCC 6538. The number of bacteria (cfu/ml) extracted from each mouse is represented by the symbol for the corresponding experimental group. The median value of the data for each group is shown as a horizontal bar. CS: Commercial solution; LP 0: 0-ASt-emulsions with LP; MHLP 0: 0-MHASt-emulsions with LP; CT 0: 0-ASt-emulsions with CT; MHCT 0: 0-MHASt-emulsions with CT.

The present study demonstrated that MHASt-emulsions were highly efficient in eradicating *S. aureus*-induced superficial infection. The clinical implications of the data herein presented suggest the possibility of substituting systemic antibiotic treatment by local treatment. Furthermore, topical treatment may have an advantage over systemic treatment to achieve rapid reduction of *S. aureus* bacterial loads in superficial skin infections. This would result in decreased drug exposure and the associated side effects, thus potentially increasing patient compliance. In addition, to these possible therapeutic benefits, a rapid bacterial death and short therapy regimens with MHASt-emulsions could ultimately result in reducing treatment costs and minimizing bacterial resistance.

3.5.2 Skin histology

Histological analysis of the wounds included staging the wound healing process and scoring the extent/severity of inflammatory cell infiltration, as described in section 2.2.8.2. Detailed results and representative micrographs are shown in Table 3.2.8 and Figure 3.2.10, respectively.

Table 3.2.8 - Histopathological analysis: semi-quantification of epidermal and dermal healing stage, and severity of inflammatory cell infiltration [21].

Group	Epidermis	Dermis	Inflammation
Untreated	3	2	moderate
CT0	4	4	mild
MHCT0	4	4	mild
LP0	3	4	mild
MHLP0	4	5	minimal to mild
CS	5	4	mild

CT 0: 0-ASt-emulsions with CT; MHCT 0: 0-MHASt-emulsions with CT; LP 0: 0-ASt-emulsions with LP; MHLP 0: 0-MHASt-emulsions with LP; CS: Commercial solution.

Epidermal reparation is a crucial step in cutaneous restoration of irritated skin and wound healing. It involves the combination of two cellular processes, i.e. proliferation and migration of epidermal cells. Simultaneously, dermal reparation occurs and generally follows several stages: inflammation, tissue formation, and finally remodeling [21]. In the present study, re-epithelization of the epidermis was seen in all groups. Untreated mice displayed severe hyperplasia, with crust formation, still with no hair follicle or adnexal gland differentiation/formation, and with important inflammatory cell infiltration and

active tissue formation in the dermis. In contrast, for all other groups, epidermal healing was generally at advanced stages of healing, hyperplastic but already with hair follicles and adnexal gland formation; the dermis was at late stages of remodeling and inflammatory cell infiltration was generally mild. In comparison with all other treatment groups, MHLP0 mice showed mildly decreased inflammatory cell infiltration. Some authors demonstrated that MH could markedly reduce the *in vivo* inflammatory activity. Thus, the present study corroborates the concomitant anti-inflammatory synergistic action on MH antibacterial activity [5].

Of note, for the starch-based formulations (groups CT0 e MHCT0), the epidermis was seen to display prominent irregular hyperplasia of the epithelium with tongue-like epithelial projections into the dermis. This is a reactive pattern of hyperplasia, which contrasts with the epidermal hyperplasia typically seen in the setting of wound healing and in all other groups, and appears to be induced by this vehicle. Only scarce bacteria were seen at the wound surface, in all groups.

In sum, these results suggest MH encapsulated in Pickering emulsions may be a useful and promising approach for the treatment of superficial bacterial infection such as rosacea and impetigo [51, 52] .

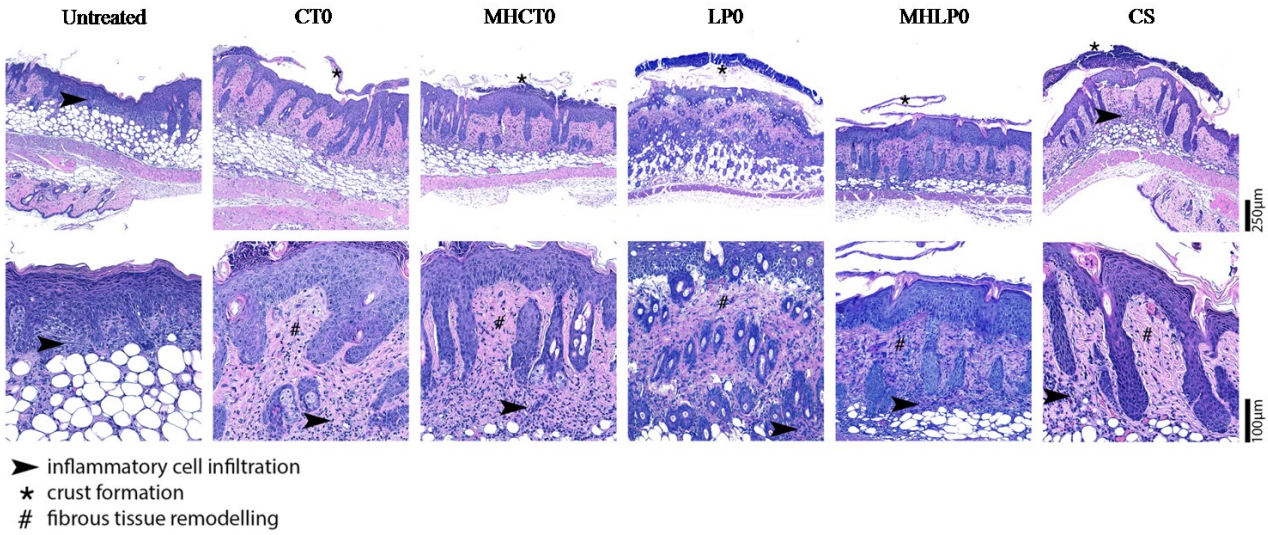

Fig. 3.2.10 - Hematoxylin and eosin-stained sections of tape-stripping lesions in BALB/c mice. Experimental groups included: untreated; CT0, 0-ASt-emulsions with CT; MHCT0, 0-MHASt-emulsions with CT; LP0, 0-ASt-emulsions with LP; MHLP0, 0-MHASt-emulsions with LP; CS, Commercial solution; all previously preceded by epicutaneous bacterial infection.

4 Conclusions

The results of this study demonstrated that ASt-emulsions are suitable systems for topical MH formulation, since the simple composition of MHASt-emulsions allowed drug solubilization and deposition onto the skin.

In vitro release studies showed a prolonged release of the MH, with an initial burst effect. Regarding *in vitro* permeation studies, MH did not passed through the entire skin layer, suggesting a minimal potential for the systemic absorption of the MH upon topical administration, and demonstrating its target delivery and safety profile. Furthermore, MHASt-emulsions have no toxicity on HaCat cells in the concentration range of its anti-staphylococcal MICs. These properties make MHASt-emulsions a suitable carrier to be used against superficial *S. aureus* skin infections. The *in vitro* antibacterial activity studies for MHASt-emulsions revealed that the drug released exceeded the MIC of MH against *S.aureus* and ASt-emulsions presented no antibacterial effect on the microorganism.

The topical administration of MH provides a concentrated drug-delivery to the infected lesion site, and leads to fast treatment, while avoiding the side effects common in the oral MH treatment.

In conclusion, Pickering emulsion technology seems to be a potential candidate for further research studies and, in the future, to expand the market of topical antibiotics.

5 References

1. Sung JH, Hwang M-R, Kim JO, Lee JH, Kim YI, Kim JH, Chang SW, Jin SG, Kim JA, Lyoo WS. Gel characterisation and in vivo evaluation of minocycline-loaded wound dressing with enhanced wound healing using polyvinyl alcohol and chitosan. International Journal of Pharmaceutics. 2010;392(1):232-240.

2. Barajas-Nava LA, López-Alcalde J, Roqué i Figuls M, Solà I, Bonfill Cosp X. Antibiotic prophylaxis for preventing burn wound infection. The Cochrane Library. 2013.

3. Kassem AA, Ismail FA, Naggar VF, Aboulmagd E. Comparative Study to Investigate the Effect of Meloxicam or Minocycline HCl In Situ Gel System on Local Treatment of Periodontal Pockets. AAPS PharmSciTech. 2014;15(4):1021-1028.

4. Schwartz BS, Graber CJ, Diep BA, Basuino L, Perdreau-Remington F, Chambers HF. Doxycycline, not minocycline, induces its own resistance in multidrug-resistant, community-associated methicillin-resistant Staphylococcus aureus clone USA300. Clinical Infectious Diseases. 2009;48(10):1483-1484.

5. Leite LM, Carvalho AGG, Ferreira PLT, Pessoa IX, Gonçalves DO, de Araújo Lopes A, dos Santos Góes JG, de Castro Alves VC, Leal LKA, Brito GA. Anti-inflammatory properties of doxycycline and minocycline in experimental models: an in vivo and in vitro comparative study. Inflammopharmacology. 2011;19(2):99-110.

6. Goulden V, Glass D, Cunliffe W. Safety of long-term high-dose minocycline in the treatment of acne. British Journal of Dermatology. 1996;134(4):693-695.

7. Cherian P, Gunson T, Borchard K, Tai Y, Smith H, Vinciullo C. Oral antibiotics versus topical decolonization to prevent surgical site infection after Mohs micrographic surgery—a randomized, controlled trial. Dermatologic Surgery. 2013;39(10):1486-1493.

8. McClain RW, Yentzer BA, Feldman SR. Comparison of skin concentrations following topical versus oral corticosteroid treatment: reconsidering the treatment of common inflammatory dermatoses. Journal of Drugs in Dermatology: JDD. 2009;8(12):1076-1079.

9. Joks RO, Durkin HG, inventors; The Research Foundation For The State University Of New York, assignee. Topical minocycline ointment for suppression of allergic skin responses. United States2012.

10. Renvert S, Lessem J, Dahlen G, Lindahl C, Svensson M. Topical minocycline microspheres versus topical chlorhexidine gel as an adjunct to mechanical debridement of incipient peri-implant infections: a randomized clinical trial. Journal of Clinical Periodontology. 2006;33(5):362-369.

11. Group F. Minocycline foam successfully treats impetigo with no side-effects in Phase II trial. BMIResearch. 2012.

12. Xu L, Wang Y, Nguyen VT, Chen J. Effects of Topical Antibiotic Prophylaxis on Wound Healing Following Flapless Implant Surgery: A Pilot Study. Journal of Periodontology. 2015;(0):1-9.

13. Marto J, Gouveia L, Jorge IM, Duarte A, Gonçalves LM, Silva SMC, Antunes F, Pais AACC, Oliveira E, Almeida AJ, Ribeiro HM. Starch-based Pickering emulsions for topical drug delivery: A QbD approach. Colloids and Surfaces B: Biointerfaces. 2015;135:183-192.

14. Zhang Y, Huo M, Zhou J, Zou A, Li W, Yao C, Xie S. DDSolver: an add-in program for modeling and comparison of drug dissolution profiles. AAPS J. 2010;12(3):263-271.

15. Costa P, Sousa Lobo JM. Modeling and comparison of dissolution profiles. European Journal of Pharmaceutical Sciences. 2001;13(2):123-133.

16. Costa FO, Sousa JJS, Pais AACC, Formosinho SJ. Comparison of dissolution profiles of Ibuprofen pellets. Journal of Controlled Release. 2003;89(2):199-212.

17. Khan K. The concept of dissolution efficiency. Journal of Pharmacy and Pharmacology. 1975;27(1):48-49.

18. OECD. Test No. 428: Skin Absorption: In Vitro Method. OECD Publishing.

19. Standards NCfCL. Performance Standards for Antimicrobial Disk Susceptibility Tests: Approved Standards: National Committee for Clinical Laboratory Standards; 2006.

20. Kugelberg E, Norström T, Petersen TK, Duvold T, Andersson DI, Hughes D. Establishment of a superficial skin infection model in mice by using Staphylococcus aureus and Streptococcus pyogenes. Antimicrobial Agents and Chemotherapy. 2005;49(8):3435-3441.

21. Kumar V, Abbas AK, Fausto N, Aster JC. Robbins and cotran pathologic basis of disease, Professional Edition: Expert Consult-Online: Elsevier Health Sciences; 2014.

22. Zbinovsky V, Chrekian GP. Minocycline. In: Klaus F, editor. Analytical Profiles of Drug Substances: Academic Press; 1977. p. 323-339.

23. EP. European Pharmacopoeia 8. Strasbourg: Council Of Europe : European Directorate for the Quality of Medicines and Healthcare; 2014.

24. Marku D, Wahlgren M, Rayner M, Sjöö M, Timgren A. Characterization of starch Pickering emulsions for potential applications in topical formulations. International Journal of Pharmaceutics. 2012;428(1–2):1-7.

25. Matos M, Timgren A, Sjöö M, Dejmek P, Rayner M. Preparation and encapsulation properties of double Pickering emulsions stabilized by quinoa starch granules. Colloids and Surfaces A: Physicochemical and Engineering Aspects. 2013;423(0):147-153.

26. Tadros TF. Emulsion formation and stability. Weinheim: Wiley-VCH ;; 2013.

27. Ascenso A, Salgado A, Euletério C, Praça FG, Bentley MVLB, Marques HC, Oliveira H, Santos C, Simões S. In vitro and in vivo topical delivery studies of tretinoin-loaded ultradeformable vesicles. European Journal of Pharmaceutics and Biopharmaceutics. 2014;88(1):48-55.

28. Lopes R, Eleutério CV, Gonçalves LMD, Cruz MEM, Almeida AJ. Lipid nanoparticles containing oryzalin for the treatment of leishmaniasis. European Journal of Pharmaceutical Sciences. 2012;45(4):442-450.

29. Korn M, Killmann E, Eisenlauer J. Infrared and microcalorimetric studies of the adsorption of monofunctional ketones, esters, ethers, and alcohols at the silica/carbon tetrachloride interface. Journal of Colloid and Interface Science. 1980;76(1):7-18.

30. Frelichowska J, Bolzinger MA, Valour JP, Mouaziz H, Pelletier J, Chevalier Y. Pickering w/o emulsions: drug release and topical delivery. International Journal of Pharmaceutics. 2009;368(1-2):7-15.

31. Ritger PL, Peppas NA. A simple equation for description of solute release II. Fickian and anomalous release from swellable devices. Journal of Controlled Release. 1987;5(1):37-42.

32. Wei Z, Wang C, Liu H, Zou S, Tong Z. Facile fabrication of biocompatible PLGA drug-carrying microspheres by O/W pickering emulsions. Colloids and Surfaces B: Biointerfaces. 2012;91:97-105.

33. Wei Z, Wang C, Liu H, Zou S, Tong Z. Halloysite nanotubes as particulate emulsifier: Preparation of biocompatible drug-carrying PLGA microspheres based on pickering emulsion. Journal of Applied Polymer Science. 2012;125(S1):E358-E368.

34. Frelichowska J, Bolzinger MA, Pelletier J, Valour JP, Chevalier Y. Topical delivery of lipophilic drugs from o/w Pickering emulsions. International Journal of Pharmaceutics. 2009;371(1-2):56-63.

35. Wissing S, Müller R. Solid lipid nanoparticles as carrier for sunscreens: in vitro release and in vivo skin penetration. Journal of Controlled Release. 2002;81(3):225-233.

36. Lou H, Qiu N, Crill C, Helms R, Almoazen H. Development of W/O Microemulsion for Transdermal Delivery of Iodide Ions. AAPS PharmSciTech. 2013;14(1):168-176.

37. Ishii H, Todo H, Terao A, Hasegawa T, Akimoto M, Oshima K, Sugibayashi K. Why does a hydrophilic drug permeate skin, although it is not soluble in white petrolatum? Drug Development and Industrial Pharmacy. 2009;35(11):1356-1363.

38. Barrett C. Skin penetration. Journal of Society of Cosmetic Chemists. 1969;20:487-499.

39. Hauser M, Richter H, Schanzer S, Lademann J, editors. Cosmetic Oils in comparison: penetration and occlusion of paraffin oil and vegetable oils. Journal Der Deutschen Dermatologischen Gesellschaft; 2011: WILEY-BLACKWELL COMMERCE PLACE, 350 MAIN ST, MALDEN 02148, MA USA.

40. Hafeez F, Maibach H. Occlusion effect on in vivo percutaneous penetration of chemicals in Man and monkey: partition coefficient effects. Skin Pharmacology and Physiology. 2013;26(2):85-91.

41. Zhai H, Maibach HI. Occlusion vs. skin barrier function. Skin Research and Technology. 2002;8(1):1-6.

42. OECD. Test No. 439: In Vitro Skin Irritation Reconstructed Human Epidermis Test Method: Reconstructed Human Epidermis Test Method. OECD Publishing; 2010.

43. Nair B, Yamarik TA. Final report on the safety assessment of aluminum starch octenylsuccinate. International Journal of Toxicology. 2002;21 Suppl 1:1-7.

44. Djekic L, Primorac M. The influence of cosurfactants and oils on the formation of pharmaceutical microemulsions based on PEG-8 caprylic/capric glycerides. International Journal of Pharmaceutics. 2008;352(1-2):231-239.

45. Zanatta CF, Ugartondo V, Mitjans M, Rocha-Filho PA, Vinardell MP. Low cytotoxicity of creams and lotions formulated with Buriti oil (Mauritia flexuosa) assessed by the neutral red release test. Food and Chemical Toxicology. 2008;46(8):2776-2781.

46. Bos JD, Meinardi MM. The 500 Dalton rule for the skin penetration of chemical compounds and drugs. Experimental Dermatology. 2000;9(3):165-169.

47. Raposo S, Salgado A, Gonçalves L, Pinto P, Urbano M, Ribeiro H. Safety Assessment and Biological Effects of a New Cold Processed SilEmulsion for Dermatological Purpose. BioMed Research International. 2013;2013:10.

48. Torres FG, Commeaux S, Troncoso OP. Starch-based biomaterials for wound-dressing applications. Starch-Stärke. 2013;65(7-8):543-551.

49. Santander-Ortega M, Stauner T, Loretz B, Ortega-Vinuesa J, Bastos-González D, Wenz G, Schaefer U, Lehr C. Nanoparticles made from novel starch derivatives for transdermal drug delivery. Journal of Controlled Release. 2010;141(1):85-92.

50. Fargier A, Sacha M, Keck C, Haltner E. Skin disc antibiogram: a new in-vitro model to test pharmaco-dynamic equivalence of anti-bacterial topic formulations. Wissenschaftliche Posterausstellung. 2015;16(18):3-5.

51. Culp B, Scheinfeld N. Rosacea: a review. Pharmacy and Therapeutics. 2009;34(1):38.

52. Hartman-Adams H, Banvard C, Juckett G. Impetigo: diagnosis and treatment. American Family Physician. 2014;90(4):229-235.

4 Starch-based nanocapsules

This page was intentionally left blank

Section 1

A Quality by Design (QbD) approach on starch-based nanocapsules: a promising platform for topical drug delivery

This Section was adapted from the submitted paper in:

J Marto, LF Gouveia, LM Gonçalves, DP Gaspar, P Pinto, FA Carvalho, E Oliveira, HM Ribeiro, AJ Almeida (2016) A Quality by Design (QbD) approach on starch-based nanocapsules: a promising platform for topical drug delivery. Colloids and Surfaces B: Biointerfaces.

This page was intentionally left blank

Graphical Abstract

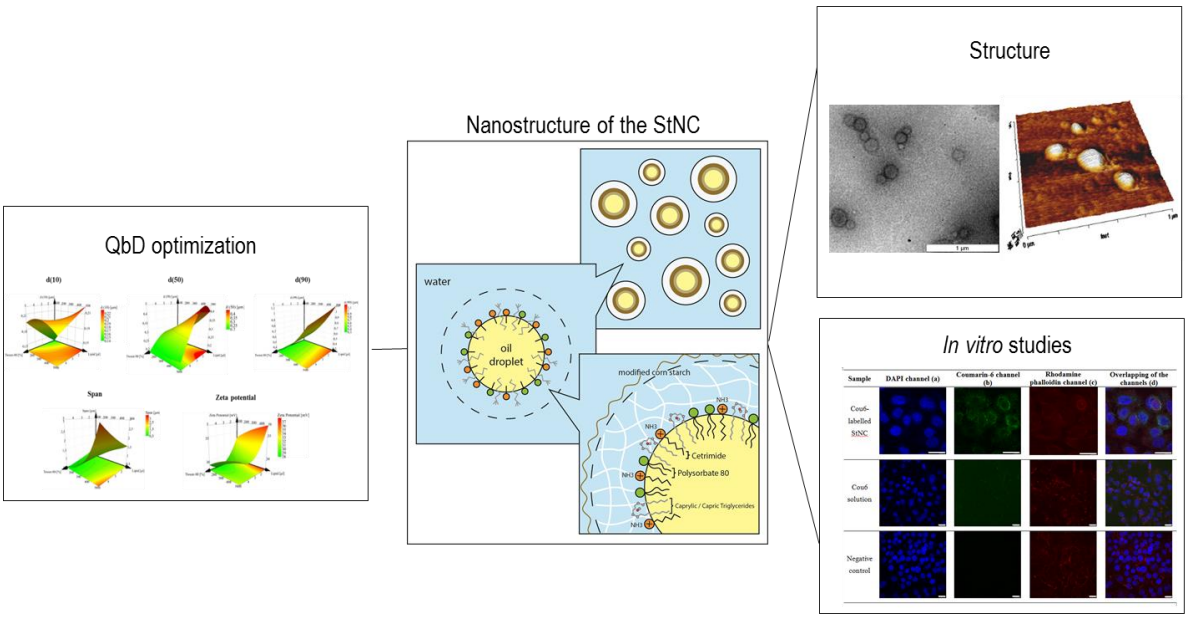

Highlights:

- A QbD approach was successfully applied to develop starch-based nanocapsules.
- Formulation and process parameters allowed the control of particle size distribution.
- Lipid amount and surfactant concentration highly influenced nanocapsules physical stability.
- Starch-based nanocapsules were non-irritant and suitable for skin application.

This page was intentionally left blank

1 Introduction

The technological development of new dosage forms has been a promising approach to increase and control drug skin penetration. Polymeric and lipid-based nanoparticles are a suitable strategy to improve percutaneous drug absorption due to the capacity to enhance the rate and extent the transport across the skin as a result of their surface area [1-4].

Both the advantages and limitations of using nanocarriers arise from their unique features: reduced particle size, high surface energy, composition, architecture, among others. Thus, detailed characterization, analytical evaluation, toxicological and pharmacological assessment are necessary to determine the efficacy of using these nanostructures as drug delivery systems [5]. In this way, the use of well-known polysaccharides as drug vehicles has additional benefits regarding safety and toxicity as well as availability [6]. Polymeric nanoparticles are an excellent option for topical delivery because they can be tailor-made in different sizes and it is possible to modify the surface polarity in order to improve skin penetration [5, 7]. Moreover, nanoparticle carriers made of bioadhesive materials, such as starch, can prolong the residence time by increasing the permeation of loaded drugs [6]. Particularly, starch nanocapsules are attracting major attention as novel colloidal drug carrier for topical applications. This system combines the advantages and avoids the drawbacks of several colloidal carriers of its class (polymeric nanoparticles). These nanocapsules gained significant popularity due to its simple, green process for preparation without the use of hazardous organic solvents and the inconvenience of removing them afterwards. On the other hand, emulsion-solvent evaporation method arises as an advantageous alternative to obtain starch nanoparticles. The interest in using emulsion-solvent evaporation method for nanocapsules synthesis arises mainly from the versatile nature of the system such as mild reaction conditions simple procedure, cost effectiveness, formation of very small particle size and its scalability [8].

In addition, pharmaceutical industry is under enormous pressure to continuously improve product quality, reduce manufacturing costs and increase the speed to develop new pharmaceutical products. One of the areas with major impact on quality and cost parameters is the formulation development. In order to achieve these challenging goals, a quality by design (QbD) approach can be used to support and accelerate the pharmaceutical development and optimize novel formulations [9, 10].

Therefore, the major aim of this research study was to develop and characterize an innovative and sustainable starch-based nanocarrier as a potential platform for topical drug delivery. Hence, a QbD approach was performed not only to extract the maximum amount

of information from the collected data, but also to establish the influence of several factors on the formulation and physical properties of starch-based nanocapsules. *In vitro* studies demonstrated the successful application of starch nanocapsules on pharmaceutical and cosmetic fields.

2 Materials and methods

2.1 Materials

Caprylic/capric triglycerides (Tegosoft® CT) (CT) a kind gift from Evonik Industries AG (Essen, Germany). Cetrimonium bromide (Cetrimide) was a gift from DS Produtos Químicos (São Domingos de Rana, Portugal). Polysorbate 80 (Tween® 80) was obtained from Merck (Kenilworth, USA). Ethanol was obtained from Carlo Erba Reagents (Cornaredo, Italy). Pregelatinized modified starch (Instant Pure-Cote® B793) was a gift from Grain Processing Corporation (Washington, USA). Coumarin-6 was obtained from Sigma-Aldrich (Dorset, Germany). Purified water was obtained by reverse osmosis, electrodeionization (Millipore, Elix 3) followed by filtration (pore 0.22 µm). A spontaneously immortalized human keratinocyte cell line, HaCaT (CLS, Germany) was used and all culture media components were obtained from Life Technology (UK).

2.2 Methods

2.2.1 Design of starch nanocapsules (StNC) formulations

2.2.1.1 Preparation of StNC

The StNC were emulsion-solvent evaporation method, using prepared by capric/caprylic triglycerides (CT) as the lipid component, Tween®80 and cetrimide as surfactants, pregelatinized modified starch as a polymer and ethanol. Briefly, capric/caprylic triglycerides were dissolved in cationic surfactant ethanol solution and then added to the aqueous phase containing Tween®80 and the hydrated polymer, under constant magnetic stirring. The nanoparticle dispersion was then kept under stirring at 25 ± 2 ˚C. When incorporating the coumarin-6 (Cou6), the probe was added to the lipid.

2.2.1.2 Particle size analysis and zeta potential (ZP) measurements

The particle size analysis was performed according to the procedure described previously in Chapter 3, section 2.2.1.1. In addition, in order to achieve an acceptable turbidity, about 5 ml of each formulation, corresponding to an obscuration between 10% - 20%, was added

to the sample chamber containing 120 ml of filtered purified water using a stirrer at 1750 rpm during 5 min and ultra-sonication at 25%.

The surface charge (zeta potential, ζ) was determined by electrophoretic light scattering in a Zetasizer Nano Z (Malvern Instruments, UK) at 25˚C. For the measurements, samples were diluted appropriately with filtered purified water (pH 5.6).

2.2.1.3 Fourier transform infrared spectroscopy (FTIR)

Fourier transform infrared spectra of starch, cetrimide and StNC were obtained using a Fourier transform infrared spectrometer (IRAffinity-1, Shimadzu, Kyoto, Japan). Baseline was corrected and the samples were scanned against a blank KBr pellet background at a wave number ranging from 4000-400 cm^{-1} with a resolution of 2.0 cm^{-1} with 30 scans. The characteristic peaks were recorded.

2.2.1.4 Differential scanning calorimetry (DSC)

The DSC analyses were performed according to the procedure described previously in Chapter 2, section 2.2.3.2. The thermograms were recorded at temperature range of 10 – 240 ˚C at a scan speed of 10 °C/min.

2.2.1.5 Transmission electron microscopy analysis

Particle morphology analysis was performed using transmission electron microscopy (TEM) according to the method described by Ferreira *et al.[11]*. Briefly, the StNC optimized formulation was applied to the cooper grid and dried at room temperature and analysed on Hitachi 8100 with ThermoNoran light elements EDS detector and digital image acquisition at IST of Technical University of Lisbon.

2.2.1.6 Atomic force microscopy

Particle size distribution and morphology were confirmed by atomic force microscopy (AFM). A NanoWizard II equipment (JPK Instruments, Germany) mounted on the top of an Axiovert 200 inverted microscope (Carl Zeiss, Germany) was used for imaging the samples. The AFM head is equipped with a 15 µm z-range linearized piezoelectric scanner and an infrared laser. The StNC optimized formulation was diluted (1:250) in Milli-Q water and deposited on freshly cleaved muscovite mica for 20 min. After subsequent washes, the samples were allowed to air dry at room conditions. StNC imaging was performed in air by tapping mode. Oxidized sharpened silicon tips (ACL cantilevers,

Applied Nanostructures, CA) with a tip radius of 6 nm, resonant frequency of about 190 kHz and spring constant of 58 N/m were used for the imaging. Scanning speed was optimized to 0.5 Hz and 512x512 points matrixes were acquired. Imaging data were analysed with the JPK image processing v.5.1.8 (JPKInstruments, Berlin, Germany).

2.2.2 Identification of quality target product profile (QTPP) and critical quality attributes (CQAs)

The identification of QTPP was performed according to the procedure described previously in Chapter 3, Section 1, section 2.2.3. The most important features of polymeric nanocapsules are their particle size distribution, e.g., d(10), d(50), d(90), span and zeta potential (ZP), as the particle size and surface charge influences many characteristics, especially the stability. Thus, the list of the key QTPP is given in Table 4.1.1.

Table 4.1.1 - QTPP of StNC.

QTPP element	Target
Route of administration	Topical
Dosage form	Nanoparticle (nanocapsule) < 1 µm [12]
	Particles size distribution [13] : • d(10) - 0.1-0.3 µm • d(50) - 0.2-0.5 µm • d(90) - 0.3-0.9 µm • Span - 0.5-2.0
Stability	Zeta potential > 30 mV [14]
	At least 12 month shelf-life at 5±3°C [15]
Biological effects	Non-sensitizing and non-irritant

2.2.3 Risk Analysis of CQAs

Risk analysis was performed according to the procedure described previously in Chapter 3, Section 1, section 2.2.4. With the information collected, Ishikawa diagrams were constructed to identify the potential risks. Particle size distribution, namely d(10), d(50), d(90), span and ZP were defined and further delineated to identify potential risks and after the analysis, three variables were identified for optimization in the following studies.

2.2.4 Response surface analysis

Both the manufacturing process and the formula of the StNC's were simultaneously optimized using a three-factor central composite design (CCD). The independent variables

were the stirring time (St), the percentage of nonionic surfactant, Tween® 80 (T) and the amount of lipid - capric/caprylic triglycerides (L). The chosen CCD α value to ensure design rotability was 1.682. This design required 17 experimental runs, including three replicated center points for the estimation of the prediction variance over the entire design space (Table 4.1.2). Data were analyzed as described in Chapter 3, Section 1, section 2.2.5. and the following mathematical quadratic model was fitted to the data:

Equation 1: $Y = \beta_0 + \beta_1 X_1 + \beta_2 X_2 + \beta_3 X_3 + \beta_{12} X_1 X_2 + \beta_{13} X_1 X_3 + \beta_{23} X_2 X_3 + \beta_{11} X_1^2 + \beta_{22} X_2^2 + \beta_{33} X_3^2$

Table 4.1.2 - CCD matrix and experimental matrix.

ID	Design Matrix			Experimental Matrix		
	T (%, w/v)	L (mg)	St (min)	T (%, w/v)	L (mg)	St (min)
F1	-1	-1	-1	1.5	152	42
F2	1	-1	-1	4.5	152	42
F3	-1	1	-1	1.5	448	42
F4	1	1	-1	4.5	448	42
F5	-1	-1	1	1.5	152	108
F6	1	-1	1	4.5	152	108
F7	-1	1	1	1.5	448	108
F8	1	1	1	4.5	448	108
F9	-1.682(-α)	0	0	1.0	300	75
F10	1.682 (α)	0	0	5.0	300	75
F11	0	-1.682(-α)	0	3.0	100	75
F12	0	1.682 (α)	0	3.0	500	75
F13	0	0	-1.682(-α)	3.0	300	30
F14	0	0	1.682 (α)	3.0	300	120
F15	0	0	0	3.0	300	75
F16	0	0	0	3.0	300	75
F17	0	0	0	3.0	300	75

T - % of Tween® 80; L - Capric/caprylic triglycerides amount; St - Stirring time

2.2.5 Physical stability of StNC

When applicable, the stability studies followed the ICH Q1A (R2) guideline on stability testing of new drug substances and products. All formulations were stored during 12 months at 5 ± 3°C [15]. Samples were analyzed for macroscopic appearance (visual inspection), particle size distribution and ZP immediately after preparation and at 1, 6 and 12 months of storage.

2.2.6 *In vitro* cytotoxicity studies

2.2.6.1 Cell culture conditions

The cell culture conditions are described in Chapter 2, section 2.2.4.1.

2.2.6.2 In vitro cell uptake studies

HaCat cells were grown in 96 well plates at $2x10^5$ cells/ml 24h before the uptake studies. Culture medium was replaced by 100 µl of different concentrations of Cou6-loaded StNC in the test wells.

Measurements of fluorescence were performed at excitation wavelength of 485 nm and emission 520 nm, for both Cou6-loaded StNC in microplate reader (FLUOstar Omega, BMGLabtech, Germany). These measurements were performed immediately after particle addition and after 1h of incubation (37 °C, 5 % CO_2). After the incubation time with labeled StNC, cells were rinsed 3 times with 10 mM PBS containing 20 mM Glycine at pH 7.4 pre-warmed at 37 ºC. The PBS solution was removed and then cells were disrupted with 100 µl of 1 % Triton X100 solution and the fluorescence was again measured to determine the internalized amount of particles. The internalized particles were determined as a percentage of the initial amount feed to cells. Using the quantification of the fluorescence of particles in function of their concentration it was possible to determine the amount of particles internalized by cells.

2.2.6.3 Confocal laser scanning microscopy (CLSM) of interactions between StNC and cells

HaCat cell cultures were performed at same conditions as described in section 2.2.6.1, in terms of incubation times of Cou6-loaded StNC tested and cell density. Cells grown on 12 multi-well plates containing sterile glass slides (Greiner, Germany). After the incubation time with labeled particles, cells were rinsed 3 times with 10 mM PBS containing 20 mM glycine at pH 7.4 before and after being fixed for 15 min at room temperature protected from light with 4 % (w/v) paraformaldehyde. After cell fixation, and, for actin staining with rhodamine phalloidin, cells were permeabilized with 0.1 % Triton X100 for 4 min, then cells were also rinsed 3 times with 10 mM PBS containing 20 mM glycine at pH 7.4. The 6.6 µM phalloidin-TRITC solution in 10 mM PBS was added to the cells for 30 min at room temperature. After cells rinsed 3 times with 10 mM PBS containing 20 mM glycine at pH 7.4, and air dried, cell slides were mounted in fluorescent mounting medium ProLong® Gold antifade reagent with DAPI. Afterwards, particles fluorescence in contact with cells was observed using CLSM, with an AOBS SP5X microscope (Leica GmbH,

Germany), which acquires images through different detectors for fluorescent signals, which, in this case, were got by a white light laser (WLL). A drop of immersion oil was added on glass slides in order not to be refracted until it passes the interface from the coverslip into the mounting medium. Laser excitation wavelengths of 405, 488 and 561 nm were used to scan the samples and fluorescent emissions from DAPI (emission λ= 424 - 475 nm), coumarin-6 (emission λ= 500 - 550 nm) and rhodamine phalloidin (emission λ= 575- 625 nm) were collected using separate channels, respectively. Images were acquired with a magnification of 63x, using an oil immersion lens (HCX PL APO CS). The gray scale images obtained from each scan were pseudo-coloured green (coumarin-6), blue (DAPI) and red (rhodamine phalloidin) and overlapped afterward (LAS AF, Leica Confocal Software, Leica GmbH, Germany) to obtain a multicoloured image.

3 Results and discussion

3.1 Quality by design approach

3.1.1 Risk analysis of CQAs

The first and most important step when using QbD to support formulation and process development is to pre-define the desired final QTPP. This study focused on several critical formulation and process dependent quality attributes: particle size distribution, zeta potential and stability. The factors potentially affecting the quality attributes of the StNC were divided into two categories: formula and process related. Within these two categories, critical variables were identified (Fig. 4.1.1) and the effects of these variables on the particle size distribution, ZP and stability were studied varying one factor at a time.

As a first step, multifunctional and well-known ingredients were selected, as a way to produce a simple but innovative StNC formulation. Different approaches for ingredients and process selection can be considered in order to achieve a new and more sustainable formula and process. A cold-water soluble polymer was selected in order to obtain a clear and stable dispersion with low polymer concentrations, as well as a biocompatible pH value, selecting the pregelatinized modified starch. Other multifunctional and well-known pharmaceutical excipients were selected, such as, cetrimide as cationic surfactant, Tween® 80 as non-ionic surfactant and ethanol as preservative and solvent.

The influence of process variables were also investigated, such as concentration of polymer and surfactants, amount of oil, homogenizer types (magnetic stirrer or high-speed mixer) and solvent evaporation rate, as critical variables that determine the characteristics

of StNC. Thus, the major critical variables identified as possible cause of product variability were the stirring time, amounts of nonionic surfactant and lipid. The screening study and risk analysis have the advantage of maintaining as low as possible the number of experiments required to identify the most critical factors affecting the response under assessment.

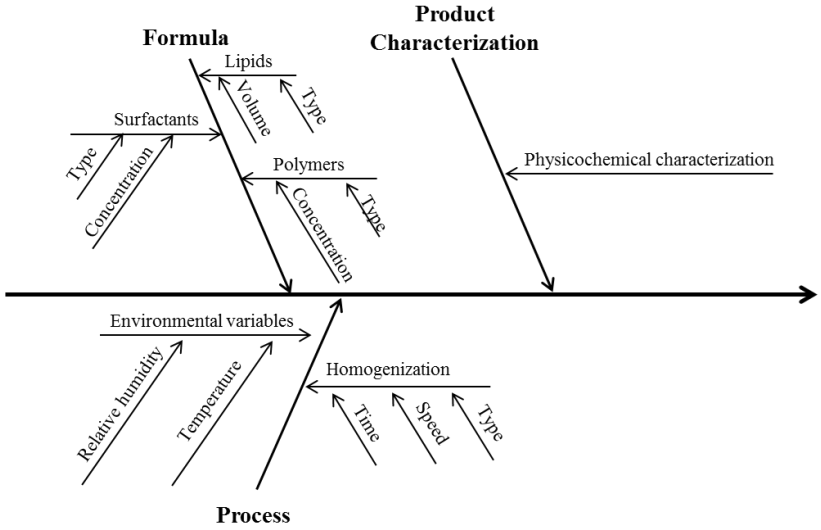

Fig. 4.1.1 - Ishikawa diagram illustrating factors that may have impact on the physicochemical characterization of StNC.

3.1.2 Response surface analysis

The choice of variables is a task of paramount importance, because it limits both results and interpretation. The choice must be based on the particular characteristics of the system. The current option is to use one variable composition, e.g. the lipid concentration, that establishes a relationship between the inner phase and the system as a whole and, implicitly, between the inner and external phases. The surfactant concentration was referred to the whole system, and the respective choice is based on the fact that the surfactant is an interface component, which can be found in both inner and external phases. Finally, the influence of the solvent evaporation rate was assessed through stirring time.

As preliminary results clearly indicated the system is highly influenced by the amount of lipid, surfactant concentration and evaporation solvent rate (results not shown), in this design, the 3 variables were studied. It should be noted that these elements are widely recognized as major factors influencing the size of polymeric nanoparticles [12].

The data obtained by using the experimental design were analyzed and second degree polynomial models were fitted and its statistical significance assessed using ANOVA. The model was statistically significant as $p < 0.1$ for all critical quality attribute except for the

zeta potential (Table 4.1.3). The adequacy of the established models was estimated by lack of fit and R^2. The lack of fit estimates the error variance independently of the model, comparing the model error and the replicate error. All models presented good fit to the data, that is, the model has no lack of fit ($p > 0.1$). An acceptable correlation between the observed and predicted values was obtained as indicated by the resulting R^2 values in the range 0.87 to 1.00 for all variables.

Table 4.1.3 - Summary of ANOVA and lack of fit for testing models.

Critical quality attribute	ANOVA		Lack of fit (p)
	R^2	p	
d(10)	0.937	0.002	0.909
d(50)	0.967	0.001	0.548
d(90)	0.993	0.000	0.472
Span	0.998	0.000	0.184
Zeta potential	0.870	0.081	0.964

Table 4.1.4 illustrates the statistical results using MODDE® Pro 11 software. The regression coefficients are scaled and centered, improving the interpretability of the model. This means that they are no longer expressed according to the original measurement scales of the factors, but have been re-expressed to be related to the levels. Therefore, the constant term relates to the estimated response at the design center point, that is, when the factors have the value zero in the level unit, thus, the values of the regression coefficients of the variables are associated with the influence on the CQAs.

Table 4.1.4 - Summary of regression analysis results for measured responses, for formula optimization.

	d(10)		d(50)		d(90)		Span		Zeta potential	
	Coeff	± SE	Coeff	± SE	Coeff	± SE	Coeff	± SE	Coeff	± SE
k	0.198	0.004	-0.468	0.014	-0.259	0.011	0.023	0.008	30.315	1.058
T	0.007	0.003	-0.095	0.012	-0.057	0.009	-0.039	0.006	-2.808	0.957
L	0.020	0.003	0.089	0.010	0.239	0.009	0.262	0.006	NS	NS
St	NS	NS	NS	NS	NS	NS	-0.019	0.007	NS	NS
T^2	NS	NS	-0.130	0.022	-0.046	0.019	NS	NS	3.300	1.466
L^2	-0.012	0.005	NS	NS	0,046	0.020	0.063	0.014	NS	NS
St^2	NS	NS	NS	NS	NS	NS	0.137	0.014	NS	NS
T*L	-0.024	0.004	-0.045	0.017	0.035	0.013	0.173	0.009	4.852	2.064
T*St	NS	NS	NS	NS	0.050	0.013	-0.108	0.009	NS	NS
L*St	NS	NS	NS	NS	NS	NS	NS	NS	NS	NS

Coeff– Coefficient Scaled and centered; SE – Standard Error; k – Constant; NS (no significant) – $p > 0.10$

A general interpretation indicates that an increase in St and in percentage of surfactant and a decrease in lipid amount originates lower particles size distribution. Due to the second order and interaction terms of the model, some combinations of the variables do not follow the general trend. The regression analysis results of the fitted models are shown in Table 4.1.4.

Considering the CCD results, the statistically significant variables ($p < 0.10$) affecting d(10), d(50) and d(90) were the percentage of Tween® 80 and the amount of lipid, while for span all factors had statistical significance. Thus it can be inferred that an increase in the amount of surfactant and decrease in the lipid amount, as well as longer stirring times, produces smaller nanocapsules with lower span, confirming previous publications [16, 17]. It was also observed that the main effect of stirring time is a borderline case according to the confidence interval assessment. However, this term was allowed to stay in the span model because it contributes to a highly significant two-factor interaction and quadratic term.

In the CCD data set, the strong main effect of percentage of Tween® 80 and lipid amount and two-factor interaction between amount of Tween® 80 and lipid amount drives this choice. Fig. 4.1.2 shows response contour plots and 3D plots created with the factors amount of Tween® 80 and lipid amount as axes, and stirring time fixed at its centre level.

According to Fig. 4.1.2 all plots present a curved surface and the possibility of modelling curvature is due to the presence of the quadratic terms. Consequently, for d(10), d(50), d(90) and span only one negative two-factor interaction, between lipid content and percentage of surfactant was meaningful. For high lipid amounts an increase in the surfactant concentration was required because a decrease of o/w interfacial tension is related to a reduction in the size of the nanocapsules [16, 17].

The low influence of Tween® 80 concentration in d(10) and d(50) sizes, combined with significant oil influence, suggesting particle size variation according to the ingredients proportion, could be due to a special molecular arrangement in the StNC, mainly during capsules formation.

Indeed, a negative correlation was observed for stirring time in the span response, meaning that an increase in the stirring time will contribute to a narrower particles size distribution, apparently, because different interfacial organizations occurred between the organic and aqueous phases, limiting solvent diffusion. Thus, the slow diffusion of the solvent during the evaporation step, makes nanocapsule formation easy [12].

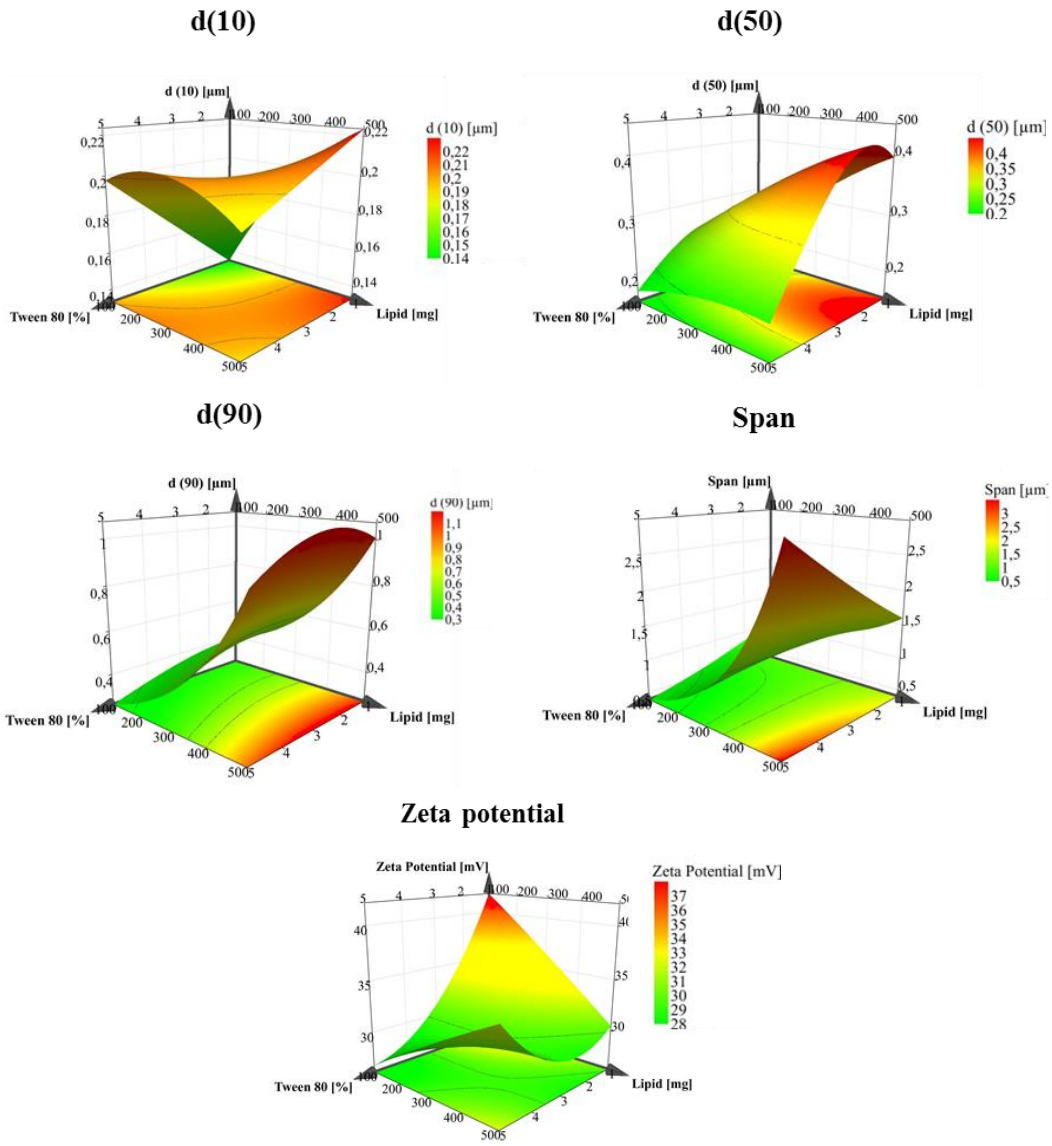

Fig. 4.1.2 - Isoresponse curves (graph floor) and response surface plots on relative particle size distribution and zeta potential.

The amount of surfactant, lipid and stirring time exerted no significant influence on particle surface charge. All StNC formulations presented a zeta potential of ca. +33.6 ± 6.7 mV, indicating the nanocapsule suspensions are physically stable. In addition, the presence of charge (positive) can improve nanocapsules interaction with skin components, due to the negative charge of the skin at normal physiological pH, as it is expected for cationic particles to have higher skin retention and penetration compared with neutral or anionic ones [18]. Thus, StNC appear to be promising pharmaceutical dosage forms for topical application.

Finding the optimal region, called design space (DS) is an objective often used to link the gap between screening and optimization studies. The DS is a mathematically and statistically defined combination of factor space and response space that results in a product that reliably meets its quality characteristics with a high degree of assurance. Thus, the particle size can be successfully predicted and controlled. Leaving the DS n-dimensional space is considered as a relevant change from the regulatory standpoint as it is expected to impact the product quality.

In this study, response surface methodology was applied to establish the DS. The factors that had been demonstrated to affect StNC quality were used to create the DS (Fig. 4.1.3). Every single point corresponds to a combination of percentage of surfactant and lipid amount. The green area corresponds to a range of combinations for which the particle size and zeta potential remains within the pre-defined acceptable limits. The optimal design setpoint is located at the center of the DS hypercube, thus, the dotted frame in the DS plot defines the optimal conditions that can be inserted into the irregular DS volume. The setpoint in the DS communicates and helps to define the acceptable value for individual factors to ensure that all CQA are fulfilled.

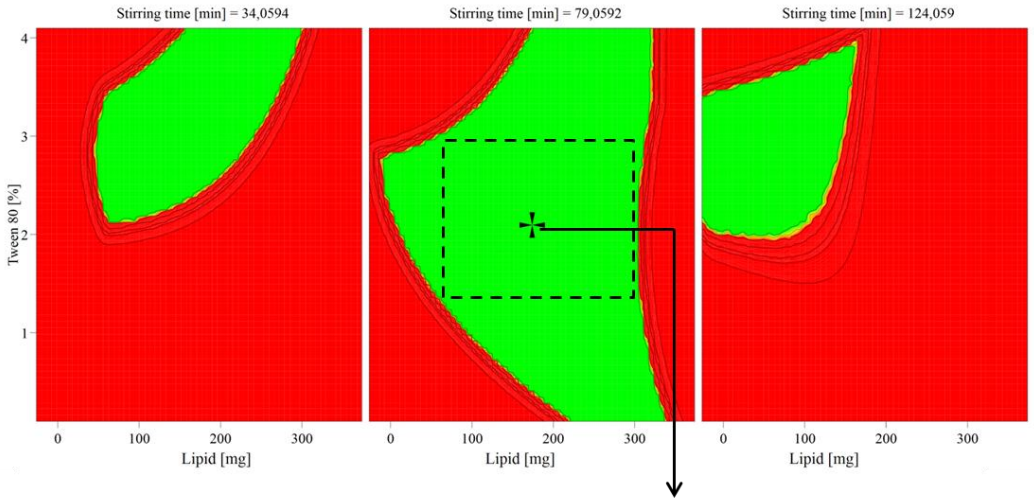

Factor	Setpoint	Factor contribution
Stirring time (min)	79.0	13.72
Tween 80 (%)	2.1	38.78
Lipid (mg)	172.8	47.50
Cetrimonium bromide (%)	0.25	-
Pregelatinized modified starch (%)	0.07	-
Ethanol (%)	32.53	-
Water (%)	65.21	

Fig. 4.1.3 - Overlay plot evidence the DS for the optimization study.

3.1.3 Stability of the StNC

The purpose of stability testing is to provide experimental evidence on how the product quality varies over time under the influence of a variety of environmental factors such as the temperature, humidity, and light, in order to establish a shelf life for the drug product and to define suitable storage conditions. During the formulation development, the main objective of the stability testing is to prove the compatibility between the excipients and/or define adequate packaging conditions in order to establish a suitable shelf life [15].

In general, the performed stability tests during the formulation development were done in accordance to the ICH, particularly the ICH Q1A (R2). For new products intended for storage in a refrigerator, this guideline defines the storage conditions: long term (5 ± 3 °C during ate 12 months) and accelerated (25 ± 2 °C / 60 ± 5% RH during ate least 6 months) [15].

Nevertheless, in the present academic work we are studying the stability, not determining the shelf-life of the StNC. The stability of the StNC was assessed by visual observation in order to detect the occurrence of phase separation or other instability phenomena. Refrigerated storage was selected because it is the most common temperature reported in the literature for the storage of polymeric nanoparticles formulations. As expected, the temperature highly influenced the rate of degradation of the polymers, because the effect of the temperature itself could be magnified by the autocatalytic effect of carboxylic chain ends [19].

At evaluation time points of 6 and 12 months, several StNC suspensions at 5 ± 3 °C showed a slight phase separation. These results can be explained by the different effect of each factor as demonstrated in the optimization study. The droplet size analysis was in accordance to the latter observations as several StNC showed a significant change in droplet size distribution after 6 months, which was more pronounced after 12 months. This phenomenon can be explained by rearrangement processes that occur in the interface, especially those produced by lipid (capric/caprylic triglycerides) and non-ionic surfactants (Tween® 80). The span and zeta potential did not suffer any significant changes over time. Thus, the stability studies of StNC suspensions at 5 ± 3 °C demonstrated that the physical properties remained within specifications for up to 6 months. Despite the physical properties remained fairly constant, the abrupt increase in d(50) and d(90) requires further studies or additional approaches to ensure stability, such as lyophilization technology to obtain dry powders.

According to several authors, nanoencapsulation improves the stability, solubility and bioavailability of encapsulated drugs and promotes its controlled release in comparison with nanoemulsions [20, 21]. Other authors reinforced that the presence of a polymeric shell can increase the associated drug concentrations within the nanocarriers and the chemical stability of drug during storage, as well as maintained the balance between free and associated drug [22].

3.1.4 Physicochemical characterization

3.1.4.1 FTIR

The intermolecular interactions of the StNC ingredients were evaluated resorting to FTIR technique, which also might give an insight of the nanostructure. The FTIR spectra of solid raw materials (cetrimide and pregelatinized modified starch) and optimized StNC are shown in Fig. 4.1.4. In what concerns the spectrum of pregelatinized modified starch, the O−H stretching and the C−H stretching vibrations give strong signals at 3414 and 2924 cm^{-1}, respectively. The bands at 1160, 1082 and 1022 cm^{-1} represent the C-O stretching on the polysaccharide skeleton. A strong band at 1453 cm^{-1} is characteristic of the C-H bending vibration.

In the case of cetrimide, the broad band at 3408 cm^{-1} is associated with O-H stretching vibration of water that remains after drying. A band at 912 cm^{-1} is related with the N-H vibration and a strong band at 1473 cm^{-1} is characteristic of the C-H bending vibration. Cetrimide also showed one band at 3450 - 3311 cm^{-1}, having a peak at 3429 cm^{-1} due to the N–H stretch of a N–substituted amine.

In comparison with pregelatinized modified granular starch and cetrimide, FTIR spectrum of StNC showed some differences, i.e. a new absorption band at 1747 cm^{-1}. This phenomenon could be related to the presence of the carbonyl group of the used lipid. The absorption peak at 1464 cm^{-1} suggested that a new interaction was formed between N-O, since the vibrations of nitro compounds reside in this region, which suggests the interactions among the hydroxyl groups weakened of the starch and the anime of cetrimide. Finally, most of the remaining profile can be directly related to features arising from cetrimide and pregelatinized modified starch.

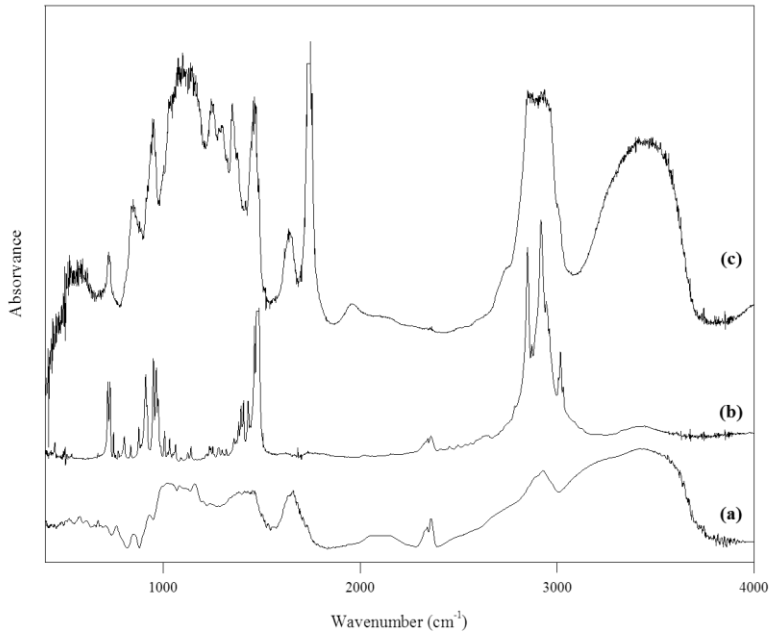

Fig. 4.1.4 - FTIR spectra of (a) pregelatinized modified starch, (b) cetrimide and (c) StNC.

3.1.4.2 DSC

The DSC analysis was performed with the purpose to detect the physical thermodynamic changes of the samples when they are submitted at a temperature ramp throughout time. The physical characterization of the StNC optimized formulation was performed by DSC analysis. The DSC patterns of pure pregelatinized modified starch, cetrimide, Tween® 80, capric/caprylic triglycerides and StNC are presented in Fig. 4.1.5. No significant thermal events occurred in the raw materials Tween® 80 and capric/caprylic triglycerides (liquid lipid). Pregelatinized modified starch and cetrimide showed endothermic events at approximately 140 °C and 106 °C, respectively. The pregelatinized modified starch peak was attributed to the melting of non-complex amylose crystalline [23]. The cetrimide peak is consistent with the literature, reminding the similar peaks observed in some long-chain n-alkanes and n-alkylhalides [24].

No significant thermal events occurred in the StNC when compared to the raw materials. Nevertheless, the relatively low amounts of the pregelatinized modified starch and cetrimide in the StNC could prevent the visualization of any discrete events as the phase transition of the pregelatinized modified starch and cetrimide.

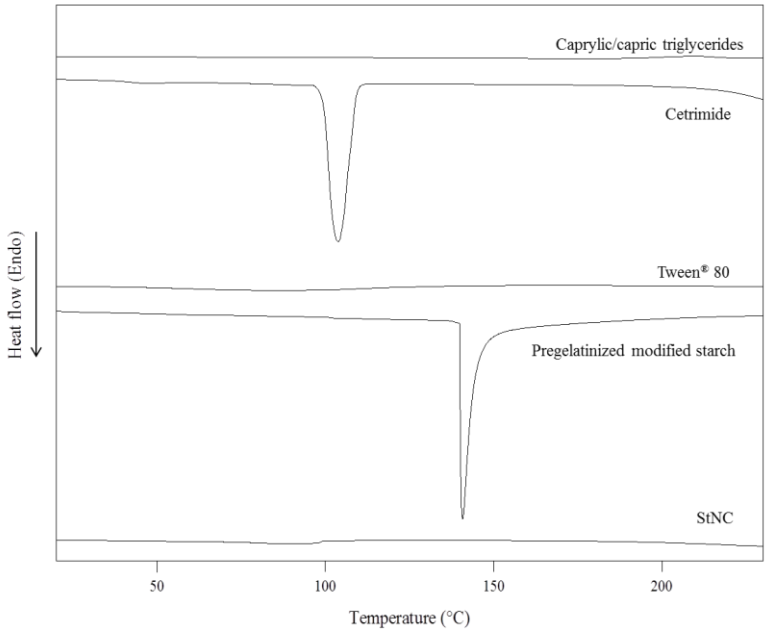

Fig. 4.1.5 - DSC thermograms of capric/caprylic triglycerides, cetrimide, Tween® 80, pregelatinized modified starch and StNC.

3.1.5 Nanostructure of the StNC

Synergistically merging the evidences of starch (biocompatibility, low cost, low toxicity and common in pharmaceutical technology) and capsular advantages (a large inner cavity and favourable interfaces properties), starch-based nanocapsules (StNC) with nanosize have gained interest in pharmaceutical drug delivery.

Overall, this study describes the development of a new drug nanocarrier consisting of an oily core surrounded by a starch shell (Fig. 4.1.6). The rationale beneath the design of this carrier was as follows: the oily core is intended to allocate significant amounts of lipophilic drugs whereas the external polymer shell is expected to improve the stability of the encapsulated drug and control its release rate.

In view of the results, a hypothetical model for the microstructure of the StNC may be proposed with a certain degree of exactitude. Fig. 4.1.6 (a) depicts the model whereby the stabilization of StNC involves two main mechanisms: 1) the presence of a nonionic surfactant (Tween® 80) combined with a cationic surfactant (cetrimide); and 2) the presence of a gelatinized starch network.

In general, surfactants stabilize the emulsion by reducing the interfacial tension of the colloidal system. Non-ionic surfactants can be used alone or in combination with charged surfactants to increase emulsion stability. The former tend to have large head groups that point away from the oil droplet. These polar head groups clash with head groups on water

phase, sterically impeding droplet coalescence, which is the case of Tween® 80. The charged surfactants have relatively high water/ethanol solubility and thus usually produce o/w emulsions. In this specific case, cetrimide, a cationic surfactant was either used as stabilizer. Cetrimide coat the oil droplets and the positive charges on the outside of the oil droplets electrostatically repel each other, decreasing the potential for coalescence [25, 26]. Thus, the polar groups of each surfactant are in an optimal position for the interaction with the bulk phase, i.e. with the aqueous starch network. Modified pregelatinized starch is a cold-water-swelling granular starch excipient, so it will disperse in cold water but not completely dissolved, producing a starch network, which presents a negative charge. The presence of the starch network is likely to stabilize the interfaces and due to the electrostatic attraction, the starch network covered itself around the lipid core, creating the starch shell. Consequently, modified pregelatinized starch suspensions are able to stabilize the water-in-oil interface and form a shell surrounded the lipid core. The mechanism of suspension is related to the presence of a starch network. Thus, the process that was used for the assembly of capsules relied in a simple idea: a poorly charged polymer (modified pregelatinized starch) was added to the oppositely charged core, due to positive charge of cetrimide [12].

The optimized StNC were observed by TEM and AFM, which are rapid, powerful techniques that can provide information on morphology and particle size distribution of these nanocarriers. Fig. 4.1.6 shows the TEM and AFM images and the cross-section profiles from the height and error images of the optimized StNC. Particle sizes obtained using TEM and AFM images are similar to those established from the LD analysis. The nanostructure of StNC is evident in Fig. 4.1.6b, where a polymeric capsule shell can be noticed surrounding a lipid core, thus confirming the topology described above. Concerning AFM analysis, Fig. 4.1.6c (1 and 2) shows isolated discoid structures, but with differences in size and height. A detailed inspection of the three-dimensional image and the cross-section profiles (Fig. 4.1.6c (3 and 4) showed the diameter of the capsules corresponds to the width of the peak at the base of the graphic. The height is the maximum value of the y axis in the cross-section profiles. The regular trace of the graphs indicates that particles present low surface roughness. After measuring the width from each cross-section, a width frequency count histogram (Fig. 4.1.6 (c5)) was built. The results acquired from the width histogram (Fig. 4.1.6 (c6)), after applying the Gaussian model, showed that StNC sample is a heterogeneous sample, with different size distinguishable subpopulations with different average cross-sectional widths.

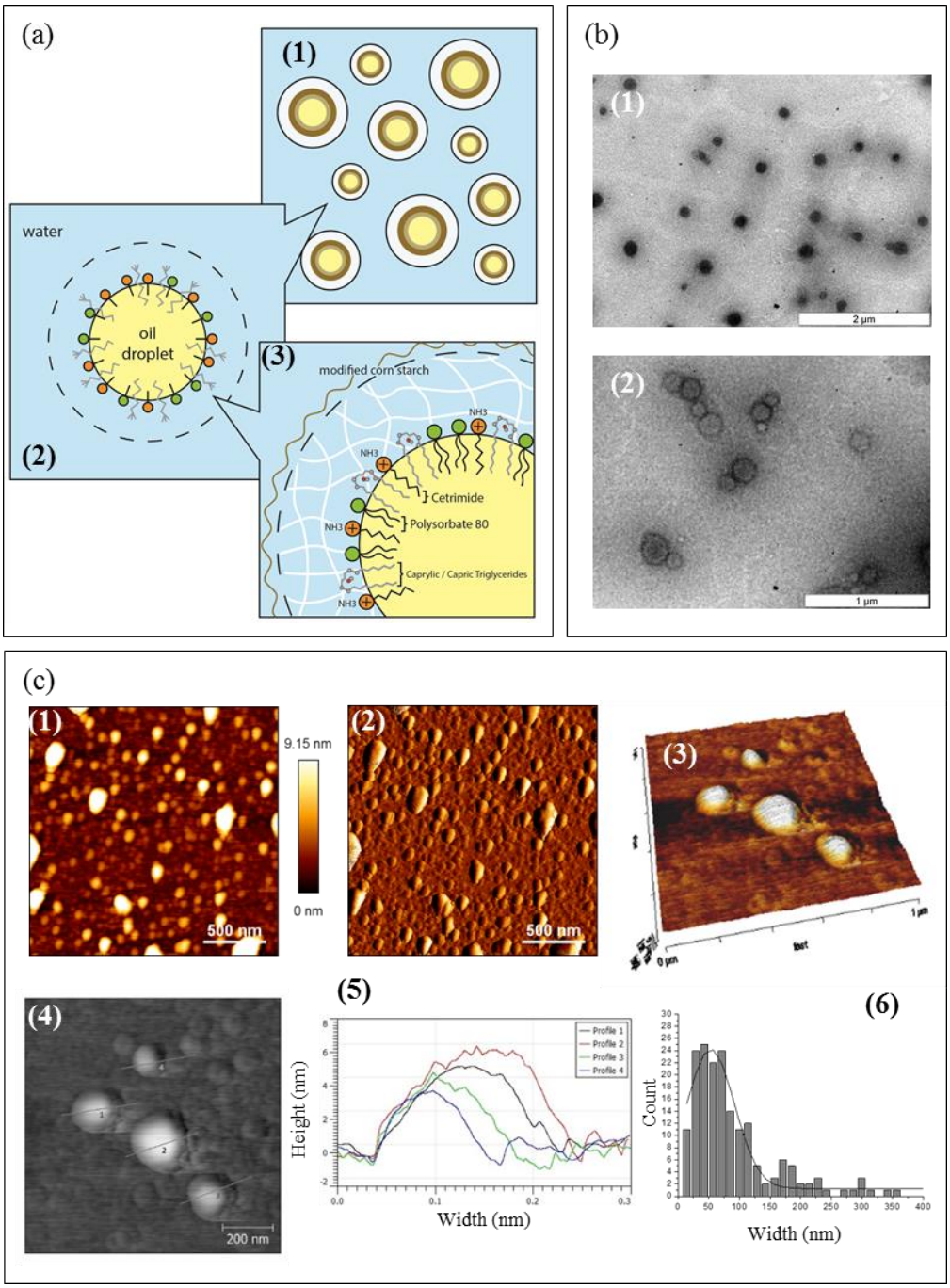

Fig. 4.1.6 – (a) Possible schematic representation for the structure of the StNC. 1) General representation of a suspension of StNC containing nanocapsules in the water phase; 2) schematic representation of a StNC; 3) schematic representation of the molecules involved in the interfacial phenomenon. (b1 and b2) TEM micrographs of optimized StNC in two different magnifications. (c) AFM images for the optimized StNC: (1) height image and respectively error image (2), (3) 3D representation of a height image and (4 and 5) examples of cross-section height profiles performed to quantitatively measured the width of the particles. (6) The right-down panel shows the histogram of the width of the nanoparticles after performing about 180 cross-section profiles of different nanoparticles.

3.1.6 *In vitro* studies of interactions between StNC and cells

The uptake by HaCaT cells of Cou6-labelled StNC was performed to predict their uptake by *in vivo* skin cells (Fig. 4.1.7). Confocal microscopy was used to follow the intracellular trafficking of Cou6-labeled StNC and their uptake by HaCat cells. Moreover, after 1 h of incubation, the StNC aqueous dispersion led to a mean fluorescent intensity three times higher than that of the Cou6 solution (9.9 ± 0.25 % *vs*. 2.9 ± 0.65 %, respectively), indicating that StNC are clearly and efficiently taken up by HaCat cells. On the other hand, CLSM is a technique that allows elucidating the uptake and interactions between the nanocarriers and cells, using a triple fluorescent labelling, i.e., green coumarin-6 for StNCs, blue DAPI for the cell nuclei and red rhodamine phalloidin for the cell actin. The obtained results corroborated the previous results from quantitative uptake, i.e., CLSM images clearly showed that StNC were highly internalized by HaCat cells as indicated by the presence of green fluorescence (StNCs) in the cytoplasm (red staining), being homogenously distributed throughout the cell, presenting some clusters of StNCs observed as larger green spots within them. In addition, Cou6-labelled StNC showed a green core entrapped inside the starch shell, which means this lipophilic fluorescent probe is a useful tool to study the nanoencapsulation of hydrophobic drugs (Fig. 4.1.7). Indeed, these results corroborate a good affinity and biocompatibility between the StNC formulations and skin model cells. This conclusion holds even when internalization takes place, which is especially relevant in the case of contact with skin [27].

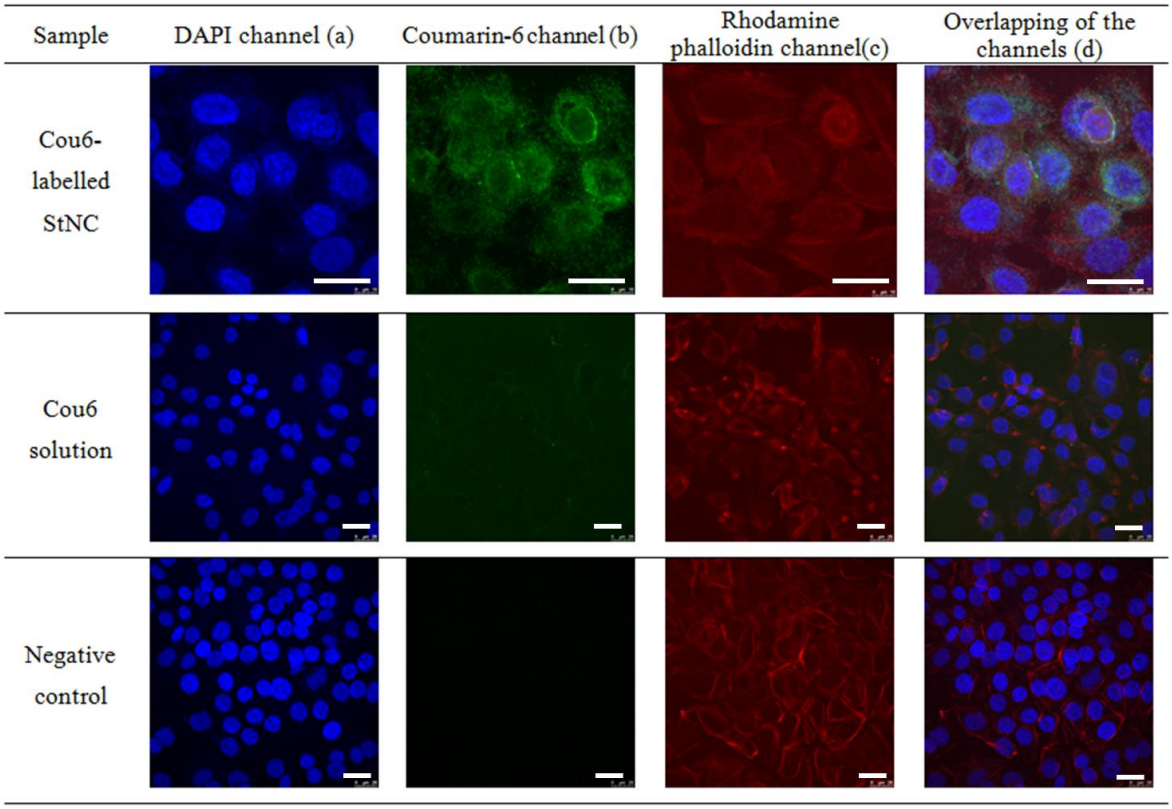

Fig. 4.1.7 - Confocal imaging of HaCat cells incubated with Cou6-labelled StNC. (a) nuclei were stained with DAPI (blue); (b) Cou6-labelled StNC (green); (c) actin were stained with rhodamine phalloidin; (d) overlapping of the three channels (Scale bar: 25µm).

4 Conclusion

The design planning methodology revealed its usefulness in the optimization of process and formula and, consequently, this work provides a framework for understanding the formation of starch-based nanocapsules. The production of StNC was optimized in terms of composition and process using a QbD approach, enabling to successfully develop StNC with an optimized nanometric particle size and acceptable stability.

The results were reinforced by the complementary analyses by DSC and FTIR, which provided some insight in the intermolecular structure, consistent with rationales extracted from the experimental design. TEM and AFM techniques allowed direct visualization of particle size and morphology, corroborating size measurements by LD. The *in vitro* studies confirmed the potential use of StNC for skin application.

In conclusion, the StNCs developed are a smart and promising strategy for topical delivery of lipophilic drugs.

5 References

1. Rodriguez-Cruz IM, Merino V, Merino M, Diez O, Nacher A, Quintanar-Guerrero D. Polymeric nanospheres as strategy to increase the amount of triclosan retained in the skin: passive diffusion vs. iontophoresis. Journal of Microencapsulation. 2013;30(1):72-80.

2. Guterres SS, Alves MP, Pohlmann AR. Polymeric Nanoparticles, Nanospheres and Nanocapsules, for Cutaneous Applications. Drug Target Insights. 2007;2:147-157.

3. Neubert RHH. Potentials of new nanocarriers for dermal and transdermal drug delivery. European Journal of Pharmaceutics and Biopharmaceutics. 2011;77(1):1-2.

4. Almeida AJ, Souto E. Solid lipid nanoparticles as a drug delivery system for peptides and proteins. Advanced Drug Delivery Reviews. 2007;59(6):478-490.

5. Escobar-Chávez JJ. Current Technologies to Increase the Transdermal Delivery of Drugs: Bentham Science Publishers; 2010.

6. Liu Z, Jiao Y, Wang Y, Zhou C, Zhang Z. Polysaccharides-based nanoparticles as drug delivery systems. Advanced Drug Delivery Reviews. 2008;60(15):1650-1662.

7. Escobar-Chávez JJ. Nanocarriers for transdermal drug delivery. Skin. 2012;19:22.

8. Chin SF, Azman A, Pang SC. Size controlled synthesis of starch nanoparticles by a microemulsion method. Journal of Nanomaterials. 2014;2014:9.

9. Yu LX, Amidon G, Khan MA, Hoag SW, Polli J, Raju GK, Woodcock J. Understanding pharmaceutical quality by design. AAPS J. 2014;16(4):771-783.

10. Marto J, Gouveia L, Jorge IM, Duarte A, Gonçalves LM, Silva SMC, Antunes F, Pais AACC, Oliveira E, Almeida AJ, Ribeiro HM. Starch-based Pickering emulsions for topical drug delivery: A QbD approach. Colloids and Surfaces B: Biointerfaces. 2015;135:183-192.

11. Ferreira IS, Bettencourt AF, Goncalves LM, Kasper S, Betrisey B, Kikhney J, Moter A, Trampuz A, Almeida AJ. Activity of daptomycin- and vancomycin-loaded poly-epsilon-caprolactone microparticles against mature staphylococcal biofilms. Internation Journal of Nanomedicine. 2015;10:4351-4366.

12. Mora-Huertas CE, Fessi H, Elaissari A. Polymer-based nanocapsules for drug delivery. International Journal of Pharmaceutics. 2010;385(1–2):113-142.

13. Quintanar-Guerrero D, Allémann E, Fessi H, Doelker E. Preparation techniques and mechanisms of formation of biodegradable nanoparticles from preformed polymers. Drug Development and Industrial Pharmacy. 1998;24(12):1113-1128.

14. Riddick T. Zeta-meter manual1968.

15. ICHQ1A(R2). ICH of Technical Requirement for Registration of Pharmaceuticals for Human Use, Stability Testing of new Drugs and Products. www.ich.org; 2003.

16. Vitorino C, Carvalho FA, Almeida AJ, Sousa JJ, Pais AA. The size of solid lipid nanoparticles: an interpretation from experimental design. Colloids and Surfaces B: Biointerfaces. 2011;84(1):117-130.

17. Martins S, Tho I, Souto E, Ferreira D, Brandl M. Multivariate design for the evaluation of lipid and surfactant composition effect for optimisation of lipid nanoparticles. European Journal of Pharmaceutical Sciences. 2012;45(5):613-623.

18. Abdel-Mottaleb MM, Moulari B, Beduneau A, Pellequer Y, Lamprecht A. Surface-charge-dependent nanoparticles accumulation in inflamed skin. Journal of Pharmaceutical Sciences. 2012;101(11):4231-4239.

19. Lemoine D, Francois C, Kedzierewicz F, Preat V, Hoffman M, Maincent P. Stability study of nanoparticles of poly (ε-caprolactone), poly (d, l-lactide) and poly (d, l-lactide-co-glycolide). Biomaterials. 1996;17(22):2191-2197.

20. Abbas S, Karangwa E, Bashari M, Hayat K, Hong X, Sharif HR, Zhang X. Fabrication of polymeric nanocapsules from curcumin-loaded nanoemulsion templates by self-assembly. Ultrasonics Sonochemistry. 2015;23:81-92.

21. He W, Lu Y, Qi J, Chen L, Hu F, Wu W. Nanoemulsion-templated shell-crosslinked nanocapsules as drug delivery systems. International Journal of Pharmaceutics. 2013;445(1):69-78.

22. Schaffazick S, Pohlmann A, Guterres S. Nanocapsules, nanoemulsion and nanodispersion containing melatonin: preparation, characterization and stability evaluation. Die Pharmazie - An International Journal of Pharmaceutical Sciences. 2007;62(5):354-360.

23. Liu H, Yu L, Simon G, Dean K, Chen L. Effects of annealing on gelatinization and microstructures of corn starches with different amylose/amylopectin ratios. Carbohydrate Polymers. 2009;77(3):662-669.

24. Bezrodna T, Puchkovska G, Styopkin V, Baran J, Drozd M, Danchuk V, Kravchuk A. IR-study of thermotropic phase transitions in cetyltrimethylammonium bromide powder and film. Journal of Molecular Structure. 2010;973(1–3):47-55.

25. Rosen MJ, Kunjappu JT. Surfactants and Interfacial Phenomena: Wiley; 2012.

26. Raposo S, Salgado A, Eccleston G, Urbano M, Ribeiro HM. Cold processed oil-in-water emulsions for dermatological purpose: formulation design and structure analysis. Pharmaceutical Development and Technology. 2014;19(4):417-429.

27. Vitorino C, Almeida J, Gonçalves LM, Almeida AJ, Sousa JJ, Pais AACC. Co-encapsulating nanostructured lipid carriers for transdermal application: From experimental design to the molecular detail. Journal of Controlled Release. 2013;167(3):301-314.

Section 2

Starch nanocapsules containing a novel neutrophil elastase inhibitor with improved pharmaceutical performance

This page was intentionally left blank

Graphical Abstract

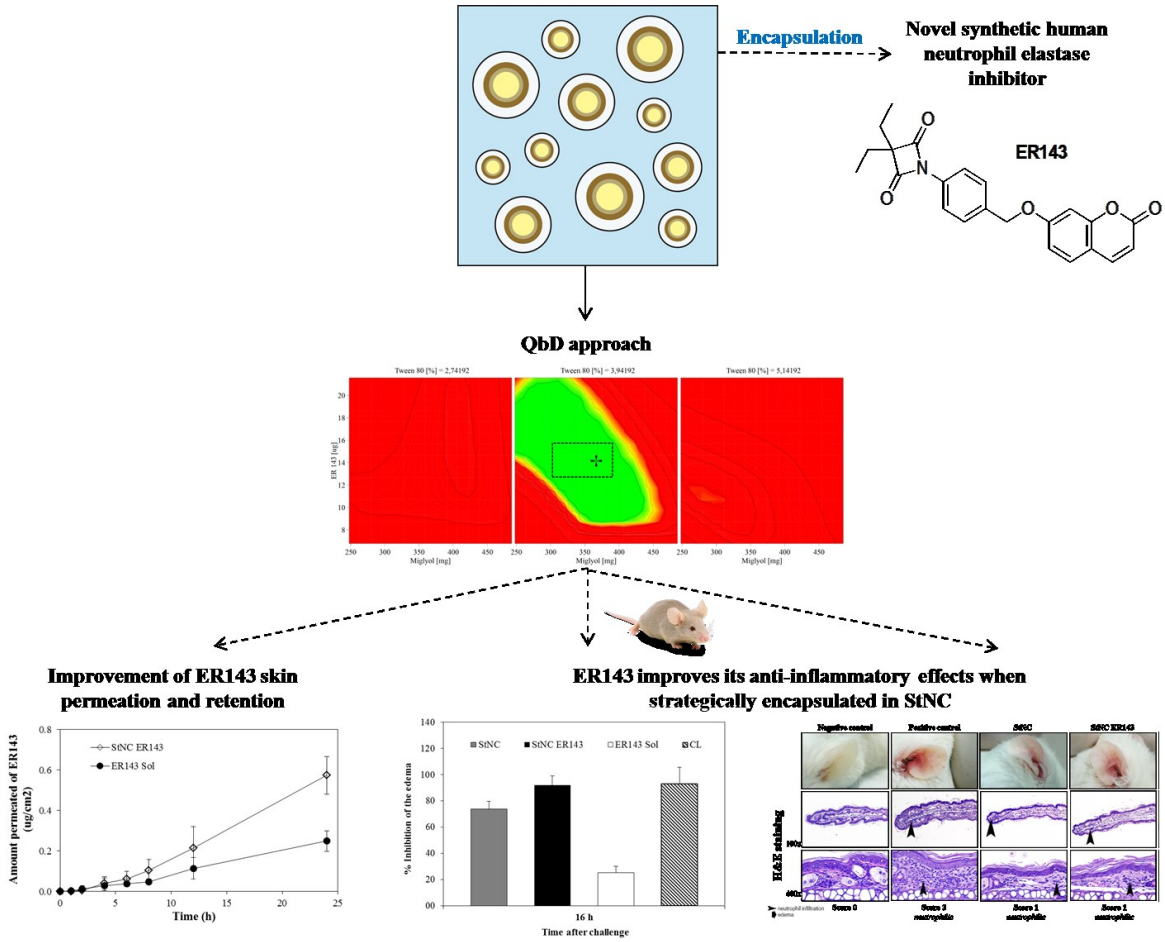

Highlights:

- The incorporation of a novel synthetic human neutrophil elastase inhibitor (ER143) into starch nanocapsules (StNC) proved to be a simple and smart strategy to improve ER143 skin permeation and retention.
- StNC provide a ER143 sustained release profile.
- ER143-loaded StNC showed an improved anti-inflammatory effect compared to ER143 solution.
- A QbD approach was successfully applied to obtain ER143-loaded StNC.

This page was intentionally left blank

1 Introduction

Currently, topical drug delivery is one of the most promising routes of drug administration. Nevertheless, the s*tratum corneum* (SC) is the main biological barrier for the delivery of drugs, which makes the topical drug delivery a challenge. Topical formulations are selected due to their localized effects at the site of the application taking advantage of drug permeation into the deeper layers of skin. However, an effective topical delivery of drugs remains a challenge to the drug delivery field, since approximately 40% of the novel promising molecules present poor solubility, and thus topical delivery is often associated with low absorption and poor bioavailability [1, 2]. To overcome these bioavailability demands, several formulation strategies have been reported, including the use of polymeric and lipid based nanoparticles to improve percutaneous absorption due to their capacity to enhance the rate and extent of the transport across the skin as a result of their high specific surface area [3-6].

Nanoparticulate carriers can provide important advantages over the conventional drug delivery systems, namely a higher physicochemical stability and drug carrying capacity, the possibility to modulate the drug release by modifying some of its characteristics as well as the ability to deliver both hydrophilic and hydrophobic drugs. In addition, these colloidal vehicles that carry drugs to the target in a controlled manner may offer further advantages such as reducing the dose frequency, increasing therapeutic control, reducing side effects, and, consequently, improving patient compliance [7].

Particularly, starch-based nanocapsules have attracted increasing interest as potential topical drug delivery vehicles, largely due to their simple and green process of preparation not requiring the use of hazardous organic solvents as well as the possibility to incorporate a wide range of drugs. They can also enhance topical bioavailability by both reducing the carrier size, increasing the rate of absorption, and by forming an occlusive layer on the skin surface that decreases water evaporation and creates wider diffusion channels [8].

These advantages increased the search for an alternative topical drug delivery system in the form of starch-based nanocapsule. The drug selected for this study is a novel inhibitor of human neutrophil elastase (HNE), presenting low water solubility and putative anti-inflammatory action. HNE is a proteolytic enzyme that is thought to play a central role in diverse inflammatory diseases. An imbalance between HNE and its endogenous inhibitors lead to severe tissue injuries triggering various disease as for instance rheumatoid arthritis, chronic obstructive pulmonary disease, psoriasis or delayed wound healing [9, 10]. The HNE is present inside the migrating neutrophils in the reticular dermis and dermal papillae,

as well as outside the cells in micro-abscesses in psoriatic skin. Hence, psoriatic skin contains low concentrations of specific elastase tissue inhibitor, which results in an excessive *in vivo* hydrolytic activity of neutrophil elastase released from migrating cells [11].

Therefore, HNE is an attractive therapeutic target and the design of new HNE inhibitors is a demanding field. MedChem group from iMed.ULisboa has been intensively dedicated to this area in order to provide new inhibitors with new architectures, including the potent oxo-β-lactam class [12]. In the present work, a coumarin-based oxo-β-lactam was designed as to be an irreversible HNE inhibitor that behaves as a turn-on probe as upon HNE inhibition releases the fluorescent hydroxy-coumarin, allowing appropriate signalization for skin permeation studies.

Thus, the purpose of this study was to develop and characterize novel starch-based nanocarrier for topical delivery of a novel HNE inhibitor in order to increase its bioavailability. Hence, a quality by design (QbD) approach was performed not only to extract the maximum amount of information from the collected data, but also to establish the influence of several factors on the formulation and physical properties of starch-based nanocapsules. The *in vitro* release and permeation studies and the *in vivo* efficacy studies were also evaluated in detail, demonstrating the successful application of starch nanocapsules and highlighting their potential for sustained drug release, acting as a promising vehicle for topical delivery of HNE inhibitors.

2 Materials and methods

2.1 Materials

The materials used are described in Chapter 4, Section 1, section 2.1.

2.2 Methods

2.2.1 HNE inhibitor synthesis

Synthesis of 3,3-diethyl-1-(4-(((2-oxo-2*H*-chromen-7-l)oxy)methyl)phenyl)azetidine-2,4-dione (ER143)

Chemical structure of ER143 is presented in Fig. 4.2.1. The synthesis of ER143 was made as herein described. To a solution of 6-hydroxycoumarin (100 mg, 0.616 mmol) in acetone (1 ml) was added potassium carbonate (94 mg, 0.677 mmol) and the resulted solution was subjected a stirring for 20 minutes. Then, was added a solution of the respective bromo precursor (193 mg, 0.622 mmol) in the same solvent (1 ml), dropwise, and the reaction was

stirred for 6 h at 60 °C. The reaction mixture was diluted with water (5 volumes) and the product extracted with 3xEtOAc (5 volumes). The organic layers were combined, dried with anhydrous Na_2SO_4, filtered and concentrated.

ER143 is a novel neutrophil elastase inhibitor with potential anti-inflammatory activity. It has a molecular weight (MW) of 391.42 g/mol and a LogP of 3.85, making it a suitable candidate for topical delivery.

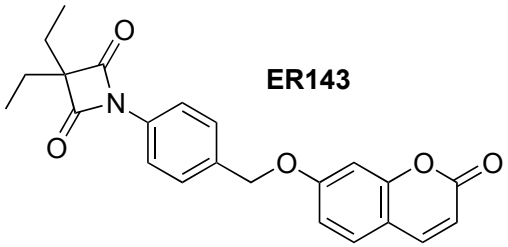

Fig. 4.2.1 – Chemical structure of ER143.

2.2.2 Biological assays

2.2.2.1 Enzymatic inhibition assay

Fluorometric assays for the HNE (Merck, Germany) inhibition activity were carried out in 200 µl assay buffer (0.1 M HEPES pH 7.5 at 25 °C) containing 20 µl of 0.17 µM HNE (stock solution 1.7 µM in 0.05 M acetate buffer, pH 5.5), 155 µl of assay buffer and 5 µl of each concentration of tested inhibitors. After 30 min of incubation at 25 °C, the reaction was initiated by the addition of 20 µl of fluorogenic substrate to a final concentration of 200 µM (MeO-Suc-Ala-Ala-Pro-Val-AMC, Merck, Germany). The Michaelis-Menten constant (K_m) of this substrate of HNE was previously determined to be 185 µM (data not shown). For all assays, saturated substrate concentration was used, throughout, in order to obtain linear fluorescence curves. Controls were performed using enzyme alone, substrate alone, enzyme with DMSO and a positive control (Sivelestat sodium salt hydrate, Sigma Aldrich, UK) [13].

2.2.2.2 Fluorescence microscopy with human neutrophils

Human neutrophils were isolated from healthy volunteers with Dextran sedimentation followed by Ficoll-Paque Plus density gradient (GE Healthcare Bio-Sciences AB, Uppsala, Sweden) and used as effector cells, as described elsewhere [14]. Human neutrophils after 30 min (at room temperature) of contact with ER143 (final concentration 8 µM) were washed with 10 mM PBS, containing 20 mM of glycin (PBS) and, then cells were fixed

with 0.4 % paraformaldehyde (15 min at room temperature), washed twice with PBS, and mounted with mounting medium (ProLong Antifade, Life Technologies, UK), containing DAPI (for nuclei labeling, blue). The fluorescence was observed and recorded on an Axiovert 40CFL fluorescence microscope (Carl Zeiss, Germany) (100x objective) equipped with an Axiocam MR3 (Carl Zeiss, Germany) camera. Images were processed with the software AxioVision Rel.4.8 (Carl Zeiss).

2.2.3 Preparation of neutrophil elastase inhibitor-loaded starch-based nanocapsules (StNC ER143)

StNC ER143 were prepared by emulsion-solvent evaporation method according to the procedure described previously in Chapter 4, Section 1, section 2.2.1.1. According to solubility studies (results not shown), caprylic/capric triglycerides allowed maximal solubility for ER143 (30 µg/mg lipid). Thus, the drug (ER143) was dissolved on capric/caprylic triglycerides and then added to the ethanolic phase, obtaining StNC ER143 nanocapsules. The different concentrations of ER143 used in design of experiment (DoE) were selected based on preliminary solubility studies of ER143 in caprylic/capric triglycerides.

2.2.4 Particle size analysis and zeta potential measurements

The particle size analysis and zeta potential measurements were performed according to the procedure described previously in Chapter 4, Section1, section 2.2.1.2.

2.2.5 Encapsulation efficiency and drug loading

After preparation, non-incorporated ER143 was separated from the StNC dispersions by size exclusion chromatography on Sephadex G-25/PD-10 columns (Sigma Aldrich, UK). The ER143 incorporation in StNC was determined after dissolving the nanocapsules with acetonitrile, which promoted the precipitation of the lipid and polymeric phase. The encapsulated ER143 remained in the supernatant, which was separated by centrifugation. The amount of free drug in the aqueous phase was measured in the supernatant at 360 nm (excitation) and 460 nm (emission) wavelengths using a fluorescence microplate reader (FLUOstar BMGLabtech, Germany). The supernatant of non-loaded nanocapsules was used as basic correction.

The ER143 encapsulation efficiency (EE) and drug loading (DL) in StNC were calculated according to the following equations:

Equation 1: $\mathrm{EE}(\%) = \frac{W_{\text{free drug}}}{W_{\text{initial drug}}} \times 100$

Equation 2: $\mathrm{DL}(\%) = \frac{W_{\text{free drug}}}{W_{\text{lipid}}} \times 100$

where $W_{\text{initial drug}}$ is the weight of the drug used, $W_{\text{free drug}}$ is the weight of free drug detected in the supernatant after centrifugation of the aqueous dispersion and W_{lipid} represents the weight of the lipid vehicle.

2.2.6 Fourier transform infrared spectroscopy (FTIR)

FTIR analysis were performed according to the procedure described previously in Chapter 4, Section1, section 2.2.1.3

2.2.7 Differential scanning calorimetry (DSC)

DSC measurements were performed according to the procedure described previously in Chapter 4, Section1, section 2.2.1.4

2.2.8 Quality by design (QbD) approach

2.2.8.1 Identification of quality target product profile (QTPP) and critical quality attributes (CQAs)

The identification of QTPP was performed according to the procedure described previously in Chapter 3, Section 1, section 2.2.3. The important features of StNC are particle size distribution, zeta potential and encapsulation efficiency, which influence other relevant characteristics, such as physicochemical stability and *in vivo* efficacy. Thus, a list of the QTTP that will be herein studied and the respective acceptance limits is given in Table 4.2.1.

2.2.8.2 Risk analysis of CQAs

Risk analysis was performed according to the procedure described previously in Chapter 3, Section 1, section 2.2.4. With the collected information, Ishikawa diagrams were constructed to identify the potential risks. The particle size, zeta potential, encapsulation efficiency and drug loading were defined and further delineated to identify potential risks and, after the analysis, the variables were identified for optimization in the following studies.

Table 4.2.1 - QTPP of StNC ER143.

QTPP element	Target
Route of administration	Topical [11]
Dose	100 µg
Dosage form	Nanoparticle (nanocapsule) [15]
	Particles size distribution: • d(10) - 0.1 - 0.3 µm • d(50) - 0.2 - 0.5 µm • d(90) - 0.3 - 0.9 µm • Span - 0.5 - 2.0
	Encapsulation efficiency > 75%
	Drug loading > 0.5%
Stability	Zeta potential > 30 mV [16]
	At least 12 month shelf-life at 5 ± 3 °C [17]
Drug product quality attributes [18]	Residual solvents Identification Assay Water content Degradation products Impurities
In vivo efficacy [19]	Anti-inflammatory activity: • Inhibition of the edema – 90-100% • Inhibition of the erythema

2.2.8.3 Response surface analysis

Response surface analysis was performed as previously described in Chapter 4, Section 1, section 2.2.4. The formula of the StNC ER143 was optimized using a central composite design (CCD). The independent variables were the percentage of nonionic surfactant, Tween® 80 (T), the amount of drug (ER143) and the amount of lipid (L). The chosen CCD α value with the aim to ensure design rotability was 1.682 (Table 4.2.2).

Table 4.2.2 - Experimental design conditions, design and experimental matrixes.

ID	Design Matrix			Experimental Matrix		
	T (%, w/v)	ER143 (µg/mg lipid)	L (mg)	T (%, w/v)	ER143 (µg/mg lipid)	L (mg)
F1	-1	-1	-1	1.8	7.6	181.1
F2	1	-1	-1	4.2	7.6	181.1
F3	-1	1	-1	1.8	22.4	181.1
F4	1	1	-1	4.2	22.4	181.1
F5	-1	-1	1	1.8	7.6	418.9
F6	1	-1	1	4.2	7.6	418.9
F7	-1	1	1	1.8	22.4	418.9
F8	1	1	1	4.2	22.4	418.9
F9	-1.682(-α)	0	0	0.9	15	300
F10	1.682 (α)	0	0	5.0	15	300
F11	0	-1.682 (-α)	0	3.0	2.6	300
F12	0	1.682(α)	0	3.0	27.4	300
F13	0	0	-1.682 (-α)	3.0	15	100
F14	0	0	1.682 (α)	3.0	15	500
F15	0	0	0	3.0	15	300
F16	0	0	0	3.0	15	300
F17	0	0	0	3.0	15	300

T - % of Tween® 80; ER143 - ER143 amount; L - Capric/caprylic triglycerides amount.

2.2.9 *In vitro* ER143 release studies from StNC

Prior to the release studies, the nanodispersions were desalted on Sephadex G-25 medium pre-filled PD-10 columns (GE Healthcare Life Sciences). The release of ER143 was carried out by incubating the nanoparticles (~ 0.75 mg) in a release medium comprising water:ethanol (7:3) with horizontal shaking at 37 ºC. At appropriate time intervals, individual samples were centrifuged in a high-speed centrifuge (Allegra™ 64R centrifuge, Beckman Coulter) at 40000×g for 30 min at 22 ºC. The amount of released ER143 was evaluated in the supernatants by fluorescence in a microplate reader (FLUOstar Omega, BMG Labtech, Germany) (excitation filter of 360 nm and emission filter 495 nm) (n = 6).
The obtained data from *in vitro* release studies were fitted as described in Chapter 3, Section 2, section 2.2.4.

2.2.10 Topical delivery studies of *StNC ER143*

2.2.10.1 In vitro skin permeation

Skin permeation studies were performed according to the procedure described previously in Chapter 3, Section 2, section 2.2.5.1. Water:ethanol (7:3) was used as the receptor phase that assured perfect sink conditions during all experiment period. The ER143 content in the

withdrawn samples was determined as above described. A control solution with the same ER143 concentration and six replicates for each sample were used. The cumulative amount of permeated ER143 (Qt) through excised newborn pig skin was plotted as function of time and determined based on the following equation:

Equation 3: $Qt = \frac{Vr \times Ct + \sum_{t=0}^{t-1} Vs \times Ci}{S}$

Where, Ct is the drug concentration of the receptor solution at each sampling time, Ci the ER143 concentration of the sample applied on the donor compartment, and Vr and Vs the volumes of the receptor solution and the sample, respectively. S represents the skin surface area (1 cm^2). The slope and intercept of the linear portion, between 4 and 24 h for StNC ER143 and ER143 solution of the plot were derived by regression using the GraphPad PRISM® 5 software (San Diego, CA, USA). ER143 fluxes (J, μg cm^{-2} h^{-1}) through the skin were calculated from the slope of the linear portion of the cumulative amounts permeated through the human skin per unit surface area versus time plot. The permeability coefficients (Kp, cm h^{-1}) were obtained by dividing the flux (J) by the initial drug concentration (C_0) in the donor compartment applying the Fick's 2nd law of diffusion (Equation 4), and it was assumed that under *sink conditions* the drug concentration in the receptor compartment is negligible compared to that in the donor compartment.

Equation 4: $M(t) = k\ l\ c_0 \left[\frac{D\,t}{l^2} - \frac{1}{6} - \frac{2}{\pi^2} \sum_{n=1}^{\infty} \frac{(-1)^n}{n^2} \exp(-Dn^2 \pi^2 \frac{t}{l^2})\right]$

2.2.10.2 In vitro skin retention

Skin retention studies were performed according to the procedure described previously in Chapter 3, Section 2, section 2.2.5.2. StNC ER143 and ER143 solution (0.3 ± 0.1 g) were spread over the newborn pig skin (1 cm^2) in contact with 3 ml of receptor phase as described before. In this extraction process, 3 ml of ethanol for ER143 assay was added to the SC tapes and ED pieces. The final solution was centrifuged (30000 rpm, 10 min) and the supernatant was filtered (0.2 μm) and assayed as above described to quantify the amount (%) of ER143 retained in these skin layers (SC + ED).

2.2.11 *In vivo* anti-inflammatory activity studies

The croton oil-induced ear inflammation model was used for investigating anti-inflammatory effects of a novel neutrophil elastase inhibitor that has potent inhibitory

effects on the production of proinflammatory cytokines from neutrophils [19]. The model was performed using female BALB/c mice (Instituto Gulbenkian de Ciências, Oeiras, Portugal). Mice were used after 1 week acclimatization to the laboratory environment. All animal experiments were carried out with the permission of the local animal ethical committee in accordance with the EU Directive (2010/63/EU), Portuguese law (DL 113/2013) and all relevant legislations. The experimental protocol was approved by Direcção Geral de Alimentação e Veterinária.

The inside of an animal ear was challenged with 10 µl of 5 % croton oil dissolved in acetone and left to dry. After the challenge, each animal was kept individually in a separate cage. One hour after the challenge, tested formulations (StNC, StNC ER143, ER143 solution and commercial lotion (CL) with hydrocortisone butyrate 1 mg/ml was used as a positive control) were applied (10 µl) on the challenged area and left to dry. The resulting edema was determined 16 h later. The ear thickness was measured with a Mitutoya® micrometer (Ascona Tools, Redwood City, USA) with three readings per ear. The degree of edema inhibition was calculated as a percentage of inhibition, determined by comparing the drug treated group with untreated controls. Six mice per group were used. Data were analyzed using the GraphPad PRISM 5 software (San Diego, CA, USA) and the groups were considered significant when the estimated *p* values were lower than 0.1 (the chosen α error), to increase statistical power.

2.2.12 Mouse ear histology

In order to evaluate the surroundings of the site of application, animals were sacrificed 16 h after the treatment with StNC, ER143 solution, StNC ER143 and CL. An ear challenged with 10 µl of 5 % croton oil dissolved in acetone was used as positive control and a native ear as negative control. The ears were resected and fixed in 10 % buffered formalin solution and cut into four strips of equal size. Strips were processed for routine histology and embedded in paraffin. A section of skin with 5µm thick was stained with hematoxylin and eosin (H&E). Lesions were scored by a pathologist blinded to experimental groups, based on the nature and the extent/severity of the lesions. Briefly, lesions were characterized by focally extensive inflammation expanding the dermis, between epidermis and the pinnal cartilage, resulting in diffuse thickening, invariably more severe at the ear tip. Infiltrate corresponded to granulation tissue with marked neutrophilic component. Occasionally, cellular infiltration was accompanied by edema. Lesions were individually scored (0–4 increasing severity; 0, absent; 1, minimal; 2, mild; 3, moderate; 4, severe).

2.2.13 Statistical analysis

According to the method described in Chapter 3, Section 2, section 2.2.9.

3 Results and discussion

3.1 Synthesis of HNE inhibitor ER143

MedChem group from iMed.ULisboa has been engaged with the development of HNE inhibitors, namely the ones based on the oxo-β-lactam scaffold as the proved to be highly potent when compared with the existent portfolio of HNE inhibitors [20, 21]. Moreover, as covalent inhibitors of HNE these can be drawn as activity based probes that provide appropriate signalling for HNE activity detection [22]. Hence, they have synthesized ER143 from the bromo derivative (***i***, previously reported by MedChem group [20], Fig. 4.2.2), by nucleophilic substitution of the bromine atom by hydroxycoumarin that will be used as tag for skin permeation studies and HNE activity detection. The desired compound was the following:

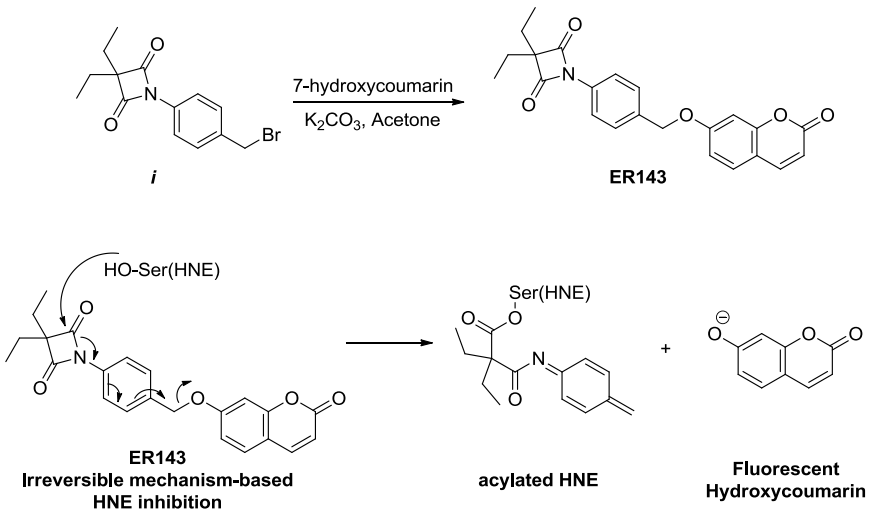

Fig. 4.2.2 - Synthetic approach to ER143 and mechanism of action against HNE.

ER143 was envisaged as a "turn-on" probe to make possible the determination of the HNE inhibitor in the permeation studies. The fluorescent properties of ER143 change as a result of enzymatic cleavage of the ester releasing a molecule of coumarin. In the present studies, a solution of NaOH was used to mimic the cleavage of ER143 by the –OH group of HNE Ser195. Therefore, using this technique was possible to quantify the inhibitor in the *in vitro* release study and in the *in vitro* skin permeation and retention studies.

3.2 Biological assays

3.2.1 Enzymatic inhibition assay

In order to evaluate the inhibitory activity of ER143, *in vitro* assays were performed against HNE and this was shown to be in the sub-nanomolar range with IC_{50} value of 0.67±0.19 nM (Fig. 4.2.3). In order to get kinetic insight, ER143 and substrate were added to the enzyme and product formation was monitored for 120 min, at different inhibitor concentrations. The resulting progress curves are depicted in Fig. 4.2.3 an show concentration but no time-dependence, which may indicate a competitive mechanism [13].

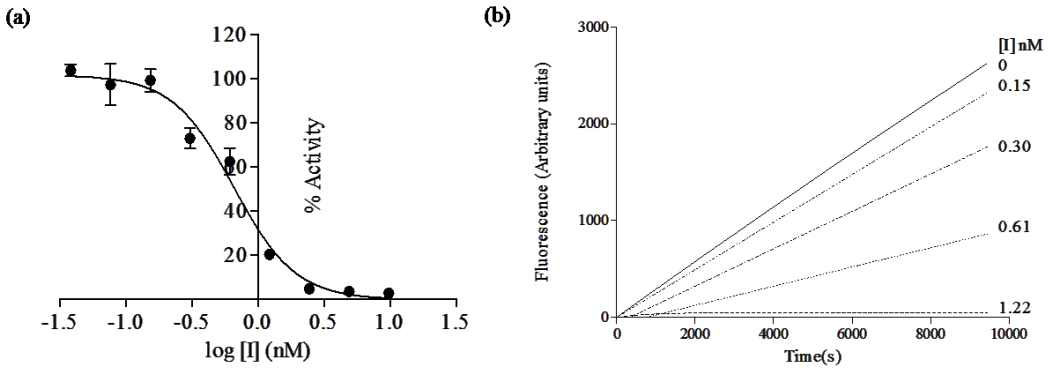

Fig. 4.2.3 - (a) The IC_{50} curve for ER143 (IC_{50}= 0.67 ± 0.19 nM); (b) Plots of progress curves for HNE inhibition by 0.15 to 1.22 nM of compound ER143. No time dependent inhibition was observed and lines indicate linear best fits.

3.2.2 Fluorescence microscopy with human neutrophils

The ability of ER143 to be cleaved *in vitro* in human leukocytes cells was observed by inspection of human leukocytes incubated with ER143, using fluorescence microscopy (Fig.4.2.4).

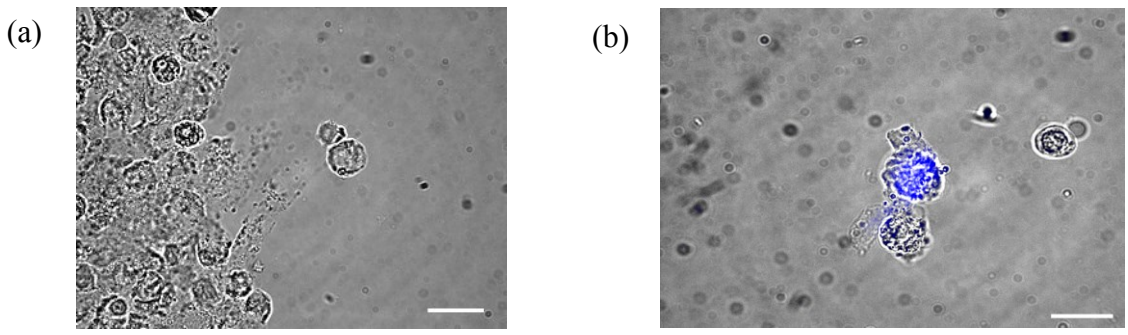

Fig. 4.2.4 - Fluorescence microscopy micrograph of human neutrophils incubated with (a) PBS and (b) ER143 (Scale bar: 10 µm).

3.3 Quality by design approach

3.3.1 Risk analysis of CQAs

Based on the previous finding, the focus of the present work was the skin delivery of ER143 after topical administration of ER143-loaded nanocapsules. Thus, the following step was to quantify the factors that potentially can affect the quality attributes of the StNC ER143. Critical variables were identified (Fig. 4.2.5) and the effects of these variables on the particle size distribution, zeta potential, encapsulation efficiency and drug loading were studied using DoE. Thus, the major critical variables identified as possible cause of product variability were the amounts of nonionic surfactant (Tween® 80), ER143 and lipid.

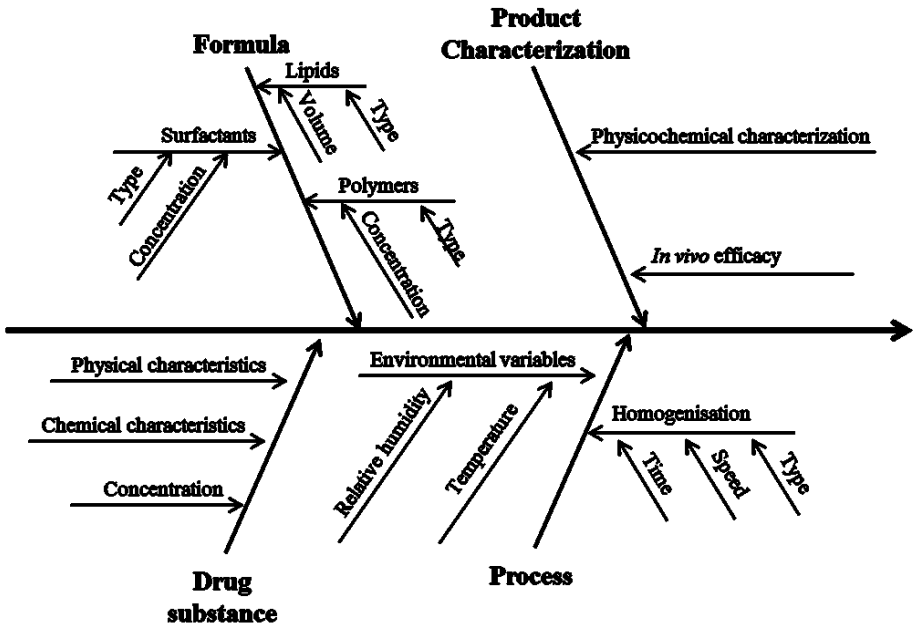

Fig. 4.2.5 - Ishikawa diagram illustrating factors that may have impact on the physicochemical characterization and *in vivo* efficacy of StNC ER143.

3.3.2 Response surface analysis

In previous work, the optimization of experimental conditions to obtained stable StNC was established and, pharmaceutically acceptable formulations were achieved. This previous work clearly indicates that StNC characteristics are highly influenced by the amount of lipid and surfactant concentration. In this design, such variables were studied as a consequence of the previous results.

The data obtained by using the experimental design were analyzed and second degree polynomial models were fitted and its statistical significance assessed using ANOVA. The model was statistically significant as $p < 0.1$ for all critical quality attribute (Table 4.2.3).

The suitability of the fit was estimated by lack of fit, and all models presented good fit to the data, that is, the model has no lack of fit ($p > 0.1$). An acceptable correlation between the observed and predicted values was obtained as indicated by the resulting R^2 values in the range 0.92 to 1.00 for all variables.

Table 4.2.3 - Summary of ANOVA and lack of fit for testing models.

Critical quality attribute	ANOVA		Lack of fit
	R^2	*p*	(*p*)
d(10)	0.994	<0.001	0.157
d(50)	0.953	0.001	0.164
d(90)	0.950	0.001	0.173
Span	0.984	<0.001	0.277
Zeta potential	0.928	0.008	0.176
EE	0.963	<0.001	0.161
DL	0.985	<0.001	0.153

EE – Encapsulation efficiency; DL – Drug loading

Table 4.2.4 illustrates the statistical analysis results using MODDE® Pro 11 (Umetrics, Sweden) software. A positive value indicates an effect that increases the response, and a negative value represents an inverse effect between the response and the factor.

Table 4.2.4 - Summary of regression analysis results for measured responses, for formula optimization.

	d(10)		d(50)		d(90)		Span		Zeta potential		EE (%)		DL (%)	
	Coeff	± SE	Coeff	± SE	Coeff	± SE	Coeff	± SE	Coeff	± SE	Coeff	± SE	Coeff	± SE
k	-0.779	<0.001	-0.588	<0.001	-0.355	<0.001	1.831	<0.001	29.602	<0.001	52.130	<0.001	0.770	<0.001
T	NS	NS	NS	NS	NS	NS	0.069	0.004	-1.225	0.019	12.282	<0.001	0.193	<0.001
ER143	0.019	0.002	0.0278	0.008	0.025	0.030	-0.1596	<0.001	NS	NS	-2.9389	0.030	0.247	<0.001
L	0.042	0.002	0,073	<0.001	0.089	<0.001	-0.175	<0.001	2.063	<0.001	3.774	0.010	0.087	0.004
T^2	0.020	0.002	0.030	0.007	0.034	0,011	-0.103	<0.001	1.777	0.003	3.335	0.026	NS	NS
$ER143^2$	NS	NS	NS	NS	NS	NS	NS	NS	NS	NS	NS	NS	-0.050	0.044
L^2	NS	NS	NS	NS	NS	NS	-0.075	0.003	NS	NS	NS	NS	NS	NS
T*ER143	0.024	0.002	0.032	0.012	0.040	0.013	-0.063	0.027	NS	NS	NS	NS	0.098	0.011
T*L	NS	NS	NS	NS	NS	NS	NS	NS	NS	NS	3.515	0,041	NS	NS
ER143*L	NS	NS	NS	NS	NS	NS	NS	NS	NS	NS	4.893	0.010	0.113	0.005

Coeff– Coefficient Scaled and centered; SE – Standard Error; k – Constant; NS (no significant) – p>0.10; EE – Encapsulation efficiency; DL – Drug loading; T - percentage of Tween® 80; ER143 - amount of drug (ER143); L - amount of lipid;

A general interpretation indicates that a decrease in lipid and ER143 amount originates lower mean particle size, and, as expected, an increase in lipid amount and in Tween® 80 concentration and a decrease in ER143 amount, increases the encapsulation efficiency.

Considering the CCD results, the statistically significant variables affecting d(10), d(50) and d(90) were the amount of ER143 and the lipid, while, for span, all factors had statistical significance ($p < 0.10$). Thus, it can be inferred that a decrease in the amount of ER143 and a decrease in the lipid amount, as well as higher amounts of surfactant, produces smaller nanocapsules with lower span. For d(10), d(50) and d(90), only one positive two-factor interaction, between ER143 content and percentage of Tween® 80, was statistically significant. For high ER143 and lipid amounts, an increase in the Tween® 80 concentration was required because a decrease of o/w interfacial tension is related to a decrease in the size of the nanocapsules.

Concerning the incorporation results, it is clear that all independent variables significantly affected the ER143 EE and DL, specifically the presence of Tween® 80. This result suggests that part of the encapsulated ER143 may be embedded in the non-ionic surfactant layer. Similar results were obtained with other lipophilic drugs incorporated in other nanocarriers [23]. Probably, the high influence of each independent variable for EE and DL is due to the selected preparation method (emulsification-solvent evaporation method), because, the solubility of ER143 in dispersion medium increased as the ethanol (good solvent for ER143) diffused into the aqueous phase. Consequently, other strategies are crucial to increase the incorporation of the ER143, including the use of suitable ingredients, namely, lipids and surfactants.

Concerning zeta potential, it is seen that the main parameter influencing surface charge is the lipid amount, followed by the quadratic term of Tween® 80 concentration and, to a lesser extent, the Tween® 80 concentration.

Generally, it is also seen that, in this model, the isolated effect of each parameter is stronger than the corresponding interactions and quadratic terms.

Thus, it is important to decide which response contour plots are most meaningful. In the CCD data set, the strong main effect of percentage of ER143 amount and lipid amount drives this choice. Fig. 4.2.6 shows response contour plots and 3D plots created with the factors ER143 amount and lipid amount as axes, and percentage of fixed Tween® 80 at its optimized center level. According to Fig. 4.2.6 and 4.2.7, all plots present an insignificant curved surface and the possibility of modelling curvature is due to the presence of the quadratic terms.

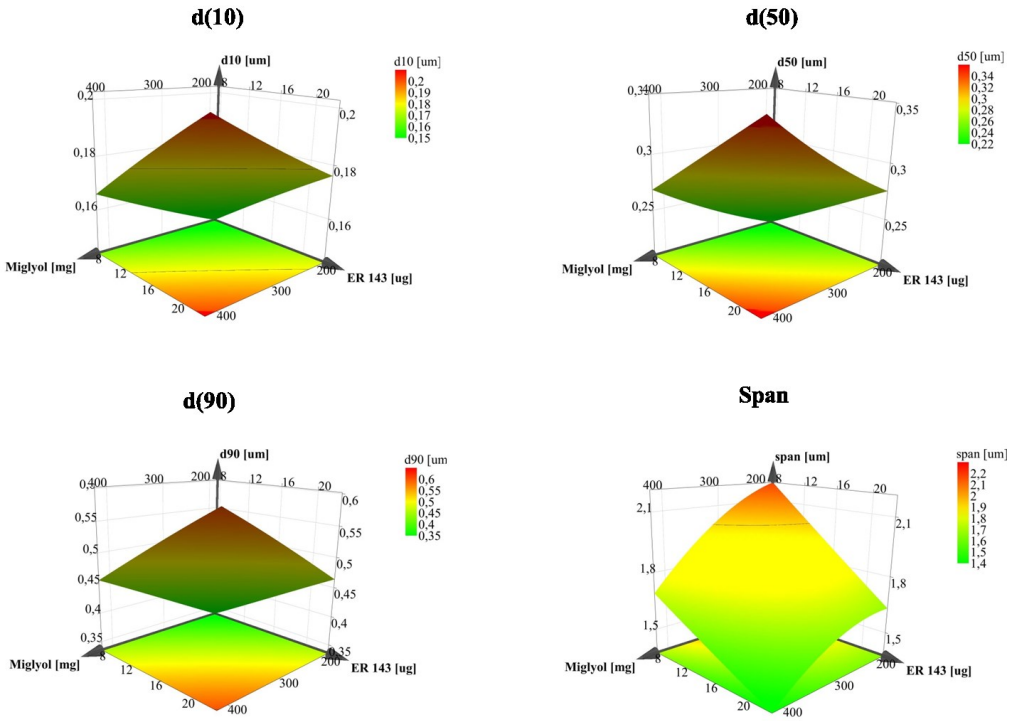

Fig. 4.2.6 - Isoresponse curves (graph floor) and response surface plots on relative particle size distribution (µm), respectively, d(10), d(50), d(90) and Span.

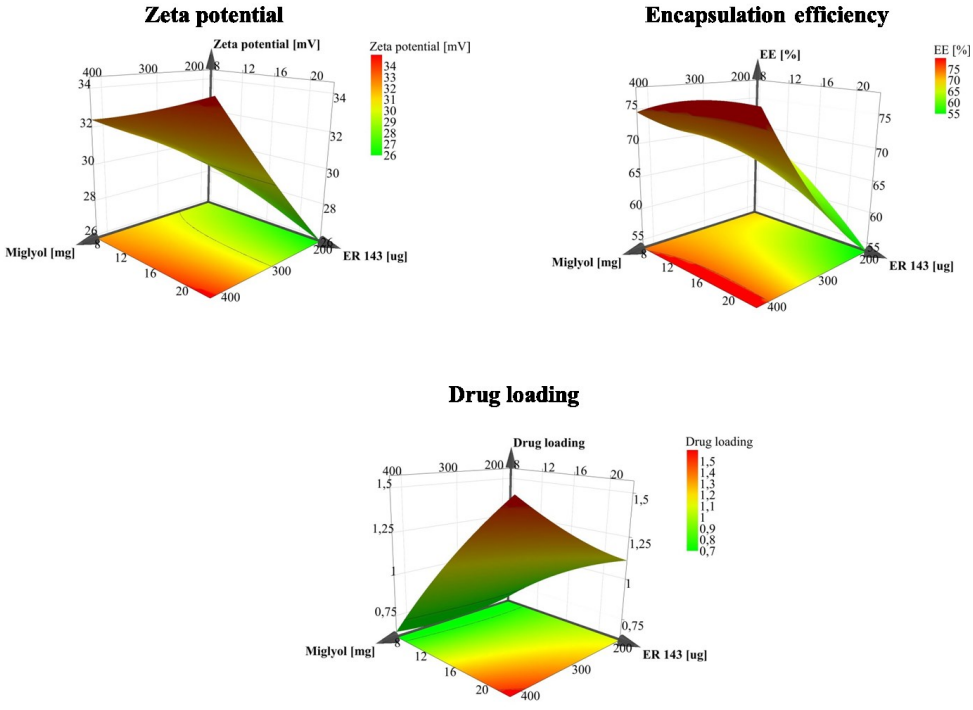

Fig. 4.2.7 - Isoresponse curves (graph floor) and response surface plots on relative zeta potential, encapsulation efficiency and drug loading.

In this study, response surface methodology was applied to establish the Design Space (DS). The factors that had been demonstrated to affect StNC ER143 quality were used to

create the DS (Fig. 4.2.8). Every single point corresponds to a combination of percentage of ER143 and lipid amount. The green area corresponds to a range of combinations for which the particle size, zeta potential, encapsulation efficiency and drug loading remain within the pre-defined acceptable limits. The optimal design setpoint is located inside the DS hypercube, thus, the dotted frame in the DS plot defines the optimal conditions that can be inserted into the irregular DS volume (Proven Acceptable Range – PAR). The setpoint in the DS communicates and helps to define the acceptable value for individual factors to ensure that all CQAs are fulfilled.

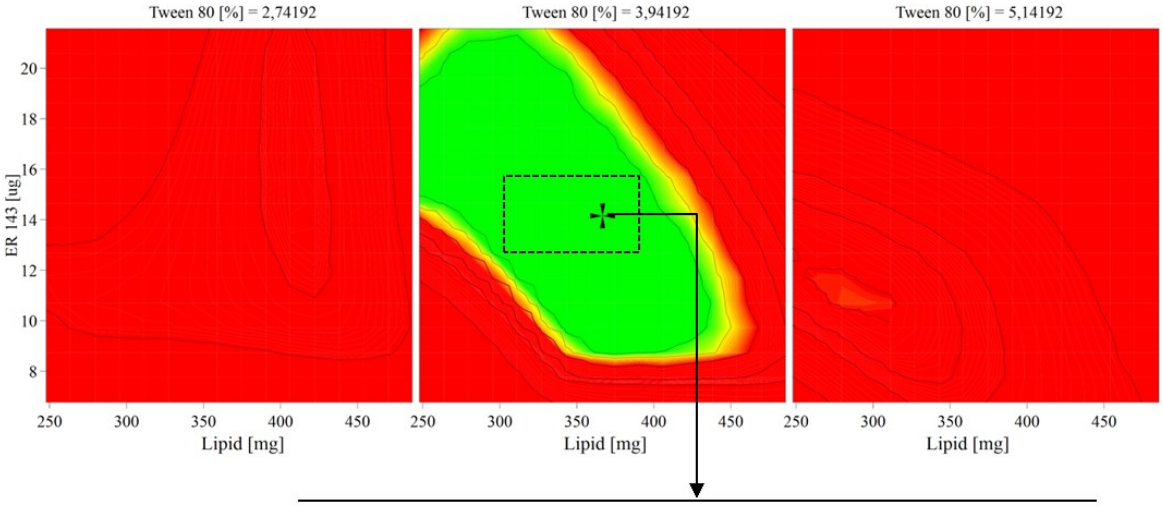

Factor	Setpoint	Factor contribution
ER143 (µg)	14.1	30.7
Tween® 80 (%)	3.9	34.5
Lipid (mg)	366	34.7
Cetrimonium bromide (%)	0.25	-
Pregelatinized modified starch (%)	0.07	-
Ethanol (%)	32.53	-
Water (%)	62.88	-

Fig. 4.2.8 - Overlay plot evidence the DS for the optimization study.

3.4 ER143-StNC interaction by DSC and FTIR

The physicochemical characterization of nanocapsules was performed by DSC analysis. The DSC patterns of pure pregelatinized modified starch, cetrimide, Tween® 80, caprylic/capric triglycerides, ER143, StNC and StNC ER143 are presented in Fig. 4.2.9. In what concerns the thermograms of raw materials and StNC, they are described in detail in Chapter 4, Section 1, section 3.1.4.2.

Concerning ER143, the powder has a crystalline structure that did not change during the heating until reaching its melting temperature, i.e. 122 °C. No significant thermal events occurred in the StNC and StNC ER143 when compared to the raw materials. The literature is scarce on DSC date concerning starch nanocapsules, which makes these findings hard to compare. Nevertheless, the relatively low amounts of the pregelatinized modified starch and cetrimide in the StNC and StNC ER143 could prevent the visualization of any discrete events as the phase transition of the pregelatinized modified starch and cetrimide. The absence of the ER143 melting can be ascribed to the amorphous or molecularly dispersed structure of the ER143 in the lipid matrix.

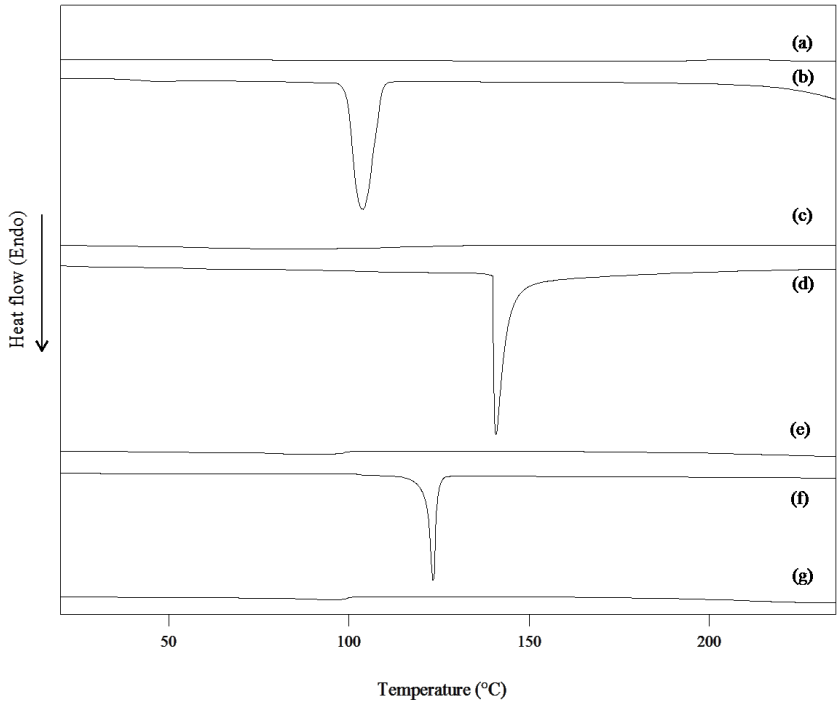

Fig. 4.2.9 - DSC thermograms of (a) caprylic/capric triglycerides, (b) cetrimide, (c) Tween® 80, (d) pregelatinized modified starch, (e) StNC, (f) ER143 and (g) StNC ER143.

In addition, the FTIR spectra for solid raw materials (cetrimide, pregelatinized modified starch and ER143) and for both optimized StNC and StNC ER143 were obtained to evaluate eventual changes on the StNC structure due to the presence of ER143 (Fig. 4.2.10). In what concerns the spectra of raw materials and StNC, they are described in detail in Chapter 4, Section 1, section 3.1.4.1.

The ER143 also showed one predominant band at 3097-3016 cm^{-1}, having a peak at 3078 cm^{-1} due to the C–H stretch of aromatic groups, with C=O stretch of a carboxylate anion and an amide group at 1732 and 1614 cm^{-1}, respectively. Furthermore, no major differences between StNC and StNC ER143 were observed since both spectra present coincidental absorption bands (Fig. 4.2.10). The spectrum profile when ER143 was loaded into StNC nanocapsules was fairly superimposable with respect to the main absorptions peaks, suggesting entrapment of the ER143 (Fig. 4.2.10).

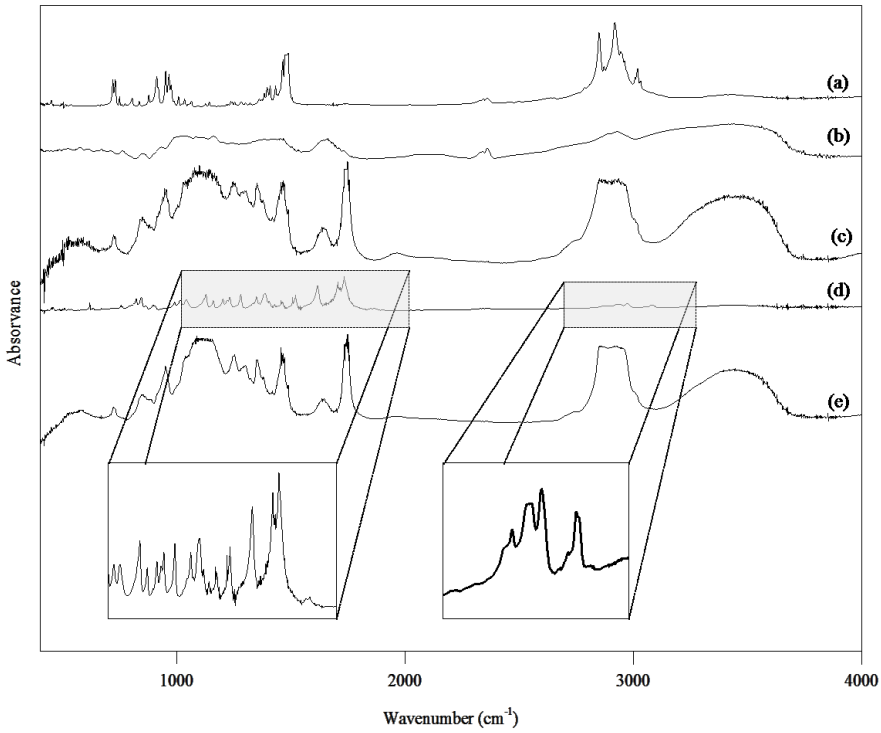

Fig. 4.2.10 - FTIR spectra of (a) cetrimide, (b) pregelatinized modified starch, (c) StNC, (d) ER143 and (e) StNC ER143.

3.5 *In vitro* ER143 release studies from StNC

The cumulative released of ER143 from StNC (Fig. 4.2.11) shows a sustained release profile that is faster between 0 and 4h and slower afterwards.

The release data were fitted to different mathematical models to describe the release profile (Table 4.2.5). When the full curve is considered, the best fit is obtained with the Weibull function, which had the highest values for $R^2_{adjusted}$ and model selection criterion (MSC) and lowest values for Akaike Information Criterion (AIC) and thus, statistically described the best drug release mechanism, followed by the Higuchi and first order models, with similar performance [24, 25]. Korsmeyer-Peppas and zero order functions are not adequate

for the dissolution curve corresponding to StNC ER143 formulation. Focusing on the Weibull model, the shape parameter (β) characterizes the curves as exponential (β = 1), sigmoidal (β > 1), with an upward curvature followed by a turning point, or parabolic (β < 1), with a higher initial slope and after that consistent with the exponential [26]. According to the results, β < 1 (0.77), which is classified in the literature as "a diffusion-controlled mechanism of release with contribution of another release mechanism" [27]. In fact, the dissolution profile is suggestive of a diffusion-controlled release over time period. According to Higuchi [28], this behavior is due to the dispersion of ER143 in a homogeneous and uniform matrix, which acts as the diffusional medium (lipid core), indicating a uniform drug distribution over the StNC. In addition, the first order explains the polymer dissolution at the interface with the surrounding medium, enhancing the drug mobility and diffusion [29, 30]. In general terms, one can only conclude that this profile represents a combined release mechanism that needs further confirmation. Finally, the slow release of ER143 from the nanocapsules is confirmed by the low DE at 24h (63.3±3.8%).

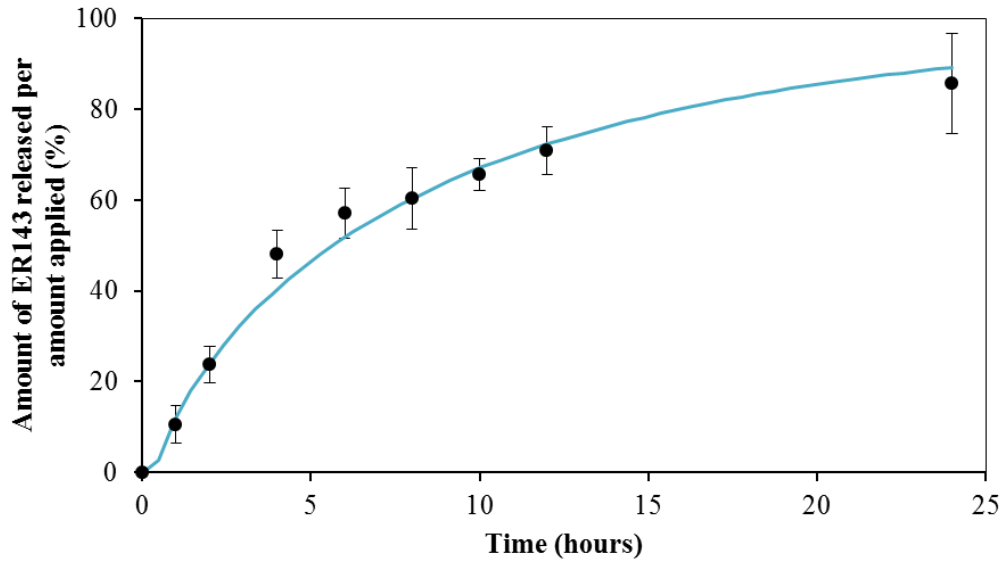

Fig. 4.2.11 - Release profile and fitting curve of Weibull model for ER143 from StNC in water:ethanol (7:3) at 37 ºC (mean ± SD, n = 6).

Table 4.2.5 - Kinetic parameters obtained after fitting the release data from the StNC ER143 to different release models (mean ± SD, n=6).

Model	K	$R^2_{adjusted}$	AIC	$T_{50\%}$ (min)	$T_{90\%}$ (min)	$DE_{24\,h}$ (% ± SD)
Zero order	4.93	0.815	75.9	7.06	12.71	63.3 ± 3.8
First order	0.14	0.956	56.0	6.13	20.36	
Higuchi	19.76	0.957	56.2	5.65	18.32	
Korsmeyer-Peppas	14.465 / n 0.65	0.921	67.4	6.05	13.28	
Weibull	α 5.21 / β 0.77 / Ti 0.40	0.982	47.8	8.33	14.66	

K – release constant; $R^2_{ajusted}$ - adjusted coefficient of determination; AIC - Akaike Information Criterion; $T_{50\%}$ - time required for 50% dissolution; $T_{90\%}$ - time required for 90% dissolution; DE_{24h} – dissolution efficiency at 24h of release study; n - release exponent; α – scale parameter; β – shape parameter; Ti – location parameter.

3.6 Topical delivery studies of StNC ER143

3.6.1 *In vitro* skin permeation and retention

The ER143 is a novel neutrophil elastase inhibitor with potential anti-inflammatory activity. It has a molecular weight (MW) of 391.42 g/mol and a logP of 3.85, making it a suitable candidate for topical delivery [31]. However, solubility in the vehicle is an important characteristic for the successful development of drugs and their penetration across biological barriers [32]. According to solubility studies (results not shown), caprylic/capric triglycerides allowed maximal solubility for ER143 (30 µg/mg lipid).

Permeation profiles showed that only after 12 h, StNC ER143 is statistically different (p<0.05) from ER143 solution (Fig. 12). These profiles are typical of infinite dose experiments where the applied dose is so high that the depletion of the permeant in the donor chamber caused by evaporation or diffusion into and through the barrier is negligibly low [33]. After an initial lag period, the cumulative amount of ER143 in the receptor fluid will increase linearly with time, i.e., the flux across the skin will reach a steady state. The fluxes, permeability coefficients (Kp) and lag time (Table 4.2.6) were obtained fitting the single curves of the permeation profiles in the linear region (between 4 and 24 h).

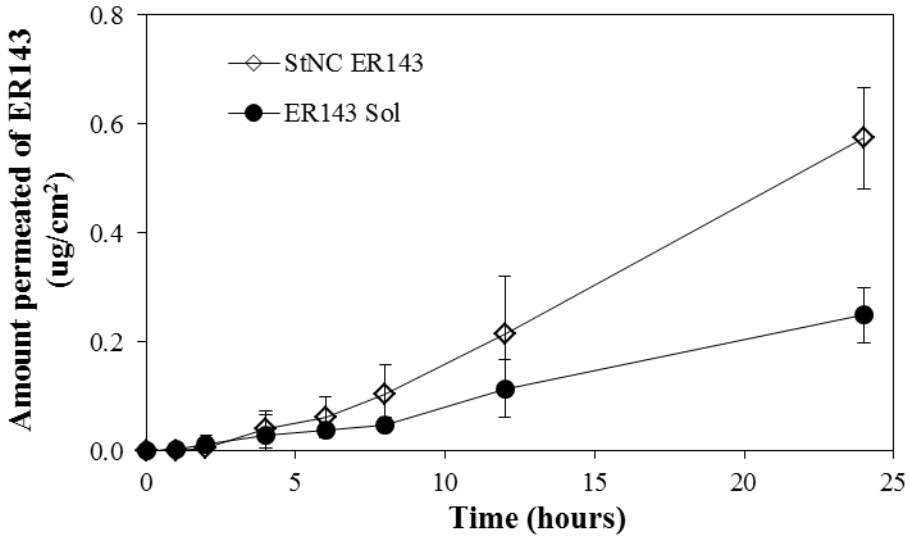

Fig. 4.2.12 - Permeation profile of ER 143 from StNC ER143 and a solution of ER143 in water:ethanol (7:3) through newborn pig skin at 37 °C (mean ± SD, n = 6).

Table 4.2.6 – Permeation flux, Kp and lag time of ER143 through newborn pig skin membrane for StNC ER143 and ER143 solution (mean ± SD, n= 6).

Formulation	Jss ($\mu g\ cm^{-2}\ h^{-1}$)	EnRt of Jss	Experimental Kp ($cm\ h^{-1}$)	EnRt of Kp	Lag time (h)	Q24 ($\mu g\ cm^{-2}$)	Theoretical Kp ($cm\ h^{-1}$)	TEnRt of Kp
ER143 Sol	0.012 ± 0.001	-	$8.20x10^{-4} \pm 1.12x10^{-4}$	-	3.53 ± 0.47	0.57 ± 0.09	4.05×10^{-3}	2.0
StNC ER143	0.029 ± 0.006	2.4	$2.73x10^{-3} \pm 0.53x10^{-3}$	3.3	2.97 ± 0.56	0.24 ± 0.05		6.7

Jss - Flux at steady-state; Kp - Permeability coefficient; EnRt - Experimental enhancement ratio. For the calculation of EnRt, ER143 Sol was considered as reference; TEnRt - Theoretical enhancement ratio. For the calculation of TEnRt, theoretical Kp was considered as reference; Q24 - Cumulative amount of ER143 permeated after 24 h.

In this study we demonstrated that the permeation profiles of ER143, StNC ER143 and ER143 solution were influenced by the selected vehicle. The different permeation rates can be explained regarding the different natures of the vehicles, since StNC are a complex vehicle whereas ER143 solution is only a simple water-ethanol solution. In addition, the high permeation through the skin was also due to the small MW and to the octanol-water partition coefficient (LogP) of ER143. The Potts and Guy equation [31] demonstrates that permeability of a drug from an aqueous solution through the SC can be suitably predicted using only two parameters, the LogP and the MW (Equation 5).

Equation 5: $\text{Log Kp}\ (\text{cm h}^{-1}) = -2.74 + 0.71\ \text{LogP} - 0.0061\ \text{MW}$

Briefly, Kp increases directly with the lipophilicity of the penetrating molecule and inversely with its MW. From the Pots and Guy equation, ER143 presents a Kp value of 4.05 x 10^{-4} cm h^{-1} (Table 4.2.6). Thus, the enhancement ratios comparing the theoretical and experimental values of Kp for ER143 formulations can be explained regarding the excipients and selected dosage form.

Thus, the enhancement ratios comparing the theoretical and experimental values of Kp for ER143 formulations can be explained regarding the excipients and selected dosage form.

The presence of ethanol in both formulations (StNC ER143 and ER143 solution) could also justify the permeation enhancement. In fact, low molecular weight of alkanols, like ethanol, acts by enhancing the solubility of the drug in the SC lipid matrix by extraction of hydrophobic alcohols, disrupting its integrity and modify the penetration rate [34, 35]. Moreover, the presence of ethanol, a well-known penetration enhancer, contributes to the percutaneous penetration of ER143. Besides lowering the skin barrier function, ethanol also increased the ER143 solubility in the vehicle.

The ability of StNC to enhance the penetration of ER143 was previously studied and has been attributed to the size and to the adhesion of nanocapsules to the skin that leads to the formation of a film, and consequently, the occlusive effect can increase the skin permeation. This enhancement does not result from isolated factors such as the size, the nature of the dosage form or the type of enhancer, but from a synergistic effect between them.

Several authors demonstrated that the use of solvents in combination with a potential penetration enhancer may offer synergistic enhancement [2, 36]. Vitorino *et al*. [2] demonstrated that the combination of ethanol and fatty acids significantly increased the percutaneous absorption of simvastatin and olanzapine through newborn pig skin. This enhancement effect was superior when compared with the enhancement caused by ethanol alone. Fatty acids (capric acid) are also well-established skin permeation enhancers. Their penetration enhancing effects are attributed to an increased drug solubility in the vehicle and increased partitioning into the skin [37].

However, not only the presence of the fatty acids (capric acid) and ethanol, as explained before, contributed to the increase on Kp, but also the presence of surfactants, such as Tween® 80. Surfactants can also act as penetration enhancers, solubilizing SC lipids and interacting with the keratin leading to the disruption of the SC [38].

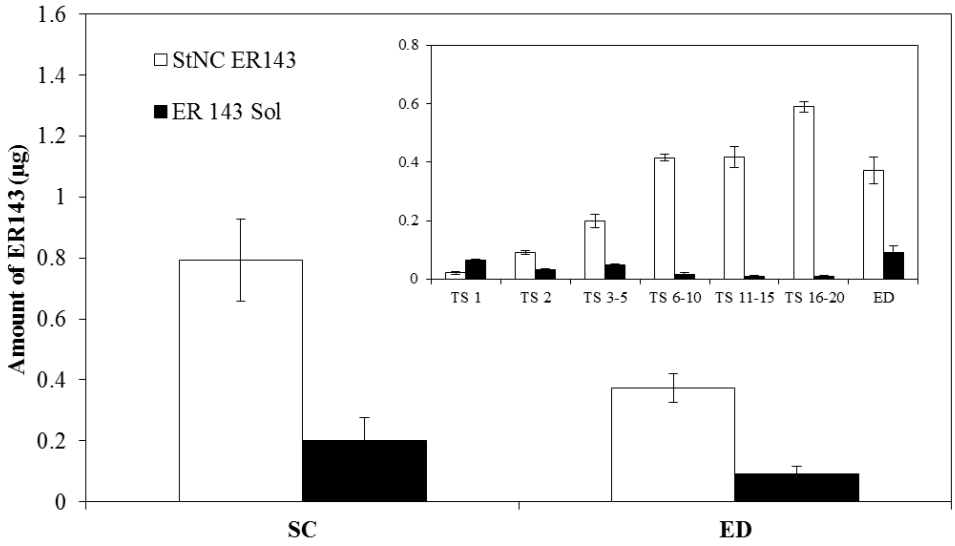

Fig. 4.2.13 - Penetration of StNC ER143 and ER143 solution (ER143 Sol) in the SC (from tape stripping, TS) and viable skin layers (epidermis and dermis - ED) after 24h. Inner graphic: Penetration of StNC ER143 and ER143 in the different tape strip layers (TS) and in the viable skin layers (ED). Statistical analysis was performed using one-way ANOVA ($p < 0.05$) (mean ± SD, n=6).

The tape stripping technique is useful to determine the dermatopharmacokinetic of topically applied substances especially if all procedures are standardized and validated, as it was previously performed in this work.

ER143 extraction from the skin by tape stripping was performed for StNC ER143 and ER143 solution (Fig. 4.2.13). The values of ER143 obtained were 0.79 ± 0.13 µg (22.70 ± 3.97 %) and 0.20 ± 0.08 µg (5.14 ± 0.82 %) for StNC ER143 and ER143 solution, respectively, in the SC, and 0.37 ± 0.05 µg (10.64 ± 1.20 %) and 0.09 ± 0.02 µg (2.25 ± 0.54 %) for StNC ER143 and ER143 solution, respectively, in the viable skin layers (epidermis and dermis - ED). The statistical analysis indicated a significant difference in the amounts of ER143 for ER143 solution compared with the StNC ER143 ($p < 0.05$) for the SC and for the viable skin layers.

Attending that neutrophil elastase receptors are located in the dermis layer, the skin permeation and retention of the ER143 is desirable [39]. In the StNC ER143, the molecule is protected by a polymer coating (starch), which probably allowed retention of the drug in the skin for 24 h, due to the control of ER143 release. According to the literature, the interaction of the drug with the skin surface is limited by the drug diffusion from the

nanocarrier and, also, this carrier could have a depot effect in the SC being continuously released to the rest of the skin and dermal vasculature [40, 41].

The skin permeation and retention results show that besides the low skin retention of ER143 after topical application of ER143 solution, when suitably formulated, ER143 can cross the SC barrier and accumulate in deeper layers, thus being applicable to topical vehicles in the treatment of anti-inflammatory diseases. Overall, the incorporation of ER143 into StNC proved to be a simple and smart strategy to improve ER143 skin permeation and retention.

3.7 *In vivo* studies

As observed with commercial lotion (CL), topical application of StNC ER143 strongly inhibited the acute inflammatory response, as evaluated by inhibition of neutrophil infiltration, erythema and edema (Fig. 4.2.14 and 4.2.15).

StNC ER143 treatment remarkably reduced edema with an inhibition of 92 ± 7 %, which was comparable to the CL, showing an inhibition of 93 ± 12 % and, these results present no statistically significant differences ($p > 0.1$). In addition, topical StNC treatment inhibited edema formation in 73 ± 6 %, while the ER143 solution could only inhibit 25 ± 5% of the edema formation.

Histological analysis of naïve mice (unchallenged) ear skin did not reveal morphological alterations neither cell infiltration signs. Both positive control and ER143 solution displayed focally extensive inflammation expanding the dermis, between epidermis and the pinnal cartilage, resulting in diffuse thickening, invariably more severe at the ear tip (arrowhead) (histopathological score, 3) (Fig. 4.2.15). For the ears treated with ER143, cellular infiltration was also accompanied by diffuse edema (block arrow). Lesions observed in skin sections of ears treated with CL were similar to those observed in the positive control but of lower severity and only focal, at the ear tip (histopathological score 2, mild); and even less severe in the StNC ER143 and StNC groups (histopathological score 1, minimal).

Interestingly, topical application of StNC inhibited the acute inflammatory response. Some authors demonstrated that glucose and mannose residues from polysaccharides could markedly reduce the *in vivo* inflammatory activity. Thus, the present study proved the synergistic action of starch on the anti-inflammatory activity of ER143 [42]. Despite the low anti-inflammatory activity of ER143 solution, ER143 improves its anti-inflammatory effects when strategically encapsulated in StNC.

This suggests that ER143 encapsulated in StNC may be a useful and promising approach for the treatment of cutaneous inflammatory diseases such as dermatitis and psoriasis.

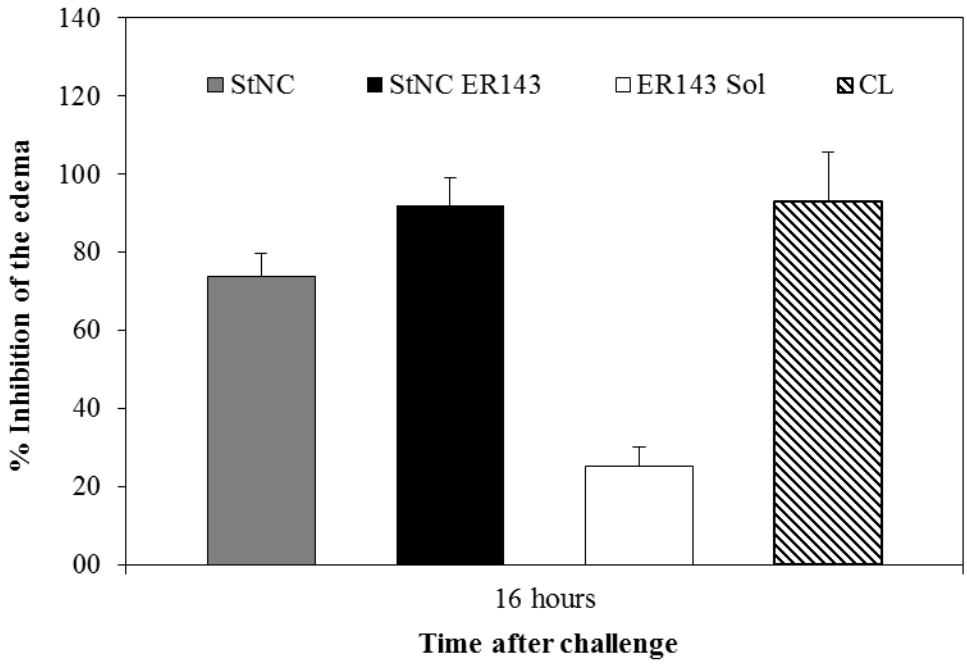

Fig. 4.2.14 - Effect of treatment with StNC, StNC ER143, ER143 solution and commercial lotion (CL) on the percentage of inhibition of the edema on a mouse ear, challenged with croton oil (mean ± SD, n=6).

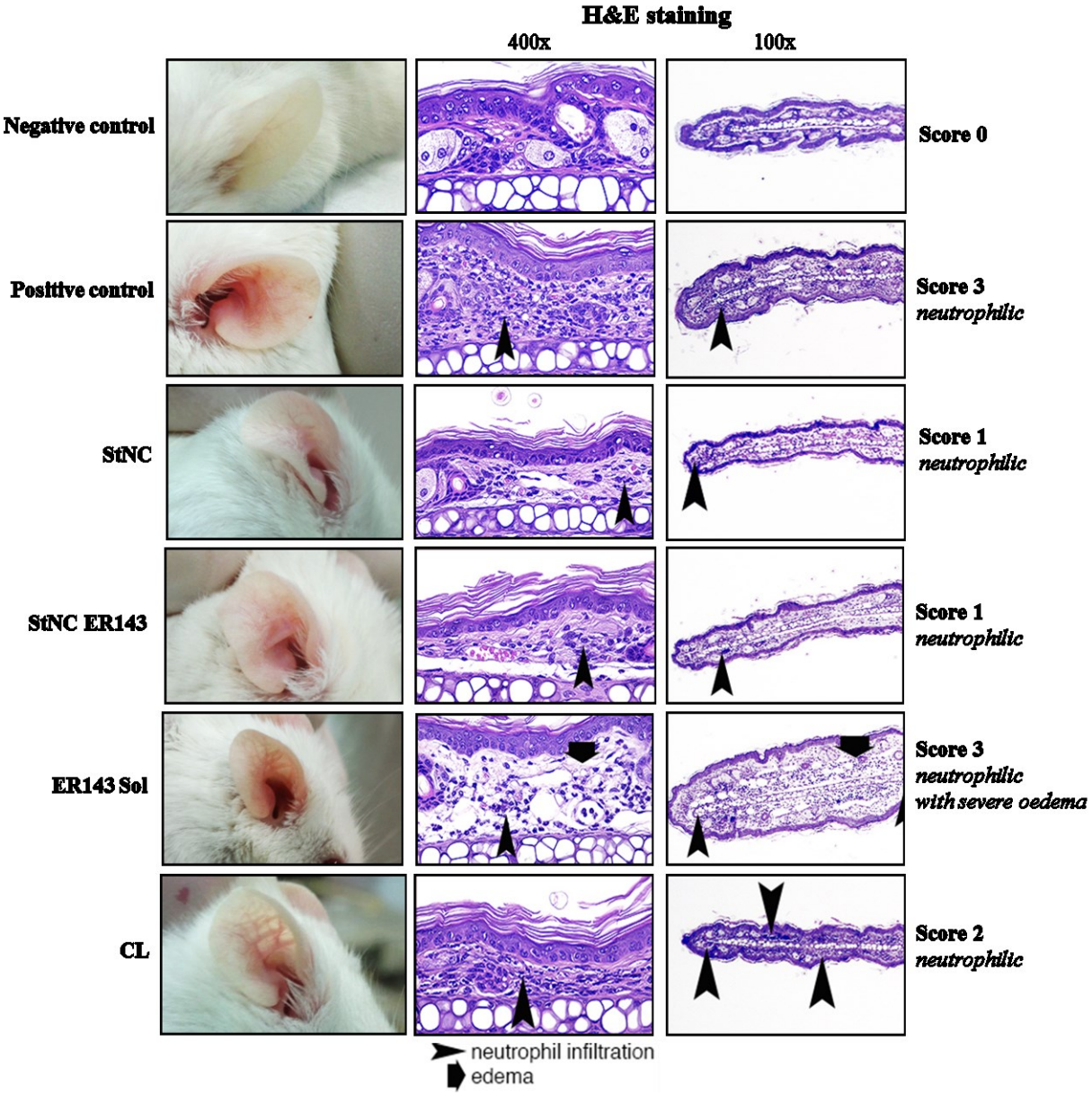

Figure 4.2.15 - Representative hematoxylin and eosin-stained sections of ear pinna of mice challenged with different samples and their solvents: (Negative control) unchallenged ear; (Positive control) ear from mouse challenged with croton-oil in the absence of any treatment; (StNC) ear from mouse challenged with croton-oil post-treated with StNC; (StNC ER143) ear from mouse challenged with croton-oil post-treated with StNC ER143; (ER143 Sol) ear from mouse challenged with croton-oil post-treated with ER143 solution; (CL) ear from mouse challenged with croton-oil post-treated with commercial lotion (CL).

4 Conclusions

A novel elastase inhibitor (ER143) was successfully formulated in starch-based nanocapules with suitable properties (particle size distribution, surface charge and encapsulation efficiency) for topical application. The *in vitro* studies demonstrated these starch nanocapsules are suitable vehicles for the delivery of ER143, increasing its skin permeation with maximum efficacy in the treatment areas. The improved pharmacological performance resulting from ER143 nanoencapsulation was confirmed *in vivo,* compared to a commercial lotion containing an anti-inflammatory corticosteroid. These results demonstrate that the incorporation of ER143 into starch-based nanocapsules has scientific merit, which is a promising strategy for the treatment of inflammatory skin diseases.

5 References

1. Kumari A, Yadav SK, Yadav SC. Biodegradable polymeric nanoparticles based drug delivery systems. Colloids and Surfaces B: Biointerfaces. 2010;75(1):1-18.

2. Vitorino C, Almeida J, Gonçalves LM, Almeida AJ, Sousa JJ, Pais AACC. Co-encapsulating nanostructured lipid carriers for transdermal application: From experimental design to the molecular detail. Journal of Controlled Release. 2013;167(3):301-314.

3. Rodriguez-Cruz IM, Merino V, Merino M, Diez O, Nacher A, Quintanar-Guerrero D. Polymeric nanospheres as strategy to increase the amount of triclosan retained in the skin: passive diffusion vs. iontophoresis. Journal of Microencapsulation. 2013;30(1):72-80.

4. Guterres SS, Alves MP, Pohlmann AR. Polymeric Nanoparticles, Nanospheres and Nanocapsules, for Cutaneous Applications. Drug Target Insights. 2007;2:147-157.

5. Neubert RHH. Potentials of new nanocarriers for dermal and transdermal drug delivery. European Journal of Pharmaceutics and Biopharmaceutics. 2011;77(1):1-2.

6. Almeida AJ, Souto E. Solid lipid nanoparticles as a drug delivery system for peptides and proteins. Advanced Drug Delivery Reviews. 2007;59(6):478-490.

7. Desai D, Shah D. Implication of nanoparticles for controlled drug delivery system. International Journal of Pharmceutical Sciences and Research. 2013;4:2478-2488.

8. Wissing SA, Müller RH. The influence of solid lipid nanoparticles on skin hydration and viscoelasticity – in vivo study. European Journal of Pharmaceutics and Biopharmaceutics. 2003;56(1):67-72.

9. Lucas SD, Costa E, Guedes RC, Moreira R. Targeting COPD: advances on low-molecular-weight inhibitors of human neutrophil elastase. Medicinal Research Reviews. 2013;33(S1):E73-E101.

10. Siedle B, Gustavsson L, Johansson S, Murillo R, Castro V, Bohlin L, Merfort I. The effect of sesquiterpene lactones on the release of human neutrophil elastase. Biochemical Pharmacology. 2003;65(5):897-903.

11. Glinski W, Jarzabek-Chorzelska M, Kuligowski M, Pierozynska-Dubowska M, Glinska-Ferenz M, Jabłonska S. Basement membrane zone as a target for human neutrophil elastase in psoriasis. Archives of Dermatological Research. 1990;282(8):506-511.

12. Areias L, Ruivo E, Gonçalves L, Duarte M, André V, Moreira R, Lucas S, Guedes R. A unified approach toward the rational design of selective low nanomolar human neutrophil elastase inhibitors. RSC Advances. 2015;5(64):51717-51721.

13. Lucas SD, Gonçalves LM, Carvalho LA, Correia HF, Da Costa EM, Guedes RA, Moreira R, Guedes RC. Optimization of O 3-Acyl Kojic Acid Derivatives as Potent and Selective Human Neutrophil Elastase Inhibitors. Journal of Medicinal Chemistry. 2013;56(23):9802-9806.

14. Nauseef WM. Isolation of human neutrophils from venous blood. Neutrophil Methods and Protocols: Springer; 2014. p. 13-18.

15. Mora-Huertas CE, Fessi H, Elaissari A. Polymer-based nanocapsules for drug delivery. International Journal of Pharmaceutics. 2010;385(1–2):113-142.

16. Riddick T. Zeta-meter manual.1968.

17. ICHQ1A(R2). ICH of Technical Requirement for Registration of Pharmaceuticals for Human Use, Stability Testing of new Drugs and Products. www.ich.org; 2003.

18. ICHQ8(R2). ICH Harmonised tripartite guideline pharmaceutical development Q8(R2). www.ich.org; 2012.

19. Muramoto K, Goto M, Inoue Y, Ishii N, Chiba K-i, Kuboi Y, Omae T, Wang YJ, Gusovsky F, Shirota H. E6201, a novel kinase inhibitor of mitogen-activated protein kinase/extracellular signal-regulated kinase kinase-1 and mitogen-activated protein kinase/extracellular signal-regulated kinase kinase kinase-1: in vivo effects on cutaneous inflammatory responses by topical administration. Journal of Pharmacology and Experimental Therapeutics. 2010;335(1):23-31.

20. Mulchande J, Oliveira R, Carrasco M, Gouveia L, Guedes RC, Iley J, Moreira R. 4-Oxo-beta-lactams (azetidine-2,4-diones) are potent and selective inhibitors of human leukocyte elastase. Journal of Medicinal Chemistry. 2010;53(1):241-253.

21. Areias LRP, Ruivo EFP, Goncalves LM, Duarte MT, Andre V, Moreira R, Lucas SD, Guedes RC. A unified approach toward the rational design of selective low nanomolar human neutrophil elastase inhibitors. RSC Advances. 2015;5(64):51717-51721.

22. Carvalho LAR, Ruivo EFP, Lucas SD, Moreira R. Activity-based probes as molecular tools for biomarker discovery. MedChemComm. 2015;6(4):536-546.

23. Lopes R, Eleutério C, Gonçalves L, Cruz M, Almeida A. Lipid nanoparticles containing oryzalin for the treatment of leishmaniasis. European Journal of Pharmaceutical Sciences. 2012;45(4):442-450.

24. Zhang Y, Huo M, Zhou J, Zou A, Li W, Yao C, Xie S. DDSolver: an add-in program for modeling and comparison of drug dissolution profiles. AAPS J. 2010;12(3):263-271.

25. Akaike H. Factor analysis and AIC. Psychometrika. 1987;52(3):317-332.

26. Costa P, Sousa Lobo JM. Modeling and comparison of dissolution profiles. European Journal of Pharmaceutical Sciences. 2001;13(2):123-133.

27. Papadopoulou V, Kosmidis K, Vlachou M, Macheras P. On the use of the Weibull function for the discernment of drug release mechanisms. International journal of pharmaceutics. 2006;309(1–2):44-50.

28. Huguchi T. Mechanism of sustained-action medication. Journal of Pharmaceutical Sciences. 1963;52:1145-1149.

29. Arifin DY, Lee LY, Wang C-H. Mathematical modeling and simulation of drug release from microspheres: Implications to drug delivery systems. Advanced Drug Delivery Reviews. 2006;58(12–13):1274-1325.

30. Raj CA, Kumar PS, Kumar KS. Kinetics and drug release studies of isoniazid encapsulated with PLA-co-PEG/gold nanoparticles. International Journal of Pharmacy and Pharmaceutical Sciences. 2012;4:398-404.

31. Potts RO, Guy RH. Predicting skin permeability. Pharmaceutical research. 1992;9(5):663-669.

32. El Maghraby GM, Alanazi FK, Alsarra IA. Transdermal delivery of tadalafil. I. Effect of vehicles on skin permeation. Drug Development and Industrial Pharmacy. 2009;35(3):329-336.

33. Selzer D, Abdel-Mottaleb MA, Hahn T, Schaefera UF, Neumannc D. Finite and infinite dosing: Difficulties in measurements, evaluations and predictions. Advanced Drug Delivery Reviews. 2013;65(2):278-294.

34. Kikwai L, Kanikkannan N, Babu RJ, Singh M. Effect of vehicles on the transdermal delivery of melatonin across porcine skin in vitro. Journal of Controlled Release. 2002;83(2):307-311.

35. Marto J, Baltazar D, Duarte A, Fernandes A, Gouveia L, Militao M, Salgado A, Simoes S, Oliveira E, Ribeiro HM. Topical gels of etofenamate: in vitro and in vivo evaluation. Pharmaceutical Development and Technology. 2014:1-6.

36. Raposo S, Tavares R, Gonçalves L, Simões S, Urbano M, Ribeiro HM. Mometasone furoate-loaded cold processed oil-in-water emulsions: in vitro and in vivo studies. Drug Delivery. 2014;(0):1-11.

37. Aungst BJ, Blake JA, Hussain MA. Contributions of drug solubilization, partitioning, barrier disruption, and solvent permeation to the enhancement of skin permeation of various compounds with fatty acids and amines. Pharmaceutical Research. 1990;7(7):712-718.

38. Williams AC, Barry BW. Penetration enhancers. Advanced Drug Delivery Reviews. 2012;64:128-137.

39. Starcher B, O'Neal P, Granstein RD, Beissert S. Inhibition of neutrophil elastase suppresses the development of skin tumors in hairless mice. Journal of Investigative Dermatology. 1996;107(2):159-163.

40. Fischer TW, Greif C, Fluhr JW, Wigger-Alberti W, Elsner P. Percutaneous penetration of topically applied melatonin in a cream and an alcoholic solution. Skin Pharmacology and Physiology. 2004;17(4):190-194.

41. Da Silva ALM, Contri RV, Jornada DS, Pohlmann AR, Guterres SS. Vitamin K1–loaded lipid-core nanocapsules: physicochemical characterization and in vitro skin permeation. Skin Research and Technology. 2013;19(1):e223-e230.

42. Garbacki N, Gloaguen V, Damas J, Hoffmann L, Tits M, Angenot L. Inhibition of croton oil-induced oedema in mice ear skin by capsular polysaccharides from cyanobacteria. Naunyn-Schmiedeberg's Archives of Pharmacology. 2000;361(4):460-464.

5 Starch-based vehicles: a safety and effective platform for dermatological purpose

This page was intentionally left blank

Graphical Abstract

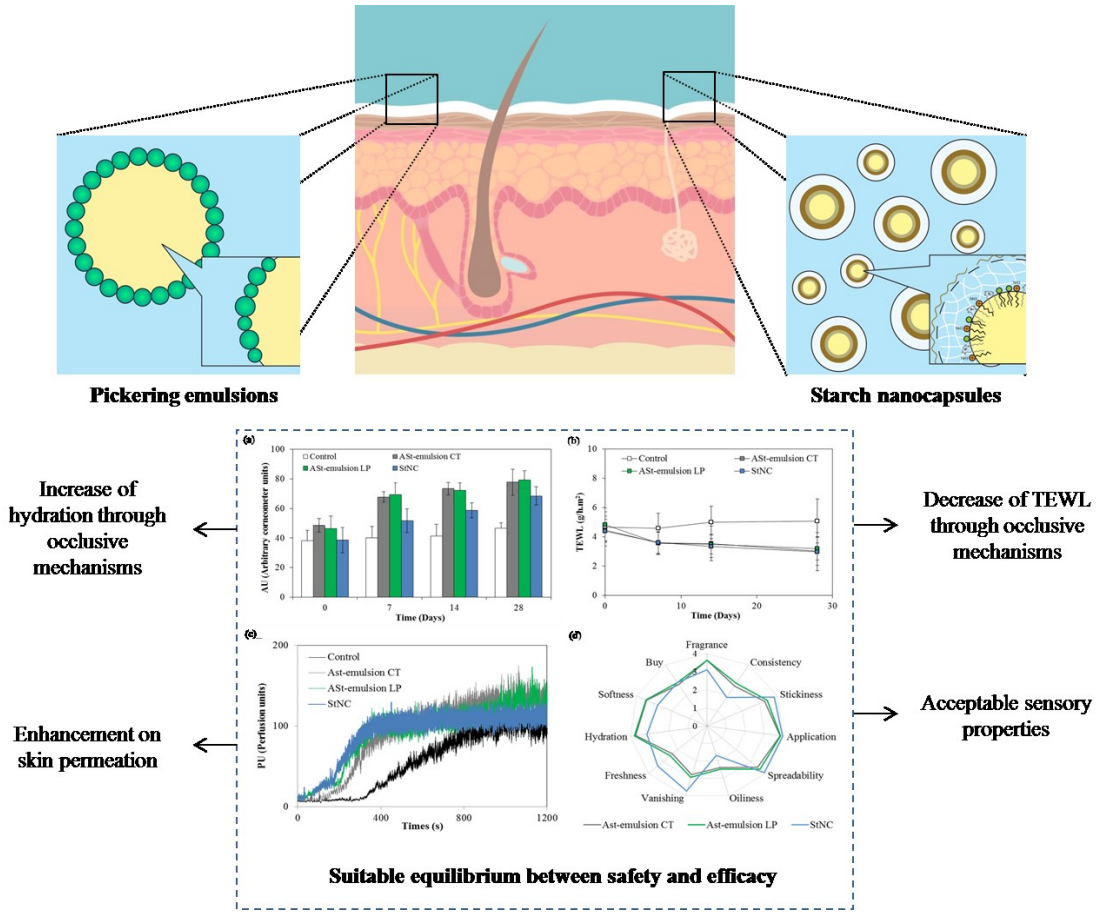

Highlights:

- Starch-based vehicles (St-BV) are non-irritant and suitable for skin application.
- Biological effects demonstrated that St-BV increased both the skin hydration and microcirculation, with good acceptance by the consumers, boosting patient comfort for maximum compliance and treatment results.
- St-BV can be considered safe in the normal and reasonably foreseeable use.

This page was intentionally left blank

1 Introduction

Emulsions and, more recently, nanoparticles have been widely used in pharmacy and cosmetics for their therapeutic properties and, as vehicles to deliver drugs and cosmetic agents to the skin. These pharmaceutical dosage forms have to fulfill a number of requirements, e.g. acceptable physical and chemical stability, satisfactory safety and efficacy profile and an attractive appearance to reach at the same time optimal sensory attributes. In addition, they must be non-irritant to the skin and easily applied. In order to provide all these attributes, several excipients have been investigated often resulting in complex, multi-component formulations containing several emulsifiers, co-emulsifiers, polymers, emollients and preservatives [1, 2]. Thus, it is crucial to evaluate the safety profile of these ingredients used in such vehicles, particularly those of special concern in terms of safety assessment, such as, preservatives, solubilizers and surfactants. Although human external contact with these ingredients hardly results in their penetration through the skin and significant systemic exposure, since skin care products mainly produce local exposure, human systemic exposure to their ingredients can rarely be completely excluded [3].

For instance, cosmetics do not penetrate into the body to modify the physiological functions. Nevertheless, when a substance or ingredient comes into contact with the skin, it cannot be excluded that, in specific circumstances, that substance might cause a reaction. This is why before their introduction in the market all cosmetic products must undergo an extensive safety assessment, including skin acceptability or compatibility studies carefully conducted on volunteers to confirm their good tolerance [4].

Human studies may also be conducted to measure skin benefits and document product claims, or to collect consumer's feedback before the product is launched in the market. In all these studies, any undesirable health effect is taken into account to complement and strengthen the overall safety assessment on the product [5].

Cosmetic products fall under the general requirements of the EC Cosmetics Regulation 1223/2009 [6], whereby the toxicological profile of all used ingredients and detailed knowledge of the product-specific exposure are required as fundamental for the safety assessment. As imposed by the European legislation, cosmetics are considered to be safe for the consumer. Although this appears to be self-evident, there is a whole scientific exercise preceding this "obvious" conclusion [5]. The safety of a cosmetic product is determined based on the safety assessment of its ingredients, which is performed using

literature data, *in vitro* tests and human tests since, in European Union (EU), finished cosmetic products are no longer tested in animals.

The key factors in the management of topical diseases are not only related to the use of effective topical agents but also in providing skin hydration and barrier repair. The selected ingredients to such vehicles are extremely important and should present a suitable equilibrium between safety and efficacy [7]. Emollients or moisturizers are often used in the treatment of topical diseases with the aim of improving skin hydration and barrier repair [8].

Therefore, the major aim of this research study was to evaluate the safety profile and biological effects of starch-based vehicles (St-BV), using the literature data and a systematic approach for the safety assessment, comparing it with *in vitro* and *in vivo* data obtained using methods of skin bioengineering and tests performed on human volunteers, such as trans-epidermal water loss (TEWL), epidermal capacitance, skin surface lipids and microcirculation. It should be referred that St-BV can be market as cosmetic products thus, it is of great importance to study their safety profile and biological effects according to the relevant European regulatory framework.

2 Materials and methods

2.1 Materials

The materials used are described in Chapter 2, section 2.1. and Chapter 4, Section 1, section 2.1.

2.2 Methods

2.2.1 Preparation of starch-based vehicles (St-BV)

2.2.1.1 Preparation of starch-stabilized emulsions (ASt-emulsion)

ASt-emulsions were prepared according to the procedure described previously in Chapter 3, Section 1, section 2.2.2. (Table 5.1).

2.2.1.2 Preparation of starch nanocapsules (StNC)

StNC were prepared by emulsion-solvent evaporation method according to the procedure described previously in Chapter 4, Section 1, section 2.2.1.1. (Table 5.1).

Table 5.1 - Qualitative and quantitative composition of the optimized St-BV.

Ingredients	Quantitative Composition (%, w/w)			Main functions/additional functions
	ASt-emulsion with LP	ASt-emulsion with CT	StNC	
Phase A (external)				
Liquid paraffin	69	-	-	Emollient
Caprylic/capric acid triglyceride	-	69	-	Emollient
Phase B (solid particles)				
Aluminum starch octenylsuccinate	6	6	-	Absorbent and viscosity controlling
Phase C (internal)				
Purified water	25	25	-	Solvent
Phase A (Ethanolic phase)				
Ethanol	-	-	32.53	Solvent and preservative
Cetrimonium bromide	-	-	0.25	Emulsifying
Capric/caprylic triglycerides	-	-	0.55	Emollient
Phase B (Aqueous phase)				
Purified water	-	-	65.47	Solvent
Polysorbate 80	-	-	1.13	Emulsifying
Pregelatinized modified corn starch	-	-	0.07	Polymer

2.2.2 Safety assessment of St-BV

The safety assessment of St-BV was accomplished according to the Scientific Committee on Consumer Safety's (SCCS) Notes of Guidance for Testing of Cosmetic Ingredients and their Safety Evaluation [4]. The information for each ingredient was obtained from the respective supplier.

2.2.2.1 Hazard identification

The results of the *in vitro* and *in vivo* tests, clinical studies, physical, chemical and toxicological properties of each ingredient were considered to recognize if the ingredient has the potential to damage human health.

2.2.2.2 Dose-response assessment

The dose-response assessment describes the change in effect on an organism caused by different levels of exposure to a chemical after a certain exposure time. In the case of an effect with a threshold, the dosage at which no observed adverse effect level (NOAEL) is determined [4].

2.2.2.3 Exposure assessment

The amount and the frequency of human exposure to the St-BV were determined using the systemic exposure dose (SED) that was calculated for each ingredient, according to the Equation 1.

Equation 1: $\text{SED} = \text{E (mg/kg/bw/day)} \times \frac{C(\%)}{100} \times \frac{DA(\%)}{100}$

Where *E* is the amount of the ingredient expected to enter the blood stream per kg body weight (bw) and per day, *C* is the concentration of the ingredient in the St-BV and *DA* is the dermal absorption reported as a percentage of the test dose to be applied under conditions simulating those of real-life.

2.2.2.4 Risk characterization

The probability that the substances under study cause damage to human health was considered. In the case of a threshold effect, the margin of safety (MoS) was calculated according to the Equation 2.

Equation 2: $Mos = \frac{NOAEL}{SED}$

2.2.3 EpiSkin™ assay

The validated reconstructed human epidermis EpiSkin™ skin irritation test method was used [9]. The EpiSkin™ tissues were supplied by SkinEthic Laboratories (www.skinethic.com) consisting in a reconstructed organotypic culture of adult human keratinocytes reproducing a multilayered and well differentiated epidermis.

The method used following the instruction of the producer, the 12 well plates, containing 12 inserts of tissues (0.38 cm^2), were transferred into 12 wells plates containing 2 ml of maintenance medium and incubated at 37 ºC (5 % CO_2, 95 % humidified atmosphere). After 24 h, the second column of each plate was filled with maintenance medium preheated at 37 ºC.

An amount of 10 mg of St-BV were applied directly and contacted during 15 min with the epidermis samples. Phosphate buffer saline (PBS) was used as negative control and sodium dodecyl sulfate (SDS) (5 % in distilled water) as positive control.

Cell viability was determined with the MTT assay. Tissues were transferred to wells containing 2 ml of a 0.3 mg/ml MTT solution and incubated for 3 h (37 ºC, 5 % CO_2, 95 %

humidified atmosphere). After incubation, the epidermis tissues were put in contact with acidic isopropanol (0.5 ml/tube) to extract the intracellular formazan.

The tubes were incubated for 4 h in dark with periodic vortexing, after that, a duplicate of 200 µl was transferred to a 96-well flat bottom microtiter plate. Absorbance was read at 570 nm with acidified isopropanol as blank and viability was calculated considering 100% for the negative control.

2.2.4 *In vivo* studies

2.2.4.1 Human Repeat Insult Patch Test (HRIPT)

A safety evaluation study was performed on St-BV, using the Marzully and Maibach [10] HRIPT protocol. Briefly, the product was applied on the back of 50 healthy volunteers that previously signed the informed written consent. Subjects with dermatological or other medical or physical conditions precluding the topical application of the testing product were excluded, along with pregnant and nursing women. For the induction period of a possible allergic reaction, a series of 9 patches (Finn Chamber standard) were performed over a period of 3 weeks. An occlusive patch containing 20 mg of the formulation was applied on the left side of the back where it remained for 48 h. After that period, the patch was removed, the skin was evaluated and a new patch was applied. Reactions after patching were scored according to the recommendations of the International Contact Dermatitis Research Group [11].

A 2 weeks rest period was followed without application of the testing product. During the challenge period, new patches were prepared and fixed in the same manner as in the induction period, but also on the right side of the back (i.e. a virgin site). The patches were removed after 48 h and the skin reactions were evaluated as before at 48, 72, and 96 h after patching using the same scoring system.

This protocol was approved by the local Ethical Committee and respected the Helsinki Declaration and the AFSSAPS regulations on performed HRIPT studies on cosmetic products. The study was conducted under the supervision of a dermatologist who participated in the evaluation of irritation/allergic reactions to the tested formulations.

2.2.4.2 Biological effects of St-BV

A total of 20 healthy volunteers, aged between 18 and 45, were selected, and provided informed written consent. This protocol was approved by the local Ethical Committee.

Volunteers applied the St-BV formulations on the forearm during 28 days and the results were compared with a defined control area (anatomically equivalent and without product). The trans-epidermal water loss (TEWL), epidermal capacitance (Hydration) and skin surface lipids were evaluated with a Tewameter TM210, Corneometer CM820 and a Sebumeter SM810 (C+K Electronics GmbH, Germany) respectively, during 28 days. At the end of the study, the microcirculation was measured with a laser Doppler perfusion monitor (PF5010, Perimed, Järfärlla, Sweden). An amount of 0.1 M aqueous solution of methyl nicotinate was applied for exactly 60 sec using a saturated filter paper disc. Immediately after removing the paper disc, the alterations on the blood flow (in perfusion units, PU) were measured for 20 min using a two-probe. Measurements were performed under standardized conditions, at room temperature according to the Good Clinical Practices rules [12]. Statistical evaluation of data was performed using two-way analysis of variance (ANOVA) and the groups were considered significant when the estimated *p* values were lower than 0.1 (the chosen α error), to increase statistical power.

2.2.4.3 Sensory analysis

A sensory analysis was adapted from ISO 11136:2014, using the same panel of 20 volunteers. The panel was questioned to scale characteristics of the St-BV. Each volunteer answered a few questions about the St-BV sensory attributes, such as texture (fragrance, consistency and stickiness), skin feel during application (ease of application, spreadability and oiliness), skin feel after application (vanishing, hydration, softness of the skin and freshness) and the intent to acquire the product. Responses were given in a scale from 1 (very bad) to 4 (very good). Sensory parameters were evaluated by a small amount of each formulation applied between the fingertips and rubbed into the skin.

2.2.5 Statistical analysis

According the method described in Chapter3, Section2, section 2.3.3.

3 Results and discussion

3.1 Safety assessment of St-BV

3.1.1 Hazard identification

Many parameters affect the skin penetration and permeation, including the physicochemical properties of each ingredient (Table 5.2). The chemical structures and

physical properties of the ingredients used in the St-BV formulations, namely, the emollients, surfactants and polymers are complex. However, it is recognized that the safety of a final product is determined based on the theoretical safety assessment of its ingredients. Molecules in the solid state and with a molecular weight (MW) greater than 500 Da do not penetrate the skin. In addition, if a chemical is excessively hydrophilic or too strongly lipophilic, it will not partition or it will partition more readily into the *stratum corneum* (SC), respectively. In general, a LogP of between 1 and 3 is considered to be ideal for skin penetration. Thus, when no permeation data is available, the value considered is 100% according to OCDE, however in case of molecular weight > 500 Da and LogP < -1 or > 4, the value of 10% for dermal absorption is considered [13-15].

These limits on MW and LogP result from the physical arrangement of lipids between adjacent corneocytes of the SC. Considering the MW of the ingredients presented in Table 5.2, it is concluded that solid particles (aluminum starch octenylsuccinate) and the polysorbate 80 are not able to penetrate the SC. On the other hand, the ingredients with higher probability to penetrate into the SC are liquid paraffin, caprylic/capric acid triglyceride, ethanol, cetrimide and pregelatinized modified corn starch.

Table 5.2 - Chemical properties of the ingredients presented in the St-BV.

Ingredient (Chemical name/INCI name)	CAS number	Molecular weight (g/mol)	Impurities*	LogP
Purified water/aqua	7732-18-5	18.0	-	-1.38
Liquid paraffin/ paraffinum liquidum	8012-95-1 / 8042-47-5	n.a.	Polycyclic aromatic hydrocarbons < 0.057%	n.a.
Caprylic/capric acid triglyceride	73398-61-5	408.57	Ash < 0.01% Heavy metals < 10 mg/kg	3.59
Aluminum starch octenylsuccinate	9087-61-0	n.a.	Arsenic < 1.0mg/kg Lead < 2.0mg/kg	n.a.
Ethanol/alcohol	64-17-5	46.1	Alcohol (methyl-2-propanol-1) < 0.5 g/hl Ethyl acetate < 1.3 g/hl Aldehydes < 0.5 g/hl Furfural – n.a.	-0.1
Cetrimonium bromide	57-09-0	364.45	Amine HBr < 0.3 % Sulphated ash < 0.5%	2.69
Polysorbate 80	9005-65-6	604.8	-	4.99
Pregelatinized modified corn starch	68584-86-1	-	Sulfur dioxane < 50ppm Iron < 20 ppm Ash < 0.5 %	n.a.

*Data from the literature and from MSDS the supplier [16, 17]. INCI – International Nomenclature of Cosmetic Ingredients

Concerning the impurities of the ingredients and according the manufacture of liquid paraffin, there are eight impurities which can be detected in this excipient. All of these impurities are listed in the Annex II (List of substances prohibited in cosmetic products)

and they are: benzo[def]chrysene (benzo[a]pyrene), dibenz[a,h]anthracene, benz[a]anthracene, benzo[e]pyrene, benzo[j]fluoranthene, benz(e)acephenanthrylene, benzo(k)fluoranthene and chrysene. However, according to the article 17 of the Regulation (EC) No 1223/2009, the non-intended presence of a small quantity of a prohibited substance, stemming from impurities of natural or synthetic ingredients, the manufacturing process, storage, migration from packaging, which is technically unavoidable in good manufacturing practice, shall be allowed to provide that such presence is in conformity with Article 3 (Safety). The other impurities or traces present in the ingredients are related to the production process or raw materials, their concentrations being very low [6].

The biological safety evaluation requires that cytotoxicity, sensitization and irritation or intracutaneous reactivity are determined and the risk of chronic toxicity, carcinogenicity, reproductive/development toxicity or other organ-specific toxicities based on specific nature and duration of exposure of the product are assessed (Table 5.3) [4].

The main ingredient present in ASt-emulsions is a liquid lipid (LP or CT). Liquid lipids are widely used in cosmetic products due to their moisturizing, occlusive and emollient properties. Moreover, it is well known that after topical application of one product, only a very small amount is able to penetrate the skin due to the SC properties. There are several mechanisms of hydration but the majority of the oils act by occlusion, e.g., they avoid the evaporation of endogenous water, decreasing the trans-epidermal water loss [18]. In fact, LP and CT act as skin moisturizers in the skin surface, decreasing the trans-epidermal water loss and thus, they do not penetrate through the skin barrier. Medium-chain triglycerides are a family of triglycerides, containing predominantly, caprylic (C(8)) and capric (C(10)) fatty acids with lesser amounts than caproic (C(6)) and lauric (C(12)) fatty acids, exhibiting very low levels of toxicity in a variety of laboratory animals and in humans when administered orally, parenterally or by the dermal route [19]. On the other hand, the polycyclic aromatic hydrocarbons from LP can penetrate into the SC. It was demonstrated that in the worst case scenario only 56% of these substances are absorbed through the skin [20].

Table 5.3 - Summary of the biological safety of the ingredients.

Ingredient (Chemical name/INCI name)	Acute toxicity	Dermal Irritation	Ocular irritation	Sensitization	Genotoxicity / carcinogenicity	Ref
Purified water/aqua	n.a.	n.a.	n.a.	n.a.	n.a.	-
Liquid paraffin/ paraffinum liquidum	Rat (oral) LD_{50} > 5000 mg/kg	Rabbit (OECD 404): Non irritant	Rabbit (OECD 405): non- irritant	OECD 406: non sensitiser	Ames test: negative	[21, 22]
Caprylic/capric acid triglyceride	Rat (oral) LD_{50} > 36.000 mg/kg bw	Non-irritating or were only mildly irritating	Non-irritating	Non-sensitizing	*Salmonella typhimurium* (OECD 471): no mutagenic	[19]
Aluminum starch octenylsuccinate	-	Human volunteers: no irritant	Ocular irritant in humans	Guinea pig: non sensitizer	No evidence of genotoxicity or mutagenicity	[23]
Ethanol/alcohol	Mouse (oral) LD_{50} > 8300 mg/kg	Rabbit (dermal) LD_{50} > 20000 mg/kg; Rabbit (OECD 404): non-irritant	Rabbit (OECD 405): moderately irritating	Guinea pig: non sensitizer Human: non sensitizer	*Salmonella typhimurium* (OECD 471): no mutagenic	[24]
Cetrimonium bromide	Rat (oral) LD_{50} > 400 < 600 mg/kg	Rabbit: Irritant	Potent irritant	Sensitizer	*Salmonella typhimurium* (OECD 471): no mutagenic	[25]
Polysorbate 80	Rat (oral) LD_{50} > 63840 mg/kg	Rabbit (OECD 404): moderately irritating	Rabbit (OECD 405): moderately irritating	-	No evidence of genotoxicity or mutagenicity	[26]
Pregelatinized modified corn starch	Toxicological information (e.g. acute toxicity, NOAEL, mutagenicity, LD_{50}/LC_{50}-value) is not available for this product. Due to the fact that it is a food grade raw material, there is no reason to determine toxicity data. When applied correctly, the raw material will have no negative adverse effects in humans.*					

* Data from material safety data sheet; INCI – International Nomenclature of Cosmetic Ingredients; n.a. – not available; LD_{50} - the median lethal dose; LC_{50} - the median lethal concentration; OECD - The Organisation for Economic Co-operation and Development; NOAEL - No Observed Adverse Effect Level; bw – body weight.

The ingredients in the solid state are not able to penetrate the SC if not solubilized. The ASt are not soluble in water neither in oils [14], being formulated in suspension, which does not allow skin penetration. Given the negligible, dermal penetration of ASt when applied on skin, and in consideration of the low toxicity observed, the calculation of a margin of safety (MoS) is not relevant for this assessment [23]. Concerning the ASt, it was demonstrated that it has unimportant acute toxicity in animals, and no toxicity was reported following chronic administration. In addition, this ingredient was not recognized as an ocular irritant in rabbits. Oral studies using ASt produced no adverse systemic, reproductive, or developmental effects. ASt may produce minor skin irritation, but in general this ingredient is not irritating at concentrations used in cosmetics, and neither sensitizer nor photosensitizer [23].

Concerning the StNC formulation, in the particular case of ethanol, Pendlington *et al*. [27] described the only study in the literature about serum ethanol levels in humans after using a body deodorant spray. Despite the high amounts of ethanol and the large exposure surfaces, the serum concentration was 0.4 mg/l [28].

Emulsifiers are of particular concern due to their skin irritative potential [34, 35], because they have the potential to act as penetration enhancers by decreasing surface tension and conditioning the SC, thus facilitating or enhancing diffusion of other molecules through the skin [36]. The emulsifiers present in StNC are polysorbate 80 and cetrimonium bromide.

Polysorbates are a series of polyoxyethylenated sorbitan esters that are used as hydrophilic, nonionic surfactants in a variety of cosmetic products, that are not irritant, or only very slightly irritant to the skin of rabbits and humans [26]. However, increased TEWL was induced by some polysorbates, indicating an invisible impairment of the SC barrier function [29]. In addition, acute and long-term oral toxicity in animals indicates a low order of toxicity with oral ingestion of the polysorbates. In particular, polysorbate 80 was shown to be non-mutagenic in the Ames[1] and micronucleus tests and this ingredient was non-carcinogenic in laboratory animals [30]. The available data indicate this ingredient is used in numerous preparations without clinical reports of significant adverse effects.

Cetrimonium bromide is a quaternary ammonium salt used for a variety of purposes in cosmetic products at concentrations of up to 10%. This ingredient applied dermally is

[1] The Ames test is a widely employed method that uses bacteria to test whether a given chemical can cause mutations in the DNA of the test organism. More formally, it is a biological assay to assess the mutagenic potential of chemical compounds [30].

slowly absorbed into the skin. Dermal irritation, sensitization and ocular irritation are often seen with this quaternary ammonium salt. It has been described as embryotoxic and teratogenic in mice following intraperitoneal injection of 35 mg/kg, although only teratogenic effects were observed with 10 mg/kg [25, 31].

Concerning the pregelatinized modified corn starch, it was demonstrated that starch has little acute or short-term toxicity in animals, and no toxicity was noted following chronic administration. This ingredient was classified as minimal irritating to the rabbit eye. Pregelatinized modified corn starch (7.5%) did not induce cumulative skin irritation in 26 subjects or skin sensitization in 113 subjects tested. This ingredient is neither sensitizer nor photosensitizer. At concentrations higher than used in cosmetics, pregelatinized modified corn starch caused moderate erythema in HRIPT studies [32].

On the whole, it is concluded that all ingredients are safe for use in cosmetics at present concentrations of use. However, these data clearly suggest the ingredients of special concerns are cetrimonium bromide and ethanol because they present suitable physical characteristics to penetrate the skin. Moreover, ethanol is present in the formulation in a relatively high concentration and cetrimonium bromide showed to be irritant to the skin and it is a sensitizer.

3.1.2 Exposure assessment

The St-BV are intended for use on intact skin of adults. They can be used as a vehicle in antibioteraphy and anti-inflamatory therapy or an adjuvant in these therapies upon application to the affected area in the desired quantity once or twice a day.

They will be supplied for use as a leave-on cosmetic product, which is intended to stay in prolonged contact with the skin. According to the SCCS opinion, the exposed skin surface area for a body lotion is 15670 cm^2. All St-BV will be considered as body creams or body lotions. The estimated daily amount applied for a body cream is 7.82 g/day and the frequency of application is 2.28/day, which is translated in a daily exposure of 123.2 mg/kg/bw/day. Applying the previous equation 1, the SED values were calculated for each ingredient [4].

Tables 5.4 and 5.5 show the estimated SED for the ingredients present in the St-BV. In the lack of dermal absorption studies, the worst-case scenario of 100% of dermal penetration should be taken into consideration [4]. In addition, a large number of studies suggest that

solid particles do not penetrate healthy or sunburnt human skin deep enough to reach live cells of the epidermis, as a result, the dermal absorption considered for ASt was 0%.

Table 5.4 - Exposure data of ASt-emulsions ingredients.

Ingredient (Chemical name/INCI name)	Daily exposure (mg/kg bw/day)	% in the ASt-emulsion LP	% in the ASt-emulsion CT	Dermal absorption* (%)	SED (mg/kg/bw/day) for ASt-emulsion with LP	SED (mg/kg/bw/day) for ASt-emulsion with CT
Purified water/aqua	123.2	25	25	100	30.8	30.8
Liquid paraffin/ paraffinum liquidum	123.2	69	-	100	85.0	-
Caprylic/capric acid triglyceride	123.2	-	69	100	-	85.0
Aluminum starch octenylsuccinate	123.2	6	6	0	7.4	7.4

*when no permeation data is available, the value considered is 100%. INCI – International Nomenclature of Cosmetic Ingredients; SED - systemic exposure dose; bw – body weight; CT – Caprylic/capric acid triglyceride; LP – Liquid paraffin.

Table 5.5 - Exposure data of StNC formulation ingredients.

Ingredient (Chemical name/INCI name)	Daily exposure (mg/kg bw/day)	% in the StNC	Dermal absorption* (%)	SED (mg/kg/bw/day)
Purified water/aqua	123.2	65.47	100	80.66
Ethanol/alcohol	123.2	32.53	0.04**	0.02
Cetrimonium bromide	123.2	0.25	100	0.31
Capric/caprylic triglycerides	123.2	0.55	100	0.68
Polysorbate 80	123.2	1.13	100	1.39
Pregelatinized modified corn starch	123.2	0.07	100	0.09

*when no permeation data is available, the value considered is 100%; **data from the literature [24, 27]. INCI – International Nomenclature of Cosmetic Ingredients; SED - systemic exposure dose; bw – body weight; StNC – Starch-based nanocapsules.

3.1.3 Dose-response assessment

The NOAEL is mainly derived from repeated dose animal studies (90 day, developmental toxicity studies). As far as the determination of critical effects in repeated dose toxicity studies is concerned, the available repeated dose toxicity data should be evaluated in detail for a characterization of the health hazards upon repeated exposure. The NOAEL values found out for cetrimonium bromide and ethanol were 100 and 2400 mg/kg/day, respectively [24, 25].

3.1.4 Risk characterization

The MoS is used to extrapolate from a group of test animals to an average human being, and subsequently from average humans to sensitive subpopulations. The world health organization proposes a minimum value of 100, and it is generally accepted that the MoS should at least be 100 to declare a substance safe for use. The value of 100 consists of a factor 10 for the extrapolation from animal to man and another factor 10 taking into account the inter-individual variations within the human population [4].

For the two ingredients of special concerns (cetrimonium bromide and ethanol), the MoS was calculated according to Equation 2 (above). The value obtained for cetrimonium bromide was 333.3, which is above of the threshold value of 100, suggesting that the ingredient can be considered to pose no consumer risks on systemic toxicity effects. However, it should be emphasized that this is a very conservative approach. In fact, the actual safety margins of cosmetic ingredients tend to be higher than theoretical values, since calculated MoS data represents a worst-case scenario. For example, it was considered a skin penetration of 100 %, which not corresponds to the reality. In this case *in vitro* and *in vivo* tests will be useful to decide about the safety of this ingredient. Concerning ethanol, the obtained MoS value was 120000.

3.2 EpiSkin™ assay

The *in vitro* safety topical use of St-BV was tested on reconstituted human epidermis. The Episkin™ model mimics morphologically and biochemically living skin and is useful to classify skin irritants able to produce a reduction in cell viability, as evaluated by a MTT assay [33]. The tissue viability calculated as percentage of cytotoxicity compared to the negative control (PBS), was 98.0 ± 8.6 %, 95.6 ± 9.0 % and 84.0 ± 5.0 % for ASt-emulsion with LP, ASt-emulsion with CT and StNC, respectively, whereas in the positive control (SDS), it was 34.0 ± 4.0 %. A product is considered non-irritant when its viability is not reduced by 50 % [34]. Thus, the absence of skin-irritant effects at the tested concentrations indicated St-BV are safe for topical use.

3.3 *In vivo* studies

Concerning the HRIPT assay, no reactions or skin sensitization/irritation were observed in the initial 3 weeks of contact and even after the final challenge contact. Thus, very good

skin compatibility and absence of allergenic potential were obtained for St-BV, justifying the claim "dermatological tested" and making them skin-friendly vehicles.

In addition, SC hydration is a decisive factor to keep the skin flexible and permeable to molecules [33]. An increased TEWL is a sensitive measure of barrier damage and an indication of the skin permeability. On the other hand, SC water retention and skin surface lipids properties are crucial factors in keeping the skin supple and flexible and influence skin permeability to molecules. The chosen methodological procedure allowed the identification of positive results regarding TEWL, skin water dynamics, expressed in terms of epidermal capacitance changes and skin lipids expressed in terms of sebum [35, 36].

The long term *in vivo* study demonstrated a decrease in TEWL value, but not significant (p>0.1), in the treatment area when compared with control area, during 28 days. St-BV reduced the TEWL through occlusive mechanisms that increase the water content on the skin.

The principal mechanisms of hydration are humectancy, emolliency and occlusion. The hydration provided by St-BV is attributed to the occlusives (LP or StNC) or emollients (LP and CT). In fact, occlusives provide a layer of oil or nanocapsules on the surface of the skin and promote water retention within the SC, whereas emollients smooth the skin by filling spaces between skin flakes and adding a complementary occlusive activity which contributes to SC hydration [37]. In addition, this study revealed a better skin hydration for all St-BV, comparing with the control area, after 28 days of two daily applications (Fig. 5.1). Concerning the ASt-emulsions hydration results, these may be due to LP and CT occlusive and emollient or only emollient characteristics, respectively. Once applied to the skin, emollient lipids resemble those naturally found on skin improving the rate of barrier repair. Consequently, the SC is soften and hydrated, reducing water loss. In relation to StNC, this may be due to its occlusive ability to form a layer on the surface of the skin and moisturize by retarding the water evaporation. Due to their high surface area, StNC provide partial occlusion that hydrates and improves the appearance of the SC, making the skin soft and flexible [38].

On the other hand, St-BV did not significantly increase skin surface lipids compared to the control (p > 0.1).

Concerning the microcirculation results and following a long term application of St-BV, there was an enhancement on skin permeation in the first 5 min (Fig. 5.1c). The ASt-emulsions present this characteristic as a result of their water retention and hydration ability (consequence of occlusive and emollient capacities), providing a healthier skin

barrier with a higher permeation aptitude. The skin is hydrated and exists in a swollen state, therefore more void spaces within the skin create wider diffusion channels [39]. Additionally, Pickering emulsions already showed higher adhesion to the skin [40].

The StNC also present this characteristic as a result of their occlusive effect to form a layer on the surface of the skin and, moisturize by decreasing the water evaporation [41]. Additionally, ethanol is a permeation enhancer and can exert its permeation enhancing activity through various mechanisms, namely, lipid extraction, increased lipid fluidity, enhancement of drug solubility in SC lipids and effects on solvent drugs (increasing the solubility of the drug in the vehicle) [42]. These findings suggest that not only the drug itself but also the vehicle plays a significant role in the treatment efficacy.

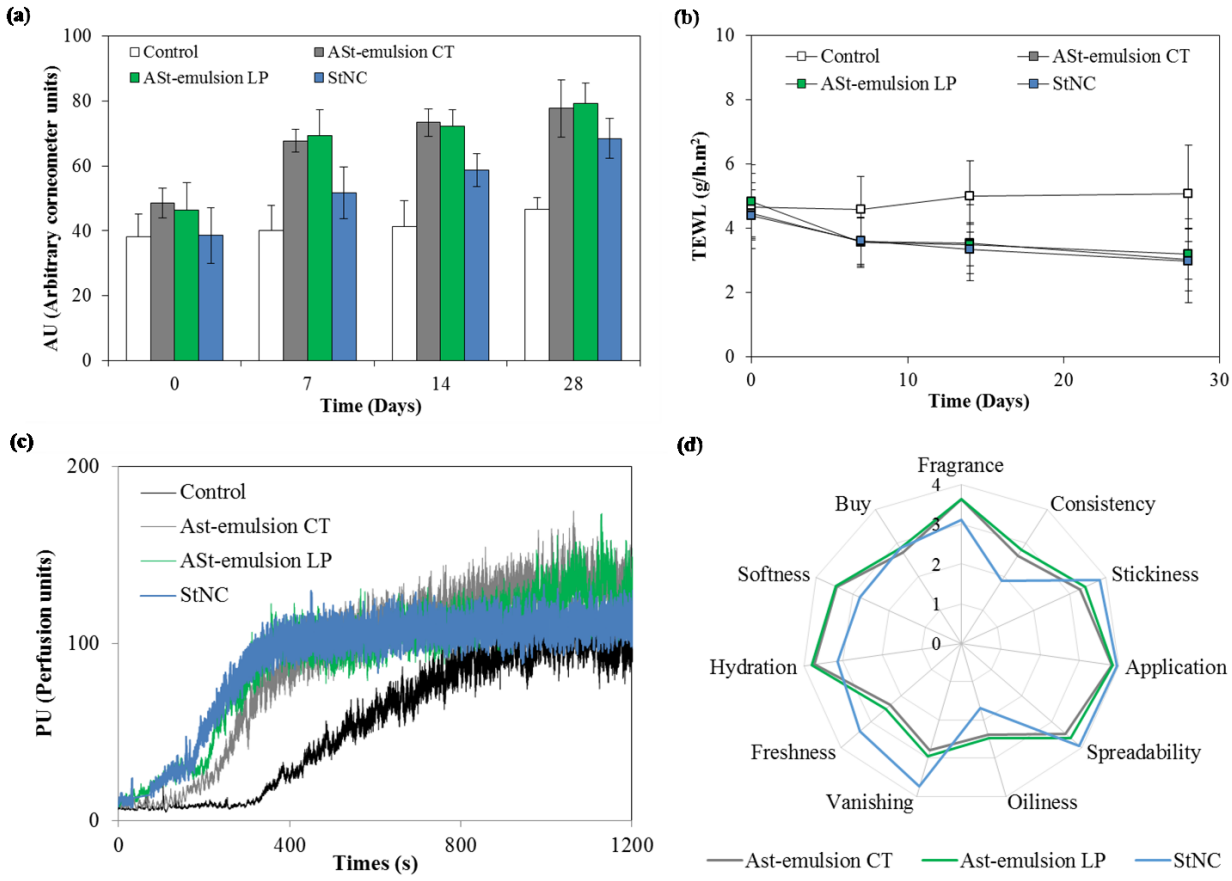

Fig. 5.1 - Comparison of (a) TEWL and (b) skin hydration values in terms of capacitance during 28 days between St-BV and control; c) skin's microcirculation after application of methyl nicotinate measured using a two-probe laser Doppler perfusion monitor (mean ± SD, n=20); d) sensory profile of St-BV.

The cosmetic properties of St-BV were assessed using a simple sensory questionnaire in which the basic characteristics, i.e. texture and skin feel were evaluated by volunteers, during and after application (Fig. 5.1d). Results showed that St-BV met consumer appeal and acceptance requirements. The general opinion is truly optimistic and so, St-BV present the highest score for spreadability, stickiness and skin feel on application. ASt-emulsions present a low score for the freshness and StNC present a low score for the oiliness and consistency. However, the volunteers did not find significant differences between Ast-emulsion CT and ASt-emulsion LP. The fragrance was well accepted by the volunteers and they considered that was easy to apply and quick to spread. In the after feel, volunteers reported hydration and softness and the intent to buy was high. These observations are in accordance with the results obtained so far in epidermal capacitance, TEWL and sebometry (Fig. 5.1).

4 Conclusion

Considering the composition of the St-BV, the physicochemical characteristics, the toxicological profile of the ingredients, the risk characterization and the *in vitro* and *in vivo* results, all St-BV can be considered safe in the normal and reasonably foreseeable use.

EpiSkin™ assay showed that the tissue viability after the application of St-BV was between 98.0 ± 8.6% and 84.0 ± 5.0 % and, thus considered non-irritant to the skin. The *in vivo* studies confirmed that the St-BV are not skin irritant and did not induce any sensitization on the volunteers, being safe for human use. Moreover, biological effects demonstrated that St-BV increased both the skin hydration and microcirculation, being attractive topical vehicles. Therefore, a suitable equilibrium between safety and efficacy was demonstrated.

5 References

1. Raposo S, Salgado A, Eccleston G, Urbano M, Ribeiro HM. Cold processed oil-in-water emulsions for dermatological purpose: formulation design and structure analysis. Pharmaceutical Development and Technology. 2014;19(4):417-429.

2. Raposo SC, Simões SD, Almeida AJ, Ribeiro HM. Advanced systems for glucocorticoids' dermal delivery. Expert Opinion on Drug Delivery. 2013;10(6):857-877.

3. Nohynek GJ, Antignac E, Re T, Toutain H. Safety assessment of personal care products/cosmetics and their ingredients. Toxicology and Applied Pharmacology. 2010;243(2):239-259.

4. SCCS. The SCCS'S Notes of Guidance for the Testing of Cosmetic Ingredients and Their Safety Evaluation: 9th Revision: European Union; 2015.

5. Pauwels M, Rogiers V. Human health safety evaluation of cosmetics in the EU: a legally imposed challenge to science. Toxicology and Applied Pharmacology. 2010;243(2):260-274.

6. EC. Regulation (EC) No 1223/2009 of the European Parliament and of the Council of 30 November 2009 on cosmetic products. In: EC, editor.: Official Journal of the European Union; 2009.

7. Serup J. Efficacy testing of cosmetic products*. Skin Research and Technology. 2001;7(3):141-151.

8. Carneiro R, Salgado A, Raposo S, Marto J, Simões S, Urbano M, Ribeiro HM. Topical emulsions containing ceramides: Effects on the skin barrier function and anti-inflammatory properties. European Journal of Lipid Science and Technology. 2011;113(8):961-966.

9. OECD. Test No. 439: In Vitro Skin Irritation Reconstructed Human Epidermis Test Method: Reconstructed Human Epidermis Test Method. OECD Publishing; 2010.

10. Marzulli FN, Maibach HI. Contact allergy: predictive testing in man. Contact Dermatitis. 1976;2(1):1-17.

11. Fregert S, Bandmann HJ. International Contact Dermatitis Research Group patch testing. New York: Springer-Verlag. 1975:8-10.

12. ICHE6(R1). ICH harmonised tripartite guideline: guideline for good clinical practice E6 (R1). International Conference on Harmonisation of Technical Requirements for Registration of Pharmaceuticals for Human Use.1996.

13. Potts RO, Guy RH. Predicting skin permeability. Pharmaceutical Research. 1992;9(5):663-669.

14. Bos JD, Meinardi MM. The 500 Dalton rule for the skin penetration of chemical compounds and drugs. Experimental Dermatology. 2000;9(3):165-169.

15. Brain KR, Chilcott RP. Physicochemical Factors Affecting Skin Absorption. Principles and Practice of Skin Toxicology: John Wiley & Sons, Ltd; 2008. p. 83-92.

16. EC. Cosmetic ingredient database – CosIng. European Comission.

17. Tetko IV, Gasteiger J, Todeschini R, Mauri A, Livingstone D, Ertl P, Palyulin VA, Radchenko EV, Zefirov NS, Makarenko AS, Tanchuk VY, Prokopenko VV. Virtual

computational chemistry laboratory--design and description. Journal of Computer-aided Molecular Design. 2005;19(6):453-463.

18. Boekschoten MV, Schouten EG, Katan MB. Coffee bean extracts rich and poor in kahweol both give rise to elevation of liver enzymes in healthy volunteers. Nutrition Journal 2004;3:7-7.

19. Traul K, Driedger A, Ingle D, Nakhasi D. Review of the toxicologic properties of medium-chain triglycerides. Food and Chemical Toxicology. 2000;38(1):79-98.

20. Dooms-Goossens A, Degreef H. Contact allergy to petrolatums. (I). Sensitizing capacity of different brands of. Contact Dermatitis. 1983;9(3):175-185.

21. Nash J, Gettings S, Diembeck W, Chudowski M, Kraus A. A toxicological review of topical exposure to white mineral oils. Food and Chemical Toxicology. 1996;34(2):213-225.

22. EFSA. Scientific opinion on the safety assessment of medium viscosity white mineral oils with a kinematic viscosity between 8.5 – 11 mm²/s at 100 °C for the proposed uses as a food additive. European Food Safety Authority. 2013;11(1):1-21.

23. Nair B, Yamarik TA. Final report on the safety assessment of aluminum starch octenylsuccinate. International Journal of Toxicology. 2002;21 Suppl 1:1-7.

24. OECD. Ethanol. OECD SIDS; 2004.

25. Becker LC, Bergfeld WF, Belsito DV, Hill RA, Klaassen CD, Liebler D, Marks JG, Shank RC, Slaga TJ, Snyder PW. Safety Assessment of Trimoniums as Used in Cosmetics. International Journal of Toxicology. 2012;31(6 suppl):296S-341S.

26. Moore J. Final report on the safety assessment of polysorbates 20, 21, 40, 60, 61, 65, 80, 81, and 85. International Journal of Toxicology. 1984;3:1-82.

27. Pendlington RU, Whittle E, Robinson JA, Howes D. Fate of ethanol topically applied to skin. Food and Chemical Toxicology 2001;39(2):169-174.

28. Lachenmeier DW. Safety evaluation of topical applications of ethanol on the skin and inside the oral cavity. Journal of Occupational Medicine and Toxicology. 2008;3:26.

29. Bárány E, Lindberg M, Lodén M. Unexpected skin barrier influence from nonionic emulsifiers. International Journal of Pharmaceutics. 2000;195(1):189-195.

30. Mortelmans K, Zeiger E. The Ames Salmonella/microsome mutagenicity assay. Mutation Research/Fundamental and Molecular Mechanisms of Mutagenesis. 2000;455(1):29-60.

31. Andersen F. Final report on the safety assessment of cetrimonium chloride, cetrimonium bromide, and steartrimonium chloride. International Journal of Toxicology. 1997;16(3):195-220.

32. Belsito M, Hill RA, Klaassen CD, Liebler DC, Marks Jr JG. Safety Assessment of Plant Polysaccharide Gums as Used in Cosmetics. Cosmetic Ingredient Review. 2014:1-45.

33. Raposo S, Salgado A, Gonçalves L, Pinto P, Urbano M, Ribeiro H. Safety Assessment and Biological Effects of a New Cold Processed SilEmulsion for Dermatological Purpose. BioMed Research International. 2013;2013:10.

34. Wallin R, Arscott E. A practical guide to ISO 10993-5: Cytotoxicity. Medical Device and Diagnostic Industry. 1998;20:96-98.

35. Agner T, Serup J. Skin reactions to irritants assessed by non-invasive bioengineering methods. Contact Dermatitis. 1989;20(5):352-359.

36. Pinnagoda J, Tupker R, Coenraads P, Nater J. Measurement of transepidermal water loss. Contact Dermatitis. 1989;20(2):159-160.

37. Kraft J, Lynde C. Moisturizers: what they are and a practical approach to product selection. Skin Therapy Lett. 2005;10(5):1-8.

38. Wissing SA, Müller RH. The influence of solid lipid nanoparticles on skin hydration and viscoelasticity – in vivo study. European Journal of Pharmaceutics and Biopharmaceutics. 2003;56(1):67-72.

39. Lou H, Qiu N, Crill C, Helms R, Almoazen H. Development of W/O Microemulsion for Transdermal Delivery of Iodide Ions. AAPS PharmSciTech. 2013;14(1):168-176.

40. Frelichowska J, Bolzinger M-A, Valour J-P, Mouaziz H, Pelletier J, Chevalier Y. Pickering w/o emulsions: Drug release and topical delivery. International Journal of Pharmaceutics. 2009;368(1–2):7-15.

41. Lou H, Qiu N, Crill C, Helms R, Almoazen H. Development of w/o microemulsion for transdermal delivery of iodide ions. AAPS PharmSciTech. 2013;14(1):168-176.

42. Marto J, Baltazar D, Duarte A, Fernandes A, Gouveia L, Militao M, Salgado A, Simoes S, Oliveira E, Ribeiro HM. Topical gels of etofenamate: in vitro and in vivo evaluation. Pharmaceutical Development and Technology. 2015;20(6):710-715.

6 Pickering emulsion sunscreen

This page was intentionally left blank

Melatonin-based Pickering emulsion sunscreen for skin's photoprotection

This Chapter was adapted from the published papers in:

J Marto, LF Gouveia, BG Chiari, A Paiva, V Isaac, P Pinto, P Simões, A.J Almeida, HM Ribeiro (2016) The green generation of sunscreens: Using coffee industrial sub-products. Industrial Crops and Products. 80: 93-100.

J Marto, A Ascenso, LM Gonçalves, LF Gouveia, P Manteigas, P Pinto, P Simões, E Oliveira, A.J Almeida, HM Ribeiro (2016) Melatonin-based Pickering emulsion for skin's photoprotection. Drug Delivery. 11:1-14.

This page was intentionally left blank

Graphical Abstract

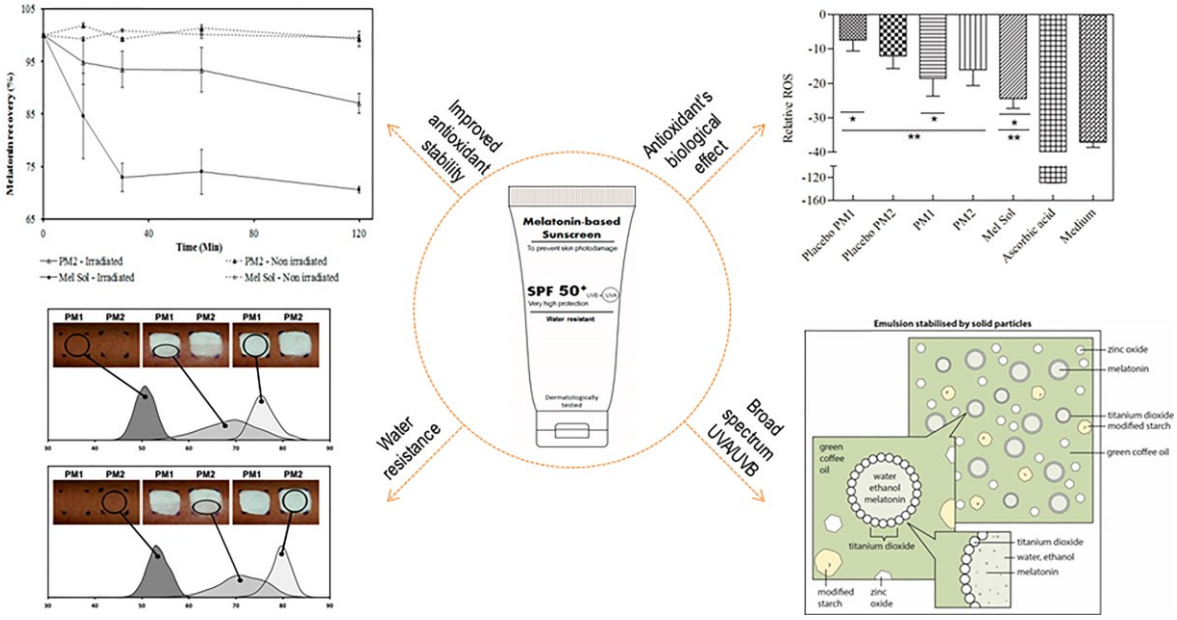

Highlights:

- Broad spectrum melatonin-based sunscreen offer protection against UV light and free radicals.
- Modified starch and green coffee oil boost UV protection over the whole UVA/B spectrum, reducing the amount of UV filters.
- Pickering emulsion sunscreens with suitable rheological and mechanical properties.
- Pickering emulsions sunscreens proved to be a promising solution to protect melatonin from photodegradation.
- Novel melatonin-based sunscreens were non-irritant and safe for skin application.

This page was intentionally left blank

1. Introduction

Skin cancer is one of the most common types of cancers worldwide with an increasing incidence, mainly the non-melanoma skin cancer (NMSC). In addition, there is an emerging group of high-risk patients treated with immunosuppressive drugs and submitted to surgeries, chemotherapy and radiotherapy, which have an increased risk of developing NMSC, either as basal cell carcinoma or squamous cell carcinoma [1, 2]. Ultraviolet radiation (UVR) from sun exposure is the main etiological agent for skin cancer [3, 4]. The UV-induced cell damage can mainly occur by two mechanisms, such as: a) development of cyclobutan dimers [5]; b) generation of reactive oxygen species (ROS), which are also involved in carcinogenesis. Avoiding sun exposure, covering the skin and applying sunscreens with a high degree of protection are the main strategies recommended to prevent UV-induced cell damage. The UV filters of sunscreens can be divided in two groups: a) organic or chemical filters which absorb UVR and are "not visible" on skin surface, being more unstable and reactive; and b) inorganic or physical filters, which reflect UVR. However, the main limitations of the physical filters are related to their poor spreadability and less cosmetic appearance on the skin [6]. Therefore, the research of new UV filters, or at least, an alternative to reduce their concentration without affecting the total photoprotection of the sunscreen product should be promoted to obtain effective, greener and safer sunscreen formulations.

The efficacy of sunscreen products has been recognized as an important public health issue and is usually expressed by the sun protection factor (SPF), which is defined as the UV energy required to produce a minimal erythema dose (MED) on protected skin, divided by the UV energy dosage required to produce a MED on unprotected skin [7]. Thus, the determination of SPF represents the first approach to evaluate the ability of sunscreens to prevent skin damage by UVR [8].

The photoprotection afforded by topical sunscreens against solar UVR exposure can be determined *in vitro* and *in vivo,* ideally in human volunteers. *In vivo* SPF determination has been used for many years. Although useful and precise, it is also a time consuming, complex and expensive process, particularly when the determination of the protection against long wavelength (UVA) is also required [9]. Thus, *in vitro* evaluation can be an alternative and a faster way to obtain information about the photoprotective activity of the UV filters. The *in vitro* SPF can be calculated by UV spectrophotometric technique employing a very simple mathematical equation developed by Mansur *et al.* [10] or using a

specific UV spectrophotometer covering both UVB and UVA, optimized for the determination of SPF on sunscreens and cosmetic products.

Melatonin (N-acetyl-5-methoxytryptamine) is a well-known neuroendocrine mediator discovered by Lerner (1960), and mostly produced by the pineal gland that follows a circadian light-dependent rhythm of secretion [11, 12]. This hormone can be also produced by retina, bone marrow, gastrointestinal tract, gonads, immune system and skin [13]. In skin, melatonin can be synthesized by normal and malignant keratinocytes (*stratum corneum*), melanocytes (epidermis) and fibroblasts (dermis). This synthesis may be induced or modified by UVB irradiation [13, 14]. Melatonin receptors are G protein-coupled receptors, and there are two subtypes in humans (MT_1, MT_2). MT_1 receptors expression has been detected by immunocytochemistry in skin (*stratum granulosum*, *stratum spinosum*, upper and inner epithelial root sheath, eccrine sweat gland, and blood vessel endothelium). The MT_2 receptors expression has been detected in the inner epithelial root sheath, eccrine sweat gland, and blood vessel endothelium [15].

As it is involved in several physiological processes related to circadian rhythms, seasonal reproduction, retinal function, among others. Melatonin also seems to participate in seasonal and non-seasonal skin changes, hair growth and pigmentation [12, 13]. It acts as an immunomodulator, anti-inflammatory and potent antioxidant agent by down-regulating several pro-inflammatory cytokines and up-regulating antioxidant enzymes, besides being an extra- and intracellular free radical scavenger of ROS and RNS, able to quench the hydroxyl radical, among others [16]. The ability of melatonin to act as an antioxidant, by itself and through its active metabolites, makes it particularly efficient either *in vitro* or *in vivo*, even at a low concentration [17]. Several reports in the literature emphasize the superior antioxidant activity of this molecule, when compared to other antioxidants (e.g. ascorbic acid or vitamin C; vitamin E, etc.) [18, 19]. Moreover, it also inhibits the cyclic adenosine monophosphate (cAMP) signal transduction pathway when it binds to the MT_{1A} receptor and activates phospholipase C, potentiating the release of arachidonate [15, 20]. By activating cytoprotective pathways, counteracting oxidative stress and suppressing the damaged cells proliferation, melatonin has been shown to provide cellular protection against UVR damage. In fact, numerous studies have recognized the photoprotective effects of melatonin after topical application [14, 21, 22], including reduction of UV-induced erythema, protection against oxidative damage caused by UVA rays, and prevention of both photoageing and photocarcinogenesis [12].

In addition, melatonin may function as an antimutagenic and anticarcinogenic agent, capable of suppressing all three stages of carcinogenesis (initiation, promotion and progression) [12, 13, 23]. Therefore, these properties suggest that melatonin may be a promising candidate as a new and effective sun protective agent especially for immunosuppressed patients [24]. However, the short half-life (1 h) and chemical instability of melatonin may limit its therapeutic use. Consequently, melatonin is a challenging molecule for stabilization in a suitable prolonged-release sunscreen formulation. In this context, Pickering emulsions are excellent candidates to stabilize this radical scavenger on a safe and effective manner.

Pickering emulsions are surfactant-free liquid or semi-solid systems stabilized by solid particles (SP). Partial wetting of the SP surface by water and oil is the origin of the strong anchoring of these particles at the oil–water interface. In fact, only few natural and biocompatible materials are available for the successful stabilization of these emulsions since strict requirements, including the insolubility in both fluid phases and intermediate wettability, need to be met. The principal parameters of SP affecting their physicochemical properties include shape, size, surface characteristics and inner structure [25].

Therefore, several types of SP can be used for the stabilization of Pickering emulsions. Starch, a well-known pharmaceutical excipient, shows strong affinity for the oil-water interface resulting in stable emulsions [26]. In addition, starch has been chemically modified to improve many aspects of pharmaceutical emulsions, such as: spreadability, oil absorption, water repellence, and heat tolerance [27]. Some UV filters, as titanium dioxide (TiO_2) and zinc oxide (ZnO), can be also used as SP for the stabilization of these emulsions [28]. TiO_2 has been incorporated in sunscreen formulations for more than 25 years, and it has been regarded as safe and effective, bringing together two of the most desirable features in pharmaceutical market. On one hand, it is especially preferred by people with a high propensity for skin irritation, such as patients undergoing chemotherapy. On the other hand, TiO_2 is necessary for manufacturing sunscreens with a high SPF [29]. Its properties ensure that formulations can be uniformly spread on the skin, granting a better UV protection. Therefore, TiO_2 can combine both stability and SPF of the sunscreen formulation. However, following the recommendations of the European Commission Recommendation of 22 September 2006, the protection factor against UVA should be at least one-third of the overall SPF. Thus, taking into account that TiO_2 is primarily a UVB absorbing compound, it is important to add another physical filter with a

complementary protection. As ZnO is more effective in the UVA range, the combination of both filters will assure a broad-band UV protection [30].

Regarding the use of chemical filters in sunscreen formulation, it is becoming less popular nowadays due to the possible harmful effects. Thus, in order to find effective topical photoprotective agents, plant-derived products including natural oils have been gaining significant attention due to their safety and multiple biological activities on the skin and cost effectiveness. In this context, green coffee oil, a rich source of antioxidants and polyphenols, which has arisen as a potential candidate to replace the chemical filters in "green" sunscreen formulations [31].

Therefore, the major aim of this research study was to develop and characterize a melatonin-based innovative sunscreen formulation based on semi-solid Pickering emulsions stabilized by physical UV filters and natural oils associated to melatonin as a key strategy to prevent UV-induced skin damage. Physicochemical characterization as well as *in vitro* and *in vivo* testing were performed. Studies included physical testing and chemical stability of melatonin by a thorough pharmaceutical control. The SPF was evaluated and *in vitro* skin permeation and retention using newborn pig skin was also determined. The ability of melatonin-containing sunscreens to decrease ROS production was assessed *in vitro*, using cell cultures. *In vivo* biological properties of the final formulations, including the Human Repeat Insult Patch Test (HRIPT) and sunscreen water resistance were also evaluated.

2. Materials and methods

2.1 Materials

Melatonin was purchased from Alfa Aesar (Ward Hill, USA). Carrot oil, Brazil nut oil and refined raspberry seed oil and avocado oil were kind gifts from Provital Group (Barcelona, Spain), Croda do Brasil Ltda. (Campinas, Brazil), Seatons (East Yorkshire, UK) and BioChemica (Melbourne, USA), respectively. Green coffee oil (GCO) was supplied by Cooxupé – Cooperativa de Cafeicultores de Gauxupé (Minas Gerais, Brazil). Spent coffee oil (SCO) was supplied by NovaDelta – Comércio e Indústria de Cafés, S.A. (Campo Maior, Portugal). Triethoxycaprylylsilane titanium dioxide ($mTiO_2$) (Unipure White LC 987) was a gift from Sensient (Milwaukee, USA). Aluminum starch octenylsuccinate (ASt) (DryFlo® Plus) was obtained from AkzoNobel (Amsterdam, Netherlands). Zinc Oxide (ZnO) (Tego® Sun Z 500) was purchased from Evonik Industries AG (Essen, Germany). Liquid paraffin was obtained from José Vaz Pereira, S.A. (Lisbon, Portugal). Ethanol was

purchased from Merck® (Kenilworth, USA). All other reagents were HPLC grade. Purified water was obtained by reverse osmosis (Millipore, Elix 3).

2.2 Methods

2.2.1 Solid particles (SP) – mTiO2, ZnO and ASt

2.2.1.1 Wettability measurement

Contact angles of water and green coffee oil on ZnO, mTiO2 and ASt in air atmosphere were measured according to the procedure described previously in Chapter 2, section 2.2.1.2.

2.2.1.2 Particle size of SP

The particle size analysis was performed according to the procedure described previously in Chapter 3, Section 1, section 2.2.1.1.

2.2.2 Natural oils

2.2.2.1 In vitro SPF determination

All natural oils were accurately weighed (0.25 g), diluted with ethanol, followed by ultrasonication for 5 min and filtered through filter paper (Whatman™ 42). The absorption spectra of samples solution were obtained in the range of 290 to 320 nm (Hitachi U-2001, USA) every 5 nm, using a standard 1 cm quartz cell, and ethanol as the blank reagent. Triplicates were made, followed by the application of the Mansur equation – Equation

Equation 1: $SPF_{spectrophotometric} = CF \times \sum_{290}^{320} EE\ (\lambda) \times I\ (\lambda) \times Abs\ (\lambda)$

where *EE* (λ) is the erythemal effect spectrum; I (λ) is the solar intensity spectrum; Abs (λ) is the absorbance of sunscreen product and CF is the correction factor (=10) [10]. The values of EE x I are constants determined by Sayre [32].

2.2.3 Sunscreen formulations – PhotoMel 1 (PM1) and PhotoMel 2(PM2)

2.2.3.1 Preparation of PM1 and PM2

According to the pre-formulation studies (results not shown), two final formulations were selected (Table 6.1) based on macroscopic appearance, stability and SPF value. The continuous oil phase (Phase A) consisted of green coffee oil, and the aqueous phase (Phase B) composed by purified water, ethanol and melatonin. Solid particles – TiO_2, ZnO and ASt were firstly dispersed in the oil phase. The oil and aqueous phases were then mixed

using a high-speed homogenizer (UltraTurrax®, IKA-Werke GmbH & Co. KG, Germany) at room temperature (cold process).

Table 6.1- Qualitative and quantitative composition of the final formulations.

Ingredients	Quantitative Composition (%, w/w)	
	PM1	PM2
Phase A (external)		
Triethoxycaprylylsilane titanium dioxide	20	20
Zinc oxide	15	15
Aluminum starch octenylsuccinate	-	5
Green coffee oil	35	35
Phase B (internal)		
Melatonin	1	1
Ethanol	6	6
Purified water	23	18

2.2.4 Efficacy of PM1 and PM2

2.2.4.1 In vitro SPF determination

The SPF was assessed using the Optometrics SPF-290S Analyzer (Optometrics Corporation, Essex, UK). The samples were prepared by spreading 110 mg of each formulation over a Transpore® tape (70.7 x 70.7 mm) to obtain a film of 2 mg/cm^2, as specified by the European legislation [33]. Each sample was exposed to a xenon arc solar simulator, and the analyzer performed scans in 6 different spots on the Transpore® tape substrate. Each scan takes a transmittance (T) measurement every 2 nm from a wavelength ranging from 290 to 400 nm. The monochromatic protection factor (MPF) was determined for the selected wavelengths using Equation 2. The SPF value was calculated using Equation 3.

Equation 2: $\mathrm{MPF} = \frac{1}{\mathrm{T}}$

Equation 3: $\mathrm{SPF} = \frac{\sum_{290}^{400} E\lambda.B\lambda}{\sum_{290}^{400} \overline{MPF\lambda}}$

Where, (*E*) is the spectral irradiance of terrestrial sunlight under controlled conditions and (*B*) is the erythema effectiveness [34].

2.2.4.2 In vitro sunscreen water resistance

The water resistance of developed sunscreens was measured using an improved *in vitro* bath system. An amount of 2 mg/cm^2 of sunscreen formulation was dispensed onto the plate, and carefully applied with a rubber-gloved finger. After drying for 15 min, the SPF of each sample was determined using the SPF 290 analyzer (Optometrics SPF-290S Analyzer). The samples were immersed in the *in vitro* bath system (29 ± 2°C) and washed away by the water flow (150 rpm) during 20 min. The samples were allowed to air dry for 15 min and SPF was measured again. Afterwards, the samples were immersed once more and washed during 20 min. The samples were allowed to air dry for 15 min and SPF was measured to calculate the water resistance retention (%WRR) of the sunscreens, as defined by Equation .

Equation 4: $\%\ \mathrm{WRR} = \frac{(\mathrm{SPF_{wet}}-1)}{(\mathrm{SPF_{dry}}-1)} \times 100$

where, SPF_{dry} and SPF_{wet} are the SPFs before and after water immersion, respectively [35, 36].

2.2.5 Physicochemical and microbiological stability

Two batches of PM1 and PM2 emulsions were stored during 3 months at 25 ± 2 °C and under accelerated conditions (40 ± 2 °C; relative humidity 75 ± 5 %). Samples were analyzed for chemical and physical stability (melatonin assay, macroscopic appearance, pH by potentiometry and droplet size distribution) before the storage period and after 14 days, 1 and 3 months.

2.2.5.1 Melatonin chemical stability

Melatonin assay was performed by liquid chromatography using a HPLC system (Shimadzu®, Japan) with a SPD-10A UV-VIS detector at 300 nm according to a previously validated method reported in the literature [37]. Chromatographic separation was obtained using a reverse-phase chromatography column (Lichrospher 100 RP-18, 250 x 4 mm, Merck®, Germany) with a flow rate of 1.0 ml/min and an injection volume of 10 µl. The run time was approximately 10 min. The mobile phase for melatonin assay consisted of methanol: acetonitrile: 0.5 % acetic acid solution (4:1:5, v/v/v).

2.2.5.2 Droplet size distribution

The emulsions were analyzed for droplet size as previously described in Chapter 3, Section 1, section 2.2.2.2.

2.2.5.3 Microbiological stability

The microbiological stability assessment was performed according to the ISO 16212:2008, ISO 21149:2006 and ISO 21148:2005 [38-40].

2.2.6 UV degradation studies

Three UVB lamps (Sankyo Denki G8T5E, Kanagawa, Japan) with a peak emission at 312 nm were used as the UVB source, and measured with a VLX 312 radiometer equipped with a UVB sensor (Vilber Lourmat, Marne-la-Vallée Cedex, France). The formulations were exposed to a UVB radiation dose (26 mJ/cm^2) for 2 h to mimic the solar radiation exposure [41]. Non-irradiated PM1, PM2 and melatonin solution (water:ethanol, 50:50) (Mel Sol) formulations were used as negative controls of the irradiated group. Following UVB irradiation, the samples were analyzed at pre-determined time points (15, 30, 60 and 120 min), using HPLC.

2.2.7 Characterization studies

2.2.7.1 Microscopy analysis

The microscopic aspect of PM emulsions was confirmed as previously described in Chapter 3, Section 1, section 2.2.2.2.

2.2.7.2 Structural analysis

Dynamic viscosity

Shear rate *vs*. shear stress measurements were performed using a AR 2000ex rheometer (TA Instruments, USA). Rotational viscosity was determined using a cone geometry with an angle of 2 º. Flow curves were generated by ramping the shear rate from 0 to 100 s^{-1} (ascent curve) and then from 100 to 0 s^{-1} (descent curve) for 120 s each curve. All tests were performed on 1 g samples at 25.0 ± 0.5 ºC, in duplicate.

Oscillatory measurements

Oscillatory measurements were performed to investigate the behavior of these formulations when subjected to small deformations. Oscillation frequency sweep tests were performed

from 0.1 to 100 Hz. Viscoelastic experiments were carried out by exposing the samples to a forced oscillation deformation. Prior to the oscillation tests, the sweep tests were conducted at 1 Hz and 0 to 50 Pa (stress sweep test), and at 0.1 to 100 Hz and 1 Pa (frequency sweep test) for both emulsions. The creep and recovery tests were carried out with 1 Pa shear stress, allowing 360 s for creep and other 360 s for relaxation. All tests were performed on 1 g samples at 25.0 ± 0.5 ºC in duplicate.

2.2.7.3 Texture profile analysis (TPA)

TPA method is described in Chapter 3, Section 1, section 2.2.7.2.

2.2.8 Topical delivery studies

2.2.8.1 In vitro skin permeation

Skin permeation studies were performed according to the procedure described previously in Chapter 3, Section 2, section 2.2.5.1. and in Chapter 4, Section 2, section 2.2.10.1. Ethanol:water (1:1) was used as the receptor phase that assured perfect sink conditions during all experiment period. The Mel Sol was used as a control. The melatonin content in the withdrawn samples was analyzed by HPLC.

2.2.8.2 In vitro skin retention

Skin retention studies were performed according to the procedure described previously in Chapter 3, Section 2, section 2.2.5.2. and in Chapter 4, Section 2, section 2.2.10.2. In the extraction process, 3 ml of mobile phase for melatonin assay was added to the SC tapes and ED pieces. The final solution was injected in HPLC to quantify the amount (%, w/w) of melatonin retained in these skin layers (SC + ED).

2.2.9 *In vitro* cytotoxicity studies

2.2.9.1 Cell culture conditions

The cell culture conditions are described in Chapter 2, section 2.2.4.1.

2.2.9.2 Cytotoxicity assays

To determine *in vitro* emulsions effects on cell viability, cells were incubated with PM emulsions for 24 h and cell viability was determined using the MTT assay as described in detail in Chapter 2, section 2.2.5.2. The relative cell viability (%) was compared to control

cells (culture medium and sodium dodecyl sulfate (SDS) at 1 mg/ml as negative and positive controls, respectively).

2.2.9.3 Measurement of ROS production

The HaCaT sub-confluent cells were incubated for 30 min with 20 μM 2,7'dichlorodihydrofluorescein diacetate (H2-DCFDA, Life Technologies, UK) in the dark at 37 ºC, with 5 % CO_2. Fresh medium was added to the cells before exposure to PM1, PM2 and melatonin solution (1 %, w/v) and ascorbic acid (1 %, w/v) for 1 h. After hydrogen peroxide (H_2O_2, 500 μM) exposure, ROS levels were determined at 485 nm (excitation) and 520 nm (emission) wavelengths using a fluorescence microplate reader (FLUOstar BMGLabtech, Germany) [42]. Data from 6 replicates were reported as relative fluorescence units (RFU) percentage and expressed as mean fluorescence ratio (fluorescence of exposed cells/fluorescence of unexposed control from the same experiment).

2.2.10 *In vitro* EpiSkin™

The EpiSkin™ assay is described in Chapter 5, section 2.2.3.

2.2.11 Safety assessment

According to the method described in Chapter 5, section 2.2.2.

2.2.11.1 Hazard identification

According to the method described in Chapter 5, section 2.2.2.1.

2.2.11.2 Dose-response assessment

According to the method described in Chapter 5, section 2.2.2.2.

2.2.11.3 Exposure assessment

According to the method described in Chapter 5, section 2.2.2.3.

2.2.11.4 Risk characterization

According to the method described in Chapter 5, section 2.2.2.4.

2.2.12 *In vivo* studies

2.2.12.1 Human Repeat Insult Patch Test (HRIPT)

According to the method described in Chapter 5, section 2.2.4.1.

2.2.12.2 In vivo sunscreen water resistance

The water resistance of sunscreens was tested on 3 volunteers (Fitzpatrick skin type II). Volunteers cleanse their forearms using a mild cleanser and leave them to air dry for 30 min before starting the test. Initial cross polarized images are taken after the sunscreens application (2 mg/cm^2) on the inner forearm (4 cm^2).

The amount of each sunscreen formulation left before and after water bath immersion was quantified via cross-polarized imaging by means of the Visia® CA (Canfield Scientific, Faitfield, NJ). Panellists immerse their forearms into a water bath system (29 ± 2 °C) and washed away by the flow of water (150 rpm) during 40 min [36]. Their forearms were allowed to air dry for 15 min and the amount of sunscreen was measured again. This procedure was repeated and the amount of sunscreen was measured again to calculate the water resistance of the sunscreen formulations.

This method yields a series of three cross-polarized images for each panellist: clean skin (without sunscreen), immediately after sunscreen application, and post water bath. Water resistance information was obtained from the cross-polarized Visia® CA imaging mode in visible light. The RGB color space of the raw bitmap images was converted to relative luminance using ImageJ®. From these images, average L changes for each sunscreen area were obtained from histograms. Skin whiteness was defined as the change in L value before and after water immersion, and the percentage of water resistance retention (% WRR) of the sunscreens was determined according to Equation 5.

Equation 5: $\%\ WRR = \frac{L_{\text{washed protector}} - L_{\text{skin}}}{L_{\text{protector}} - L_{\text{skin}}}$

2.2.13 *Statistical analysis*

According to the method described in Chapter3, Section2, section 2.2.9.

3. Results and discussion

3.1 Solid particles (SP)

The SP chosen to formulate the PM Pickering emulsions were TiO_2, ZnO and ASt particles. TiO_2 is a common UVB filter used for manufacturing sunscreens with a high SPF [29]. Previous results clearly demonstrated the importance of the presence of TiO_2 attending that this solid particle (mainly at 20% concentration) contributed for emulsion stability and high SPF (data not shown). The addition of another filter (ZnO) was intended to ensure an adequate protection in the UVA range. Therefore, the combination of these filters resulted in a broad-spectrum UV protection [30], while improving the antibacterial and antifungal properties of the formulations [43]. ASt is a modified starch used in pharmaceutical and personal care products at concentrations up to 30% as an anticaking and a viscosity increasing agent [27], which can also function as a steric stabilizer. However, in the present work, ASt was not used due to its stabilizing properties but rather as SPF enhancer of PM Pickering emulsions (Table 6.5).

3.1.1 *Wettability measurements*

In Pickering emulsions, one of the liquid phases will probably wet the solid more than the other liquid, being the latter the disperse phase. The importance of the wettability of the particles at the oil-water interface is quantified by the contact angle (θ), which will determine the emulsion type. If the contact angle measured through the aqueous phase is < 90º, the emulsion will be o/w and, by contrast, if the contact angle is > 90º, the emulsion will be w/o. In this case, a w/o emulsion was desirable in order to guarantee the chemical stability and solubility of melatonin in the internal (aqueous) phase. Furthermore, w/o emulsions are more water resistant and provide higher SPF at the same UV filters concentration than o/w emulsions [44].

Table 6.2 - Contact angle of water, liquid paraffin and green coffee oil with $mTiO_2$, ZnO and ASt (mean ± SD, n=3).

Samples	Contact angle (θ, °)		
	Water	Liquid paraffin	Green coffee oil
$mTiO_2$	106.5 ± 0.7	0	60.1 ± 1.9
ZnO	100.2 ± 2.6	0	23.3 ± 0.1
ASt	109.0 ± 0.4	15.8 ± 1.1	0

$mTiO_2$ - Triethoxycaprylylsilane titanium dioxide; ZnO – Zinc oxide; ASt - Aluminum starch octenylsuccinate.

According to Table 6.2, $mTiO_2$, ZnO and ASt particles stabilize more effectively w/o emulsions. All SP had a contact angle with water > 90º, and simultaneously, a contact angle with paraffin and green coffee oil < 90º thus, allowing the formulation of a stable emulsion by combining these three types of particles.

3.1.2 *Particle size distribution*

It is important to prove that the particles have a size greater than 100 nm in order to ensure an environmentally friendly cosmetic product. According to the international "green" standards, nanomaterials are forbidden. Particle size distributions of $mTiO_2$, ZnO and ASt showed that all particles were larger than 100 nm, as requested to avoid regulatory issues (Table 6.3).

Table 6.3 - Particle size distribution of the different SP proposed (mean ± SD, n=6).

Solid Particles	Particle size distribution (μm)			
	Span	d (0.1)	d (0.5)	d (0.9)
$mTiO_2$	37.36 ± 1.38	0.14 ± 0.01	0.19 ± 0.01	7.12 ± 0.30
ZnO	19.51 ± 5.53	0.16 ± 0.01	0.57 ± 0.03	11.38 ± 3.74
ASt	1.04 ± 0.01	7.28 ± 0.00	13.52 ± 0.01	20.81 ± 0.00

$mTiO_2$ - Triethoxycaprylylsilane titanium dioxide; ZnO – Zinc oxide; ASt - Aluminum starch octenylsuccinate.

3.2 Natural oils

3.2.1 *SPF measurement*

Sunscreens are usually composed of synthetic chemical filters with a high capacity to absorb sun light at the region of UVB (320–290 nm) and UVA (400–320 nm) spectrum. The reduction of filter concentration in sunscreen formulations is a strategy to improve quality without affecting their properties as well as to reduce the adverse effects (e.g. estrogenic effects, disruption of human endocrine activity, among others). On the other hand, the increasing association of natural products with antioxidant activity (e.g. GCO and melatonin) may also improve the photoprotective activity of sunscreen formulations. In fact, these natural products present several advantages, such as the bioactivity, relative safety and achievement from renewable sources, low cost, besides the feasibility for application in a wide range of health care products. In this context, GCO, a rich source of antioxidants and polyphenols, which has arisen as a potential candidate to replace the

chemical filters in sunscreen PM formulations [31]. As reviewed by Scheuer *et al*. [24], topical application of melatonin conduced to a dose-dependent decrease of erythema degree and a formulation containing 1% (w/w) of melatonin proved to be effective in preventing UV-induced erythema. However, it is important to note that the ideal concentration of melatonin is still to be defined, so further studies will be needed to assess the required dose to achieve an effective photoprotection. The SPF determination for different natural oils is represented on Table 6.4.

Table 6.4 - SPF found for the natural oils (mean ± SD, n=3).

Sample	SPF
Raspberry oil	0.48 ± 0.18
Avocado oil	0
Carrot oil	0.64 ± 0.06
Green coffee oil	5.03 ± 0.23
Spent coffee oil	1.57 ± 0.07
Brazil nut oil	0.02 ± 0.05

The pure GCO showed the highest SPF (~ 5), which is in line with previous results suggesting the use of GCO as a potential natural product for improving SPF in sunscreens formulations thus, allowing to decrease the concentration of chemical or physical filters in such formulations [45]. For example, GCO showed a high synergistic effect when associated with a synthetic sunscreen as ethylhexylmethoxycinnamate, leading to an increase of 20 % in SPF [45]. Therefore, this promising oil was used as the external phase of the final PM formulations.

3.3 Efficacy of PM1 and PM2

Attending to pre-formulation studies (results not shown), two formulations (PM1 and PM2) were characterized and selected for further assessment. Although the only variable between these two emulsions was the presence (PM2) or absence (PM1) of starch, the respective results were surprisingly different, as we shall see in the following section.

3.3.1 *SPF measurement*

Based on the results showed on Table 6.5, both emulsions showed high values of SPF with a suitable UVA/UVB ratio. Although, starch had shown no photoprotection property by itself, there was a synergistic increase of SPF value (around 2 fold) when combined with physical filters as TiO_2 in PM2 formulation. Other authors also reported that the addition of 5 % starch induced a SPF enhancement of 40 % [46]. Thus, it was possible to reduce the amount of physical filters by including starch in the sunscreen formulation [47].

Differences in SPF between PM1 and PM2 formulations were only detected in the *in vitro* determinations (Optometrics SPF-290S Analyzer). However, it must be noticed that this evaluation has some limitations. According to Pissavini *et al.* [48], high SPF values are more difficult to measure due to the biological variability. Another limitation is the impossibility to detect biological effects that might affect the SPF determination, since it is a simple physical measurement. For example, a substance exhibiting antioxidant and anti-inflammatory activities may delay the appearance of erythema, which cannot be observed under *in vitro* conditions.

Therefore, the real life SPF is usually lower than the SPF obtained with the solar simulator as here observed. These SPF values would only be the same in the case of the ideal sunscreen with spectral homeostasis.

Table 6.5 - *In vitro* and *in vivo* efficacy tests of the PM1 and PM2.

Formulations	*In vitro* SPF - Optometrics SPF-290S Analyzer			*In vitro* sun product water resistance		*In vivo* sun product water resistance
	SPF	UVA/UVB	UVA	%WRR* after 1st Immersion	%WRR* after 2nd Immersion	%WRR*
PM1	43.4±6.2	0.9±0.1	33.0±5.6	55.3±6.9	54.7±7.6	70.0±2.0
PM2	82.3±10.3	0.9±0.1	71.1±10.1	62.6±4.3	50.7±6.1	71.2±0.5

* WRR – water resistance retention

3.3.2 *In vitro sun product water resistance*

The protection that sunscreens provide against sunburn is neither absolute nor tight. The photoprotection conferred by a sunscreen is extremely variable in a context of beach or pool since there are many conditions that contribute to its decline (e.g. the trips to the bathroom or the simple contact with the towel will decrease the sunscreen coverage). That is why it is strongly recommended to reapply the sunscreen after prolonged swimming or

vigorous activity. One of the many factors that can have an effect on the level of protection is the water contact, because UV absorbers present in the formulation can leach out or be physically removed by the washing action [35].

In vivo water resistance testing of topical sunscreens is time consuming, expensive and experimentally problematic [49]. Thus, initially it was opted to determine the sun product water resistance under *in vitro* conditions. This method measures the SPF following a defined water immersion procedure. A product is considered water resistant when the value for the lower 90 % one-sided confidence limit has to be greater than or equal to 50 % [35]. Analysis of Table 6.5 revealed that PM1 and PM2 formulations showed an *in vitro* % WRR ≥ 50% after both immersions. Consequently, it was possible to ensure the water resistance claim of both formulations.

3.3.3 *Physical and chemical stability*

In previous studies, the degradation profile of melatonin has already been evaluated (data not shown). These results confirmed the high degradation tendency of melatonin, particularly in the presence of an oxidizing agent. Therefore, Pickering emulsions were formulated to deliver this radical scavenger on a safe and effective manner. The stability of these emulsions in terms of melatonin content, pH and macroscopic characteristics was assessed for 3 months at 25 ± 2 ºC and under accelerated conditions (40 ± 2 ºC; relative humidity 75 ± 5 %). After this period, both PM1 and PM2 emulsions remained white with a creamy and homogeneous aspect for both storage conditions. In fact, no instability-related processes, such as creaming (or sedimentation), flocculation, coalescence or phase inversion were observed. The pH values (pH ~ 5) did not significantly vary over time as well as the droplet size (Table 6.6**)**. Melatonin assay remained within the pre-established limits [90 – 110 %] throughout the study.

Microbiological testing revealed that these formulations were stable for 3 months as the total aerobic microbial, yeast and mould count presented accepted values following the established criteria (< 10 cfu/g).

Table 6.6 - Droplet size distribution of the PM1 and PM2 emulsions (mean ± SD; n= 625) and percentage of melatonin recovered in batches 1 and 2 (mean ± SD; n=3) stored at 25 ± 2 °C and 40 ± 2 °C during 90 days, respectively.

	Time (days)	Temperature (ºC)	PM 1		PM 2	
			Batch 1	Batch 2	Batch 1	Batch 2
Droplet size distribution d(0.5) (μm)	1	25	6.2 ± 4.1	6.7 ± 4.8	5.7 ± 4.3	6.2 ± 3.6
	14	25	6.4 ± 5.8	6.4 ± 4.7	5.6 ± 6.3	6.5 ± 4.1
		40	7.1 ± 8.5	6.5 ± 4.2	5.3 ± 3.8	5.9 ± 5.7
	30	25	5.9 ± 7.2	6.8 ± 3.9	6.5 ± 5.7	6.1 ± 3.5
		40	6.7 ± 3.4	6.2 ± 3.8	6.2 ± 5.9	5.4 ± 4.1
	90	25	6.4 ± 3.9	5.9 ± 3.8	6.1 ± 6.2	5.6 ± 5.5
		40	5.7 ± 4.1	5.8 ± 4.5	5.8 ± 3.9	6.3 ± 6.7
Melatonin recovery (%)	1	25	101.82 ± 5.47	99.23± 0.30	92.80 ± 0.61	99.29 ± 1.47
	14	25	92.63 ± 0.73	90.84 ± 1.93	92.95 ± 2.19	94.73 ± 3.14
		40	93.59 ± 1.05	95.54 ± 4.33	96.63 ± 0.73	94.95 ± 2.79
	30	25	100.26 ± 0.81	105.98 ± 4.15	100.40 ± 3.31	100.09 ± 11.24
		40	100.40 ± 6.31	100.09 ± 3.24	101.15 ± 1.12	99.57 ± 0.58
	90	25	96.96 ± 8.43	94.75 ± 4.69	94.15 ± 1.59	101.27 ± 0.31
		40	101.48 ± 7.74	107.62 ± 5.27	94.70 ± 0.37	104.23 ± 1.76

3.4 UV degradation studies

The photo-instability of melatonin is well documented [50]. As a result of its absorption at 254 nm, this compound is quite vulnerable to UV light, originating N1-acetyl-N2-formyl-5-methoxykynuramine (AFMK) as its main photodegradation product [50, 51]. Melatonin can also be attacked by the ˙OH radical, which interacts similarly with AFMK. The concentrations of these photodegradation products are directly proportional to UVR-dose and melatonin content, and their accumulation are time-dependent [52].

Thus, photodegradation studies were performed using an UVB lamp (wavelength that mostly affects the melatonin stability). An acute exposure was simulated for 2 h correspondent to the reapplication time of sunscreen, as recommended [53]. According to Fig. 6.1, Melatonin solution (Mel Sol) presented a significant decrease ($p < 0.05$) of the melatonin content to values below the inferior limit of the 90-110% specification after 15 min of UVB exposure. In contrast, PM1 and PM2 remained within the established range until the end of exposure time (120 min).

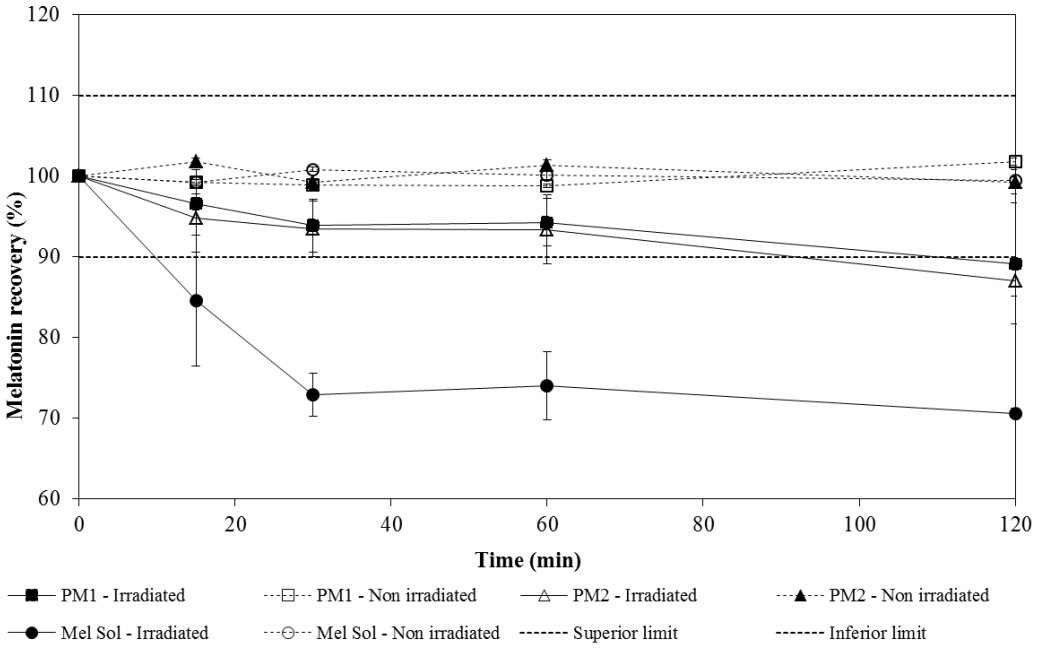

Fig. 6.1 - UV degradation studies of melatonin solution (Mel Sol) and melatonin formulations (PM1 and PM2).

Comparing the photodegradation profiles of Mel Sol and PM emulsions, it is possible to conclude that this novel sunscreen formulation (PM) is suitable for the protection of melatonin.

3.5 Characterization studies

3.5.1 *Microscopy analysis*

Light microscopy analysis showed no differences among formulations (Fig. 6.2), while polarized light micrographs revealed a positive birefringence only in PM2, which may be due to the crystalline structure of starch granules (Fig. 6.2 (d)). In fact, the semi–crystalline starch granules do not disperse in water at room temperature, which can be an advantage for the emulsion stabilization by these SP [54].

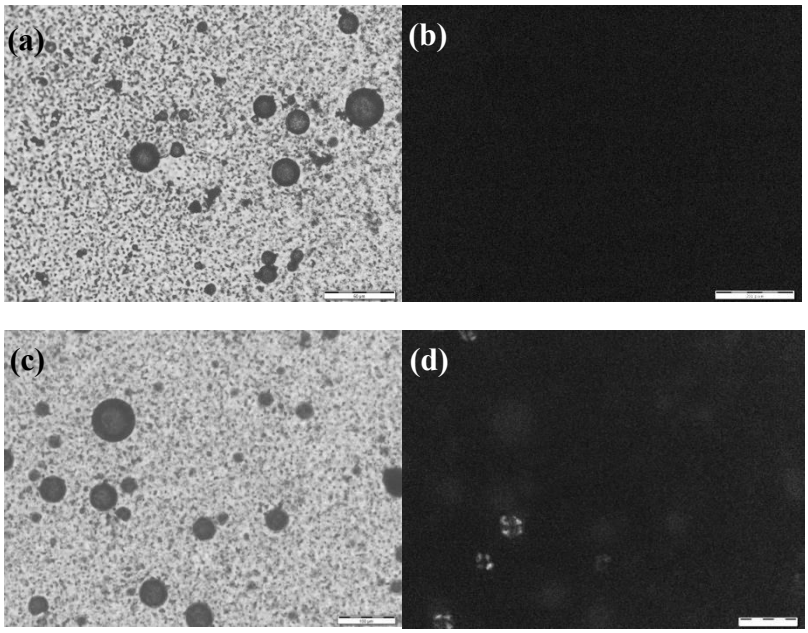

Fig. 6.2 - Micrographs of (a) PM1 under bright-field, (b) PM1 under polarized light, (c) PM2 under bright-field and (d) PM2 under polarized light (Scale bar = 50μm).

3.5.2 *Structural analysis*

The physical characterization of PM1 and PM2 emulsions has been performed using several techniques crucial for the predictive performance of the product under a variety of conditions, particularly during product filling, spreadability on the skin and easiness of product removal from the final packaging system. The flow curves (Fig. 6.3 (a)) showed that the PM emulsions were non-Newtonian fluids, which means that their viscosity is dependent on the shear rate.

These emulsions were also characterized as shear thinning fluids, since their structure need an initial tension to be deformed and start flowing (yield stress), and after that, a non-linear curves obtained as the apparent viscosity decreased with increased stress [55]. In addition, the relation between the shear stress and the shear rate was also time-dependent, particularly in the case of PM2.

Considering the time during which these formulations were submitted to different forces, it was possible to verify that the apparent viscosity was not only dependent of the shear rate magnitude, but also of the time of this shear rate application. In this context, the PM1 and PM2 emulsions exhibited rheopectic behaviors. However, at lower shear rates (around 30 s^{-1}), this behavior was altered and both emulsions began to exhibited thixotropic behavior [55].

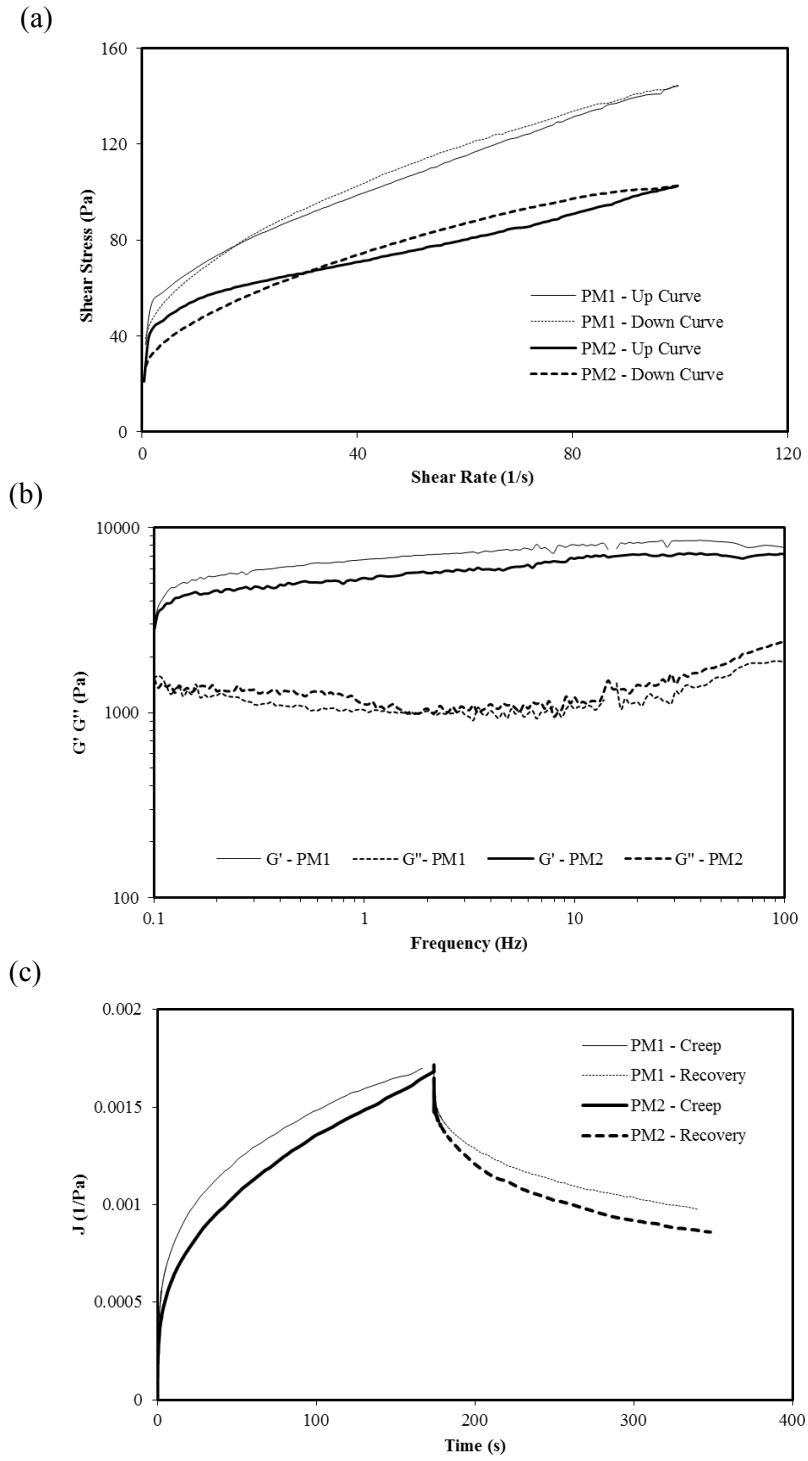

Fig. 6.3 – (a) Flow curves, (b) frequency sweep plot and (c) creep and recovery plot of PM1 and PM2 emulsions.

The shear stress sweep precedes the frequency sweep and creep/ recovery tests, making it possible to determine the values of shear stress within a linear range at which the sample does not suffer any deformation. Both emulsions were not disrupted at 0 to 5 Pa. Thus, the values of G' (elastic modulus) and G'' (viscous modulus) remained linear within this

region of linear viscoelasticity, indicating the suitable shear stress to be used in frequency sweep and creep/recovery tests.

Both emulsions exhibited a higher G' than G'' values (Fig. 6.3(b)), a solidlike behavior [56]. The frequency sweep curves of PM emulsions showed that there was practically no variation of the elastic and viscous moduli at the tested range (0.1-100 Hz).

When a viscoelastic material has a storage (or elastic) modulus higher than the viscous (or loss) modulus, the shear energy is temporarily stored during the test and can be retrieved later, as usually occurs in emulsion systems. Emulsion systems with this feature usually exhibit an high stability [57].

When the emulsions were submitted to predetermined shear stress (1 Pa for both emulsions) for 150 s (creep), and then left for another 150 s without shear stress (recovery), both PM1 and PM2 emulsions suffered deformation according to the compliance value (J) (Fig. 6.3 (c)). In the recovery part of this study, the samples could recover part of their former structure, and the elastic part of the deformation was reversed.

Regarding the TPA results, PM1 and PM2 emulsions demonstrated a wide range of mechanical properties dependent on the presence of starch (Table 6.7). In fact, the starch affected the mechanical behavior of these formulations, which may influence their adhesion on the skin.

The addition of starch caused a decrease in emulsion hardness. In contrast, PM1 emulsion (without starch) showed a greater hardness. In other words, the starch addition influenced positively this parameter. The same trend was verified for adhesiveness, which is more related to surface characteristics, and depends on a combined effect of adhesive and cohesive forces. PM2 emulsion showed a lower value of adhesiveness, which was again dependent on the presence of starch, since this was the only different ingredient between the two formulations.

Considering the elasticity, cohesiveness and compressibility results, the presence or absence of starch did not influence these parameters. So, the only parameters altered by the presence of starch were hardness and adhesiveness, attending to the decrease in both values.

Table 6.7 - Mechanical properties of the emulsions extracted from the TPA mode in batches 1 and 2 (mean ± SD, n=3).

Formulations		Hardness (g)	Adhesiveness (|g.s|)	Elasticity	Cohesiveness	Compressibility (g.s)
PM 1	Batch 1	16.7 ± 0.1	26.9 ± 0.1	1.0 ± 0.1	0.8 ± 0.1	21.4 ± 0.6
	Batch 2	16.0 ± 0.8	27.3 ± 0.2	1.0 ± 0.1	0.8 ± 0.1	22.0 ± 1.9
PM 2	Batch 1	11.2 ± 0.2	13.0 ± 0.6	1.0 ± 0.1	0.8 ± 0.1	22.0 ± 0.1
	Batch 2	11.8± 0.7	13.9 ± 0.6	1.0 ± 0.1	0.8 ± 0.1	17.6 ± 0.2

In summary, the addition of ASt promoted a reduction in the apparent viscosity of the PM2 emulsion. In fact, the presence of starch can improve the spreadability of the emulsions over the skin surface. Considering the sunscreen formulation, a maximizing photoprotection will be obtained by covering the total skin area. These phenomena can be explained by the triethoxycaprylylsilane and aluminum octenylsuccinate surface treatment of $mTiO_2$ and ASt, respectively (Fig. 6.4). According to other authors, the silane coating decreases the interaction between the alumina aggregates, present on the surface of the starch granules, decreasing the shear stress required to break the flocculation [58]. Thus, both $mTiO_2$ and ASt, surface treatment can interact results in a lower viscosity.

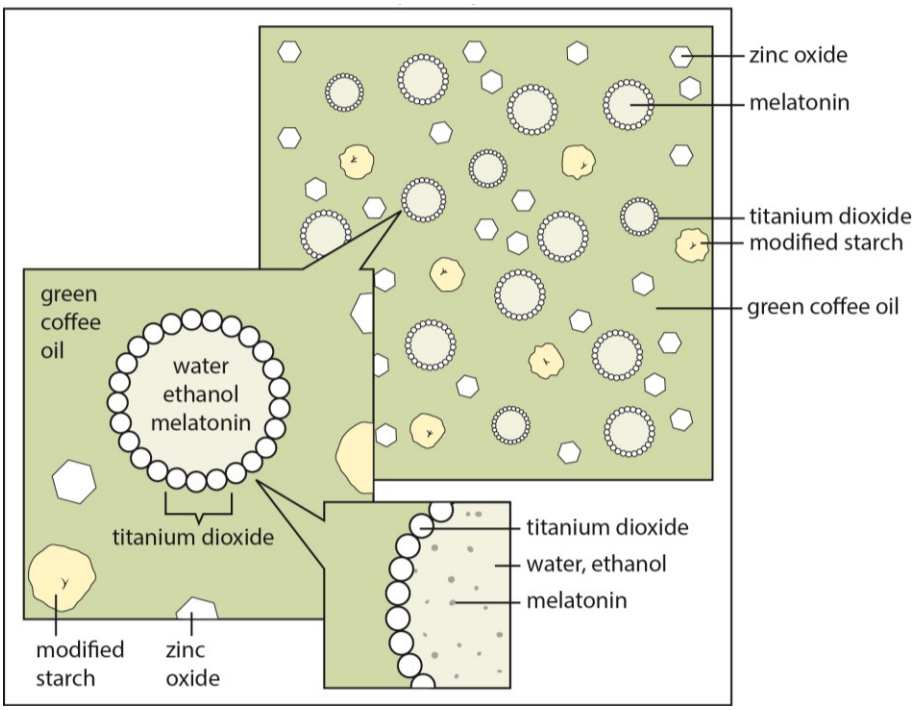

Fig. 6.4 - Schematic representation of a w/o Pickering emulsion (PM2) proposed by this research work.

3.6 Topical delivery studies

3.6.1 *Skin permeation and retention*

In vitro studies with Franz diffusion cells are a useful tool to determine the drug flow before performing *in vivo* assays [59]. Skin permeation occurs via two main routes: the transappendageal (through the sweat glands and across the hair follicles associated with the sebaceous glands) and the transepidermal (intercellular route through intercellular lipid domains and transcellular pathway through the keratinocytes). The relative importance of which route will be followed depends on the molecules physicochemical characteristics.

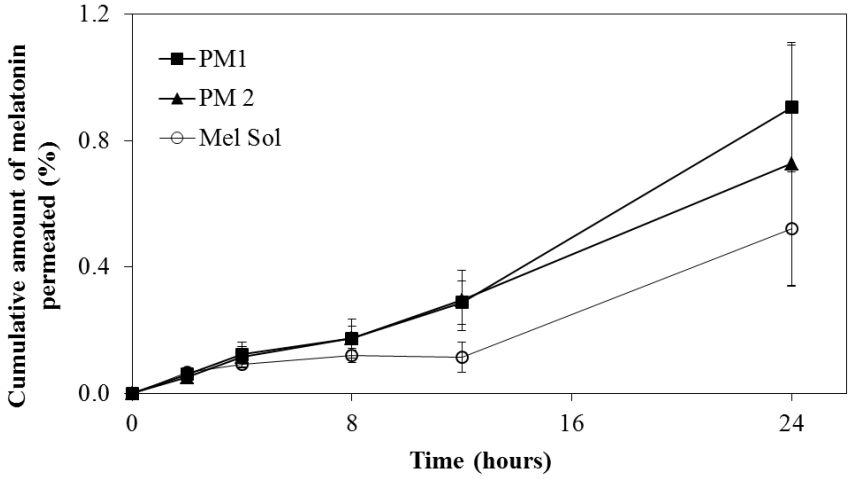

Fig. 6.5- Permeation profile of melatonin from PM1, PM2 and Mel Sol (Mel solution) through newborn pig skin (mean ± SD, n=6).

Fig. 6.5 shows the permeation profiles of melatonin from PM1, PM2 and solution (Mel Sol) through newborn pig skin, considering the cumulative amount of melatonin permeated to the acceptor compartment as a function of time for 24 h.

There was a significant increased permeation of melatonin with time for PM1 and PM2 and Mel Sol ($p > 0.05$). These profiles are typical of infinite dose experiments where the applied dose is so high that the depletion of the permeant in the donor chamber caused by evaporation or diffusion into and through the barrier is negligibly low [60]. The high permeation through the skin was also due to the small molecular size (232.278 Da) and to the LogP of melatonin. Although melatonin is usually considered an amphiphilic molecule, its LogP (~ 1.4) is relatively close to amphoteric molecules (LogP ≥ 1.7). Finally, the presence of ethanol in the tested formulations also justifies the permeation enhancement. Low molecular weight alkanols, like ethanol, act by enhancing the solubility of the drug in

the SC lipid matrix by extraction of hydrophobic alcohols, disrupting its integrity [61, 62]. Besides lowering the skin barrier function, ethanol also increased the melatonin solubility in the vehicle.

However, it should be noted that this data obtained using newborn pig skin cannot be translated to *in vivo* delivery in humans, as other factors significantly alter its permeation profile, such as cutaneous microvasculature, which prevents the accumulation of melatonin in the skin, and the cutaneous metabolism of fatty alcohols [61].

Melatonin extraction from the skin by tape stripping was performed for PM1, PM2 and Mel Sol (Fig. 6.6).

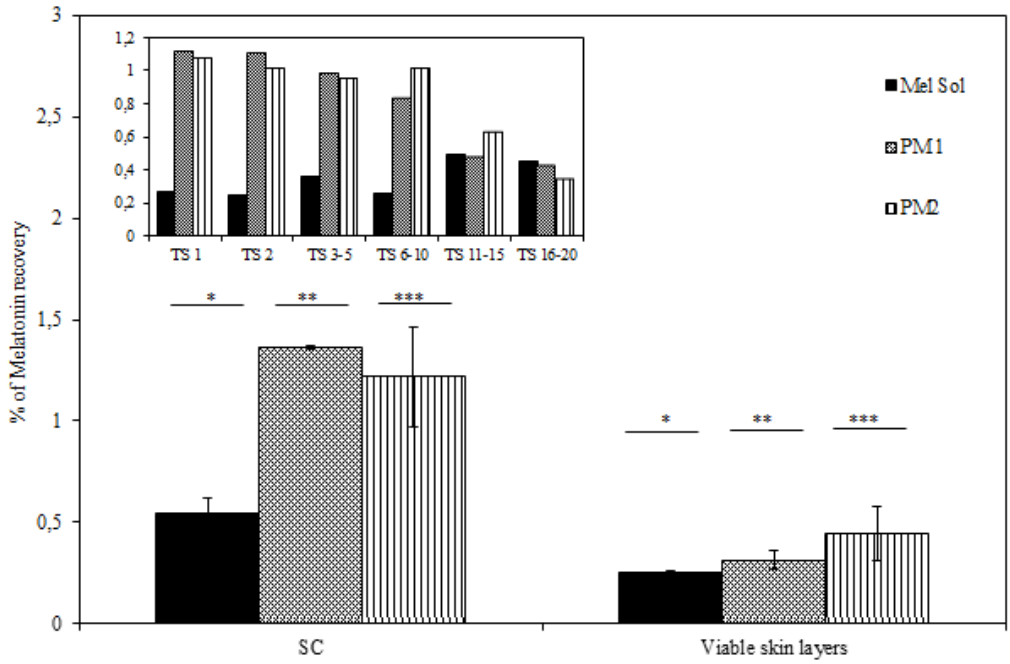

Fig. 6.6 - Penetration of PM1, PM2 formulations and melatonin solution (Mel Sol) in the SC (from tape stripping, TS) and viable skin layers (epidermis and dermis) after 24h. Inner graphic: Penetration of PM1, PM2 and Mel Sol in the different tape strip layers (TS) and in the viable skin layers (ED). Statistical analysis was performed using one-way ANOVA with Tukey's post hoc test ($p < 0.05$) (mean ± SD, n = 6).

The amount of melatonin extracted from the SC was significantly higher than from viable skin layers (epidermis and dermis) for all tested formulations, as expected attending that SC is the first main skin barrier ($p < 0.05$). This is a required outcome, as the target activity of sunscreens is in the outermost layers of the skin, reflecting UVR in order to reduce penetration to deeper viable skin layers where damage may occur.

The statistical analysis indicated that the amounts of melatonin extracted from the SC and viable skin layers are significantly lower when using Mel Sol compared to PM1 and PM2 ($p < 0.05$). However, PM1 and PM2 probably due its composition, i.e., w/o emulsions, could be more retained due to the lipohilicity of the upper skin layers, suggesting that w/o emulsions may provide advantages with respect to low penetration rates and high substantively to the SC [63].

Although PM1 and PM2 are sunscreen formulations usually considered as cosmetic products, in this case it was also incorporated an active molecule (melatonin) to offer DNA protection against UVR damage. Attending to the fact that melatonin receptors are located in epidermis layer, inner epithelial root sheath, sweat glands and blood vessel endothelium [64], the skin permeation and penetration of these formulations were desirable. Fischer *et al.* [65] also related that topical melatonin had a depot effect in the SC being continuously released to the rest of the skin and dermal vasculature.

3.7 *In vitro* ROS assay

Keratinocytes represent the major population in the skin and UVR causes damage to these cells. Thus, the possible protective effect of melatonin against oxidative damage in HaCaT cell lines was investigated *in vitro*.

To investigate the potential cytotoxicity of the melatonin, the cell viability was evaluated using HaCaT cell lines in a MTT assay. Melatonin is not cytotoxic in HaCaT cells on the range of concentrations tested, 1 – 0.015 % (w/v).

The intracellular production of reactive oxygen species (ROS) within cells was assessed with a fluorimetric technique using 2,7'dichlorodihydrofluorescein diacetate (H2-DCFDA, Life Technologies, UK). H2-DCFDA is a stable, non-fluorescent molecule that is hydrolyzed by intracellular esterases to non-fluorescent 2-7'-dichlorodihydrofluorescein (H2DCF), which is rapidly oxidized in the presence of H_2O_2, hydroxyl radicals and diverse peroxides [66] to a highly fluorescent compound (DCF) [67]. Ascorbic acid was used as a positive control due to its antioxidant properties.

Fig. 6.7 refers the difference between ROS generation in ethanol/water sample (vehicle) and in the tested formulations. It is clear that all formulations decreased the formation of ROS, particularly the melatonin-loaded emulsions due to its antioxidant activity.

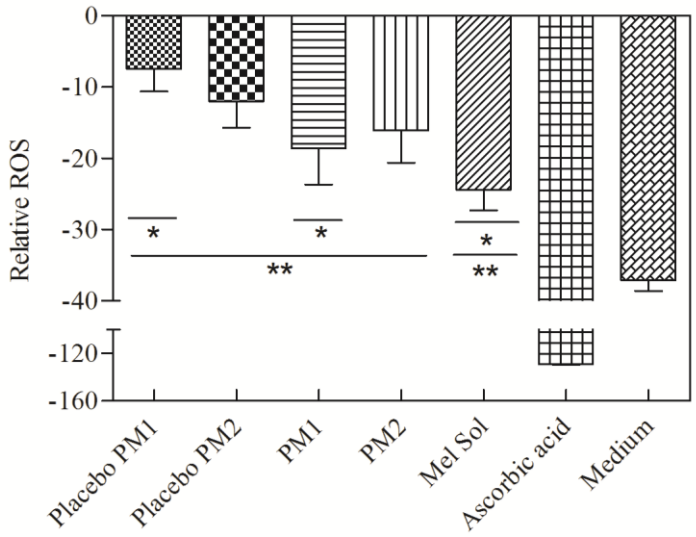

Fig. 6.7 - Relative ROS determination of HaCat cell line measured by the H2-DCFDA assay. Melatonin concentration is 1% (w/w) in all cases. Statistical analysis was performed using one-way ANOVA with Tukey's post hoc test ($p < 0.05$) (mean ± SD, n = 6).

All formulations and melatonin solution led to an increase of ROS formation when compared to ascorbic acid and the statistical analysis indicated that the Mel Sol provides a significant better protection than PM1 and PM2. This phenomenon can be explained probably due to the presence of ethanol, once ethanol may induce ROS production *per se and* due to the incomplete release of melatonin from Pickering emulsion [68]. Furthermore, some studies refer the cytotoxicity of ZnO nanoparticles, which may be associated not only with its action as an antibacterial, disinfecting and drying agent but also with its capacity to enhance ROS production [69]. This suggests that the excipients of these formulations could have an oxidant activity, and that by themselves may induce ROS formation. On the other hand, ascorbic acid (vitamin C) was used as a positive control due to its potent antioxidant properties and because it possesses a variety of other topical advantages including photoprotection from UVR, inhibition of melanogenesis and improvement of a variety of inflammatory skin disorders. However, despite of its potential as a topical antioxidant, the instability of this water-soluble vitamin, together with difficulties associated with its topical delivery, proved that ascorbic acid is unattractive for topical application [70].

3.8 *In vitro* EpiSkin™

The *in vitro* safety topical use of PM emulsions was tested on reconstituted human epidermis by the EpiSkin™ model and is useful to classify skin irritants able to produce a reduction in cell viability [71]. The tissue viability measured as optical density by the MTT assay and calculated as percentage of cytotoxicity compared to the negative control (PBS), was 84.0 ± 5.0 % and 81.0 ± 4.0 % for PM1 and PM2, respectively, whereas for the positive control (SDS) it was 36.0 ± 4.0 %. A product is considered an irritant when viability is reduced by 50 %. The absence of skin-irritant effects at the tested concentrations indicated that both formulations could be safe for topical use.

3.9 Safety assessment

3.9.1 *Hazard identification*

Many variables affect the skin penetration and permeation, including the physicochemical parameters of each ingredient (Table 6.8). The chemical structures and physical properties of the ingredients used in the PM emulsions, namely, the emollient and modified SP are complex, hindering to predict interactions between them. However, it is recognized that the safety of a final product is determined based on the theoretical safety assessment of its ingredients [72].

Table 6.8 - Chemical properties of the ingredients presented in the PM1 and PM2.

Ingredient (Chemical name/INCI name)	CAS number	Molecular weight (g/mol)	LogP
Water (aqua)	7732-18-5	18.02	-
Green coffee oil (Coffea arabica seed oil)	84650-00-0	-	-
Fatty acids *			
Palmitic acid (16:0)	57-10-3	256.42	7.23
Stearic acid (18:0)	57-11-4	284.48	8.02
Oleic acid (18:1)	112-80-1	282.46	7.78
Linoleic acid (18:2)	60-33-3	280.44	7.70
Linolenic acid (18:3)	463-40-1	278.43	6.5
Titanium dioxide* and Triethoxycaprylylsilane	13463-67-7 2943-75-1	356.38	-
Zinc oxide*	1314-13-2	81.38	-
Aluminum starch octenylsuccinate	9087-61-0	-	-
Melatonin*	73-31-4	232.3	1.2
Ethanol (alcohol)*	64-17-5	46.06	-0.19

*Data from the literature [31, 73-77]. INCI – International nomenclatura of Cosmetic Ingredients

Assessment of the safety for human health of the finished product shall take into consideration the toxicological profile of each ingredient, its chemical structure and its levels of exposure (Table 6.9). *In vitro* and *in vivo* studies make it possible to investigate the toxicological profile of a cosmetic ingredient, namely, the cytotoxicity, sensitization and irritation or intracutaneous reactivity, the risk of carcinogenicity, mutagenicity or teratogenicity based on period of exposure of the cosmetic products [72].

The main ingredient present in PM formulations is GCO. Due to the absence of data in the literature for this emollient, it was included information about the fatty acids present in these oils and the safety profile of each ingredient was assessed. Vegetable extracts are widely used is cosmetic products due to their moisturizing, occlusive and emollient properties. Moreover, it is known that after topical application of one product only a very small amount is able to penetrate the skin due to the SC properties. There are several mechanisms of hydration but the majority of the oils act by occlusion, i.e., they avoid the evaporation of endogenous water, decreasing the transepidermal water loss. The GCO is considered a food oil and thus it is considered safe after topical application [78].

Despite the high concentration of mTiO_2 and ZnO, the toxicological profile of these ingredients does not give rise to concern in human use, since the substance is not absorbed through the skin. The ingredients in the solid state and particle size greater than 100 nm are not able to penetrate the SC if not solubilized. mTiO_2 and ZnO are not soluble in water neither in oils. Thus they are in suspension and they cannot penetrate through the skin. Given the negligible, dermal penetration of mTiO2 and ZnO when applied on skin, and in consideration of the low toxicity observed, the calculation of a margin of safety (MoS) is not relevant for this assessment [74, 75].

Concerning the ASt, this ingredient is not irritating at concentrations used in cosmetics, and neither sensitizer nor photosensitizer, and based on the available data we concluded that this ingredient is safe as cosmetic ingredient in the current concentration [27].

In the particular case of ethanol, and concerning all accessible data, it is concluded that ethanol poses no risk for the consumer in the normal and reasonably foreseeable use of this product [79, 80].

Considering the molecular weight and the LogP values (when available), the ingredient that most probably penetrates into the SC is melatonin, because PM emulsions contain potent skin enhancers (ethanol and fatty acids).

Table 6.9 - Summary of the biological safety of the ingredients.

Ingredient (Chemical name/INCI name)	Acute toxicity	Dermal Irritation	Ocular irritation	Sensitization	Photostability	Genotoxicity / Mutagenicity	Ref
Melatonin	Rat (oral) LD_{50} > 1600 mg/kg	Human volunteers: no irritant	-	OECD 429: non sensitizer	-	No evidence of genotoxicity or mutagenicity	[76]
Green coffee oil	Toxicological information (e.g. acute toxicity, NOAEL, mutagenicity, LD_{50}/LC_{50}-value) is not available for this product. Due to the fact that it is a food grade raw material, there is no reason to determine toxicity data. When applied correctly, the raw material will have no negative adverse effects in humans						[78]
Titanium dioxide Triethoxycaprylylsilane	Rat (oral) LD_{50} > 2150 mg/kg	Rabbit (OECD 404): no irritant	Rabbit (OECD 405): no irritant	Guinea pig: non sensitizer	-	*Salmonella typhimurium* (OECD 471): no mutagenic	[74]
Zinc oxide	Rat (oral) LD_{50} > 2000 mg/kg; Rat (dermal) LD_{50} > 2000 mg/kg	Rabbit (occlusive patch test): no irritant	Rabbit: no irritant	Guinea pig: non sensitizer Human: non sensitizer	UV radiation (30 J/cm^2): photo-stable and non-photoreactive	Bone marrow cytogenetic assay in rodents and host-mediated assay in mice	[75]
Aluminum starch octenylsuccinate	-	Human volunteers: no irritant	Ocular irritant in humans	Guinea pig: non sensitizer	-	No evidence of genotoxicity or mutagenicity	[27]
Ethanol (alcohol)	Mouse (oral) LD_{50} > 8300 mg/kg	Rabbit (dermal) LD_{50} > 20000 mg/kg; Rabbit (OECD 404): no irritant	Rabbit (OECD 405): moderately irritating	Guinea pig: non sensitizer Human: non sensitizer	-	*Salmonella typhimurium* (OECD 471): no mutagenic	[81]
Water	n.a.	n.a.	n.a.	n.a.	-	n.a.	-

n.a. – not available; LD_{50} - the median lethal dose; LC_{50} - the median lethal concentration; OECD - The Organisation for Economic Co-operation and Development; NOAEL - No Observed Adverse Effect Level.

3.9.2 *Exposure assessment*

The PM emulsions are proposed for use on intact skin of adults and can be used as a sunscreen. These emulsions are leave-on cosmetic products intended to stay in prolonged contact with the skin and should be applied generously and repeatedly before sun bathing, especially after spending time in water.

According to the SCCS opinion, the exposed skin surface area for a sunscreen is 17500 cm^2. The estimated daily amount applied for a sunscreen is 70.0 g/day and the frequency of application is twice a day which is converted in a daily exposure of 1166.7 mg/kg bw/day. Applying the equation 4 the SED values were calculated for each ingredient (Table 6.10) [72]. Note that both worst scenarios were used: highest skin surface and highest amount applied.

Table 6.10 shows the estimated SED from the ingredients present in the PM emulsions. In the lack of dermal absorption studies, the worst-case scenario of 100% of dermal penetration should be taken into consideration [72]. In addition, a large number of studies suggest that SP do not penetrate in healthy or sunburnt human skin deep enough to reach live cells of the epidermis, as a result, the dermal absorption considered for mTiO2, ZnO and Ast was 0%.

Table 6.10 - Exposure data of formulation ingredients.

Ingredient (Chemical name/INCI name)	Daily exposure (mg/kg bw/day)	% in the final product		Dermal absorption (%)	SED (mg/kg bw/day)		NOAEL (mg/kg bw/day)	MoS
		PM1	PM2		PM1	PM2		
Water	1166.7	19	18	100	221.7	210	-	-
Green coffee oil	1166.7	35	35	100	408.3	408.3	n.a.	-
Triethoxycaprylylsilane titanium dioxide	1166.7	20	20	0	-	-	62.5*	n.a.
Zinc oxide	1166.7	15	15	0	-	-	53.5*	n.a.
Aluminum starch octenylsuccinate	1166.7	5	5	0	-	-	n.a.	-
Melatonin	1166.7	-	1	0.7	-	0.08	200*	2500
Ethanol (alcohol)	1166.7	6	6	0.04	0.03	0.03	2400*	80000

n.a. – not available; *data from the literature [74-76, 79, 81]; bw – body weight.

3.9.3 *Dose-response assessment*

The NOAEL is an important part of the non-clinical risk assessment. The NOAEL values found out for TiO_2, ZnO and melatonin were 62.5, 53.5 and 200 mg/kg/day, respectively.

3.9.4 *Risk characterization*

The MoS is used to extrapolate from a group of test animals to an average human being, and subsequently from average humans to sensitive subpopulations. The WHO proposes a value of 100, and it is usually recognized that the MoS should at least be 100 to claim an ingredient safe for human use. The value of 100 consists of a factor 10 for the extrapolation from animal to man and another factor 10 taking into account the inter-individual variations within the human population [72]. The MoS for melatonin was calculated according to Equation 2 (Chapter 5), and the value obtained was 2500, which is above the threshold value of 100, hence the ingredient may be considered safe.

3.10 *In vivo* studies

3.10.1 *HRIPT*

The HRIPT assay intends to assure two essential conditions: the first one is the skin compatibility and the second one, the absence of allergenic potential of the tested formulations. Therefore, HRIPT was conducted to justify the claim "dermatological tested". No reactions or skin sensitization/irritation were observed in the initial 3 weeks contact and even after the final challenge contact. Thus, very good skin compatibility was obtained for these melatonin sunscreen formulations.

3.10.2 *In vivo sun product water resistance*

After ensuring the *in vitro* efficacy of these formulations, the WRR was also evaluated in humans. Human testing is considered to be the most acceptable and definitive method for claiming WRR. This method is a new *in vivo* screening approach to measure WRR using cross polarized imaging. Although it does not allow determining the exact SPF before and after the immersion, it evaluates the sunscreen loss due to the action of water. Similarly to the in *vitro* assay, the value for the 90 % lower unilateral confidence limit must be mean % WRR $\geq$ 50 %.

Skin whiteness showed a similar behavior to that obtained for water resistance. The PM1 and PM2 emulsions possess 70 – 85 % of whiteness without water exposure. However, when exposed to water for 40 min, both products showed quite similar amounts of whiteness on skin and quite perceptible, as shown in Fig. 6.8. Both emulsions presented a broad peak distribution ranging from 50 to 80 % with a median peak around 70 % of

whiteness. Thus, w/o emulsions possess a higher degree of water repellency needed to avoid products to coalesce in contact with water drops remaining on wet skin.

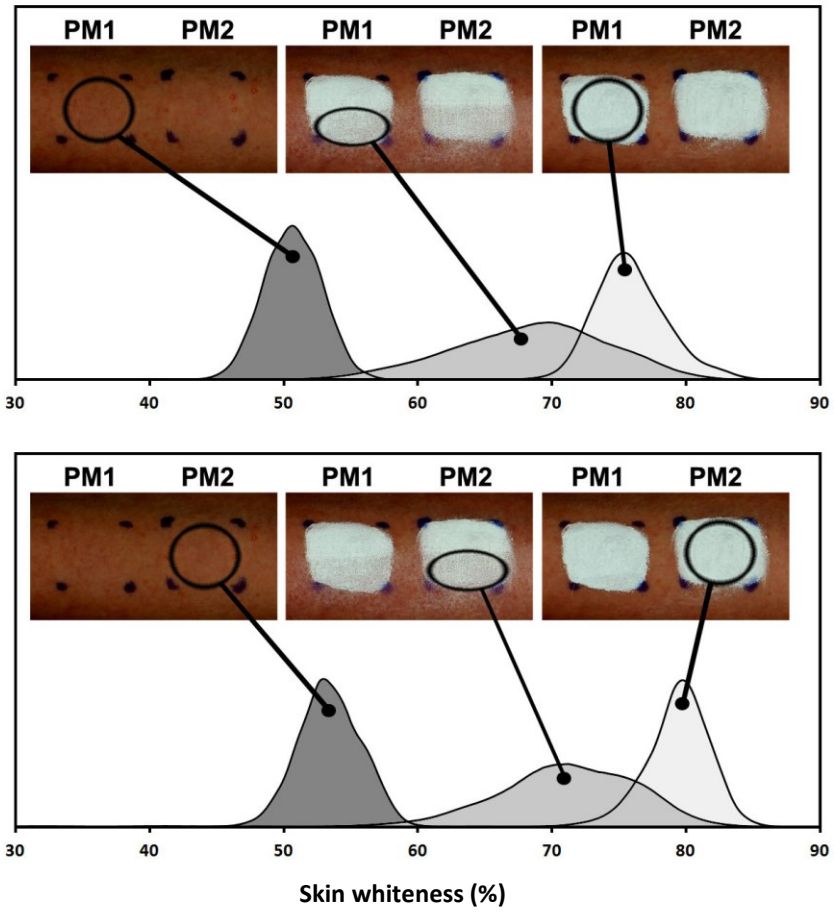

Fig. 6.8- Histograms of skin whiteness (%) resulting from sunscreens applied on dry skin and cross-polarized images of two sunscreens applied to the volar forearm of a subject: Dark grey - bare skin; light grey - fresh sunscreen applications with 30 min air drying; and grey - sunscreen after 40 min water immersion.

Based on the WRR values (Table 6.5), it is possible to claim water resistance of the product. Furthermore, these *in vivo* values were higher than those obtained *in vitro*, which may be explained by a better adhesion to human skin compared with the adhesive tape used for the *in vitro* assay.

4. Conclusions

Thus, a novel sunscreen formulation with a high UVB/A protection, biological activity and better tolerability was designed to stabilize and deliver melatonin, based on the Pickering emulsions concept. The successful formulation was possible by combining natural and multifunctional compounds. In particular, GCO (a recognized bio-antioxidant) was associated to UV physical absorbers ($mTiO_2$ and ZnO) at lower concentrations and with rigorous particles size higher than 100 nm. The UV filters concentration could be reduced due to the SPF improvement by the presence of both starch particles and GCO.

As previously outlined, melatonin may be beneficial for sun protection. Based on its free radical scavenger and antioxidant activity, the advantage of including melatonin in PM emulsions became obvious. Regarding the advantages of melatonin over other antioxidants, these are related to its several mechanisms of action such as immunomodulatory and anti-inflammatory besides potent antioxidant actions, suppressing all three stages of carcinogenesis. Moreover, melatonin can be produced in different skin cells from dermis and epidermis layers which may determine a strong effect on both NMSC and MSC as well as photoageing processes. Pickering emulsions proved to be a promising solution not only for the sunscreen development but also for the photostability of drugs. To the best of our knowledge this is the first successful formulation able to protect melatonin from photodegradation. All results revealed an excellent compromise between stability, UV protection, water resistance, topical delivery, efficacy and safety.

Our findings combined with data reported so far thus enrich existing knowledge about the potent anti-oxidant action of melatonin and highlight that melatonin-containing Pickering emulsion sunscreens could be one of the most promising segments in the personal care industry.

5. References

1. Rangwala S, Tsai KY. Roles of the immune system in skin cancer. British Journal of Dermatology 2011;165(5):953-965.

2. Hofbauer GFL, Bavinck JNB, Euvrard S. Organ transplantation and skin cancer: basic problems and new perspectives. Experimental dermatology. 2010;19(6):473-482.

3. Yaar M, Gilchrest BA. Ageing and photoageing of keratinocytes and melanocytes. Clinical and Experimental Dermatology 2001;26(7):583-591.

4. Hadshiew IM, Eller MS, Gilchrest BA. Skin aging and photoaging: The role of DNA damage and repair. Clinical and Experimental Dermatology 2000;11(1):19-25.

5. Ahmed NU, Ueda M, Nikaido O, Osawa T, Ichihashi M. High levels of 8-hydroxy-2′-deoxyguanosine appear in normal human epidermis after a single dose of ultraviolet radiation. British Journal of Dermatology 1999;140(2):226-231.

6. Ascenso A, Ribeiro H, Marques HC, Oliveira H, Santos C, Simões S. Tretinoin still as a Key Agent for UV Photoaging Management. Mini-Reviews in Medicinal Chemistry. 2014;14(8):629-641.

7. Dutra E, Oliveira D, Kedor-Hackmann E, Santoro M. Determination of sun protection factor (SPF) of sunscreens by ultraviolet spectrophotometry. Brazilian Journal of Pharmaceutical Sciences. 2004;40(3):381–385.

8. Mishra AK, Mishra A, Chattopadhyay P. Evaluation of Sun Protection Factor of Some Marketed Formulations of Sunscreens by Ultraviolet Spectroscopic Method. Journal of Current Pharmaceutical Research. 2011;5(1):32-35.

9. Gasparro FP, Mitchnick M, Nash JF. A review of sunscreen safety and efficacy. Photochemistry and Photobiology. 1998;68(3):243-256.

10. Mansur JS, Breder MNR, Mansur MCA, Azulay RD, 24. Determinação do fator de proteção solar por espectrofotometria. Anais Brasileiros de Dermatologia. 1986;61:167-172.

11. Lerner AB, Case JD, Takahashi Y. Isolation of Melatonin and 5-methoxyindole-3-acetic acid from bovine pineal glands. The Journal of Biological Chemistry. 1960;235:1992-1997.

12. Papagiannidou E, Skene DJ, Ioannides C. Potential drug interactions with Melatonin. Physiology & Behavior 2014;131:17-24.

13. Rezzani R, Rodella LF, Favero G, Damiani G, Paganelli C, Reiter RJ. Attenuation of ultraviolet A-induced alterations in NIH3T3 dermal fibroblasts by Melatonin. British Journal of Dermatology 2014;170(2):382-391.

14. Kleszczynski K, Fischer TW. Melatonin and human skin aging. Dermatoendocrinology. 2012;4(3):245-252.

15. Slominski RM, Reiter RJ, Schlabritz-Loutsevitch N, Ostrom RS, Slominski AT. Melatonin membrane receptors in peripheral tissues: distribution and functions. Molecular and Cellular Endocrinology 2012;351(2):152-166.

16. Fischer T, Wigger-Alberti W, Elsner P. Melatonin in der Dermatologie Experimentelle und klinische Aspekte. Hautarzt. 1999;50(1):5-11.

17. Kostoglou-Athanassiou I. Therapeutic applications of melatonin. Therapeutic Advances in Endocrinology and Metabolism. 2013;4(1):13-24.

18. Yalcinkaya FR, Gokce A, Guven EO, Davarci M, Cikim G, Yekeler H, Balbay MD. Protective Effect of Vitamin E and Melatonin Against Radiation Induced Damage in Testes of Rats. Journal of Animal and Veterinary Advances 2009;8(11):2335-2340.

19. Martín M, Macías M, Escames G, León J, Acuña-Castroviejo D. Melatonin but not vitamins C and E maintains glutathione homeostasis in t-butyl hydroperoxide-induced mitochondrial oxidative stress. The FASEB Journal. 2000.

20. Singh M, Jadhav HR. Melatonin: functions and ligands. Drug Discovery Today. 2014;19(9):1410-1428.

21. Slominski A, Zmijewski MA, Wortsman J, Semak I, Zbytek B, Slominski M, Tobin DJ. On the Role of Melatonin in Skin Physiology and Pathology. Endocrine. 2005;27(2):137-148.

22. Reiter RJ, Carneiro RC, Oh CS. Melatonin in Relation to Cellular Antioxidative Defense Mechanisms. Hormone and Metabolic Research Journal. 1997;29(08):363-372.

23. Pugazhenthi K, Kapoor M, Clarkson AN, Hall I, Appleton I. Melatonin accelerates the process of wound repair in full-thickness incisional wounds. Journal of Pineal Research. 2008;44(4):387-396.

24. Scheuer C, Pommergaard HC, Rosenberg J, Gogenur I. Melatonin's protective effect against UV radiation: a systematic review of clinical and experimental studies. Photodermatology, Photoimmunology & Photomedicine. 2014;30(4):180-188.

25. Folter JW, Ruijven MW, Velikov KP. Oil-in-water Pickering emulsions stabilized by colloidal particles from the water-insoluble protein zein. Soft matter. 2012;8(25):6807-6815.

26. Frelichowska J, Bolzinger MA, Pelletier J, Valour JP, Chevalier Y. Topical delivery of lipophilic drugs from o/w Pickering emulsions. International Journal of Pharmaceutics. 2009;371(1-2):56-63.

27. Nair B, Yamarik TA. Final report on the safety assessment of aluminum starch octenylsuccinate. International Journal of Toxicology. 2002;21 Suppl 1:1-7.

28. Holdich RG, Yilmaz I, Lazrigh M, Shama G. Production and evaluation of floating photocatalytic composite particles formed using Pickering Emulsions and membrane emulsification. Industrial and Engineering Chemistry Research. 2012;51(38):12509-12516.

29. Wang SQ, Tooley R. Photoprotection in the era of Nanotechnology. Seminars in Cutaneous Medicine and Surgery Journal. 2011;30(4):210-213.

30. Smijs TG, Pavel S. Titanium dioxide and zinc oxide nanoparticles in sunscreens: focus on their safety and effectiveness. Nanotechnology, Science and Applications. 2011;12:95-112.

31. Ribeiro H, Marto J, Raposo S, Agapito M, Isaac V, Chiari B, Lisboa P, Paiva A, Barreiros S, Simões P. From coffee industry waste materials to skin-friendly products with improved skin fat levels. European Journal of Lipid Science and Technology. 2013;115(3):330-336.

32. Sayre RM, Agin PP, Levee GJ, Marlowe E. Comparison of *in vivo* and *in vitro* testing of sunscreening formulas. Photochemistry and Photobiology. 1979;29(3):559-566.

33. EC. Comission Recommendation of 22 September 2006 on the efficacy of sunscreen products and the claims made relating thereto. In: EC, editor.: Official Journal of the European Union

2006.

34. Kale S, P Ghoge P, Ansari A, Waje A, Sonawane A. Formulation and in-vitro determination of sun protection factor of Nigella sativa Linn. seed oil sunscreen cream. International Journal of PharmTech Research. 2010;2(4).

35. COLIPA. Guidelines For Evaluating Sun Product Water Resistance. 2005.

36. Ahn S, Yang H, Lee H, Moon S, Chang I. Alternative evaluation method in vitro for the water-resistant effect of sunscreen products. Skin Research and Technology. 2008;14(2):187-191.

37. Zhang C, Gao Y, Zhao X, Li X. A validated HPLC method for determining Melatonin in capsule dosage form. Spatula DD. 2012;2(3):147-151.

38. Standard I. Microbiology - Enumeration of yeast and mould. Microbiology – Enumeration of yeast and mould2008.

39. Standard I. Microbiology – Enumeration and detection of aerobic mesophilic bacteria. Microbiology – Enumeration and detection of aerobic mesophilic bacteria2006.

40. Standard I. Microbiology - General instructions for microbiological examination. Microbiology - General instructions for microbiological examination2005.

41. Gonzalez H, Tarras-Wahlberg N, Stromdahl B, Juzeniene A, Moan J, Larko O, Rosen A, Wennberg A. Photostability of commercial sunscreens upon sun exposure and irradiation by ultraviolet lamps. BMC Dermatology. 2007;7(1):1.

42. Seida P, Parce JW, Seeds MS, Bass DA. Flow cytometric quantitation of oxidative produce formation by polymorphonuclear leukocytes during phagocytosis. Journal of Immunology. 1984;133:3303-3307.

43. Singh G, Joyce EM, Beddow J, Mason TJ. Evaluation of antibacterial activity of ZnO nanoparticles coated sonochemically onto textile fabrics. Journal of Microbiology, Biotechnology and Food Sciences. 2012;2(1):106-120.

44. Draelos ZD. Cosmetic Dermatology: Products and Procedures: Wiley; 2011.

45. Chiari BG, Trovattib E, Pecorarob E, Corrêaa MA, Cicarellia RM, Ribeiro S, Isaac V. Synergistic effect of green coffee oil and synthetic sunscreen forhealth care application. Industrial Crops and Products. 2014;52:389-393.

46. Guth J, Martino G, Pasapane J, Ronco D. Polymeric approaches to skin protection. Cosmetics & Toiletries. 1991;106:71-74.

47. Serpone N, Dondi D, Albini A. Inorganic and organic UV filters: Their role and efficacy in sunscreens and suncare products. Inorganica Chimica Acta. 2007;360(3):794-802.

48. Issavini M, Ferrero L, Alaro V, Heinrich U, Tronnier H, Kockott D, Lutz D, ournier V, Zambonin M, Meloni M. Determination of the in vitro SPF. Cosmetics & Toiletries. 2003;118:63-72.

49. Stokes RP, Diffey DL, Dawson LC, Barton SP. A novel in vitro technique for measuring the water resistance of sunscreens. International Journal of Cosmetic Science. 1998;20:235-340.

50. Bromme HJ, Peschke E, Israel G. Photo-degradation of melatonin: influence of argon, hydrogenperoxide, and ethanol. Journal of Pineal Research. 2008;44(4):366-372.

51. Fischer TW, Sweatman TW, Semak I, Sayre RM, Wortsman J, Slominski A. Constitutive and UV-induced metabolism of melatonin in keratinocytes and cell-free systems. The FASEB Journal. 2006;20(9):1564-1566.

52. Andrisano V, Bertucci C, Battaglia A, Cavrini V. Photostability of drugs: photodegradation of melatonin and its determination in commercial formulations. Journal of Pharmaceutical and Biomedical Analysis. 2000;23(1):15-23.

53. FDA. Labeling and Effectiveness Testing: Sunscreen Drug Products for Over-The-Counter Human Use — Small Entity Compliance Guide. In: Services; USDoHaH, editor.2012.

54. Jane J, Maningat CC, Wongsgonsup R. Starch characterization, variety and application. In: Singh BP, editor. Industrial Crops and Uses. 2010. p. 207.

55. Chhabra RP, Richardson JF. Non-Newtonian Fluid Behaviour. In: Richardson RPCF, editor. Non-Newtonian Flow and Applied Rheology (Second Edition). Oxford: Butterworth-Heinemann; 2008. p. 1-55.

56. Nikiforidis CV, Biliaderis CG, Kiosseoglou V. Rheological characteristics and physicochemical stability of dressing-type emulsions made of oil bodies–egg yolk blends. Food Chemistry. 2012;134(1):64-73.

57. Torres LG, Iturbe R, Snowden MJ, Chowdhry BZ, Leharne SA. Preparation of o/w emulsions stabilized by solid particles and their characterization by oscillatory rheology. Colloids and Surfaces A: Physicochemical and Engineering Aspects. 2007;302(1–3):439-448.

58. Lin C, Chung DDL. Nanostructured fumed metal oxides for thermal interface pastes. Journal of Materials Science. 2007;42:10.

59. Gujjar M, Banga AK. Vehicle influence on permeation through intact and compromised skin. International Journal of Pharmaceutics. 2014;472(1-2):362-368.

60. Selzer D, Abdel-Mottaleb MA, Hahn T, Schaefera UF, Neumannc D. Finite and infinite dosing: Difficulties in measurements, evaluations and predictions. Advanced drug delivery reviews. 2013;65(2):278-294.

61. Kikwai L, Kanikkannan N, Babu RJ, Singh M. Effect of vehicles on the transdermal delivery of melatonin across porcine skin in vitro. Journal of Controlled Release. 2002;83(2):307-311.

62. Marto J, Baltazar D, Duarte A, Fernandes A, Gouveia L, Militao M, Salgado A, Simoes S, Oliveira E, Ribeiro HM. Topical gels of etofenamate: in vitro and in vivo evaluation. Pharmaceutical Development and Technology. 2014:1-6.

63. Benson HAE, Sarveiya V, Risk S, Roberts MS. Influence of anatomical site and topical formulation on skin penetration of sunscreens. Journal of Therapeutics and Clinical Risk Management. 2005;1(3):209-218.

64. Slominski RM, Reiter RJ, Schlabritz-Loutsevitch N, Ostrom RS, Slominski AT. Melatonin membrane receptors in peripheral tissues: distribution and functions. Molecular and Cellular Endocrinology. 2012;351(2):152-166.

65. Fischer TW, Greif C, Fluhr JW, Wigger-Alberti W, Elsner P. Percutaneous penetration of topically applied melatonin in a cream and an alcoholic solution. Skin Pharmacology and Physiology. 2004;17(4):190-194.

66. Soh N. Recent advances in fluorescent probes for the detection of reactive oxygen species. Analytical and Bioanalytical Chemistry 2006;386:532-543.

67. Wardman P. Fluorescent and luminescent probes for measurement of oxidative and nitrosative species in cells and tissues: progress, pitfalls, and prospects. Free Radical Biology & Medicine 2007;43:995-1022.

68. Helkin AW, Nguyen HT, Samara GJ. Alcohol Induces Reactive Oxygen Species and Migration in Keratinocytes. Laryngoscope. 2010;120(S3):S35-S35.

69. Ma H, Wallis LK, Diamond S, Li S, Canas-Carrell J, Parra A. Impact of solar UV radiation on toxicity of ZnO nanoparticles through photocatalytic reactive oxygen species (ROS) generation and photo-induced dissolution. Environmental Pollution. 2014;193:165-172.

70. Murray JC, Burch JA, Streilein RD, Iannacchione MA, Hall RP, Pinnell SR. A topical antioxidant solution containing vitamins C and E stabilized by ferulic acid provides

protection for human skin against damage caused by ultraviolet irradiation. Journal of the American Academy of Dermatology. 2008;59(3):418-425.

71. Raposo S, Salgado A, Gonçalves L, Pinto P, Urbano M, Ribeiro H. Safety Assessment and Biological Effects of a New Cold Processed SilEmulsion for Dermatological Purpose. BioMed Research International. 2013;2013:10.

72. SCCS. The SCCS'S Notes of Guidance for the Testing of Cosmetic Ingredients and Their Safety Evaluation: 9th Revision: European Union; 2015.

73. EC. Cosmetic ingredient database – CosIng. European Comission.

74. SCCS. Opinion on Titanium Dioxide (nano form). COLIPA nº S75: Scientific Committee on Consumer Safety; 2013.

75. SCCNFP. Evaluation and opinion on : Zinc oxide: The scientific committee on cosmetic products and non-food products intended for consumers. 2003.

76. SCCS. Opinion on Melatonin. 2010.

77. Tetko IV, Gasteiger J, Todeschini R, Mauri A, Livingstone D, Ertl P, Palyulin VA, Radchenko EV, Zefirov NS, Makarenko AS, Tanchuk VY, Prokopenko VV. Virtual computational chemistry laboratory--design and description. Journal of Computer-aided Molecular Design. 2005;19(6):453-463.

78. Boekschoten MV, Schouten EG, Katan MB. Coffee bean extracts rich and poor in kahweol both give rise to elevation of liver enzymes in healthy volunteers. Nutrition Journal 2004;3:7-7.

79. Pendlington RU, Whittle E, Robinson JA, Howes D. Fate of ethanol topically applied to skin. Food and Chemical Toxicology 2001;39(2):169-174.

80. Lachenmeier DW. Safety evaluation of topical applications of ethanol on the skin and inside the oral cavity. Journal of Occupational Medicine and Toxicology. 2008;3:26.

81. OECD. Ethanol. OECD SIDS; 2004.

7

Concluding remarks and future work

This page was intentionally left blank

1 Concluding remarks and future work

1.1 Concluding remarks

The development of novel drug delivery systems for topical administration is a demanding task that involves not only the optimization of drugs release, permeation and retention, but also the preservation of the stability of both the drug substance and drug product.

This dissertation aimed at developing starch-based drug delivery systems built using an innovative strategy, which combined an approach that integrates simple and cost effective vehicles, methods easily transposable to the industry, and therapeutic efficacy. In summary, three different starch-based vehicles were developed with suitable physicochemical and biological properties.

The preformulation studies described in Chapter 2 revealed an enormous potential for innovative applications of starch in pharmaceutical formulations. The results obtained confirm a high variability related to its botanical origin, and demonstrated that preformulation studies are crucial to select the best starch type for the intended purpose.

In the first section of Chapter 3, the QbD approach successfully help building the quality of Pickering emulsions, allowing the development of hydrophilic drug-loaded emulsions stabilized by starch with desired organoleptic and structural characteristics. The obtained results suggest these systems are a promising vehicle for topical formulations.

In the development of MH-loaded starch-based Pickering emulsions (second section of Chapter 3), *in vitro* antibacterial activity studies revealed that the prolonged drug release pattern easily exceeded the minimum inhibitory concentration of MH against *S. aureus*. In addition, MH does not pass through the entire skin layer, suggesting a minimal potential for the systemic absorption of the antibiotic upon topical administration. *In vivo* studies showed topical administration of MH was effective in the treatment of *S. aureus* superficial infections. These findings proved MHASt-emulsions as promising formulations contributing for a new perspective on topical treatment of superficial bacterial infections.

The first section of Chapter 4 (starch-based nanocapsules) revealed an excellent compromise between stability and safety, evidencing that starch nanocapsules are suitable nanocarriers for topical use, while the design planning methodology was crucial for the understanding of starch nanocapsules formation process. Starch nanocapsules proved to be a powerful strategy and a promising nanocarrier for topical lipophilic drugs.

This study was complemented by an innovative application as a carrier for the novel synthetic human neutrophil elastase inhibitor ER143 (Chapter 4, section 2). Nanocapsules provided a high control of drug release, showing starch nanocapsules platform were suitable for the delivery of lipophilic drugs. The formulation successfully attenuated erythema and edema in 98% following the local and demonstrated to be suitable for a deeper skin penetration and retention.

The *in vitro* and *in vivo* characterization of the so developed vehicles (Chapter 5) demonstrated they increase skin hydration by decreasing TEWL with a suitable equilibrium between the safety and efficacy.

However, starch particles presented no intrinsic photoprotection properties (Chapter 6), although being a SPF promoter by a synergistic effect. The combination of melatonin, three multifunctional solid particles and green coffee oil, contributed to achieve a stable and effective innovative sunscreen with a wide range of UV radiation protection.

As a conclusion, starch-based drug delivery systems, particularly Pickering emulsions and starch-based nanocapsules, were successfully developed as potential carriers for the encapsulation/incorporation of drugs with different physicochemical characteristics. The development of starch-based vehicles included optimization of composition, manufacturing process, physicochemical characteristics, *in vitro* release and permeation, stability studies, cytotoxicity, compatibility and, finally, *in vivo* performance. In this context, the QbD approach proved to be a powerful tool for the screening procedures, and system rationalization in every development step.

1.2 Future work

As a natural follow-up from the present study, the quantification of drugs remaining in dermis and epidermis would provide useful complementary results, since the skin may act as a drug reservoir. Microdialysis and tape stripping are available techniques that could give insights into drug location in the different skin layers, considering not only animal but also human skin sources. Supplementary *in vivo* experiments involving bioluminescence imaging studies would be useful to elucidate the biodistribution of drugs after skin application. Additionally, structural studies using X-ray photoelectron spectroscopy and NMR spectroscopy techniques would complement the physicochemical characterization of the starch-based vehicles, particularly starch nanocapsules.

Another objective will be the scale-up of the manufacturing processes using a QbD approach, assuring the quality of the drug product and cost–effectiveness.

Finally, while an ideal general drug-delivery platform may never be realized, hybrid drug-delivery systems that incorporate the benefits of various approaches will be tailored to address the needs of specific applications. This type of system is a unique, versatile topical dosage form, able to deliver different types of drugs. This appears as an obvious consequence of the knowledge gathered during these studies that clearly point out to the development of a hybrid drug delivery system. The hypothetical hybrid w/o Pickering emulsion stabilized by starch nanoparticles will integrate both lipophilic (within the nanoparticles) and hydrophilic drugs (in the aqueous phase), as depicted in Fig. 7.1.

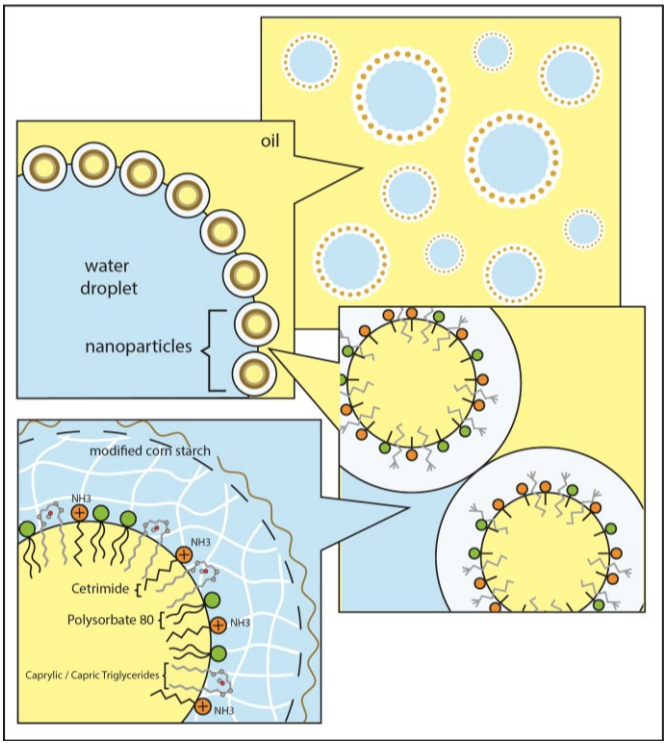

Fig. 7.1 – Hypothetical microstructure of the Pickering emulsion stabilized by lyophilized starch nanocapsules.